Some Chemistry of Metal Alkynyls: Formation of Odd and Even Bridging Carbon Chains

by

Maryka Gaudio

B.Sc. (Hons)

A Thesis Submitted Towards the Degree of Doctor of Philosophy

Department of Chemistry

December 2006

Statement of Originality

This thesis contains no material which has been accepted for the award of any other degree or diploma in any university and to the best of my knowledge and belief, contains no material previously published or written by another person, except where due reference is given.

I give consent to this thesis being made available for photocopy or loan.

Maryka Gaudio

Contents

CHAPTER THREE: Some Metal-Capped Complexes With an Odd-Numbered Bridging Carbon Chain

CHAPTER FOUR: Complexes With 1,4-Bis-Diethynylaromatic Linkers

CHAPTER FIVE: Some Cluster Chemistry

Abstract

This thesis continues the study into the synthesis and analysis of metal poly-yndiyl complexes. These molecules have shown promise as model molecular wires. Chapter one provides a general overview of the interest in carbon based molecules and introduces the need for molecular electronics. Some of the most promising classes of molecular wires are described before outlining the methods of evaluation.

Chapter two describes the synthesis of some extended chain complexes containing five or more alkynyl linkages. Several different methodologies that can be used to synthesise poly-yndiyl complexes are discussed with a gold coupling reaction providing a new and very useful route to complexes with extended carbon chains. Variations of this methodology allow for the formation of complexes containing either an even or an odd number of alkynyl linkages within the chain. The electrochemical effects of increasing chain length within the series, $\{Cp^*(dppe)Ru\}_2(C{\equiv}C)_n$ (n = 1 – 10), is examined.

Chapter three discusses the synthesis of some novel odd-membered carbon chains. Single-crystal X-ray structure determinations are reported for many of the complexes. The reactions described significantly add to the series of complexes containing the $Tp'M(CO)_2$ group (Tp' = Tp, Tp*; M = Mo, W) end-capping a carbon chain, with examples containing three, four, five and seven carbons within the chain having been obtained. Some interesting cluster-capped, even-numbered carbon chains are also described, formed by linking of the well-known carbon-tricobalt complex with the Group 6 precursors by means of the $AuX(PR_3)$ elimination reaction. The electrochemistry of each of these complexes is examined and comparisons made with similar measurements carried out on the individual end-caps.

Chapter four discusses the synthesis and electrochemistry of carbon chain complexes containing the 1,4-diethynylbenzene or 1,4-diethynyltetrafluorobenzene linkers. Comparisons on the electrochemical effects of these two linkers and polyynyl bridges of similar length are discussed. A convenient synthetic route to the organic

compounds 1,4-bis(butadiynyl)benzene and 4-(butadiynyl)phenylethyne compounds via the gold coupling reaction is also described.

Chapter five examines the synthesis of some cluster complexes. A number of new gold containing cluster complexes are prepared from the reaction of gold alkynyl complexes, M-(C≡C)-$AuPPh_3$, with the activated ruthenium carbonyl, $Ru_3(CO)_{10}(NCMe)_2$. The adducts which result from the treatment of $\{Tp(CO)_2Mo\}\equiv CC\equiv CSiMe_3$ with the cobalt carbonyl reagents $Co_2(CO)_8$ and $Co_2(CO)_6$(dppm) are also described along with the formation of the mixed metal cluster complexes $MoRu_2(CCCH_3)(CO)_8Tp$ and $MoFe_2(CCCH_3)(CO)_8Tp$.

Abbreviations

General:

[M]	general metal-ligand fragment
°	degrees
°C	degrees Celsius
Å	angstrom
Ac	acyl, -$COCH_3$
anal.	analysis
ap	2-anilinopyridinate
Atm	atmosphere
av.	average
Bu^n	normal butyl, -$(CH_2)_3CH_3$
Bu^t	tertiary butyl, -$C(CH_3)_3$
calcd	calculated
cm	centimetres
Cp	cyclopentadienyl
Cp*	pentamethylcyclopentadienyl
dbu	1,8-diazabicyclo[5.4.0]undec-7-ene
depe	1,2-bis(diethylphosphino)ethane
DF	density-functional
dippe	1,2-bis(diisopropylphosphino)ethane
DMF	*N, N*-dimethylformamide
dmpe	1,2-bis(dimethylphosphino)ethane
dmpz	3,5-dimethylpyrazolyl
dppe	1,2-bis(diphenylphosphino)ethane
dppm	bis(diphenylphosphino)methane
e^-	Electron
eq	equivalents
Et	ethyl, -CH_2CH_3
EtOH	Ethanol
eV	electron volts
h	hour(s)
HOMO	highest occupied molecular orbital
IR	Infrared
J	Joules
K	Kelvin
K_{eq}	equilibrium constant
LUMO	lowest unoccupied molecular orbital
M	Molarity

Me	methyl, -CH_3
MeOH	Methanol
mg	milligrams
MHz	megahertz
min	Minutes
mL	Millilitres
mm	millimetres
mmol	millimoles
MO	Molecular orbital
MV	mixed-valence
NIR	near-infrared
nm	nanometres
NMR	nuclear magnetic resonance
Nu	nucleophile
OPE	oligophenylethyne
ORTEP	Oak Ridge Thermal Ellipsoid Plot program
PCC	pyridinium chlorochromate
Ph	phenyl, -C_6H_5
PP	bis-phosphine
Pr^i	isopropyl, -$CH(CH_3)_2$
pz	Pyrazol-1-yl
R	general organic group
r.t.	room temperature
Ref	Reference
R_f	retention factor
s	Seconds
SAM	self-assembled monolayer
STM	scanning tunnelling microscope
SWCNT	single-walled carbon nanotube
T	temperature (K)
TCNE	tetracyanoethylene
thf	tetrahydrofuran
t.l.c.	thin layer chromatography
tmeda	tetramethylethylenediamine
TMS	trimethylsilyl, $Si(CH_3)_3$
tol	*para*-tolyl, -$C_6H_4CH_3$
Tp	hydrotris(pyrazolyl)borate
Tp*	hydrotris(3,5-dimethylpyrazolyl)borate, $HB(dmpz)_3$
UV	ultraviolet
Vis	visible
X	halide

ΔG_{th}	thermal activation barrier

NMR:

d	doublet
Hz	hertz
m	multiplet
$^{n}J_{IJ}$	n bound coupling constant between nuclei I and J
ppm	parts per million
s	singlet
t	triplet
tt	triplet of triplets
δ	chemical shift

IR:

br	broad
cm^{-1}	wavenumbers (reciprocal centimetres)
m	medium
s	strong
sh	shoulder
w	weak

Mass Spectroscopy:

CID	collision-induced dissociation
ES	electrospray
FAB	fast atom bombardment
M	molecular ion
m/z	mass per unit charge
MS-MS	mass spectrometry-mass spectrometry

UV/Vis/NIR:

$(\Delta\nu_{1/2})_{theo}$	calculated band-width at half-height
Abs	absorbance
IL	intraligand
IVCT	intervalence charge transfer
LMCT	ligand-to-metal charge transfer
MLCT	metal-to-ligand charge transfer
V_{ab}	electronic coupling parameter

$\Delta\nu_{1/2}$	observed band-width at half-height
ε	extinction coefficient
λ	wavelength

Electrochemistry:

A	amperes
CE	counter electrode
E	potential
E_n	potential of n^{th} redox process
$E_{1/2}$	half-wave potential
E_a	anodic potential
E_c	cathodic potential
I	current
i_a	anodic peak current
i_c	cathodic peak current
irr.	irreversible
K_c	comproportionation constant
V	volts
ΔE	potential difference

Acknowledgments

Firstly I would like to thank my supervisor Professor Michael Bruce for both the opportunity to work in his lab and all of his help throughout my PhD. He has provided me with not only an interesting and enjoyable project but also a very pleasant working environment for the past four years. I am also very grateful for the help of my co-supervisor Dr Marcus Cole. To Professor Allan White and Dr Brian Skelton a big thankyou for their crystallography works.

I would also like to thank Professor Brian Nicholson for running many of my mass spectra as well as enabling me to spend a month at The University of Waikato, Hamilton, New Zealand, learning to use the mass spectrometers. I thoroughly enjoyed the opportunity to work as a part of your group and learn new techniques.

To the many members of labs 9 and 10, who have come and gone over the years, I would like to say thankyou for the laughs in addition to all of the technical advice. I would especially like to acknowledge Dr Benjamin Ellis for his enthusiastic introduction to organometallic chemistry, Dr Natasha Zaitseva for teaching me all that I know about growing crystals and Dr Benjamin Hall for reading and editing this Thesis.

I would also like to thank my family and friends for their unwavering support over my years of study. To my parents, a special thankyou for their support and motivation throughout my PhD. Finally I must thank Brett for his patience and understanding without which I could never have made it this far.

Chapter 1

INTRODUCTION

1.1 Carbon Molecules

While carbon is the fourteenth most abundant element on Earth, it has the sixth highest abundance in the cosmos and thus the detection of carbon molecules have been of great interest to astronomers and astrophysicists.[1] The simplest carbon molecule, C_2, is found in the atmosphere of carbon rich stars, comets, diffuse interstellar clouds and in the sun.[2] This molecule is extremely reactive generating other C_n molecules.[3]

In 1943 carbon molecules, C_n ($n < 15$), were identified in high-frequency spark discharges between graphite electrodes.[2] With the advent of laser vaporization techniques in the early 1980's carbon clusters were generated from graphite. It was observed that only even-numbered clusters, in the range from C_{40} to C_{200}, are generated in these experiments[4] and consist of a carbon cage containing a central cavity. These carbon cage structures are generally called fullerenes and are defined as all carbon molecules with the general form $C_{20 + 2m}$ composing twelve pentagons and m hexagons.[1] An exceptionally stable fullerene is the C_{60} species known as buckminsterfullerene. Although the stability and structure of this species had been predicted many years earlier[5] it was first isolated in macroscopic quantities in 1990 by a group of astronomers, from the soot produced by resistive heating of graphite under an inert atmosphere.[6]

In 1967 the synthesis of a new polymorph of elemental carbon, known as carbyne, was reported.[7] Carbyne is a linear form of carbon, consisting entirely of sp-hybridised carbon atoms. However, reports of the preparation and structure of carbynes, which are calculated to be one-dimensional conductors, remain controversial.[8] Thus an sp-hybridised carbon allotrope remains notably absent from

the list of allotropes which currently includes diamond (sp^3), graphite (sp^2) and fullerenes (sp^2) (Figure 1.1).

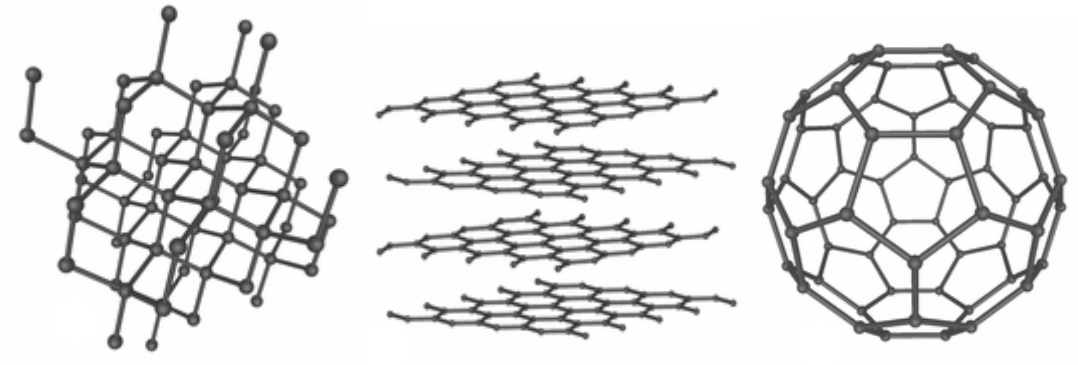

Figure 1.1: *Atomic arrangements in diamond, graphite and fullerene.*

Using a refined Hückel π-electron model Pitzer and Clementi predicted that C_n molecules would be linear in 1959. Five years latter improved calculations concluded that the C_4 acetylenic structure (**1a**) would be more stable than the double-bonded cumulene-like structure (**1b**).[2]

1a **1b**

Carbyne has presented significant synthetic and analytical challenges to date. The attraction of this elusive allotrope has stimulated a resurged interest in end-capped sp-hybridized carbon chains. It is expected that the properties of carbyne might be predicted from the trends observed in the spectroscopic data for a structurally related series of poly-ynes.[9] Three different structures are possible; two feature alternating triple and single bonds (alkynyl or poly-ynediyl) with either sp (**1c**) or sp^3 (**1d**) carbon termini and a third consisting solely of double bonds (cumulenic) with sp^2 carbon termini (**1e**).

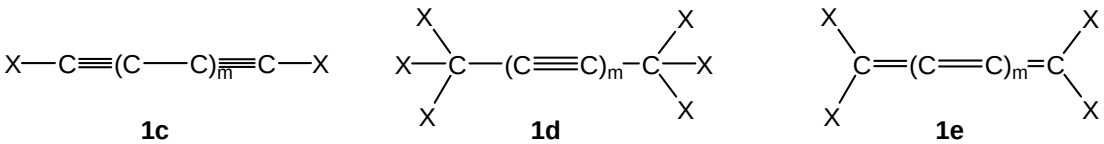

1c **1d** **1e**

The addition of transition metal centres stabilises these reactive one-dimensional carbon chains, allowing the preparation of complexes containing C_n ligands as stable entities.[10] The unique electronic, optical and physical properties of sp-hybridised carbon oligomers of the general formula $[ML_n]$-$(C{\equiv}C)_m$-$[ML_n]$, where $[ML_n]$ represents a general metal-ligand fragment, make them interesting in their own right. The X_n moieties in **1c-e** are collectively replaced by a single redox active metal capable of forming one (**1f**), two (**1g**) or three (**1h**) bonds to carbon.

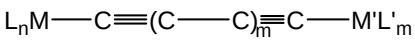

1f

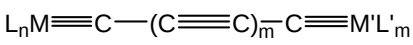

1h

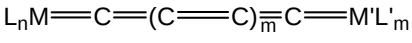

1g

These carbon-rich, bimetallic complexes contain extended π-conjugation through the poly-yndiyl (-{C≡C}$_n$-) units and are of interest for the preparation of liquid crystals,[11] metal-containing polymers,[12-15] molecular switches,[16] NLO active[17-19] and luminescent[20,21] materials. These complexes also allow through-bridge exchange of charge, as a result of their π density, which may allow the delocalisation of electrons between the remote metals.[22] Consequently their contribution is essential in the field of molecular electronics.

The field of electronics is currently driven by the continuous design of smaller devices. This is known as a 'top-down' approach. In 1965, Gordon Moore, co-founder of Intel, observed that the number of transistors per intergrated circuit was doubling every 18-24 months.[23,24] This trend became known as Moore's Law and to date has held true. However we may be approaching an intrinsic limit for micro-fabrication in the solid state, where traditional materials cease to have the electronic properties of the bulk material[25] or devices become so small that electrons may simply jump from one component to another.[26] In view of these limitations to solid state device technology the 'bottom-up' approach has been attracting interest. This is the opposite approach, where the ultimate miniaturisation is achieved by the fabrication of molecular components.

Logic chips currently being produced contain copper wires which are 90 nm wide.[27] A typical molecular component would be over one hundred times smaller in comparison to the components being fabricated today. The small size of these molecules is emphasised when one considers that in one mole (6×10^{23} molecules) of a molecular scale device, there would be more molecules than the number of transistors ever made.[27] Futhermore, this amount of material could be synthesised using a relatively small reaction flask and the physical characteristics of the device could, in principle, be changed by changing the raw materials used to make it. These key points have driven research within the electronics industry. Examples of molecular wires,[28-31] switches,[32-34] memories[35,36] and rectifiers[37,38] have all been reported, with many operating on the same principles as conventional devices.

1.2 Molecular Wires

Wires are an essential component of any electronic circuit. Their sole function is to facilitate the passage of current (electrons) between two points. A molecular wire is therefore by definition a 'one dimensional molecule allowing a through-bridge exchange of an electron/hole between its remote ends/terminal groups, themselves able to exchange electrons with the outside world.'[30] Porphyrin oligomers,[39] DNA,[40] carbon nanotubes, conjugated organic molecules and redox-active complexes have all been examined as potential molecular wires. Although the structures of these compounds are vastly different they are all able to be electron or hole-conducting, enabling a current to flow from one end of a molecule to the other.

1.2.1 Conjugated Organic Wires

Conjugated organic molecules can conduct electrons through their conjugated π-systems. The alternating single and multiple carbon-carbon bonds within these compounds provide a rigid backbone which facilitates electron transport. One class of compounds currently being investigated as potential molecular wires are oligophenylethynes (OPEs).[27,41-44] A major advantage of building electronic devices based on conjugated organic molecules is that OPEs of a precise length can be synthesised due to the range of known organic reactions. An example of an OPE, with a length of 128 Å, is shown in Figure 1.2.

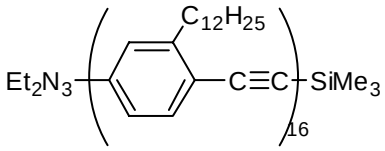

Figure 1.2: *An example of an oligophenylethyne (OPE).*

1.2.2 Carbon Nanotubes

Carbon nanotubes (CNT) consisting of a seamless cylinder of hexagonal networks were first synthesised in 1991.[45] Single wall carbon nanotubes (SWNT) are created

when a graphite film a single atomic layer thick (graphene) forms a seamless cylinder (Figure 1.3).

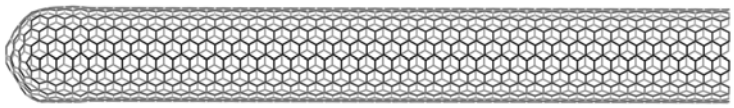

Figure 1.3: *A single wall carbon nanotube (SWNT).*[46]

If multiple concentric graphene cylinders form, then a multiwall carbon nanotube (MWNT) is created (Figure 1.4). The diameters of these structures are typically in the range of nanometers, while the length of an individual CNT can reach lengths of up to 4 cm.[47]

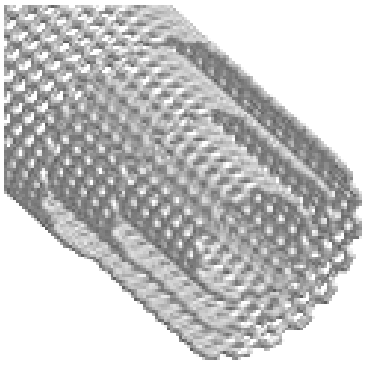

Figure1.4: *A multiwall carbon nanotube.*[48]

Since their discovery, CNTs have been regarded as potential molecular wires.[49] They readily accept electrons which can then be transported along the axis, with the conductivity varying between semi-conducting and conducting.[47] Electrical conduction seems to occur through well separated, discrete electron states that are coherent over long distances.[49] The conductivity of an individual CNT is dependent on the geometry of the tube and its diameter, with the conductivity of a MWNT solely dependant on its outermost shell.[50] The three possible wrapping angles of a CNT are shown in Figure 1.5, structure (a) is the armchair configuration while structures (b) and (c) are the zigzag and chiral forms respectively.

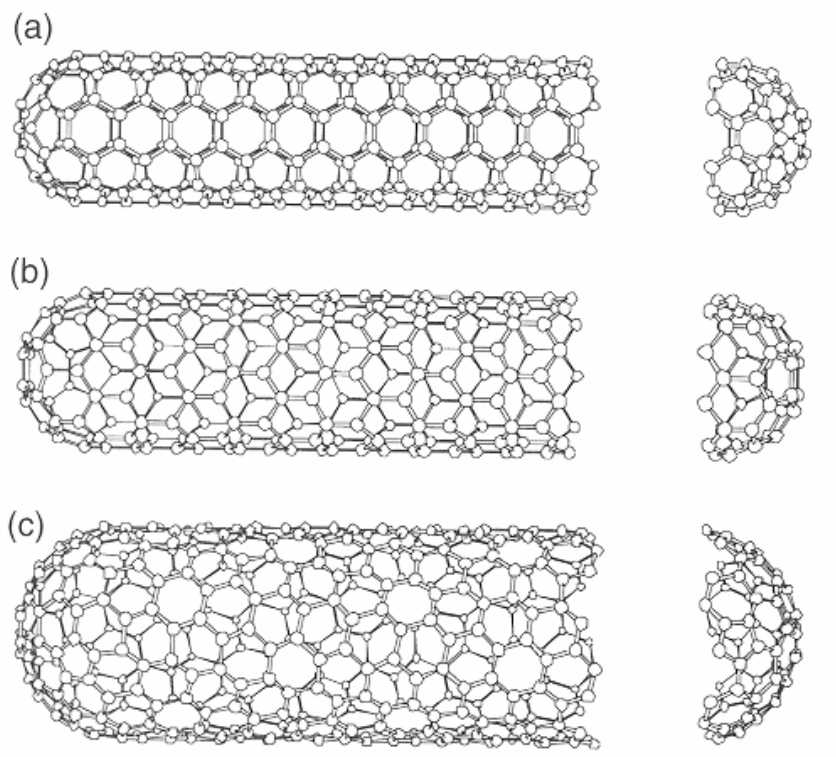

Figure 1.5: *Schematic models for; (a) armchair, (b) zigzag (c) chiral single-wall carbon nanotubes.*[48]

A major disadvantage of CNTs is a lack of synthetic control. At present there is no reliable method for the synthesis of purely conducting or semi-conducting CNT of a given size or length. Another hindrance is the formation of defects, such as pentagon-heptagon irregularities (elbow connections), which allow the charge to flow in only one direction.[28]

1.2.3 Wires with redox active termini

When termini possessing different redox states are present at each end of a wire, an odd electron species or mixed-valence (MV) compound can be generated electrochemically. Although purely organic mixed-valence compounds are known,[51] the best studied examples are dinuclear transition metal complexes.[30] The incorporation of transition metals at either end of a conjugated organic compound enables the electronic properties of the molecule to be fine tuned. The metal centres act as donor and acceptor sites for the electron transfer (ET) across the bridge. To

allow ET and therefore ensure delocalisation from one metal to the other, there must be good overlap between the d-orbitals of the metal and the π-orbitals of the bridging fragment.

There are two major advantages of using bimetallic complexes of the general form $L_nM{-}(C)_x{-}M'L'_n$ (where M is a redox active metal, L is the associated ligands of the metal and C is a conjugated carbon bridge) as molecular wires. Firstly, these complexes are redox active enabling the conductivity of the wire to be tested. Secondly, the ligands which surround the metal centre provide a site onto which other substituents may be attached allowing fabrication into a functional system.

A range of bridging ligands, including polyenes, polyynes and polyphenylenes have been investigated for their ET ability between two redox metals. However, the pioneering work in this field was carried out on the Creutz-Taube ion (Figure 1.6) in the late sixties.[52,53] The ion has an overall 5+ charge, with one ruthenium formally in the 2+ oxidation state and the other in the 3+ state. The interpretation of the electronic spectra of this MV compound has lead to a greater understanding of the electron transfer process.

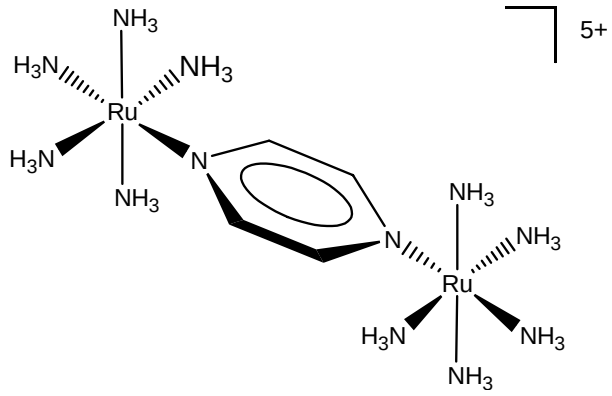

Figure 1.6: *The Creutz-Taube ion.*

Redox-active molecular wires work on the principle that an unpaired electron or hole can be transferred along the entire length of the molecule. A free electron is obtained by either the loss of an electron from the higest occupied molecular orbital (HOMO) or the addition of an electron to the lowest unoccupied molecular orbital (LUMO) of the neutral complex. This one-electron oxidation or reduction results in the

formation of a mixed-valent species in which the two metal termini are in different oxidation states. The free electron may exchange between and reside on either metal termini (Figure 1.7).

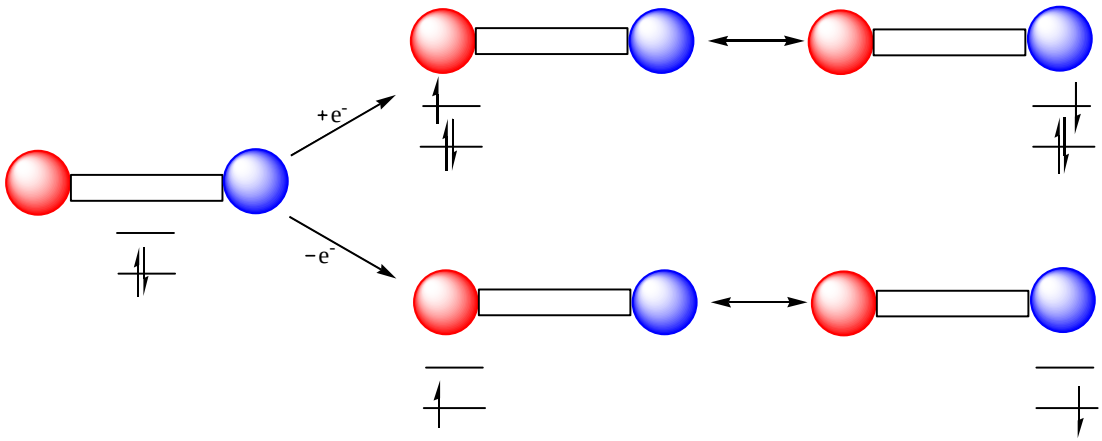

Figure 1.7: *Schematic representation of electron transfer in a redox-active molecular wire.*

The extent of electronic communcation between two metal centres in a molecular wire can be described by the Robin-Day classification of mixed-valence compounds.[54] Consider a symmetrical homometallic complex, $L_nM\text{-}(X)_x\text{-}ML_n$, in which each of the two identical redox-active centres, connected by a bridging ligand, are able to generate one-electron products by suitable redox processes. Under the Robin-Day classification there are three scenarios:

(i) The bridging ligand acts as an insulator between the two redox centres, and the charge is totally localised on one of the redox centres allowing for unique properties of each of the redox sites to be observed, with no electronic interaction between them. These complexes, which show no electronic interaction, are classified as Class I.

(ii) The metal terminii interact weakly through the bridging ligand. In this state, charge is neither totally localised nor is it totally delocalised and consequently at least one spectroscopic method is able to distinguish

between the two redox centres. Such a compound is classified as a Class II material.

(iii) There are strong interactions between the two metal centres, with the bridging ligand acting as a conductor. Such a compound may be classified as a Class III material. Oxidation of these complexes occurs in a stepwise manner, one electron at a time. In this case the charge is completely delocalised over the entire length of the molecule and no spectroscopic method can distinguish between the two redox centres. In these cases, it is perhaps misleading to use the term ‘mixed-valence’.

Recently a fourth class, between Class II and III, has been proposed.[55] Class II-III complexes exhibit an inter-valence charge transfer that is not solvent dependent, which indicates that it belongs in Class III. However it is also possible to assume there is some localisation of charge from some spectroscopic properties, such as IR and low temperature X-ray crystallography, which indicates a Class II complex. One such complex is the Creutz-Taube ion, although it is commonly assumed to be fully delocalised.[55]

1.3 Evaluation of Potential Molecular Wires

Within the molecular regime, the search for wire-like properties is related directly to the study of intramolecular electron transfer or transport (ET). At present the three techniques that are commonly used to measure intramolecular ET are; direct measurement, cyclic voltammetry and near-infrared (NIR) absorption spectroscopy. In many cases only one of these methods will facilitate the evaluation of the electronic properties of a given compound.

1.3.1 Direct Measurement

The direct measurement of electron flow requires that a single molecule spans two electrodes. The presence of a functional group, for instance a thioacetate group, at the terminus of a molecular wire provides a site at which the wire may be attached to a metal surface, typically gold.[56,57] This has been achieved by hydrolysing the thioacetate to a gold-surface thereby forming gold-thiolates. Molecular wires have been inserted into a layer of insulating molecules attached to a gold surface using this methodology (Figure 1.8).[28] The tiny tip of a scanning tunnelling microscope (STM) may then be precisely manoeuvred along the surface of the monolayer, interacting with each individual molecule chemisorbed onto the metal.[28] This contact can be used to probe the elctrochemical properties of the single molecule as when the STM tip is in contact the current can to flow freely between the STM probe and the gold electrode via the molecule.

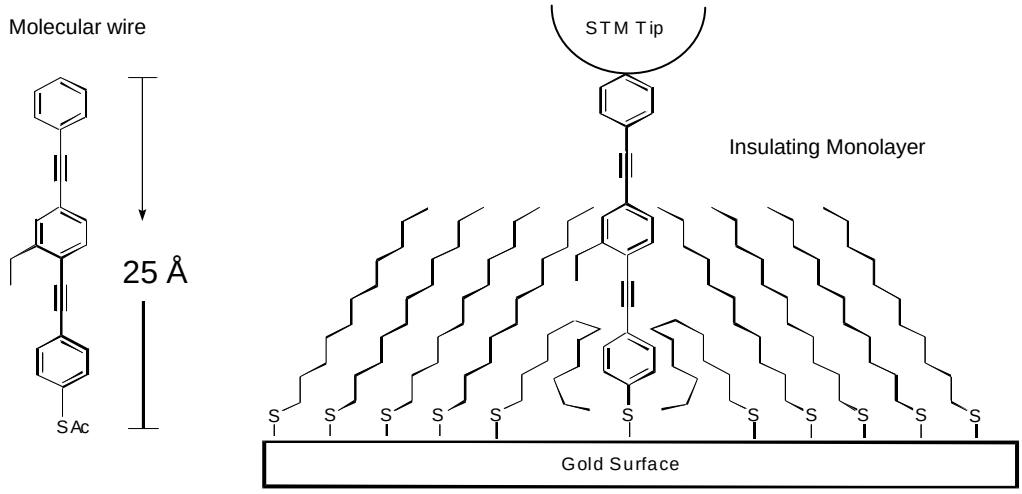

Figure 1.8: *The direct measurement of a molecular wire with an STM tip.*[28]

The direct measurement of current through a single molecule has also been achieved using molecules which may be connected to two electrodes by chemical bonds. The first experiment of this type was conducted in 1996 using a benzene-1,4-dithiol.[41] Dithiol molecules were self-assembled onto the two gold electrodes of a mechanically-controlled break junction. The electrodes were then slowly moved together in picometer increments until a single molecule bridged the gap between the two electrodes (Figure 1.9). This formed a single molecule metal-molecule-metal junction and enabled a stable conductance to be recorded. Since this initial experiment, several similar molecules have been examined using this method.[35,58]

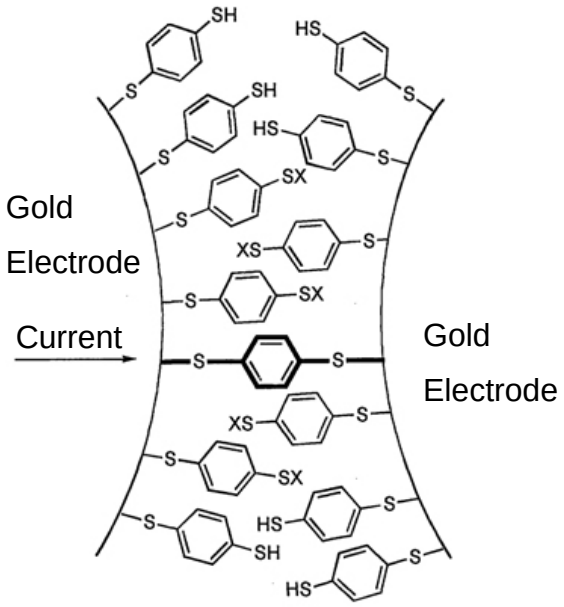

Figure 1.9: *A benzene-1,4-dithiolate self-assembled monolayer between two gold electrodes within a mechanically-controlled break junction. Where X = H or Au.*[41]

Direct measurement provides an ideal means to evaluate the electronic properties of a single molecule with potential as a molecular wire. However the two methods described above impose the prerequisites that the wire has appropriate terminals to interface with the macroscopic conductors and that the molecule itself is long enough to span the nanojunction.[30] As such these direct measurement methods are not suitable for all moleclar wire candidate molecules.

1.3.2 NIR Spectroscopy

The NIR spectral region of MV complexes contain a intervalence charge transfer (ICT) band.[30,55] This band corresponds to the optically-induced electron transfer between the two termini and thus is only observed in class II and III complexes. From the spectral characteristics of the ICT absorption, the electronic delocalisation parameter (V_{ab}) of the complex may be evaluated. The V_{ab} value is dependant on the overlap between the electronic wave function of the donor and the acceptor groups in the transition state.

These ET reactions are described by potential energy curves (Figure 1.10) where the potential energy of the complete system is plotted as a function of a reaction coordinate (Q) defining the changes in both the inner and outer coordination spheres.[30] Two such zero order curves can be constructed, corresponding to the two limiting structures of a MV complex. The reorganisation energy (λ) of a site when it is oxidised or reduced is given by the lateral displacement of the curves in the absence of electronic interaction (Figure 1.10a). However with strongly interacting sites a mixing of the wave functions results in a change in the overall energies (Figure 1.10b).

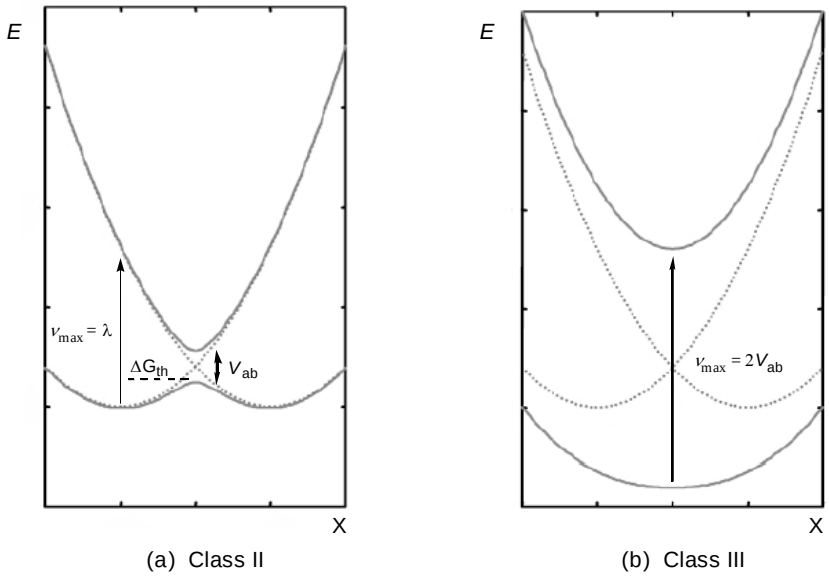

Figure 1.10: *Potential energy curves for (a) Class II and (b) Class III MV complexes. Showing the reorganisation parameter (λ), the electronic coupling parameter (V_{ab}) and the energy of the ICT transition (ν_{max}).*[30]

For Class III complexes, where the redox centres are strongly coupled, V_{ab} is directly related to the energy of the ICT band, as described by Equation 1.1.[30]

$$V_{ab} = \frac{\nu_{max}}{2} \qquad \textit{Equation 1.1}$$

While V_{ab} for class II complexes, where the redox sites are only weakly coupled, can be calculated from Equation 1.2, where ε is the molar extinction coefficient ($M^{-1}cm^{-1}$), ν_{max} is the energy of the ICT band (cm^{-1}), $\Delta\nu_{1/2}$ is the half-height width of the ICT band and $R_{MM'}$ is the effective electron transfer distance, which is often assumed to be equal to the geometric M-M' distance.[30]

$$V_{ab} = 2.05 \times 10^{-2} \frac{\sqrt{(\varepsilon\, \nu_{max}\, \Delta\nu_{1/2})}}{R_{MM'}} \qquad \textit{Equation 1.2}$$

Calculation of the theoretical band-width $(\Delta\nu_{1/2})_{theo}$ from Equation 1.3, enables compounds to be identified as either Class II or Class III. With Class II compounds having $(\Delta\nu_{1/2})_{theo}$ in either good agreement with or less than those derived from the experimentally observed ICT bands.[30]

$$(\Delta\nu_{1/2})_{theo} = \sqrt{2310\nu_{max}} \qquad \textit{Equation 1.3}$$

Once V_{ab} has been determined comparisons with related compounds can be made and conclusions on the ability of the bridging ligand to facilitate ET can then be drawn. However in order for a complex to be studied by NIR spectroscopy the MV species must be stable enough to be isolated.

1.3.3 Cyclic Voltammetry

One of the most widely used electrochemical techniques for evaluating the electronic interactions in redox-active complexes is cyclic voltammetry. The cyclic voltammetry experiment consists of a three-electrode system which analyses a solution of the potential molecular wire. The analyte is oxidised or reduced at the

working electrode. The current then flows from the working electrode to a counter electrode, while the reference electrode controls the relative potential.

During the experiment a triangular voltage is applied, as shown in Figure 1.11, to the working electrode which is stationary in an unstirred solution. Initially a forward scan is performed by increasing the potential linearly from E_{start} to E_{switch} (*switching potential*). The current response, as a function of the applied potential, of the forward scan is influenced by the concentration and nature of the analyte as well as the scan rate. A reverse scan is then carried out by decreasing the potential back to E_{end} to complete the cycle. This reverse scan provides additional information regarding the stability of the oxidised or reduced state of the analyte formed at the electrode surface.

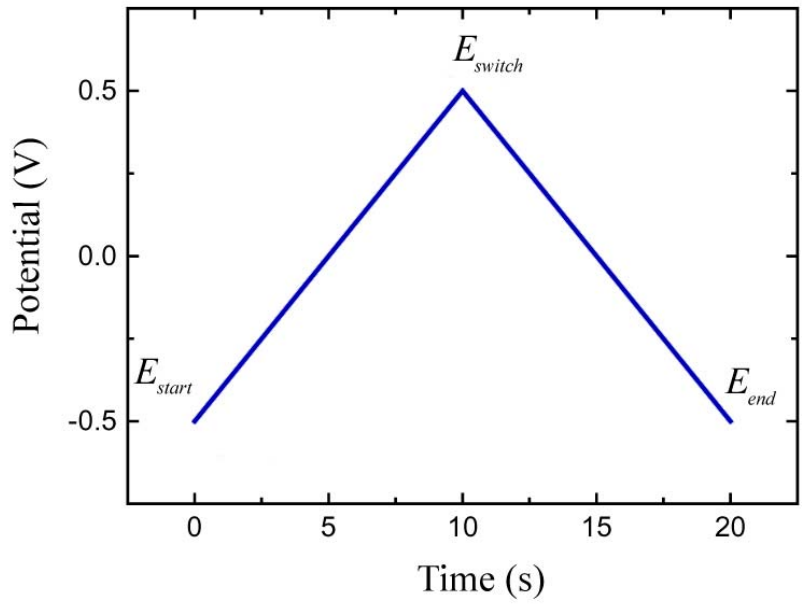

Figure 1.11: *Applied waveform used in a cyclic voltammetry experiment.*

A theoretical trace of a fully reversible one-electron process is shown in Figure 1.12. A variety of parameters can be extracted from the trace, such as the anodic and cathodic peak currents, i_a and i_c, respectively, the half-wave potential ($E_{½}$), anodic potential (E_a) and cathodic potential (E_c). In an ideal system under standard conditions, $E_{½}$ lies half-way between the oxidation (E_a) and reduction (E_c) peaks, and can be calculated from Equation 1.4.

$$E_{½} = \left|E_a - E_c\right| \qquad \textit{Equation 1.4}$$

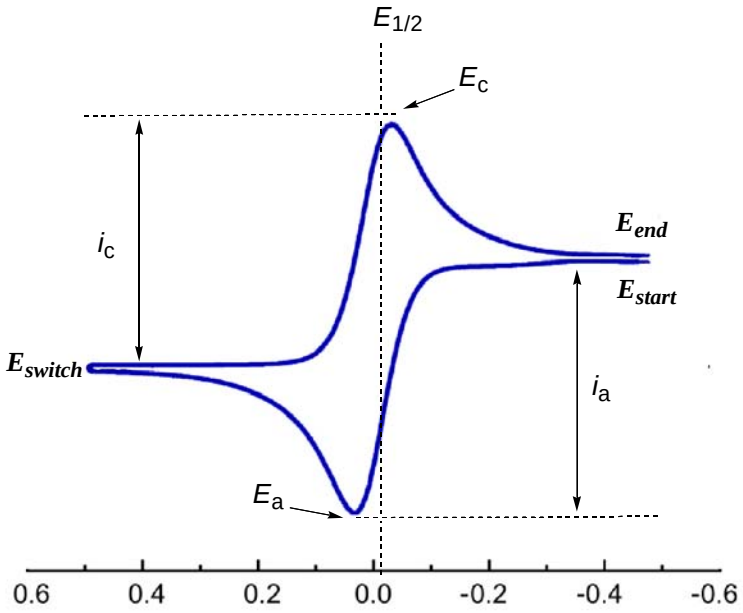

Figure 1.12: *A fully reversible one-electron process displaying various parameters that can be extracted from the trace.*

The reversibility of a redox process can be evaluated from the peak currents. For a fully reversible system the diffusion coefficients are the same for the bulk analyte and the oxidised or reduced forms, thus the ratio between the anodic and cathodic peaks will be equal ($i_a/i_c = 1$). In addition a plot of the peak current versus the square root of the scan rate will be linear for a fully reversible system.

For a symmetric molecular wire with two redox-active end-groups, the potential difference (ΔE) between the redox waves of two redox centres is commonly used to evaluate the extent of electronic interaction between two identical redox-active sites across a bridging ligand.[30,59,60] There are two extreme cases, if there is no interaction between the two redox centres (Class I) and the spacer acts as an insulator, then the two redox centres will be oxidised or reduced at almost identical potentials, differing only by a small statistical factor [ΔE = 2(RT/F)ln2]. In this case, the cyclic voltammogram will show a single redox process, with the height of the wave corresponding to a two-electron event (Figure 1.13a).[61]

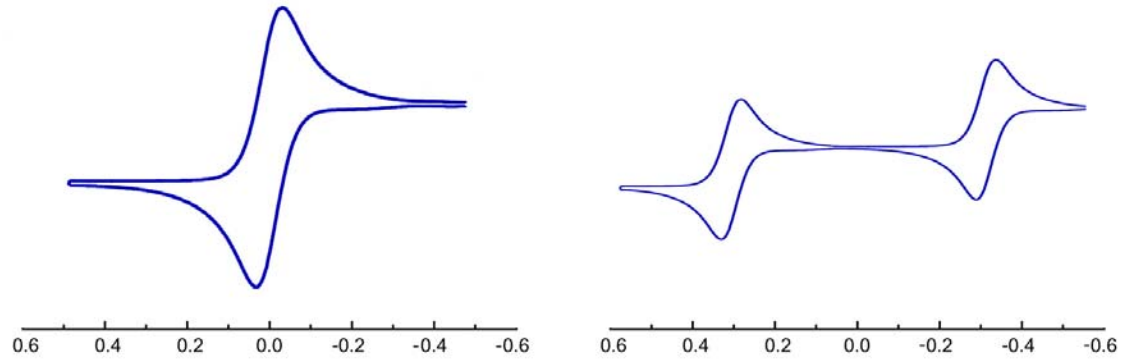

Figure 1.13 *Cyclic voltammogram of (a) Class I and (b) Class III binuclear systems.*

Conversely, if there are strong interactions between the two metal centres (Class III), and the spacer will act as a conductor and the cyclic voltammogram will show two one-electron redox waves (Figure 1.13b). The first oxidation wave represents the formation of the mono-oxidised species, while the second involves the formation of the doubly oxidised state. For symmetric Class III compounds, ΔE is usually greater than 0.2 V.[30]

Electron transfer between two molecules of the same complex in different oxidation states to give a single species with an intermediate oxidation state is known as the comproportionation reaction. The comproportionation constant K_c is the equilibrium constant for the comproportionation reaction (Scheme 1.1) and can be calculated from ΔE between two waves using Equation 1.5 which can be simplified to equation 1.6. Thus, the K_c values are an indication of the stability of an oxidised species. As the stability of an oxidised species decreases, the K_c value will decrease.

$$\text{Ox-Ox} + \text{Red-Red} \overset{K_c}{\rightleftharpoons} 2\ \text{Ox-Red}$$

Scheme 1.1

$$K_c = \frac{[\text{Ox - Red}]^2}{[\text{Ox - Ox}][\text{Red - Red}]} = \exp\left[\frac{\Delta E \times \text{F}}{\text{RT}}\right] \qquad \textit{Equation 1.5}$$

$$K_c = \exp(\Delta E / 0.0257) \qquad \textit{Equation 1.6}$$

While ΔE is often used as a measure of the degree of electronic interaction between two metal centres, it is also affected by other factors such as solvent,[59,62] counter ions,[59,63,64] and structural rearrangement upon oxidation.[65] Therefore, care needs to be taken when describing the significance of ΔE and comparisons can only be made within related systems measured under similar experimental conditions.

For example, the cyclic voltammogram of the polyalkynyl complex $\{Cp(PPh_3)_2Ru\}(C{\equiv}C)_2\{Ru(PPh_3)_2Cp\}$ shows four one-electron oxidation waves. The first three waves are fully reversible while the fourth is irreversible. The large ΔE values along with the presence of four distinct one-electron waves indicate that there are strong electronic interactions between the two runthenium centres.

The nature of the carbon chain in the four oxidation states, from the neutral to the 4^+ state, has also been investigated by theoretical calculations, infrared spectroscopy and spectroelectrochemistry.[66] The findings suggest that the complex may be represented by all three elementary valence structures (**1f-h**) depending on the oxidation state (Figure 1.14).

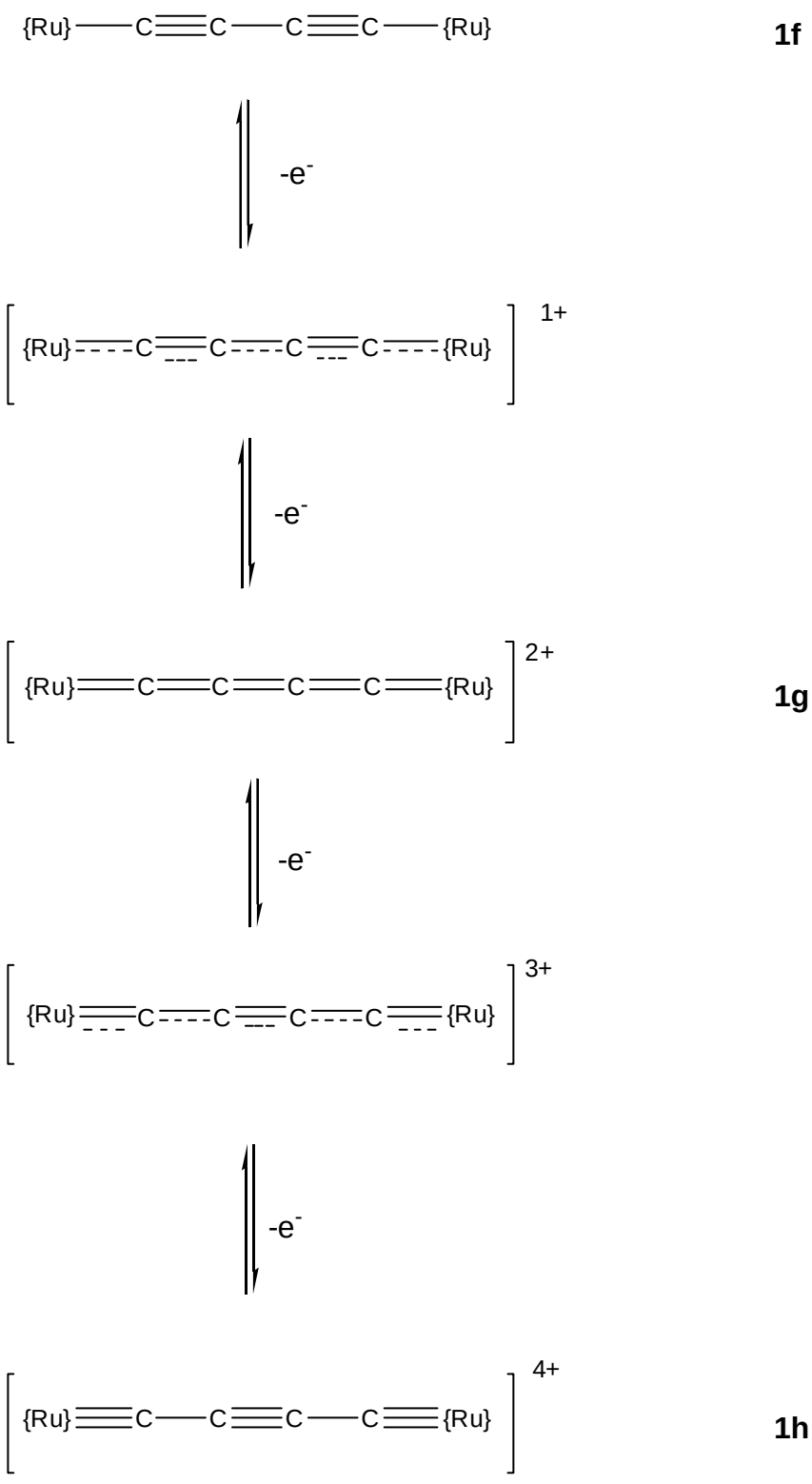

Figure 1.14: *Stepwise oxidation of the neutral complex {Cp(PPh$_3$)$_2$Ru}$_2$(C≡C)$_2$.*

Theoretical studies conducted on the simplified complex $\{Cp(PH_3)_2Ru\}(C\equiv C)_2\{Ru(PH_3)_2Cp\}$ have provided further insight into the electronic structure and properties of the oxidised complexes. To save on calculation time, PH_3 was used rather than the PPh_3 group, however it is believed that this should have little effect on the electronic structure of the chain itself.[66] A simple molecular orbital diagram (Figure 1.15) assists in the understanding of the bonding between the C_4 chain and the two ruthenium centres.

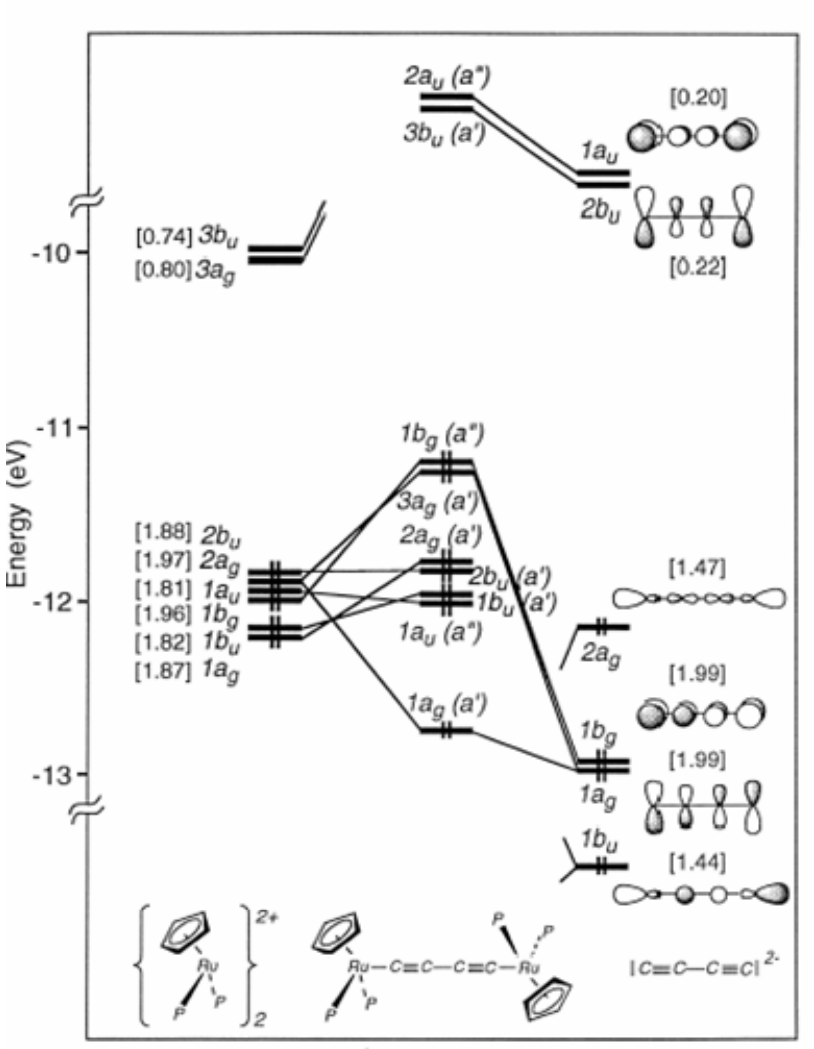

Figure 1.15: *Molecular orbital diagram of* $\{Cp(PPh_3)_2Ru\}(C\equiv C)_2\{Ru(PPh_3)_2Cp\}$[66]

For the neutral species $\{Cp(PH_3)_2Ru\}(C\equiv C)_2\{Ru(PH_3)_2Cp\}$, there are strong σ-type interactions between the high-lying metallic frontier molecular orbitals $3b_u$ and $3a_g$ and the low-lying C_4 orbitals ($1b_u$ and $2a_g$). These orbitals contribute to an electron donation from the carbon chain towards the metal. The predominant metal-carbon π-

type interactions are actually filled/filled interactions between the occupied carbon and metal π orbitals. This has the overall effect of stabilising the C_4 orbitals, while the metallic orbitals are destabilised and become the HOMOs of the neutral system. The chain carbons thus make a large contribution to the HOMOs of $\{Cp(PH_3)_2Ru\}(C\equiv C)_2\{Ru(PH_3)_2Cp\}$ through π-type interactions and the HOMOs are delocalised over the entire chain. Thus any oxidation process involving these orbitals will not be entirely metal centred.

Since the HOMOs are antibonding between ruthenium and C(α) and between C(β) and C(β') but bonding between C(α) and C(β) the computational results suggest that the ruthenium-carbon and carbon-carbon single bonds will shorten while the carbon-carbon triple bonds will lengthen upon oxidation of $\{Cp(PH_3)_2Ru\}(C\equiv C)_2\{Ru(PH_3)_2Cp\}$. The HOMOs are also well separated from the LUMOs ($2a_u$ and $3b_u$), hence $\{Cp(PH_3)_2Ru\}(C\equiv C)_2\{Ru(PH_3)_2Cp\}$ should be able to lose four electrons, giving rise to five oxidation states as observed for $\{Cp(PPh_3)_2Ru\}(C\equiv C)_2\{Ru(PPh_3)_2Cp\}$.

1.4 Synthesis of Organometallic Molecular Wires

The synthesis of compounds containing two transition metals linked by even-numbered chains containing two to eight carbon atoms has been well developed over the last decade.[67,68] The synthetic methods used depend heavily on both the nature of the metal fragment and the length of the carbon chain.

1.4.1 Binuclear Complexes Containing C_2 Chains

A number of compounds with the general formula M_nC_2 have been known for many years, although limited structural studies are reported due to their extreme tendency to detonate with mechanical shock.[10] Transition metal derivatives are assigned to one of three possible electronic structures **1i**, **1j** or **1k,** the C_2 equivalents of **1f-h**, on the basis of the central C−C separation, which can be related to those in ethyne (1.21 Å), ethene (1.34 Å) or ethane (1.53 Å).

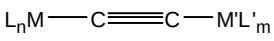

1i

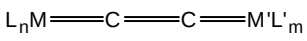

1j

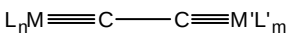

1k

Synthetic routes to C_2 complexes include;

(i) Reaction of alkali metal ethynyls with metal halides, alkyls or triflates.

(ii) Oxidative addition of dihaloethynes to metal substrates.

(iii) Metathesis of carbyne-metal complexes with alkynyl-metal complexes, or of complexes containing metal-metal triple bonds with 1,3-diynes.

1.4.1.1 Synthetic Strategy One

Complexes of the general formula $L_nM{=}C{=}CH_2$ are widely available and may be readily deprotonated, with an appropriate base, to produce the corresponding metal acetylide, $L_nMC{\equiv}CH$. Metal acetylides are considered to be nucleophilic due to the

increased back-donation from the metal centre and will readily react with electrophiles at the β carbon.

For example the diiron complex, $\{Cp^*(CO)_2Fe\}_2(\mu\text{-}C{\equiv}C)$ may be prepared from the reaction of $FeC{\equiv}CH(CO)_2Cp^*$ and $[Fe(CO)_2Cp^*(THF)]^+$ (Scheme 1.2).[69] The resulting diiron cation is then deprotonated using triethylamine to give the neutral complex in 57% yield.

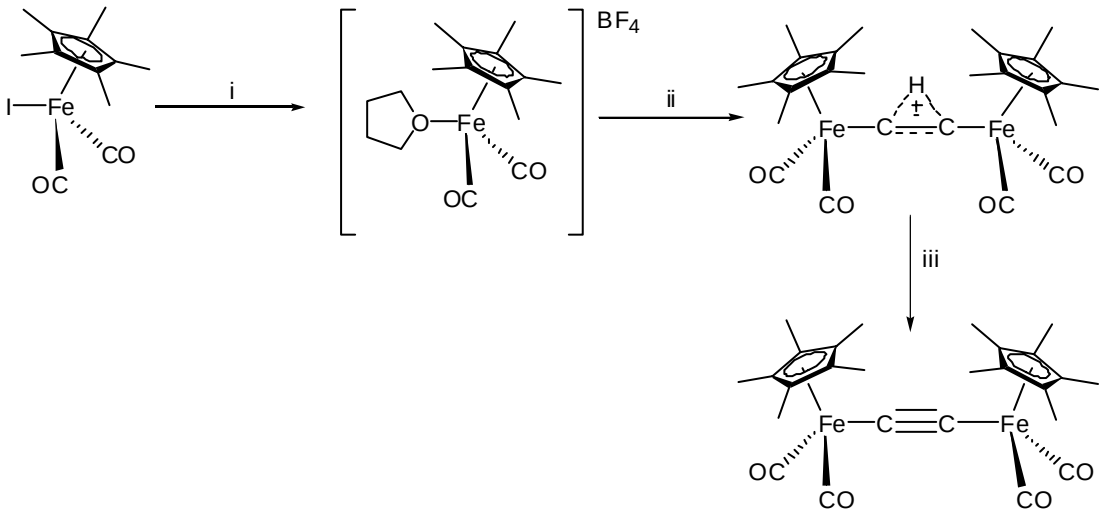

Reagents: i, $Ag[BF_4]$ / THF; ii, $FeC{\equiv}CH(CO)_2Cp^*$ / CH_2Cl_2; iii, NEt_3 / THF.

Scheme 1.2

The ruthenium ethyndiyl $\{Ru(dppe)Cp\}_2(C{\equiv}C)$ has also been prepared via a similar synthetic route. Reacting the vinylidene complex $[Ru(=C=CH_2)(dppe)Cp][PF_6]$ with two equivalents of butyllithium afforded the lithio derivative which could be treated *in situ* with $[Ru(THF)(dppe)Cp]^+$ to give the ethyndiyl $\{Ru(dppe)Cp\}_2(C{\equiv}C)$.[70]

1.4.1.2 Synthetic Strategy Two

Dihaloethynes are useful C_2-building blocks and their potential as $[C{\equiv}C]^{2+}$ equivalents has been exploited. The reaction of $IC{\equiv}CI$ with two equivalents the metal carbonyl anion $[Mn(CO)_5]^-$ gave $\{Mn(CO)_5\}_2(C{\equiv}C)$ in 15% yield (Scheme 1.3).[71] Ethynediyls have also been obtained from the reactions of $ClC{\equiv}CCl$ with

$[M(CO)_3Cp]^-$ (M = Cr, W).[72] However reactions of this type often result in side reactions such as the formation of $MI(CO)_5$, thereby explaining poor yields and in the case of $[Re(CO)_5]^-$ a failure to aquire the ethyndiyl.[71]

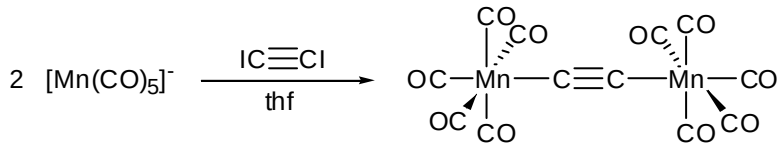

Scheme 1.3

The rhenium analogue has however been made via an alternate synthetic route in which pentacarbonyl(tetrafluoroborato)rhenium reacts with trimethyl(1-propynyl)stannane to give the ethynide bridged complex $[(OC)_5Re(C{\equiv}CH)Re(CO)_5]^+BF_4^-$. Reaction of this complex and sodium ethanolate gives the dirhenium C_2 complex $(OC)_5Re(C{\equiv}CH)Re(CO)_5$.[73]

1.4.1.3 Synthetic Strategy Three

Synthetic strategy three is somewhat unusual; nonetheless alkyne metathesis has been used to prepare a small number of ethyndiyl complexes. The ruthenium complexes $\{Ru(CO)_2Cp'\}_2(C{\equiv}C)$ (Cp' = Cp, Cp*) were obtained by metal-catalysed alkyne metathesis, where $Ru(C{\equiv}CMe)(CO)_2Cp$ reacts with $W_2(OCMe_3)_6$ to form the carbide complex $Cp(CO)_2RuC{\equiv}W(OCMe_3)_3$ with the loss of volatile $MeC{\equiv}CMe$. The carbide then reacts with a second equivalent of $Ru(C{\equiv}CMe)(CO)_2Cp$ to give $\{Ru(CO)_2Cp\}_2(C{\equiv}C)$ as a yellow precipitate in 60% yield (scheme 1.4).[72]

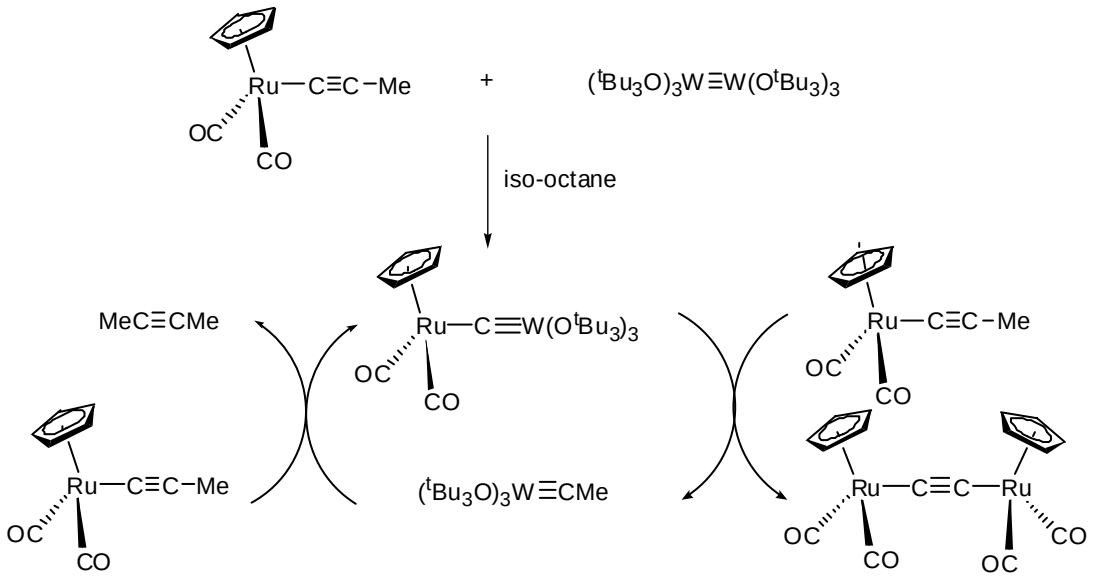

Scheme 1.4

1.4.2 Binuclear Complexes Containing C_4 Chains

Compounds that contain a bridging C_4 ligand are known as diyndiyl complexes. Generally these complexes are prepared by one of three synthetic strategies.

- *(i)* Homo-coupling between two metal ethynyl complexes;
- *(ii)* Coupling of an organic C_4 unit with two equivalents of a metal fragment;
- *(iii)* Coupling of a monometallic diynyl complex with a single equivalent of a metal fragment.

Outlined below are some literature examples demonstrating these strategies and the reaction conditions that have been used to prepare symmetrical diyndiyl complexes.

1.4.2.1 Synthetic Strategy One

Glaser oxidative coupling conditions [$Cu(OAc)_2$/pyridine/O_2] were used to prepare the rhenium diyndiyl complex $\{Re(NO)(PPh_3)Cp^*\}_2(C{\equiv}C)_2$ in 88% yield from the ethynyl complex $Re(C{\equiv}CH)(NO)(PPh_3)Cp^*$ (Scheme 1.5).[74] The tri(tolyl)phospine

analogue {Re(NO)[P(tol)$_3$]Cp*}$_2$(C≡C)$_2$ has also been prepared using Glaser oxidative coupling conditions.[75]

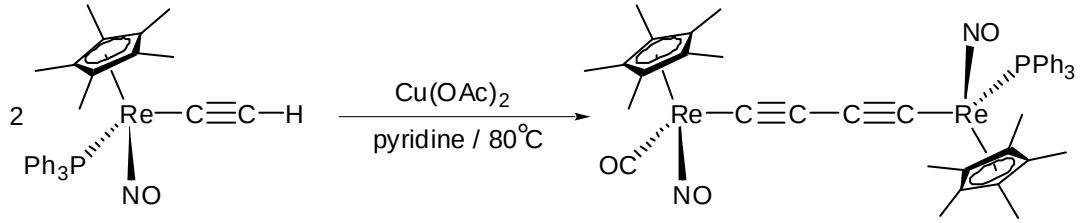

Scheme 1.5

Although Glaser coupling conditions afforded these rhenium diyndiyl complexes in excellent yield, these conditions are often too harsh for other complexes. Thus alternative conditions were used in the synthesis of the iron diyndiyl complex {Fe(dppe)Cp*}$_2$(C≡C)$_2$. Oxidation of the ethynyl complex, Fe(C≡CH)(dppe)Cp* with [FeCp$_2$][PF$_6$] generates, at low temperatures a 17-electron radical that undergoes a spontaneous carbon-carbon coupling reaction to afford an intermediate bis-vinylidene. Deprotonation of the bis-vinylidene affords the desired iron diyndiyl in 80% yield (Scheme 1.6).[76] More recently the ruthenium analogue {Ru(dppe)Cp*}$_2$(C≡C)$_2$ has been prepared by the same method.[70]

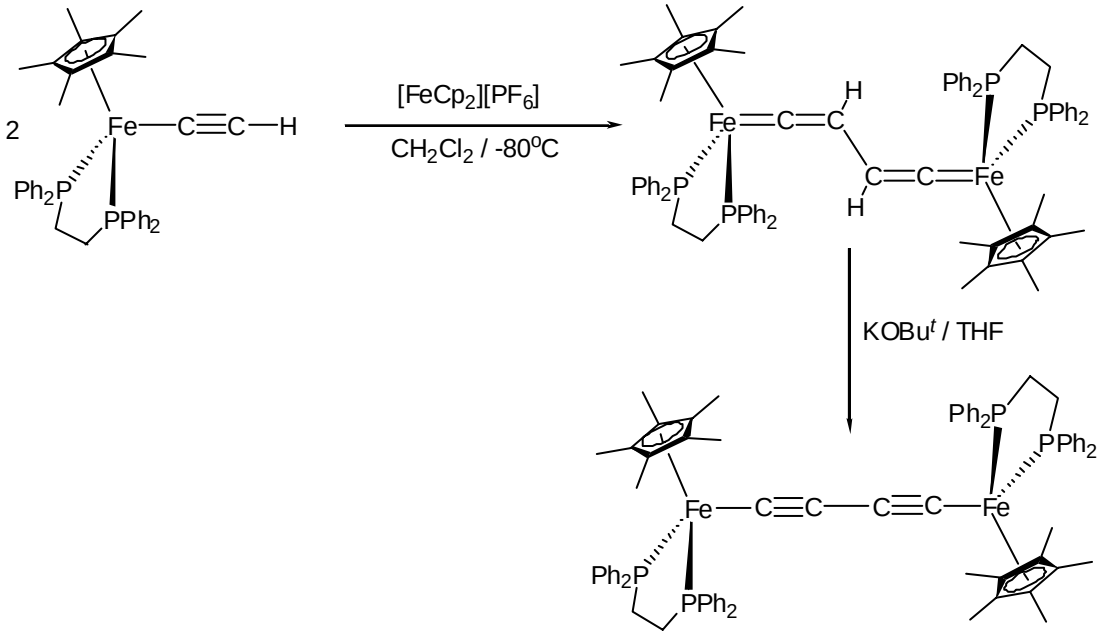

Scheme 1.6

1.4.2.2 Synthetic Strategy Two

The coupling of an organic C_4 unit with two equivalents a metal-ligand fragment is the most frequently used method to synthesise diyndyl complexes. The large number of suitable butadiynyl based starting materials available makes this method extremely versatile.

Butadiyne (HC≡CC≡CH) is the simplest and most reactive diyne molecule. This gaseous compound can be difficult to handle due to its tendency to polymerise and explosive behaviour in air. However butadiyne, prepared from the reaction of 1,4-chlorobut-2-yne with concentrated aqueous potassium hydroxide and trapped in a tetrahydrofuran (thf) solution,[77] has been used to synthesise a number of diyndiyl complexes.

The rhodium complex, $\{RhHCl(P^iPr_3)_2\}_2(C{\equiv}C)_2$, was prepared in 68% yield by the reaction of the $[RhCl(P^iPr_3)_2]_n$ with butadiyne in hexane at low temperatures (Scheme 1.7).[78] This method has also enabled the preparation of the iridium analogue $\{IrHCl(P^iPr_3)_2\}_2(C{\equiv}C)_2$ in 46% yield.[79]

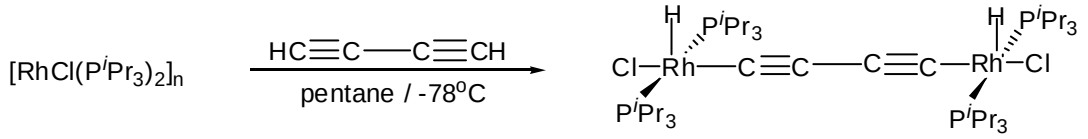

Scheme 1.7

The di-lithio derivative of butadiyne (LiC≡CC≡CLi) has also been used to prepare diyndiyl complexes. The reaction of this dianion with two equivalents of $FeCl(CO)_2Cp$ gives the corresponding diiron diyndyl complex in 40% yield with the elimination of lithium chloride (Scheme 1.8). [80]

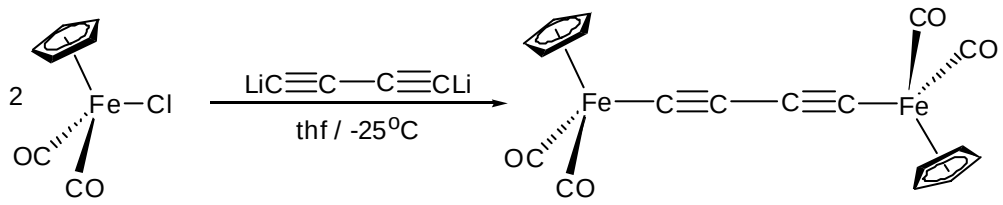

Scheme 1.8

A much more stable derivative of butadiyne is 1,4-bis(trimethylsilyl)butadiyne ($Me_3SiC{\equiv}CC{\equiv}CSiMe_3$). This compound can be prepared in large quantities by the oxidative coupling of $Me_3SiC{\equiv}CH$ under Hay coupling conditions ($CuCl/TMEDA/O_2$). This compound has also been used in the preparation of a number of diyndiyl complexes, such as $\{Ru(PPh_3)_2Cp\}_2(C{\equiv}C)_2$ which was prepared by the fluoride catalysed desilylation of 1,4-bis(trimethylsilyl)butadiyne in the presence of excess $RuCl(PPh_3)_2Cp$ (Scheme 1.9).[81]

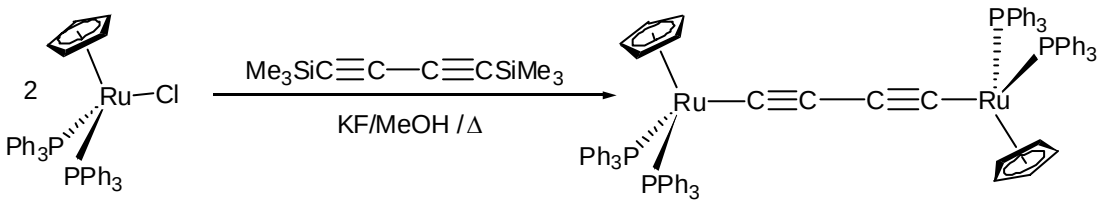

Scheme 1.9

1.4.2.3 Synthetic Strategy Three

The coupling of a monometallic diynyl complex with a single equivalent of a metal fragment has also been a useful method in the synthesis of diyndiyl complexes. For example the tungsten diyndiyyl complex $\{W(CO)_3Cp^*\}_2(C{\equiv}C)_2$ was obtained in excellent yield from the reaction of $[W(C{\equiv}CC{\equiv}CH)(CO)_3Cp^*]$ with $WCl(CO)_3Cp^*$ in the presence of copper iodide and diethylamine (Scheme 1.10).[82]

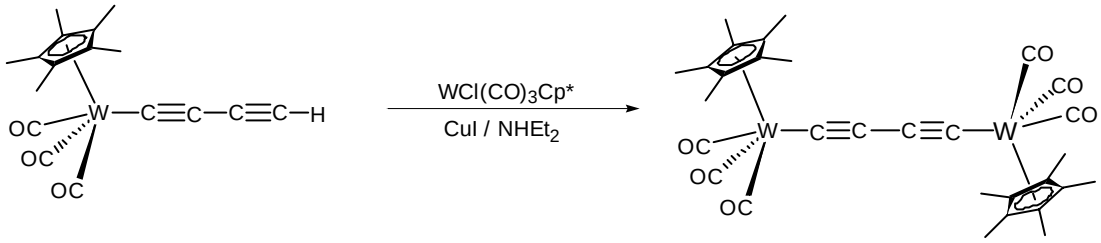

Scheme 1.10

The diiron complex $\{Fe(dippe)Cp^*\}_2(C{\equiv}C)_2$ has been prepared using alternative coupling conditions. The reaction of Fe(C≡CC≡CH)(dippe)Cp* with the iron chloride complex FeCl(dippe)Cp* in the presence of KPF_6 and $KOBu^t$ gave the diyndyl complex in 70% yield (Scheme 1.11).[83]

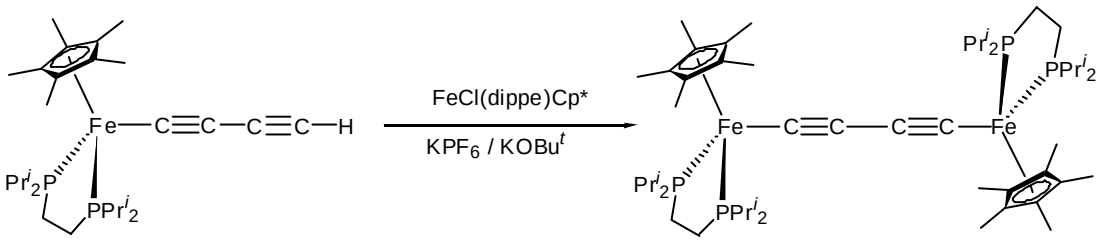

Scheme 1.11

1.4.3 Binuclear Complexes Containing C_6 and C_8 Chains

Extension of the general synthetic methods outlined for the C_2 and C_4 complexes has enabled the preparation of hexatriyndiyl (C_6) and octatetrayndiyl (C_8) complexes. Hexatriyndiyl complexes are generally prepared by coupling a preformed C_6 unit with two equivalents of a metal-halide. Octatetrayndiyl complexes may be prepared by similarly using a preformed C_8 unit. Thus treatment of the ruthenium-chloride precursor, RuCl(dppe)Cp* with half an equivalent of $Me_3Si(C{\equiv}C)_nSiMe_3$ (n = 3, 4) in methanol in the presence of the desilylating agent potassium fluoride gave $\{Ru(dppe)Cp^*\}_2(C{\equiv}C)_n$ in 57 and 89% yield respectively (Scheme 1.12).[70] The analogous bis(triphenylphosphine) complexes $\{Ru(PPh_3)_2Cp\}_2(C{\equiv}C)_n$ (n = 3, 4) have also been prepared by this methodology.[81,84]

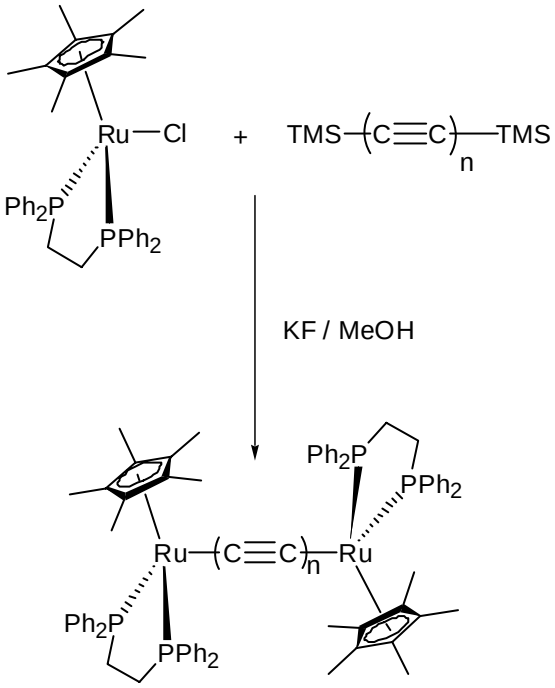

Scheme 1.12

Alternatively hexatriyndiyl complexes can be synthesised by the cross-coupling of diynyl and ethynyl complexes. For example the hexatriynediyl complex $\{Re(NO)(PPh_3)Cp^*\}_2(C{\equiv}C)_3$ was obtained in 44% yield from the oxidative coupling of a mixture of $Re(C{\equiv}CC{\equiv}CH)(NO)(PPh_3)Cp^*$ and $Re(C{\equiv}CH)(NO)(PPh_3)Cp^*$ using Glaser conditions. However the homocoupling diyndyl and ocaterayndiyl products were also formed in 14 and 15% yield respectively (scheme 1.13).[67]

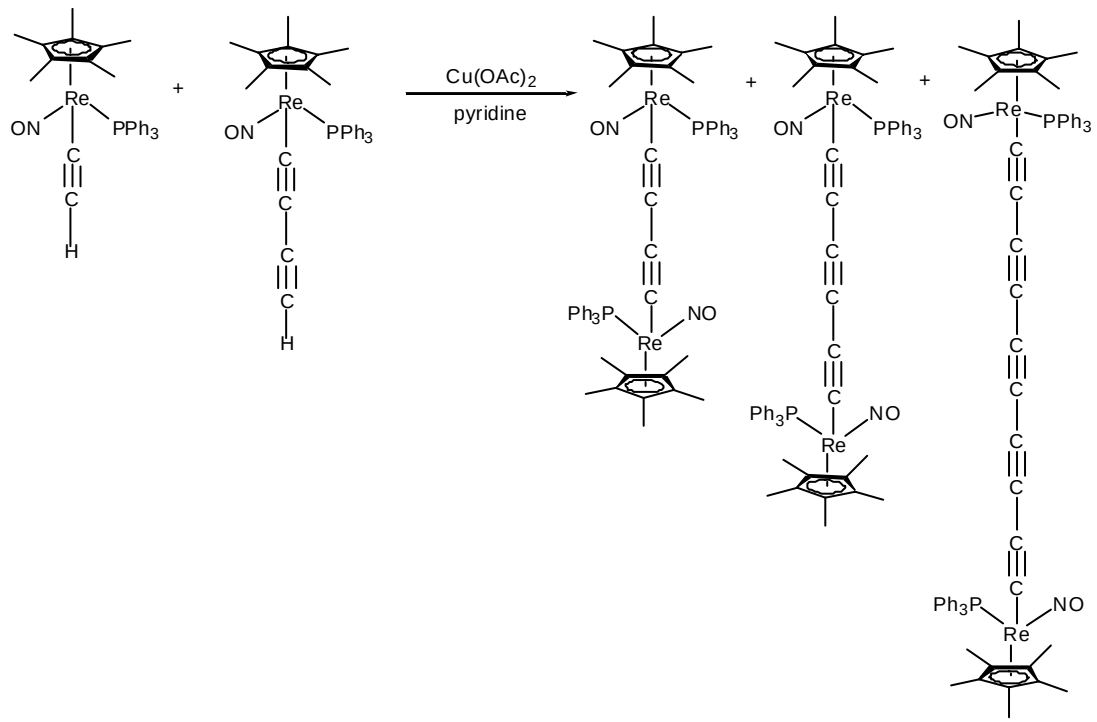

Scheme1.13

The majority of octatetrayndiyl complexes have been obtained by the oxidative coupling of diynyl complexes under either Glaser or Hay coupling conditions. Complexes featuring a C_8 chain bridging two metal centres prepared under Glaser conditions include $\{Re(NO)(PCy_3)Cp^*\}_2(C{\equiv}C)_4$,[75] $\{Fe(CO)_2Cp^*\}_2(C{\equiv}C)_4$[85] and $\{Re(NO)(PPh_2(CH_2)_6CH{=}CH_2)Cp^*\}_2(C{\equiv}C)_4$,[86] while examples of those prepared under Hay conditions include $\{M(CO)_3Cp\}_2(C{\equiv}C)_4$ (M = W, Mo)[87] and $\{Pt(p\text{-}tol_3P)_2(C_6F_5)\}_2(C{\equiv}C)_4$.[88]

1.5 Work Described within this Thesis

While the preparation of bimetallic complexes, ML_m-$(C\equiv C)_n$-ML_m, with $n < 5$ has been well developed, the preparation of extended ($n \geq 5$) and odd-membered analogues is rare. This thesis describes the development of the synthesis of some extended poly-yndiyl complexes containing the electron rich rutheninum end group Ru(dppe)Cp*. The electronic interactions between the two termini have been examined using cyclic voltammetry. Where possible, direct comparison has been made between these complexes and their shorter analogues.[70] The influence of chain length on the electronic interactions within this series is examined.

The synthesis of bimetallic complexes containing an odd-number of carbon atoms within the bridging chain is also explored. Complexes containing odd-numbered carbon chains require at least one metal-carbon multiple bond and thus an appropriate precursor is necessary in the synthesis. Here the requirement for a metal-carbon multiple bond in these complexes has been achieved using the Tp'$M(CO)_2$ group (Tp' = Tp, Tp*; M = Mo, W) to end-cap the carbon chain. Synthetic approaches include the $AuX(PR_3)$ elimination reaction between $Au(C\equiv CR)(PPh_3)$ and a halo-carbyne complexes[89] and metalla-desilylation between a trimethylsilyl-substituted alkyne and chlororuthenium precursors, such as RuCl(dppe)Cp' (Cp' = Cp, Cp*) in the presence of a base.[81] These compounds have been characterised by spectroscopic methods and where possible x-ray structure determination. Suitability as molecular wires has been established by electrochemical measurements which have been conducted and compared with analogous C_n chains containing the individual end-caps.

Cluster-capped carbon chains, formed by linking of the carbon-tricobalt carbonyl group $Co_3(\mu_3\text{-}C)(CO)_9$ with the Group 6 precursors by means of the $AuX(PR_3)$ elimination reactions are also examined. These compounds contain an even-number of carbons within the bridging chain.

The synthesis and electrochemistry of carbon chains containing 1,4-diethynylbenzene linkers has been explored. The efficient synthesis of bis-ruthenium

1,4-diethynyl benzene and 1,4-diethynyltetrafluorobenzene complexes is achieved by a fluoride-catalysed desilylation reaction. The palladium catalysed AuX((PR$_3$) elimination reaction is also examined as a convenient synthetic route to purely organic 1,4-bis(butadiynyl)benzene and 4-(butadiynyl)phenylethyne compounds.

A number of new gold containing cluster complexes are also discussed. The reaction of gold alkynyl complexes, M(C≡CR)AuPPh$_3$, with the activated ruthenium carbonyl, Ru$_3$(CO)$_{10}$(NCMe)$_2$ resulted in the formation of novel complexes containing a cluster-bound gold-phosphine group, with the alkynyl group bridging the Ru$_3$ cluster. The synthesis of mixed metal cluster complexes MoRu$_2$(C−CCH$_3$)(CO)$_8$Tp and MoFe$_2$(C−CCH$_3$)(CO)$_8$Tp through the reaction of the carbyne complex, {Tp(CO)$_2$Mo}≡CC≡CSiMe$_3$, with ruthenium and iron carbonyls is also explored.

Chapter 2

BIS-RUTHENIUM COMPLEXES WITH EXTENDED BRIDGING CARBON CHAINS

2.1 Introduction

It is generally accepted that C_{10} complexes represent the distinction between short and long sp carbon chains.[88] While many examples of shorter analogues exist, bimetallic complexes bridged by $(C{\equiv}C)_n$ chains, where $n \geq 5$, are rare. This is due to the progressive decrease in stability of these complexes and in particular, their mono-metallic congeners, as chain lengths increase. They therefore represent a greater synthetic challenge. At this time bimetallic complexes containing ten or more carbons in the chain are limited to rhenium,[67,90] iron,[91] platinum[88,92-94] and ruthenium[70,89,95] centres.

2.1.1 The Bis-Rhenium Series

The first systematic study of complexes containing long *sp* carbon chains spanning two metals was carried out by Gladysz and co-workers[90] who used the rhenium centre, $Re(NO)(PPh_3)Cp^*$, as an end-group. Di-rhenium complexes containing C_{10}, C_{12}, C_{16} and C_{20} bridging carbon chains were prepared by treating monometallic C_4 and C_6 terminal acetylides with butyllithium (^{n}BuLi) and copper iodide in thf to generate an alkynyl copper species (Scheme 2.1). In a variation of the Cadiot-Chodkiewicz reaction, this species reacts with $Br(C{\equiv}C)_nSiEt_3$ (where n = 1 or 2) to give the extended poly-ynyl complex in good yield which can be easily deprotected to the corresponding C_nH complex. Homo-coupling of these complexes using copper acetate in pyridine gives the di-rhenium species (Scheme 2.1).[90] Attempts to make analogues containing longer (n > 10) bridging carbon chains have been unsuccessful due to the decreasing stabilities of the poly-ynediyl species with hydrogen end-groups.[67]

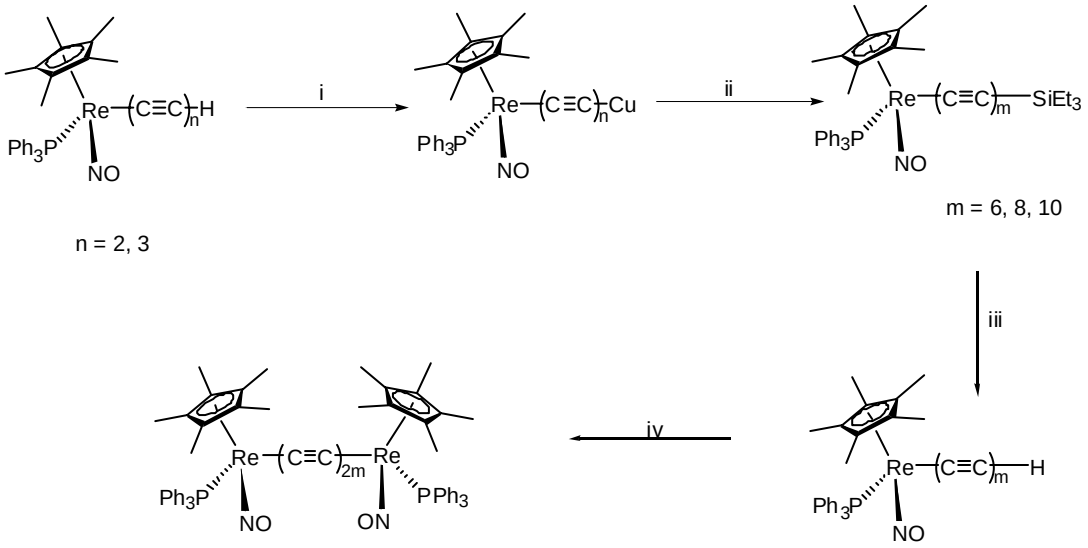

Reagents: i, ^{n}BuLi / CuI; ii, Br(C≡C)$_x$SiEt$_3$ / EtNH$_2$ (x = 1, 2); iii, wet ^{n}Bu$_4$N$^+$F$^-$; iv, Cu(OAc)$_2$ / pyridine.

Scheme 2.1

As the C_{10} analogue has an odd number of alkyne linkages, Gladysz and co-workers could not use a homo-coupling reaction for its preperation. However the cross-coupling of ReC_6H and ReC_4H enabled the preparation of the rhenium C_{10} complex in 9% yield.[67] The yield is low as the desired cross-coupling reaction competes with simultaneous homo-coupling reactions, which give the known C_{12} and C_8 bis-rhenium complexes.

These bis-rhenium complexes [M]-(C≡C)$_n$-[M], with n = 2, 3, 4, 5, 6, 8 and 10 have been reported.[67] Extension of the bridging carbon chain was found to significantly decrease the stabilities of these compounds with only the lower analogues being sufficiently stable to provide correct microanalyses. The C_{20} complex was not as stable and did not give an acceptable analysis and was characterised only by IR, Raman, UV/Vis and NMR spectroscopies. The cyclic voltammograms of lower analogues show two well-separated reversible oxidation waves indicating that there is strong electronic communication between the two rhenium centres. As the chain length increased the oxidation events become thermodynamically more difficult, with $\Delta E_{½}$ values approaching zero and a progressive decrease in reversibility suggesting a decrease in electronic communication. The C_{20} complex shows only a

single oxidation event, this is presumably a two-electron process and signifies the chain length at which the two rhenium centres begin to behave independently.[67]

2.1.2 The Bis-Platinum Series

Bis-platinum complexes, $\{PtC_6F_5(Ptol_3)_2\}_2(C{\equiv}C)_n$ [n = 2-14], have been similarly prepared by the homo-coupling of PtC_xH complexes which are generated *in situ* using tetrabutylammonium fluoride $[Bu^n{}_4N]F$ to desilylate PtC_xSi complexes. Using progressively lower temperatures, the bis-platinum C_{12}, C_{16} and C_{20} complexes were prepared in 70-88% yield (Scheme 2.2). The C_{24} complex could not be produced via this methodology, presumably because the rate of the decomposition of the intermediate $PtC_{12}H$ was too rapid.[94] However, $PtC_{12}Si$ and $PtC_{14}Si$ can be desilylated under the homo-coupling conditions to give the C_{24} and C_{28} complexes in 36% and 51% yield respectively (Scheme 2.3).[94] The C_{28} complex, $\{Pt(Ptol_3)_3\}_2(C{\equiv}C)_{14}$, is at present the longest carbon chain which bridges two metal centres. In the cyclic voltammograms of these complexes a single oxidation event was observed. With increased chain length the degree of reversibility ($i_{c/a}$, ΔE) of the oxidation event decreased dramatically and became less thermodynamically favourable.[88]

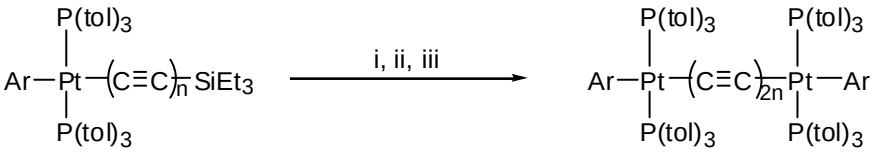

Reagents: i, wet $^nBu_4N^+F^-$ / acetone; ii, $ClSiMe_3$; iii, O_2 / cat. CuCl-TMEDA / acetone
Ar = C_6F_5, $P(tol)_3$; n = 3, 4, 5

Scheme 2.2

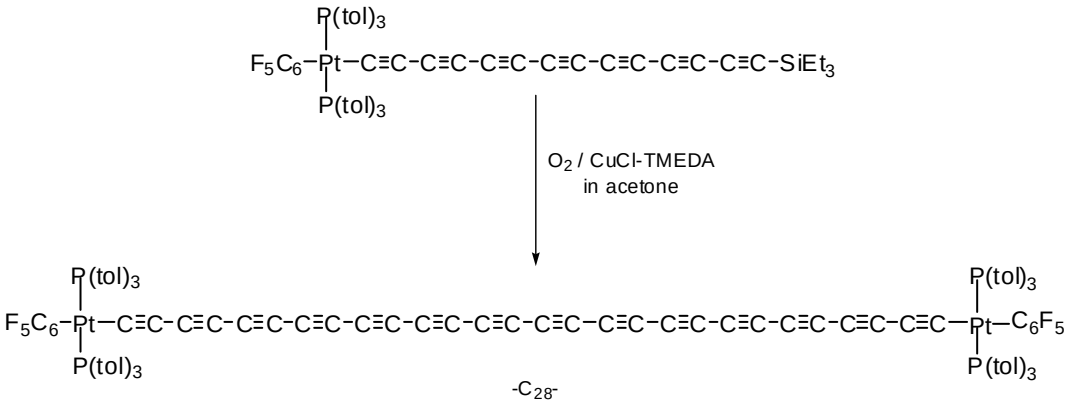

Scheme 2.3

2.1.3 Dodecahexaynediyldiiron

An iron C_{12} complex $\{Cp^*(CO)_2Fe\}_2(C{\equiv}C)_6$ has also been prepared in 73% yield by oxidative dimerisation of the monometallic hexatriynyl complex $\{Cp^*(CO)_2Fe\}(C{\equiv}C)_3H$ in the presence of a catalytic amount of CuCl·TMEDA complex (Scheme 2.4).[91] This complex was fully characterised, including molecular structure determination by X-ray crystallography. The two iron atoms, which are separated by *ca* 17.56Å, are spanned by a significantly bowed C_{12} carbon chain.[96]

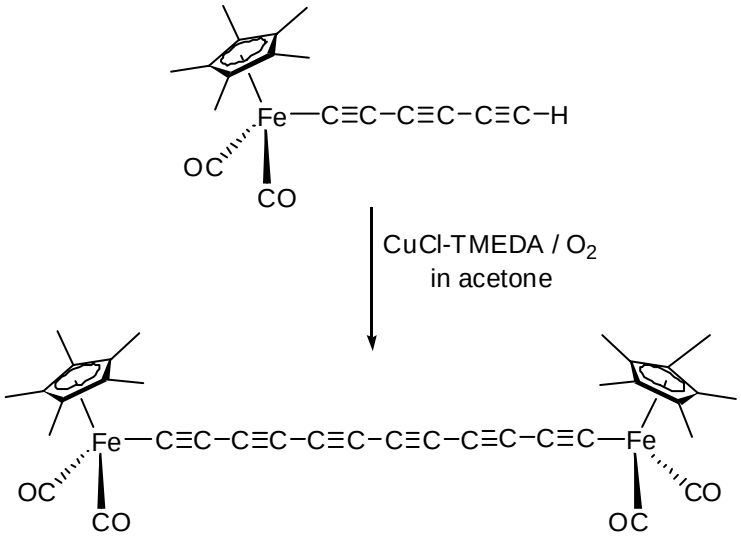

Scheme 2.4

2.1.4 Some Bis-Ruthenium Complexes

Recently, a C_{12} complex containing *trans*-$RuCl(dppe)_2$ as an end-group has been reported.[95] To prepare this complex the ruthenium acetylide complex, *trans*-$[RuCl(dppe)_2(C{\equiv}C)_3SiMe_3]$, was first obtained by reacting an excess of the lithium acetylide, $Li(C{\equiv}C)_3SiMe_3$ with the metal halide complex *cis*-$[RuCl_2(dppe)_2]$. The ruthenium acetylide can then be deprotected and homo-coupled under Eglinton conditions to give the bimetallic C_{12} complex (Scheme 2.5). Two, well separated, reversible oxidation waves were seen in the cyclic voltammogram of this C_{12} complex. Delocalisation of the charge on both metals was evidenced by the first oxidation being much easier than that of the alkynyl ruthenium $RuCl(dppe)_2(C{\equiv}C)_2SiMe_3$.[95]

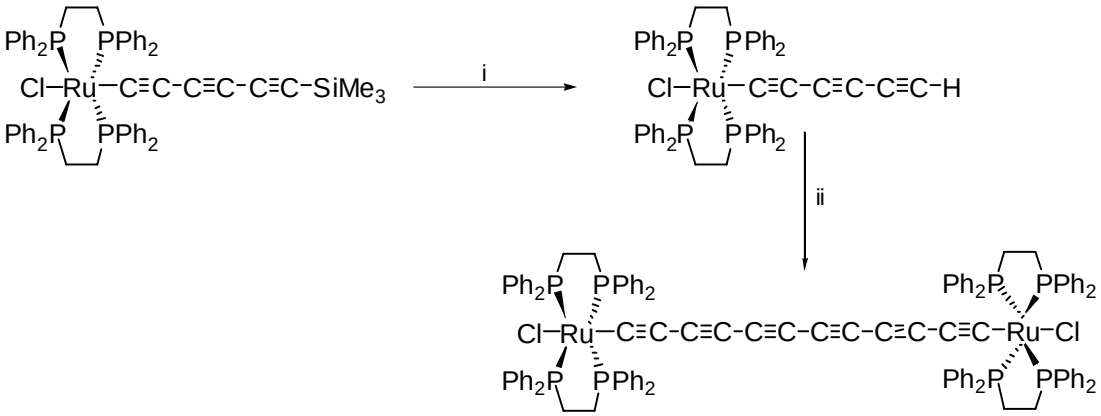

Reagents: i, $^{n}Bu_4NF$; ii, $Cu(OAc)_2$ / Pyridine / DBU

Scheme 2.5

More recently a procedure using a gold halide elimination reaction, which uses a gold poly-yne as the source of the $(C{\equiv}C)_n$ framework, has been used to prepare bis-ruthenium complexes with extended bridging carbon chains. This reaction shows great potential as an alternative method for the syntheses of complexes with extended carbons chains. There are three possible modes of chain extension via the gold halide elimination reaction (Figure 2.1).

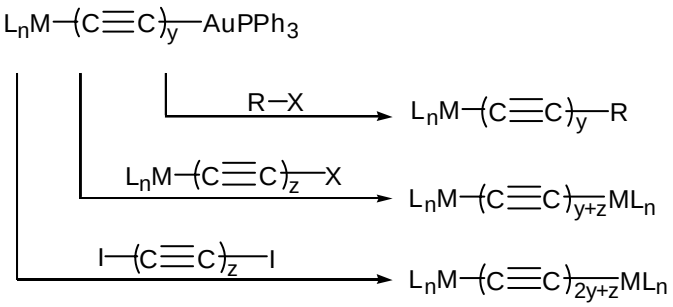

Figure 2.1: *The three modes of chain extension via the gold copling reaction.*

Treating the mixed ruthenium-gold diyndiyls Cp*(dppe)Ru(C≡C)$_n$AuPPh$_3$ [n = 2, 4] with half an equivalent of the diiodopoly-yne, I(C≡C)$_3$I, in the presence of Pd(PPh$_3$)$_4$ and CuI in a NEt$_3$/benzene mixture at 0°C gave {Ru(dppe)Cp*}$_2$(C≡C)$_m$ [m = 7, 11] in 36 and 12% yield respectively (Scheme 2.6). Coupling of the diiodohexatriyne with two Cp*(dppe)Ru(C≡C)$_2$AuPPh$_3$ fragments allowed access to a C$_{14}$ system, a chain length that had previously not been reported.

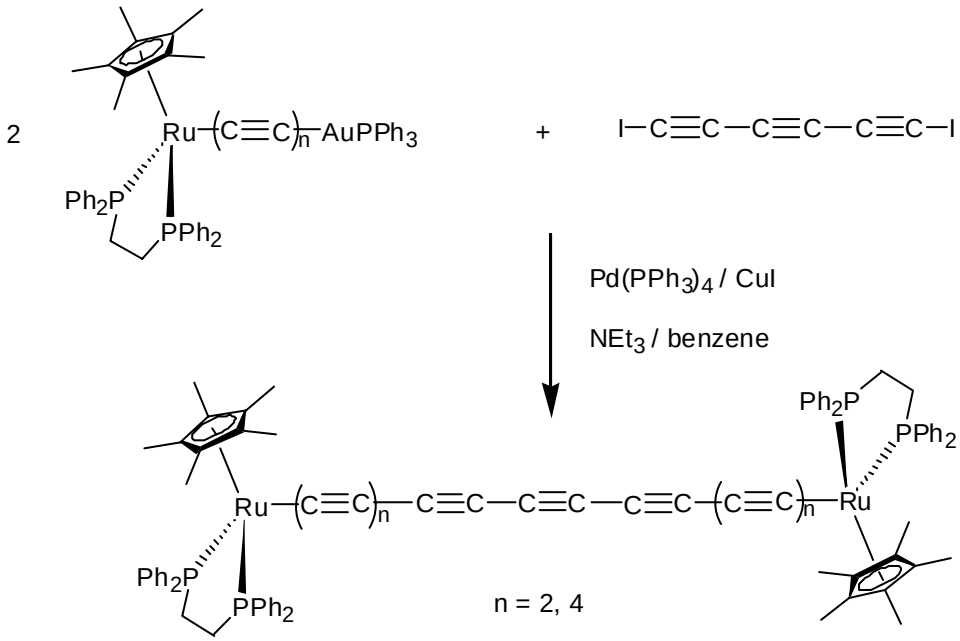

Scheme 2.6

Two independent crystals of the C$_{14}$ complex suitable for X-ray diffraction were grown from benzene/MeOH and benzene/hexane solvent mixtures. Both structures

were found to contain benzene molecules in the lattice, with the crystals grown from benzene/MeOH containing four benzene molecules and those grown from benzene/hexane containing seven benzene molecules within the unit cell. Both structures also contained a centre of inversion, with the two Cp* ligands arranged *transoid* to each other and revealed the expected pseudo-octahedral geometry around ruthenium. The alternating short and long C-C bonds confirmed the poly-yne nature of the chain carbons. An interesting feature in both structures is the slight sigmoidal-shape of the C_{14} chain. This distortion is due to the bending modes at the sp carbons that result from crystal packing forces.[88] Deviations from linearity at individual carbons vary between 1.3 and 6.2˚ with the sum of deviations totaling to 37.6˚ however the seperation of the two ruthenium centres [25.560(5) Å] is only 0.06 Å shorter than the sum of the individual ruthenium-carbon and carbon-carbon seperations.[89]

Very few bonds within poly-yne complexes are perfectly linear, however compounds with averge bond angles greater than or equal to 178.8˚ are regarded as 'essentially linear'.[96] Two common bending modes are represented in Figure 2.2. The first conformation features an inflection point at the midpoint of the chain resulting in an S-shape (**2a**). The second conformation is a symmetrically curved bow (**2b**), in which the sign of the slope changes at the midpoint of the chain. As the angles at the carbon atoms are cumulative, only small deviations from linearity are necessary to produce such effects.

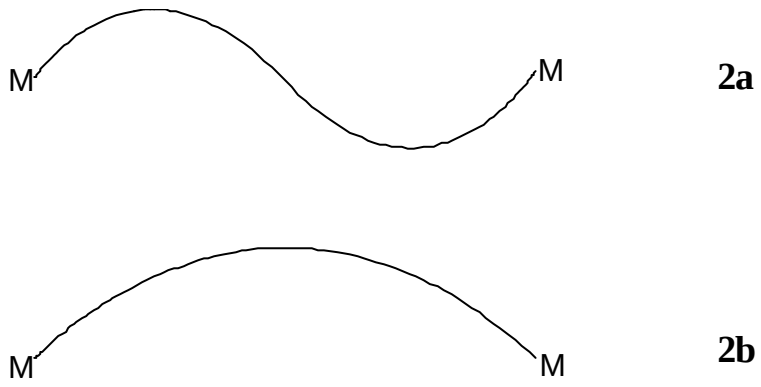

Figure 2.2: *Bending modes in poly-yndiyl complexes. (**2a**) sigmoidal and (**2b**) concave.*

Preparation of the C_{22} complex was hampered by the formation of an unidentified intensely purple coloured complex, which was the major product from the reaction. A bright purple complex also formed when the TMS-protected Cp*(dppe)Ru(C≡C)$_4$SiMe$_3$ was desilylated with [Bu$^n_4$N]F in thf. However, no such products were observed upon thermolysis of the bis-ruthenium complexes, suggesting that mono-ruthenium intermediates are the source of these products.[70] Thus, in this bis-ruthenium series, {Cp*(dppe)Ru}$_2$(C≡C)$_n$ complexes with n = 2, 3, 4, 7 and 11 have been reported. However the series remains incomplete, with the absence of the C_{10} and C_{12} analogues.

2.2 Results and Discussion

Previous studies in our group have shown that treatment of RuCl(dppe)Cp* (**1**) with half an equivalent of Me_3Si-$(C\equiv C)_4$-$SiMe_3$ in MeOH in the presence of KF gives $\{Ru(dppe)Cp^*\}_2(C\equiv C)_4$ (**2**) in 89% yield (Scheme 2.7).[70] Here an alternative synthetic route to **2** has been devised which involves the homo-coupling of $\{Ru(dppe)Cp^*\}(C\equiv C)_2H$ (**3**) by treating this compound with a catalytic amount of $Cu(OAc)_2$ in pyridine (Scheme 2.7).

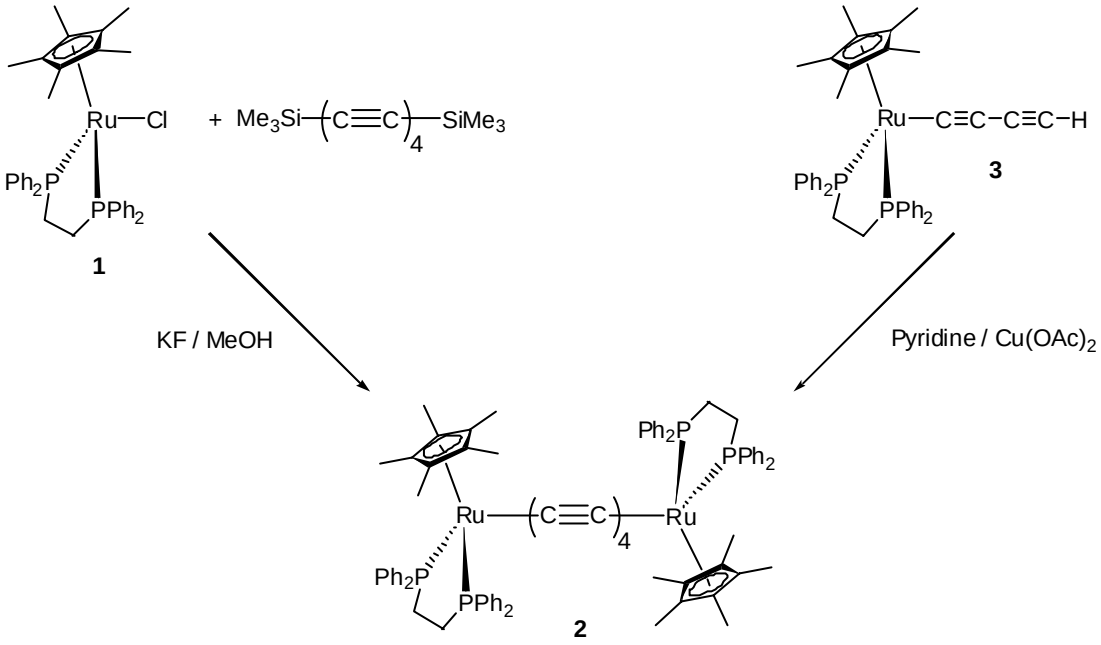

Scheme 2.7

All spectroscopic data agreed with that previously reported for **2**.[70] In the IR spectrum, two ν(C≡C) bands were found at 2107 and 1951 cm^{-1}. In the ^1H NMR spectrum a singlet at δ 1.49 assigned to the methyl protons of the Cp* ligand and the dppe protons appeared as multiplets over the expected regions. In the ^{31}P NMR spectrum a sharp singlet at *ca* δ 79.00 characteristic of the Ru(dppe)Cp* fragment was observed.

The success of this reaction demonstrates that the Ru(dppe)Cp* polyacetylene fragment is stable under these conditions. Thus it was proposed that this reaction

could provide a synthetic route to the C_{16} complex $\{Ru(dppe)Cp^*\}_2(C{\equiv}C)_8$ (**4**). This synthesis involves the homo-coupling of $\{Ru(dppe)Cp^*\}(C{\equiv}C)_4SiMe_3$ (**5**) using a catalytic amount of $Cu(OAc)_2$ in pyridine in the presence of tetrabutylammonium fluoride, $[Bu^n{}_4N]F$, to obtain **4** in 58% yield (Scheme 2.8). As observed during the successful syntheses of the C_8, C_{14} and C_{22} complexes,[70] an unidentified purple product was observed during the preparation of **4**. Thus far, all attempts to identify the purple product have been unsuccessful.

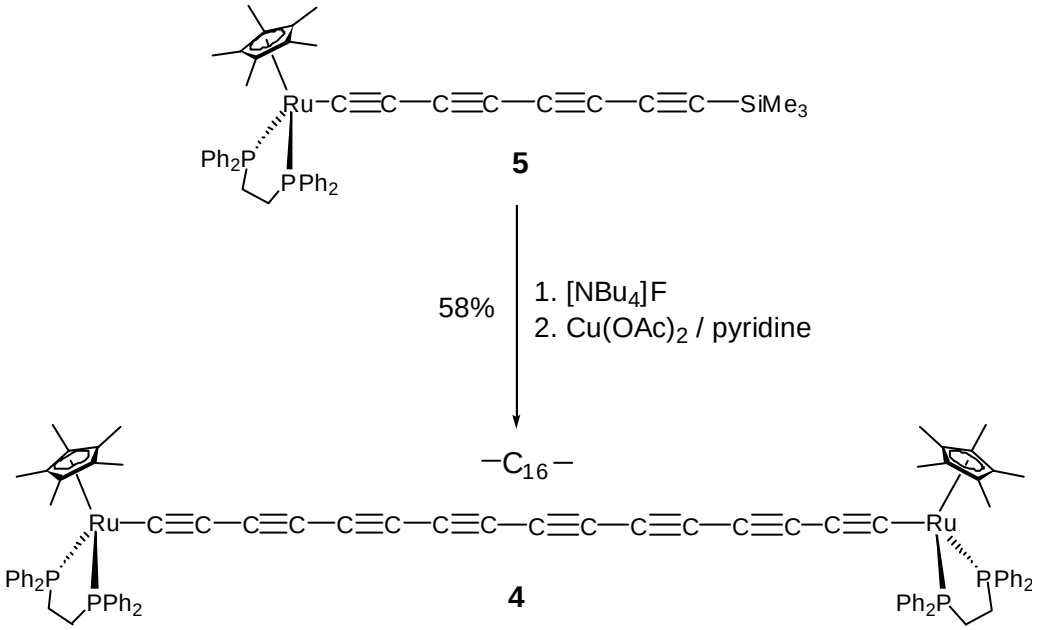

Scheme 2.8

The bis-ruthenium complex **4** was purified on a Florisil column. Solution IR spectroscopy revealed two ν(C≡C) bands at 2009 and 1927 cm^{-1}. In the ^{31}P NMR spectrum, a singlet at δ 79.68 was found for the two equivalent dppe ligands, while in the ^1H NMR spectrum, a singlet resonance for Cp* methyl protons was observed at δ 1.51. Other resonances for dppe were found as multiplets at δ 2.10 and δ 2.65 and between δ 7.13-7.71.

To better analyse the properties of this bis-ruthenium series the previously unidentified lower homologues C_{10} and C_{12} were sought. For the C_{12} complex to be made via a homo-coupling reaction the complex $\{Ru(dppe)Cp^*\}(C{\equiv}C)_3SiMe_3$ (**6**)

needed to be isolated. Recently it has been found that complexes which possess a gold(I)-phosphine centre coordinated to an alkynyl ligand can be coupled to halogen-containing complexes with the elimination of $AuX(Ph_3)$ driving the reaction to completion. The versatility of this reaction led us to re-examine the synthesis of mixed ruthenium-gold diyndiyl complexes for a more efficient synthesis of the building blocks required.

The complex $Ru\{C{\equiv}CC{\equiv}C[Au(PPh_3)]\}(dppe)Cp^*$ (**7**) has been previously synthesised through the reaction of **3** with the chloro-gold precursor $AuCl(PPh_3)$. A thf solution containing equimolar quantities of **3** and the gold chloride precursor was treated with a 1.0 M solution of $KN(SiMe_3)_2$ in toluene. The solution was stirred at room temperature for four hours to give the mixed ruthenium-gold diyndiyl as a bright yellow solid in 70% yield (Scheme 2.9).[70]

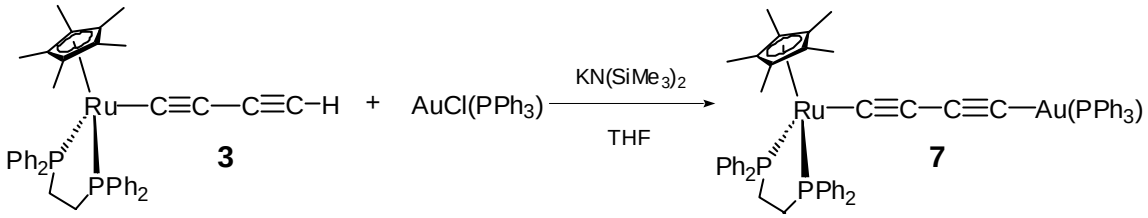

Scheme 2.9

As a part of this work, these yields have been significantly improved and the deprotecting step eliminated, by reacting equimolar quantities of $Ru(C{\equiv}CC{\equiv}CSiMe_3)(dppe)Cp^*$ **8** and the gold chloride precursor in a sodium methoxide solution (Scheme 2.10). The mixed ruthenium-gold diyndiyl crystallises directly from the reaction mixture as a bright yellow solid in 98% yield.

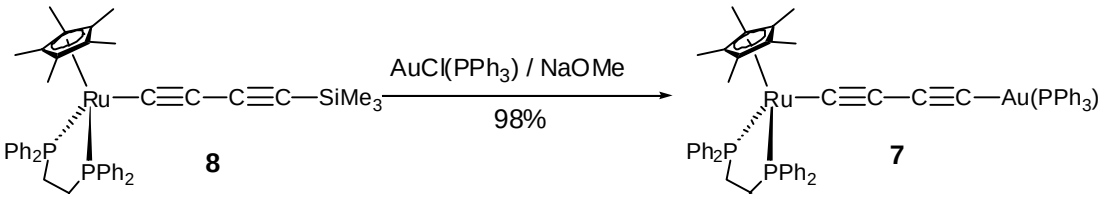

Scheme 2.10

All spectroscopic data agreed with those previously reported. Three ν(C≡C) bands were observed in the IR spectra, while in the ^{31}P NMR spectrum, two resonances in a 2:1 ratio, one at *ca* δ 80 corresponding to dppe and the second at *ca* δ 42 due to the phosphine attached to the gold centre were observed.

With the improved synthesis of **7**, it was anticipated that further chain extensions could be obtained through its reaction with $I(C{\equiv}C)_nSiMe_3$. The hexatriynyl complex **6** was prepared by treating **7** with iodo trimethylsilylethyne, $IC{\equiv}CSiMe_3$ in a thf/triethylamine mixture in the presence of $Pd(PPh_3)_4$ and CuI (Scheme 2.11). After four hours hexane was added to precipitate the remaining catalyst which was removed by filtration. The resulting orange solution was loaded directly onto a basic alumina column which was gradient eluted with triethylamine/hexane to obtain **6** as a bright yellow solid in 79% yield.

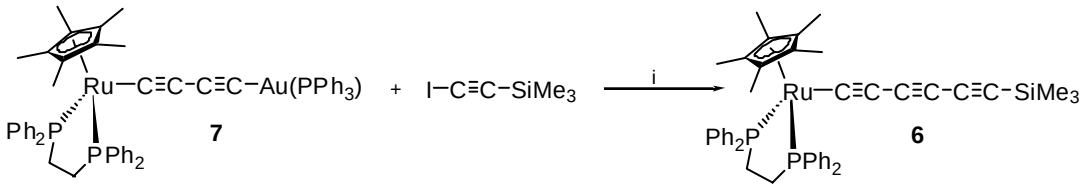

Reagents: i, $Pd(PPh_3)_4$/CuI in thf/NEt_3

Scheme 2.11

As expected, the spectroscopic features of **6** were similar to those found previously for **5**. In the IR spectrum two ν(C≡C) bands were found at 2110 and 1971 cm^{-1}. While in the ES-mass spectrum a $[M]^+$ ion was found at *m/z* 781 followed by a $[Ru(dppe)Cp^*]^+$ ion at *m/z* 635. In the ^{1}H NMR spectrum, singlets at δ 0.11 and 1.50 were assigned to the TMS and Cp* groups respectively, while multiplets at δ 1.73 and 2.42 and between δ 7.00 and 7.24 were due to the dppe ligand. The ^{31}P NMR spectrum displayed only one resonance at δ 80.43 for the Ru(dppe)Cp* fragment. Five of the six quaternary carbons of the C_6 were observed in the ^{13}C NMR spectrum between δ 49.43 and 127.62.

Crystals of the TMS-protected complex **6** were grown by the slow evaporation of a triethylamine/hexane solution. Complex **6** crystallises with two unique molecules in

the unit cell of which the ORTEP plot of one is illustrated below (Figure 2.3), while selected structural parameters are collected in Table 2.1.

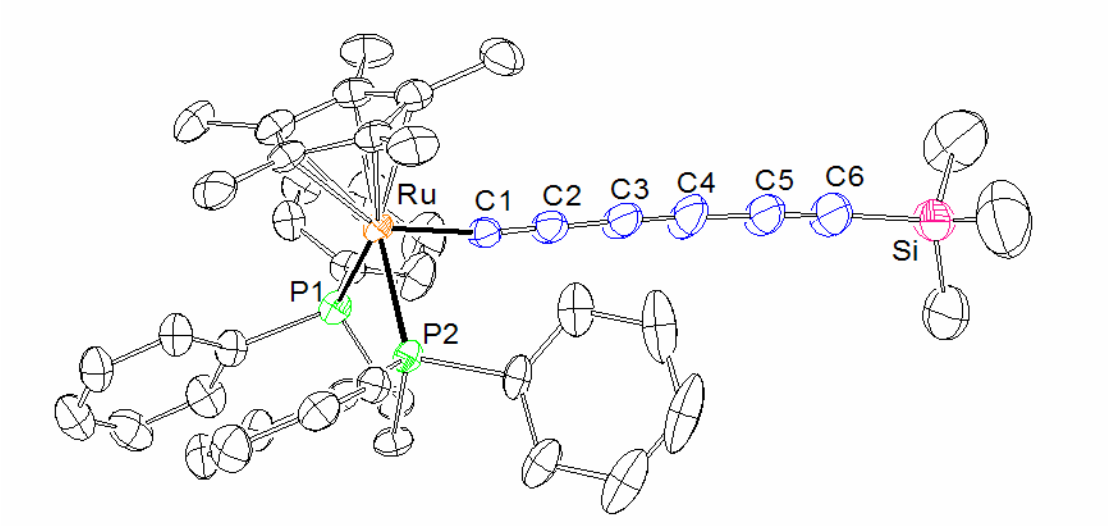

Figure 2.3: *ORTEP view of {Cp*(dppe)Ru}(C≡C)$_3$SiMe$_3$ (**6**).*

Table 2.1: *Selected structural data for {Cp*(dppe)Ru}(C≡C)$_3$SiMe$_3$ (**6**).*

Bond Distances (Å)		**Bond Angles (˚)**	
Ru-P(1)	2.270(2), *2.263(2)*	P(1)-Ru-P(2)	83.06(5), *82.70(8)*
Ru-P(2)	2.273(1), *2.280(2)*	P(1)-Ru-C(1)	81.9(2), *83.4(2)*
Ru-C(Cp*)	2.215(5) – 2.278(5), *2.218(6) – 2.280(5)*	P(2)-Ru-C(1)	87.2(1), *89.3(2)*
(av.)	2.249(5), *2.255(6)*	Ru-C(1)-C(2)	178.2(4), *173.3(5)*
Ru-C(1)	1.967(5), *1.966(5)*	C(1)-C(2)-C(3)	173.8(6), *175.4(7)*
C(1)-C(2)	1.231(8), *1.238(8)*	C(2)-C(3)-C(4)	177.7(7), *176.4(7)*
C(2)-C(3)	1.335(8), *1.357(9)*	C(3)-C(4)-C(5)	177.1(7), *174.5(9)*
C(3)-C(4)	1.220(9), *1.22(1)*	C(4)-C(5)-C(6)	176.3(8), *178.3(1)*
C(4)-C(5)	1.37(1), *1.38(1)*	C(5)-C(6)-Si	174.7(8), *174.0(8)*
C(5)-C(6)	1.20(1), *1.20(1)*		
C(6)-Si	1.833(8), *1.836(8)*		

Italicised values refer to molecule 2.

The Ru-C distance, 1.967(5) Å, is typical for a ruthenium-carbon single bond and the C≡C triple bonds are between 1.20(1) and 1.231(8) Å, with the shortest distances found furthest away from ruthenium. This feature is consistent with increased contributions from the cumulene resonance form (Scheme 2.12), as found in related systems.[74] It has been found that this effect decreases as the carbons extend out from the ruthenium[70] and bond lengths approach the typical values found in 1,3-butadiyne [C≡C, 1.217(1); C-C, 1.384(2) Å].[97]

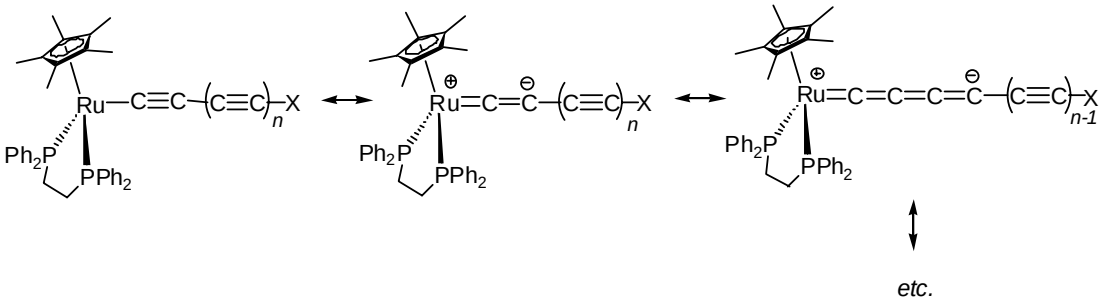

Scheme 2.12

Complex **6** was desilylated *in situ* using $[Bu^n_4N]F$ before being homo-coupled with a catalytic amount of $Cu(OAc)_2$ in pyridine and exposure to oxygen (Scheme 2.13). After one hour at 50˚C the mixture was chromatographed on a Florisil column eluting with diethyl ether to collect the bis-ruthenium C_{12} complex (**9**) as a red fraction in 82% yield. The IR spectrum showed five ν(C≡C) bands between 2280 and 1938 cm^{-1}. In the ^1H NMR a singlet was observed at δ 1.48 for Cp* and multiplets at δ 1.73 and 2.40 and between δ 6.90 – 7.71 for the dppe ligand. In the ^{31}P NMR spectrum a resonance at δ 79.43 was observed for the Ru(dppe)Cp* fragment. While no C≡C resonances were found in the ^{13}C NMR spectrum, perhaps due to decomposition at the concentration required for ^{13}C NMR acquisition, a $[M]^+$ ion at *m/z* 1415 was found in the ES-mass spectrum.

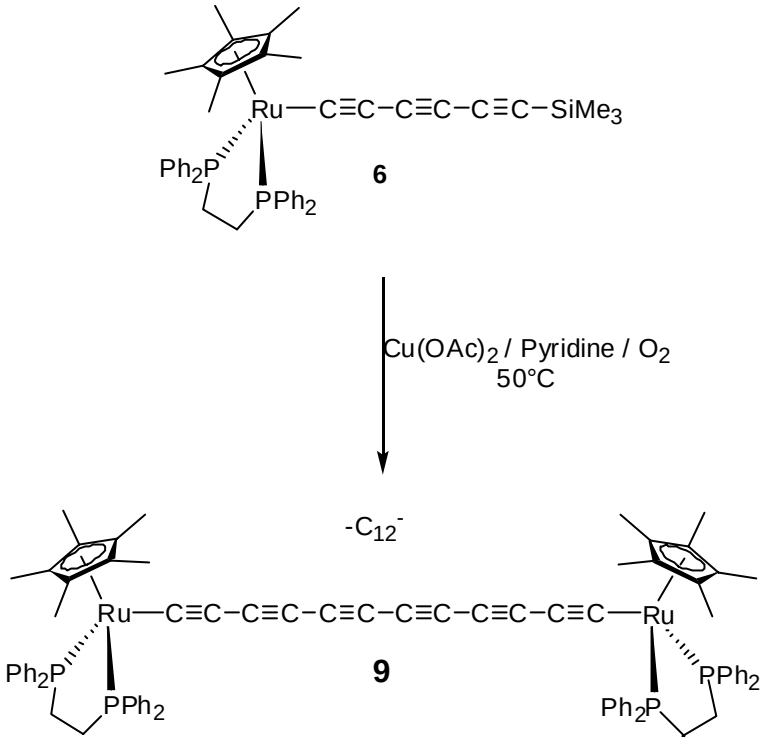

Scheme 2.13

To enable the preparation of a homologue with an odd number of alkyne linkages the complex Ru{(C≡C)$_5$SiMe$_3$}(dppe)Cp* (**10**) was sought. It was thought that the reaction of **10** with RuCl(dppe)Cp* and potassium fluoride would give the bis-ruthenium C_{10} complex (**11**), while the homo-coupling of **10** should give the bis-ruthenium C_{20} complex (**12**).

In a similar reaction to that used in the preparation of **6**, Ru{(C≡C)$_3$[Au(PPh$_3$)]}(dppe)Cp*[98] was treated with an excess of Me$_3$Si(C≡C)$_2$I in the presence of catalytic amounts of Pd(PPh$_3$)$_4$ and CuI. Purification by chromatography on a basic alumina column gave an unidentified purple complex as the major product. The pure C_{10}SiMe$_3$ complex (**10**) was isolated in only 2% yield as a red solid. The IR spectrum showed three ν(C≡C) bands between 2104 and 1966 cm^{-1}. In the ^{1}H NMR spectrum singlets were observed at δ 0.30 and 1.56 for SiMe$_3$ and Cp* respectively and multiplets at δ 2.14 and 2.62 and between δ 6.87 and 7.79 for the dppe ligand. In the ^{31}P NMR a singlet was observed at δ 79.91 for the Ru(dppe)Cp* group. In the ES-mass spectrum a [M + H]$^+$ ion was found at *m/z* 829. Due to the poor yields and instability of this complex in concentrated solutions it

could not be satisfactorily characterised by ^{13}C NMR or microanalysis. It has previously been found that the stability of the mono-ruthenium complexes [Ru](C≡C)$_n$H decreases with increasing chain length, with purple complexes formed when $n > 3$.[70] The source of this decomposition in these complexes is probably the lack of a bulky end-group at one end of the carbon chain. The *in situ* preparation and homo-coupling of **10** was also attempted, but after repeated attempts the desired bis-ruthenium C_{20} complex was not identified.

The gold coupling reaction provides an alternative method to prepare **11** without the need for extended (C≡C)$_n$H systems. Two equivalents of **7** were treated with the diiodoethyne, I(C≡C)I at 0˚C in the presence of catalytic Pd(PPh$_3$)$_4$ and CuI. After four hours hexane was added to give **11** as an analytically pure orange precipitate in 64% yield. The IR spectrum showed four ν(C≡C) bands between 2113 and 1938 cm^{-1}. In the ^1H NMR spectrum a singlet at δ 1.49 for the Cp* and multiplets at δ 1.73 and 2.40 and between δ 6.89 and 7.75 for the dppe ligand were observed. Four singlets between δ 50.8 and 91.98 were assigned to the carbons of the chain in the ^{13}C NMR spectrum. In the ^{31}P NMR spectrum a singlet was observed at δ 79.68 for the Ru(dppe)Cp* group and in the ES-mass spectrum an [M]$^+$ ion was observed at *m/z* 1390.

Table 2.2: *Spectroscopic Data for {Ru(dppe)Cp*}$_2$(C≡C)$_n$*

n	IR ν(C≡C) (cm^{-1})	NMR (δ)			Mass Spectrometry (*m/z*)	Ref
		^{1}H	^{13}C	^{31}P		
2	1973 s	1.68 (s, 30H, Cp*), 1.95, 2.72 (2m, 2 x 4H, CH_2CH_2), 7.04 – 8.05 (m, 40H, Ph)	10.09 (s, $C_5\mathit{Me}_5$), 29.11 (s, CH_2CH_2), 92.26 (s, C_5Me_5), 94.63 [t, $^2J_{CP}$ 27 Hz, C_1], 99.47 (s, C_2), 127.32 – 140.46 (m, Ph)	82.53	1318, $[M]^+$; 635 $[Ru(dppe)Cp^*]^+$	69
3	2129 w, 2057 s, 1959 m	1.61 (s, 30H, Cp*), 2.16, 2.81 (2m, 2 x 4H, CH_2CH_2), 7.20 – 7.88 (m, 40H, Ph)		79.41	1342, $[M]^+$; 635 $[Ru(dppe)Cp^*]^+$	69
4	2107m, 1951 m	1.49 (s, 30H, Cp*), 2.09, 2.67 (2m, 2 x 4H, CH_2CH_2), 7.09 – 7.66 (m, 40H, Ph)	10.23 (s, $C_5\mathit{Me}_5$), 29.79 (s, CH_2CH_2), 51.12 (s, C_4), 63.60 (s, C_3), 92.54 (s, C_2), 94.58 (s, C_5Me_5), 94.58 [t, $^2J_{CP}$ 22 Hz, C_1], 127.69 – 138.62 (m, Ph)	79.99	1398, $[M + MeOH]^+$; 1366 $[M]^+$, 635 $[Ru(dppe)Cp^*]^+$	69
5	2113m, 2046w, 1988m, 1938w	1.49 (s, 30H, Cp*), 1.73, 2.40 (2m, 2 x 4H, CH_2CH_2), 6.89 – 7.75 (m, 40H, Ph)	10.13 (s, $C_5\mathit{Me}_5$), 29.72 (s, CH_2CH_2), 50.28, 60.46, 65.79, 91.98 (4s, C≡C), 94.09 (s, C_5Me_5), 94.41 (s, br, Ru−C), 127.74 – 138.12 (m, Ph)	79.68	1390, $[M]^+$; 675 $[Ru(dppe)Cp^* + MeCN]^+$, 635 $[Ru(dppe)Cp^*]^+$	This Work
6	2280 w, 2269 w sh, 2109 w, 2048 m, 1938 br	1.48 (s, 30H, Cp*), 1.73, 2.40 (2m, 2 x 4H, CH_2CH_2), 6.90 – 7.71 (m, 40H, Ph)	10.36 (s, $C_5\mathit{Me}_5$), 30.10 (s, CH_2CH_2), 94.32 (s, C_5Me_5), 127.60 – 137.51 (m, Ph)	79.43	1414, $[M]^+$; 675 $[Ru(dppe)Cp^* + MeCN]^+$, 635 $[Ru(dppe)Cp^*]^+$	This Work
7	2058 m, 1947 br	1.45 [t, $^3J_{HP}$ 2 Hz, 30H, Cp*], 1.70, 2.36 (2m, 2 x 4H, CH_2CH_2), 6.99 – 7.68 (m, 40H, Ph)	10.39 (s, $C_5\mathit{Me}_5$), 30.01 (s, CH_2CH_2), 94.32 (s, C_5Me_5), 129.43 – 133.95 (m, Ph)	78.96	1438, $[M + Na]^+$; 635, $[Ru(dppe)Cp^*]^+$	69
8	2009 m, 1927 br	1.51 (s, 30H, Cp*), 2.10, 2.65 (2m, 2 x 4H, CH_2CH_2), 7.13-7.71 (m, 40H, Ph)		79.68	1485, $[M + Na]^+$; 635, $[Ru(dppe)Cp^*]^+$	This Work

Solutions of the bis-ruthenium complexes progressively darken in colour as the chain length is extended, from yellow (C_6), to orange (C_{10}), to deep red (C_{16}). Accordingly, the UV-visible spectra display a progressive red shift as chain length and hence the extent of conjugation increases (Figure 2.4). Molecular orbital calculations have shown that the energy difference between the HOMO and LUMO decreases as the extent of conjugation increases,[66] thus less energy is required to effect the $\pi \rightarrow \pi^*$ transition and in the bis-ruthenium series C_6 absorbs at λ_{max} = 279 nm, C_{10} absorbs at λ_{max} = 383 nm, C_{12} absorbs at λ_{max} = 419 nm and C_{16} absorbs at λ_{max} = 483 nm.

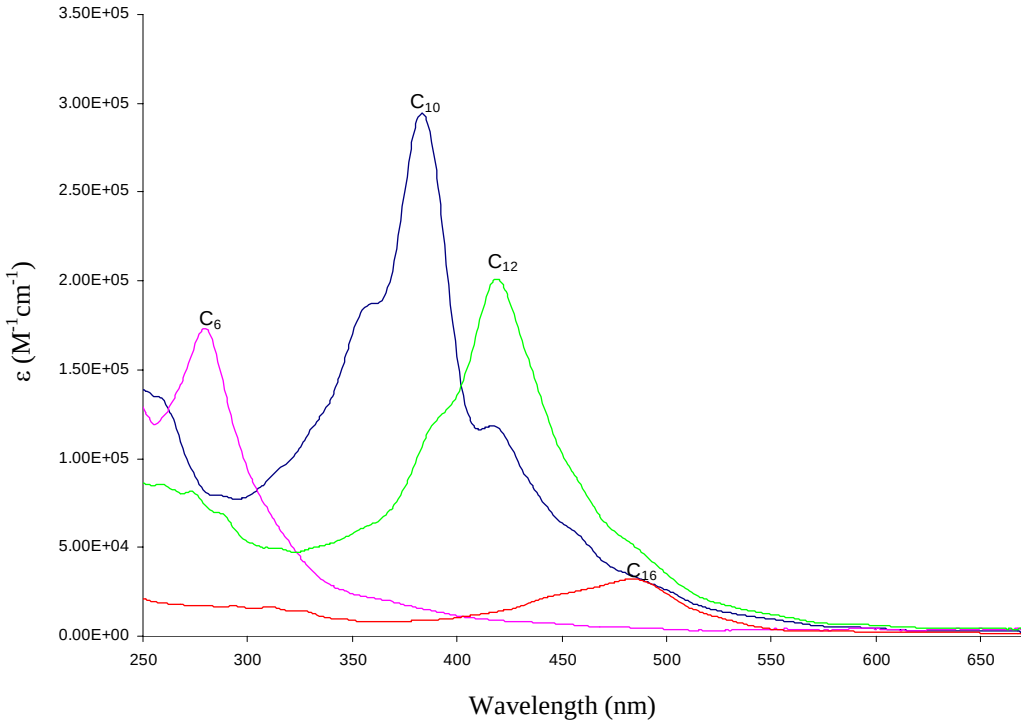

Figure 2.4: *UV-visible spectra of the {Cp*(dppe)Ru}$_2$(C≡C)$_n$ series (thf).*

2.3 Electrochemistry

The electronic interactions between two ruthenium centres across carbon chains containing 2, 4, 6, 8 and 14 carbons have previously been investigated.[70] The shorter C_2 - C_8 analogues displayed four redox processes with the first three of these processes having been found to be fully reversible while the fourth is only partially reversible. In the cyclic voltammogram of the C_{14} complex only two irreversible waves were observed. As a part of this work the electronic interactions in analogues containing 10, 12 and 16 carbons have been investigated. Cyclic voltammograms were recorded in CH_2Cl_2 under standard conditions, provided in the general experimental conditions. This gives a complete series of complexes containing from 2 to 16 carbons within the chain end-capped by Ru(dppe)Cp*. Electrochemical data are summarised in Table 2.3.

The cyclic voltammograms of the C_{10} and C_{12} complexes **11** and **9** confirm that the two metal centres interact across the carbon chain (Figure 2.5). Both complexes display three redox processes with the first two waves fully reversible and the third partially reversible. In the case of complex **11** the first and second oxidation events are found at +0.18 V and +0.45 V respectively. In **9** the first oxidation event is much higher at +0.30 V while the second oxidation event is at approximately the same value as that in **11** (+0.51 V). Thus, with an added C≡C unit in **9** the first oxidation potential increases by 120 mV and $\Delta E_{½}$ decreases from 0.26 in **11** to 0.21 in **9**. As 0.2 V is considered the distinction between Class II and Class III systems,[30] it appears that the C_{12} complex lies on the boundary of a Class II/III MV complex. Such systems usually display properties associated with both localised and delocalised electronic states and have attracted considerable interest in recent times.[55]

Table 2.3: *Electrochemical Data for {Ru(dppe)Cp*}$_2$(C≡C)$_n$*

Complex	E_1	E_2	$\Delta E_{1/2}$	K_c (0/+1/+2) [a]	E_3	E_4	ref
{Ru(dppe)Cp}$_2$(C≡C)	-0.61	+0.21	0.82	1.02 x 10^{14}	+1.06	+1.74 [b]	69
{Ru(dppe)Cp*}$_2$(C≡C)$_2$	-0.43	+0.22	0.65	1.27 x 10^{11}	+1.04	+1.54 [b]	69
{Ru(dppe)Cp*}$_2$(C≡C)$_3$	-0.15	+0.33	0.48	1.58 x 10^{8}	+1.05	+1.33 [b]	69
{Ru(dppe)Cp*}$_2$(C≡C)$_4$	+0.08	+0.43	0.35	9.5 x 10^{5}	+1.07	+1.27 [b]	69
{Ru(dppe)Cp*}$_2$(C≡C)$_5$	+0.18	+0.45	0.26	2.48 x 10^{4}	+1.11		This work
{Ru(dppe)Cp*}$_2$(C≡C)$_6$	+0.30	+0.51	0.21	2.91 x 10^{3}	+1.05		This work
{Ru(dppe)Cp*}$_2$(C≡C)$_7$	+0.42 [c]	+0.55 [b]	0.17 [d]	8.0 x 10^{2}			69
{Ru(dppe)Cp*}$_2$(C≡C)$_8$	+0.44	+0.57	0.13	1.57 x 10^{2}	+0.96		This work

Electrochemical data (V), measured in CH_2Cl_2 with $[Bu^n_4N][PF_6]$ supporting electrolyte, values referenced to $[FeCp_2]/[FeCp_2]^+$ = 0.46 V.
[a] All values calculated from ΔE and Equation 1.6. [b] Partially reversible. [c] Peak potential of an irreversible process. [d] ΔE was measured as the separation between the two anodic waves.

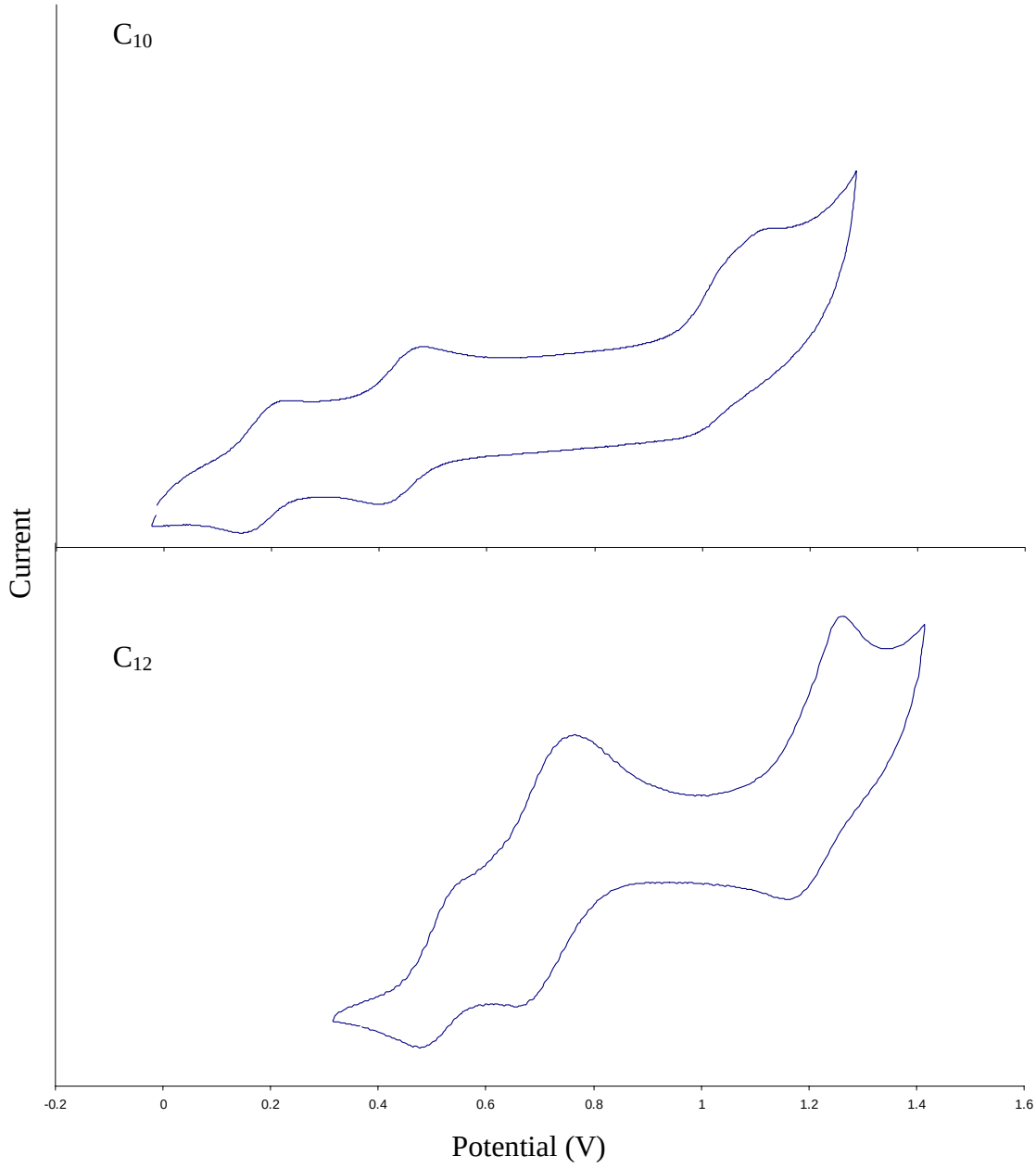

Figure 2.5: *Cyclic voltammograms of **11** and **9**, recorded in CH_2Cl_2, 0.1 M $[Bu^n_4N][PF_6]$.*

The cyclic voltammogram of the C_{16} complex shows three partially chemically reversible oxidation events. However there is little separation between the first two oxidation waves (Figure 2.6). As observed in **9**, this decrease in $\Delta E_{½}$ is due to the first oxidation event occurring at a much higher potential (+0.44 V) while the second oxidation remains relatively unaffected (+0.57 V) by the increase in chain length.

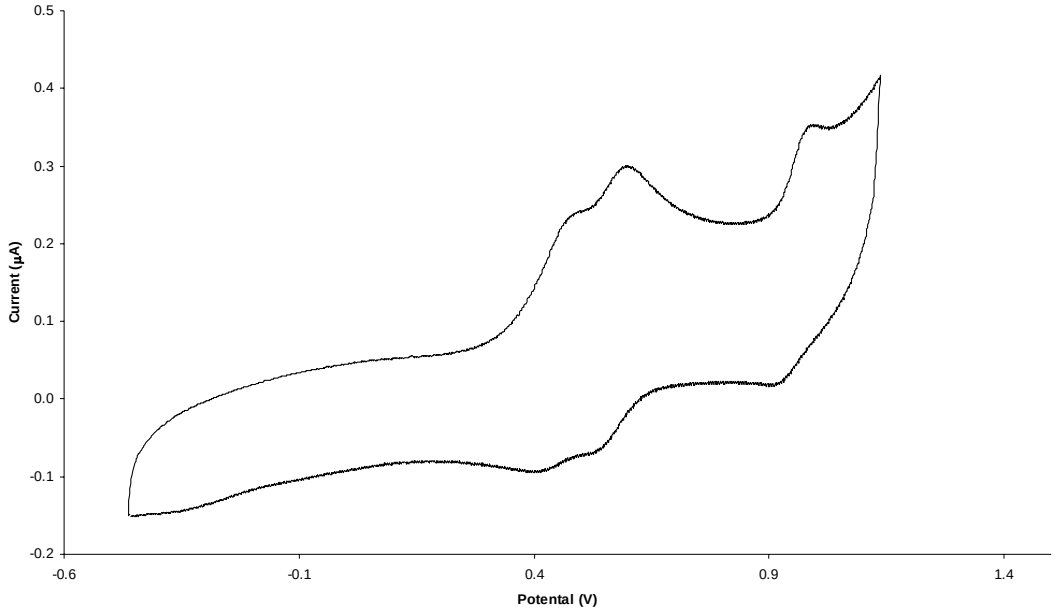

Figure 2.6: Cyclic *voltammogram of **4**, recorded in CH_2Cl_2, 0.1 M $[Bu^n_4N][PF_6]$.*

With the complete series of $\{Cp^*(dppe)Ru\}_2(C{\equiv}C)_n$ (n = 2 – 8) complexes prepared and their cyclic voltammograms recorded, the influence of chain length on the electronic interactions can now be examined fully. To this point, the separation of the first two waves (ΔE) was considered the best indication of the extent of interactions between the two redox centres.[70,99] Subtle changes in the coordinated ligands have been found to have little effect on ΔE. Thus the ethynyl complex $\{Cp(dppe)Ru\}_2(C{\equiv}C)$[70] can be included in comparisons between the longer chain complexes with the more electron-rich Ru(dppe)Cp* metal centres extending the series to n = 1 – 8. The data in Table 2.3 show that as the chain length is increased, the interactions between the two ruthenium centres decrease at a steady rate. This trend is represented graphically in Figure 2.7, which is a plot of ΔE for the first two waves against chain length.

Electron transfer between two molecules of the same chain complex in different oxidation states to give a single species with an intermediate oxidation state is known as the comproportionation reaction (Scheme 2.14).

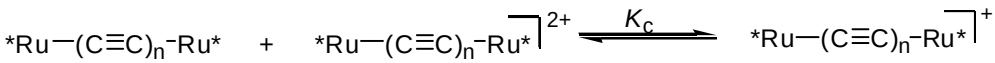

Where Ru* = Ru(dppe)Cp*

Scheme 2.14

The equilibrium constant for the comproportionation reaction can be calculated from ΔE between two waves using Equation 1.6.[65] As the magnitude of the comproportionation constant is also often taken as an indication of the strength of the electronic coupling between two redox centres, the K_c values are also given in Table 2.3. The decrease in thermodynamic stabilities of the oxidised species of the ruthenium series is evidenced by the steady decrease of K_c values with increasing chain length.

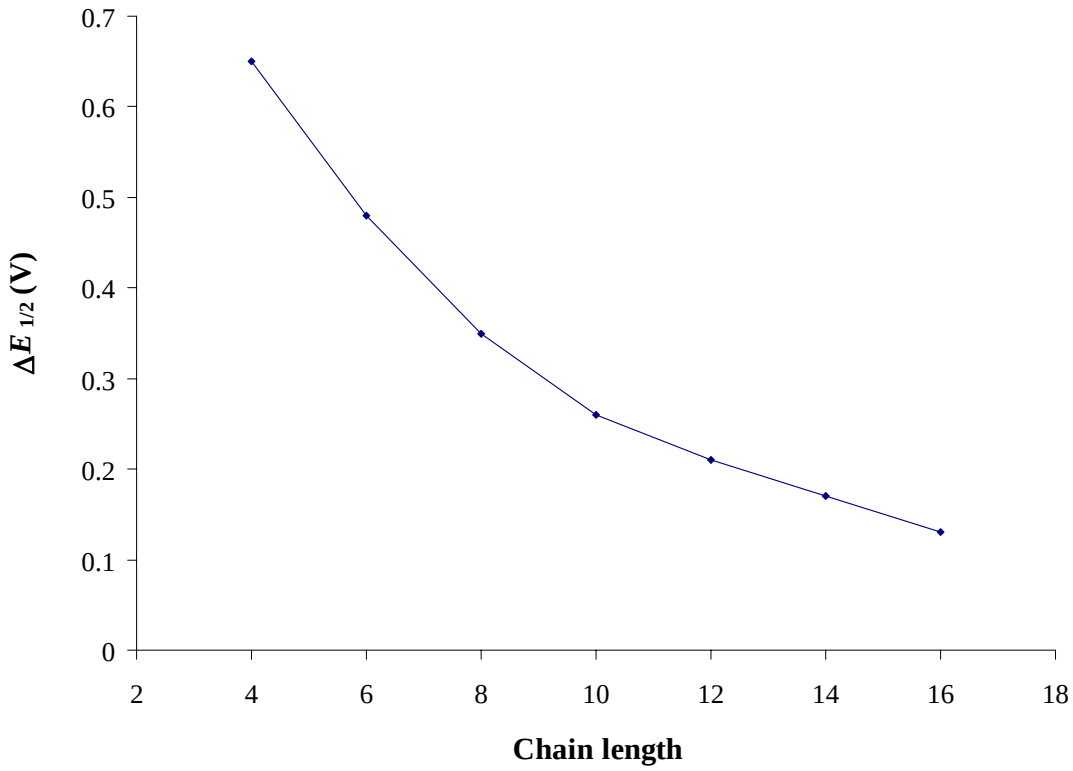

Figure 2.7: *Chain length effect on ΔE in the {Cp*(dppe)Ru}$_2$(C≡C)$_n$ series.*

Comparison of the data contained within Table 2.2 show that as the chain length is increased, E_1 becomes thermodynamically more difficult with the first redox event

occurring at -0.61 V in the C_2 complex and at 0.44 V in the C_{16} complex, a difference of more than 1 V. The E_2 processes are affected to a lesser extent by chain length and are observed between +0.21 V and +0.57 V. Similar trends were also observed in the Re(NO)(PPh_3)Cp* series. In this series ΔE values for the C_4 and C_{16} complexes were 0.53 and 0.07 V respectively, a difference of 0.6 V.[67] Therefore it can be concluded that the strength of electronic interactions across polyyndiyl ligands is enhanced by the ruthenium metal centre relative to the rhenium series. This trend is represented graphically in Figure 2.8, which is a plot of ΔE for the first two waves of both the rhenium and ruthenium series against chain length.

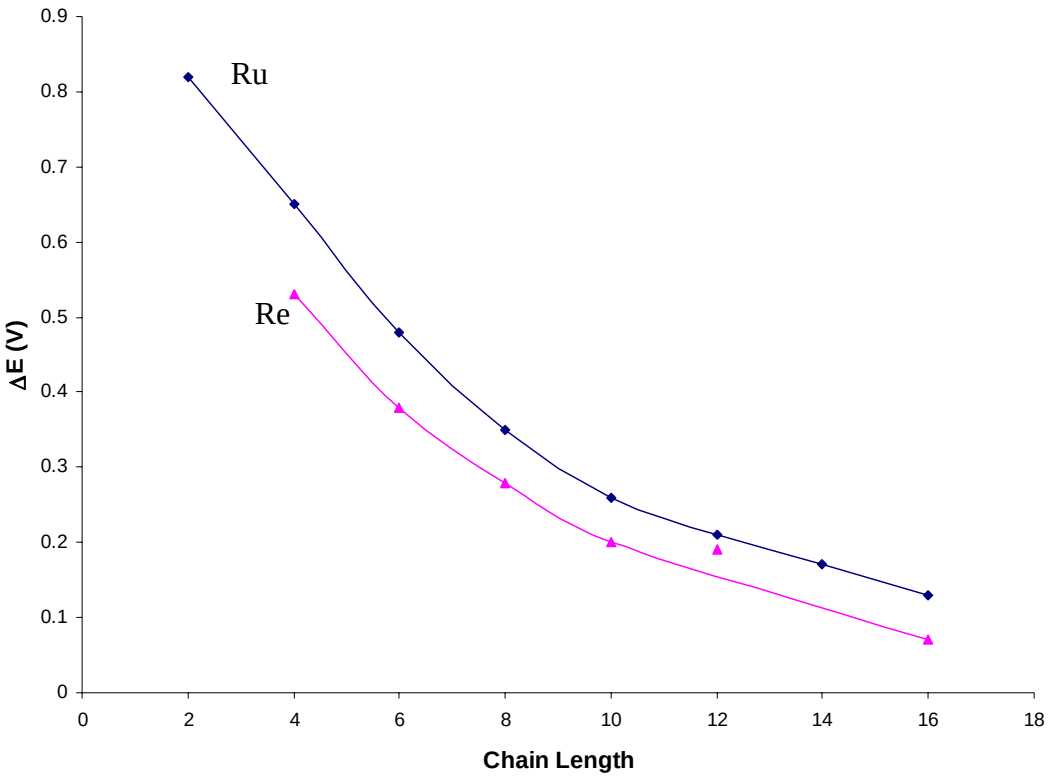

Figure 2.8: *Chain length effect on ΔE in the {Cp*(dppe)Ru}$_2$(C≡C)$_n$ vs. {Cp*(NO)(PPh_3)Re}$_2$(C≡C)$_n$ the series.*

2.4 Conclusions

This work has demonstrated several different methodologies that can be used to synthesise polyyndiyl complexes. Synthesis of the C_{12} and C_{16} complexes have been achieved by the homo-coupling reactions of $\{Cp^*(dppe)Ru\}(C{\equiv}C)_nH$ in the presence of catalytic $Cu(OAc)_2$ and pyridine. However this methodology only allows the synthesis of complexes containing an even number of alkynyl linkages.

The gold reaction has provided a new and very useful route to complexes with extended carbon chains and enables the synthesis of complexes containing both an even and an odd number of alkynyl linkages. Synthesis of the C_{10} complex was achieved by the double coupling of $\{Cp^*(dppe)Ru\}(C{\equiv}C)_4Au(PPh_3)$ with diiodoethyne in the presence of a Pd(0)/Cu(I) catalyst. As discussed above, increasing the chain length or having less sterically demanding end-groups generally decreases the stability of poly-ynes. Capping a poly-yne with $Au(PPh_3)$ in these reactions, rather than the proton, typically required for palladium-catalysed cross coupling reactions, has enabled access to higher chain-lengths by stabilisation of extended C_n chains. Historically, attempts to synthesise complexes of similar chain lengths using conventional methodologies have involved the use of $Br(C{\equiv}C)_nBr$ which are prone to detonation by mechanical shock.[67]

Cyclic voltammetry has confirmed that electronic interactions decrease with increasing chain length in the series, $\{Cp^*(dppe)Ru\}_2(C{\equiv}C)_n$. Furthermore, the change-over between Class II and Class III MV complex was identified as the C_{12} complex (ΔE = 0.21 V).

2.5 General experimental conditions

All reactions were carried out using standard Schlenk techniques, under dry high purity argon. Solvents were purified as follows: diethyl ether, pentane, THF and toluene were distilled from Na/benzophenone; benzene was distilled from Na; CH_2Cl_2 was distilled from CaH_2; NEt_3 was distilled from KOH; MeOH was distilled from Mg/I_2. Elemental analyses were performed by CMAS, Belmont, Vic., Australia.

2.5.1 Instrumentation

IR spectra were obtained on a Perkin-Elmer 1720X FT IR spectrometer (4000-400 cm^{-1}). Nujol mull spectra were obtained from samples mounted between NaCl discs. Solution spectra were obtained using a 0.5 mm path-length solution cell with NaCl windows.

NMR spectra were recorded on Bruker AM300WB or ACP300 (^{1}H at 300.13 MHz, ^{13}C at 75.47 MHz, ^{19}F at 564.24 MHz,^{31}P at 121.50 MHz) instruments. Samples were contained within 5 mm sample tubes. Chemical shifts (δ) are given in ppm relative to internal TMS (0 ppm) for ^{1}H and ^{13}C NMR spectra, external CF_3COOH (0 ppm) for ^{19}F spectra and external H_3PO_4 (76.68 ppm) for ^{31}P NMR spectra.

Cyclic voltammograms were recorded using a MacLab/400 supplied by AD Instruments or a Princeton PAR model 263A potentiostat in a conventional three electrode cell, using a platinum working electrode, platinum wire counter electrode and a pseudo-reference electrode. Experiments were carried out from CH_2Cl_2 solutions containing 0.1 M $[Bu^n_4N][PF_6]$ as the supporting electrolyte. All potentials were referenced against an internal ferrocene standard ($[FeCp_2]/[FeCp_2]^+$ = +0.46 V vs. SCE).

Processes were determined to be diffusion controlled if the plot of i_p vs. $v^{1/2}$ was linear and fully chemically reversible if $i_{pa}/i_{pc} \approx 1$ and $\Delta E_p \approx \Delta E_{p(ferrocene)}$ independent of the scan rate.

ES-mass spectra were recorded on either a VG Platform 2 or a Finnigan LCQ spectrometer. Methanol solutions were directly infused into the instrument, using chemical aids to ionisation as required.

X-ray crystal structures were determined by Professor Allan White and Dr Brian Skelton, University of Western Australia, Australia.

2.6 Experimental

The compounds $Me_3Si(C{\equiv}C)_4SiMe_3$,[55] RuCl(dppe)Cp,[100] $I(C{\equiv}C)_3I$,[55] $IC{\equiv}CC{\equiv}CSiMe_3$,[100] $IC{\equiv}CI$,[101] (use with appropriate care) $Pd(PPh_3)_4$,[100] $\{Cp^*(dppe)Ru\}(C{\equiv}C)_2SiMe_3$[70] $\{Cp^*(dppe)Ru\}(C{\equiv}C)_4SiMe_3$,[70] $\{Cp^*(dppe)Ru\}(C{\equiv}C)_2H$,[70] $AuCl(PPh_3)$,[102] $\{Cp^*(dppe)Ru\}(C{\equiv}C)_3AuPPh_3$,[98] $\{Cp^*(dppe)Ru\}(C{\equiv}C)_4AuPPh_3$,[70] $Me_3SiC{\equiv}CH$[103] and 1,4$\{Me_3Si(C{\equiv}C)\}C_6H_4$[104] were all prepared by standard literature methods. $Me_3Si(C{\equiv}C)I$ was prepared by stirring a mixture of $Me_3SiC{\equiv}CH$ (2 ml, 15 mmol) and BuLi (9.4 ml of 1.6 M solution in hexane, 15 mmol) in ether (40 ml) at –40˚C for 5 mins. Solid iodine was then added slowly until the brown colour persisted (≈2 g) and the mixture stirred for a further 10 mins before being washed with $Na_2S_2O_3$ (4 x 50 ml) followed by saturated NaCl (2 x 50 ml). The organic layer was dried with $MgSO_4$ and the solvent removed to give $Me_3SiC{\equiv}CI$ (1.54 g, 46%)

$\{Ru(dppe)Cp^*\}_2(C{\equiv}C)_4$ (2)

A Schlenk flask was charged with $Ru(C{\equiv}CC{\equiv}CH)(dppe)Cp^*$ (100 mg, 0.14 mmol), $Cu(OAc)_2$ (30 mg, 0.14 mmol), pyridine (2 ml) and dbu (18.5 mg, 0.12 mmol). The resulting mixture was opened to air and stirred at 50˚C for 30 min before the solvent was removed and the residue extracted in benzene. The extract was then chromatographed on a basic alumina column eluting with benzene/acetone gradient to collect a bright yellow fraction. The solvent was removed to give $\{Ru(dppe)Cp^*\}_2(C{\equiv}C)_4$ (78 mg, 82%). ^{1}H NMR (C_6D_6): δ 1.49 (s, 30H, Cp*), 2.09, 2.67 (2m, 2 x 4H, CH_2CH_2), 7.09-7.66 (m, 40H, Ph). ^{31}P NMR: δ 80.81 (s, dppe). ES-mass spectrum (*m/z*): 635, $[Ru(dppe)Cp^*]^+$.

$\{Ru(dppe)Cp^*\}_2(C{\equiv}C)_8$ (4)

A mixture of $Ru\{(C{\equiv}C)_4SiMe_3\}(dppe)Cp^*$ (20 mg, 0.025 mmol) and $[Bu^n{}_4N]F$ [0.007 ml, (1.0M in thf, ~5 wt. % water) 0.007 mmol] in toluene (15 ml) was stirred at 20˚C for 2 h. Pyridine (1 ml), $Cu(OAc)_2$ (5.8 mg, 0.03 mmol) and dbu (18.5 mg, 0.12 mmol) were then added and the mixture stirred open to air for a further 1 h at 50˚C. The crude product was then chromatographed on a Florisil column eluting with diethyl ether to collect a red fraction. The solvent was removed to give

{Ru(dppe)Cp*}$_2$(C≡C)$_8$ (11 mg, 58%). IR (CH_2Cl_2, cm^{-1}): ν(C≡C) 2009 m, 1927 br. ^{1}H NMR (C_6D_6): δ 1.51 (s, 30H, Cp*), 2.10, 2.65 (2m, 2 x 4H, CH_2CH_2), 7.13-7.71 (m, 40H, Ph). ^{31}P NMR: δ 79.68 (s, dppm). ES-mass spectrum (*m/z*): 1485, $[M + Na]^+$; 635, $[Ru(dppe)Cp^*]^+$.

Ru{(C≡C)$_3$SiMe$_3$}(dppe)Cp* (6)

To a stirring solution of Ru{(C≡C)$_2$AuPPh$_3$}(dppe)Cp* (400 mg, 0.35 mmol) in a 1:1 mixture of triethylamine / thf (40 ml) was added $Me_3SiC{\equiv}CI$ (200 mg, 0.89 mmol) followed immediately by $Pd(PPh_3)_4$ (50 mg) and CuI (12 mg). This mixture was stirred in the dark at room temperature for 4 h before hexane (100 ml) was added and the the preciptate removed by filtration. The filtrate was loaded directly onto a basic alumina column which was gradient eluted with triethylamine / hexane. The yellow band collected to obtain Ru{(C≡C)$_3$SiMe$_3$}(dppe)Cp* (217 mg, 79%). Single crystals suitable for X-ray were grown from triethylamine/hexane. Anal. Calcd ($C_{45}H_{48}P_2RuSi$): C, 69.21; H, 6.20. Found: C, 69.28; H, 6.31. IR (Nujol, cm^{-1}): ν(C≡C) 2110 s, 1971 s. ^{1}H NMR (C_6D_6): δ 0.11 (s, 9H, $SiMe_3$) 1.50 (s, 15H, Cp*), 1.73, 2.42 (2m, 2 x 2H, CH_2CH_2), 7.00 – 7.24 (m, 20H, Ph). ^{13}C NMR: (C_6D_6) δ 0.21 (s, $SiMe_3$), 10.05 (s, $C_5\mathit{Me}_5$), 49.43, 69.79, 77.93, 92.19 (s, C≡C) 93.90 [t, ^2J(CP) 2 Hz, C_5Me_5], 127.62 [t, ^2J(CP) 4.5 Hz, C_1], 128.29 – 138.38 (m, Ph). ^{31}P NMR: δ 80.43(s, 2P, dppe). ES-mass spectrum (*m/z*): 781, $[M]^+$; 635, $[Cp^*(dppe)Ru]^+$.

Ru{(C≡C)$_2$AuPPh$_3$}(dppe)Cp* (7)

To a stirred suspension of $AuClPPh_3$ (90 mg, 0.18 mmol) in sodium methoxide (5 mg Na in MeOH 5 ml) was added Ru{(C≡C)$_2$SiMe$_3$}(dppe)Cp* (136 mg, 0.18 mmol). This mixture was stirred at 20˚C for 1 h. The resulting yellow precipitate was collected and washed with MeOH (3 ml) followed by hexane (5 ml) to give Ru{(C≡C)$_2$AuPPh$_3$}(dppe)Cp* (195 mg, 98%). ^{1}H NMR (C_6D_6): δ 1.56 (s, 15H, Cp*), 1.86, 2.73 (2m, 2 x 2H, CH_2CH_2), 6.85-8.05 (m, 35H, Ph). ^{31}P NMR: δ 81.65 (s, 2P, dppe), 43.12 (s, 1P, PPh_3).

{Ru(dppe)Cp*}$_2$(C≡C)$_6$ (9)

A mixture of Ru{(C≡C)$_3$SiMe$_3$}(dppe)Cp* (76 mg, 0.10 mmol) and [Bu$^n_4$N]F (0.05 ml, 0.05 mmol) in thf (10 ml) was stirred at 20˚C for 1 h. Pyridine (2 ml) and Cu(OAc)$_2$ (20 mg, 0.1 mmol) were then added and the mixture opened to air before being stirred for 1 h at 50˚C. The solvent was then evaporated and the crude product chromatographed on a Florisil column eluting with diethyl ether to collect a red fraction. The solvent was removed to give {Ru(dppe)Cp*}$_2$(C≡C)$_6$ (58 mg, 82%). Anal. Calcd ($C_{84}H_{78}Ru_2P_4$): C, 71.37; H, 5.56. Found: C, 71.19; H, 5.55. IR (CH_2Cl_2, cm^{-1}): ν(C≡C) 2280 w, 2269 wsh, 2109 w, 2048 m, 1938 br. ^{1}H NMR (C_6D_6): δ 1.48 (s, 30H, Cp*), 1.73, 2.40 (2m, 2 x 4H, CH_2CH_2), 6.90 – 7.71 (m, 40H, Ph). ^{13}C NMR: δ 10.36 (s, C_5*Me*$_5$), 30.10 (s, CH_2CH_2), 94.32 (s, *C*$_5$Me$_5$), 127.60 – 137.51 (m, Ph). ^{31}P NMR: δ 79.43 (s, 2P, CH_2CH_2). ES-mass spectrum (*m/z*): 1414.7, [M]$^+$; 675.7 [Ru(dppe)Cp* + MeCN]$^+$, 635.3 [Ru(dppe)Cp*]$^+$.

Ru{(C≡C)$_5$SiMe$_3$}(dppe)Cp* (10)

To a stirring solution of Ru{(C≡C)$_3$AuPPh$_3$}(dppe)Cp* (200 mg, 0.25 mmol) in a 1:1 mixture of triethylamine / thf was added Me$_3$Si(C≡C)$_2$I (90 mg, 0.70 mmol) followed immediately by Pd(PPh$_3$)$_4$ (20 mg) and CuI (10 mg). This mixture was stirred in the dark at room temperature for 4 h before hexane (100 ml) was added. This solution was loaded directly onto a basic alumina column which was gradient eluted with triethylamine / hexane, the red band collected and the solvent removed. The residue was then washed with hexane before the product was extracted with diethyl ether. The solvent was removed to give Ru{(C≡C)$_5$SiMe$_3$}(dppe)Cp* (**9**) (4 mg, 2%). IR (CH_2Cl_2, cm^{-1}): ν(C≡C) 2104s, 2062sh, 1966s. ^{1}H NMR (C_6D_6): δ 0.30 (s, 9H, SiMe$_3$) 1.56 (s, 15H, Cp*), 2.14, 2.62 (2m, 2 x 2H, CH_2CH_2), 6.87 – 7.79 (m, 20H, Ph). ^{31}P NMR: δ 79.91(s, 2P, dppe). ES-mass spectrum (*m/z*): 829, [M + H]$^+$; 663 [Ru(dppe)Cp* + CO]$^+$.

{Ru(dppe)Cp*}$_2$(C≡C)$_5$ (11)

To a stirring solution of Ru{(C≡C)$_2$AuPPh$_3$}(dppe)Cp* (200 mg, 0.18 mmol) in a 1:1 mixture of triethylamine / thf (40 ml) at 0˚C was added IC≡CI (24 mg, 0.09 mmol) followed immediately by Pd(PPh$_3$)$_4$ (50 mg) and CuI (5 mg). This mixture was stirred in the dark at room temperature for 4 h before hexane (100 ml) was

added. The resulting orange precipitate was collected, washed with hexane and dried to give {Ru(dppe)Cp*}$_2$(C≡C)$_5$ (80 mg, 64%). Anal. Calcd ($C_{82}H_{78}Ru_2P_4$): C, 70.88; H, 5.66. Found: C, 70.90; H, 5.76. IR (CH_2Cl_2, cm^{-1}): ν(C≡C) 2113 m, 2046 w, 1988 m, 1938 w. ^{1}H NMR (C_6D_6): δ 1.49 (s, 30H, Cp*), 1.73, 2.40 (2m, 2 x 4H, CH_2CH_2), 6.89 – 7.75 (m, 40H, Ph). ^{13}C NMR: δ 10.13 (s, C_5Me_5), 29.72 (m, CH_2CH_2), 50.28, 60.46, 65.79, 91.98 (4s, C≡C), 94.09 (s, C_5Me_5), 94.41 (s, br, Ru−C), 127.74 – 138.12 (m, Ph). ^{31}P NMR: δ 79.68 (s, 2P, CH_2CH_2). ES-mass spectrum (*m/z*): 1390, $[M]^+$; 675.7 $[Ru(dppe)Cp^* + MeCN]^+$, 635.3 $[Ru(dppe)Cp^*]^+$.

Chapter 3

SOME METAL-CAPPED COMPLEXES WITH AN ODD-NUMBERED BRIDGING CARBON CHAIN

3.1 Introduction

The vast majority of complexes $L_nM{-}C_n{-}M'L'_m$ prepared to date have even-numbered bridging carbon chains. This is due to the wide use and availability of acetylenic and buta-1,3-diyne precursors. Bimetallic complexes separated by an odd number of carbons are comparatively scarce and pose a greater synthetic challenge. Complexes of the general formula $[L_nM](CC)_mC[M'L'_m]$ with an odd number of carbon atoms bridging two transition metal centres can be represented by one of the two valence structures below (Figure 3.1). Both electronic structures require at least one of the M-C attachments to involve a multiple bond. Structure **3a** is a cumulenic form, while structure **3b** is a polyalkynyl-carbyne form.

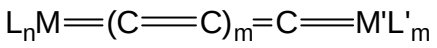

3a

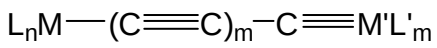

3b

Figure 3.1: *Valence structures of $[L_nM](CC)_mC[M'L'_m]$.*

3.1.1 Synthesis of Bimetallic Compounds Containing C_3 Bridging Ligands

Bimetallic compounds spanned by linear C_3 ligands have previously been obtained through three synthetic strategies:[10]

(i) Deprotonation and oxidation of hydrocarbon fragments which bridge two metal centres.

(ii) Fischer-type carbyne synthesis from the reaction of lithiated ethynyl-metal complexes with metal carbonyls. The resulting intermediate anions react with $[Me_3O]^+[BF_4]^-$ to give methoxycarbene derivatives, from which the OMe group can subsequently be removed to give the C_3 complex.

(iii) Metathesis of C≡C and M≡C triple bonds and silylpropargylidyne desilylation.

Detailed below are some literature examples that illustrate the three alternative strategies and the different reaction conditions that have been used to prepare C_3 ligands which bridge two transition metal centres.

3.1.1.1 Synthetic Strategy One

Complementary carbyne reagents may be used to synthesise C_3-bridged complexes. For example the nucleophilic β-carbon of the molybdenum vinylidene anion, $[Mo(=C=CH_2)(CO)_2Tp^*]^-$ (Tp* = Hydrotris(3,5-dimethylpyrazolyl)borate) obtained from the deprotonation of $Mo(\equiv CCH_3)(CO)_2Tp^*$, can replace the chloride of $Mo(\equiv CCl)(CO)_2Tp^*$ (Figure 3.2) to give $Tp^*(CO)_2Mo\equiv CCH_2C\equiv Mo(CO)_2Tp^*$. Treating this complex with two equivalents of KO^tBu and exposing the reaction mixture to air yields the mixed valent complex, $Tp^*(CO)_2Mo\equiv CC\equiv CMo(O)_2Tp^*$ (Scheme 3.1), in which a Mo(II) metal centre is connected to a Mo(VI) metal centre through a C_3-bridge.[105] This synthetic route can also be used to obtain the dinuclear complexes $Tp^*(CO)_2W\equiv CC\equiv CMo(O)_2Tp^*$ and $Tp^*(O)_2W\equiv CC\equiv CMo(CO)_2Tp^*$, the latter from the tungsten vinylidene anion $[Tp^*(CO)_2W=C=CH_2]^-$.[105]

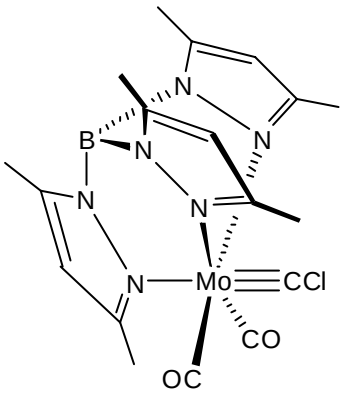

Figure 3.2: *$Mo(\equiv CCl)(CO)_2Tp^*$*

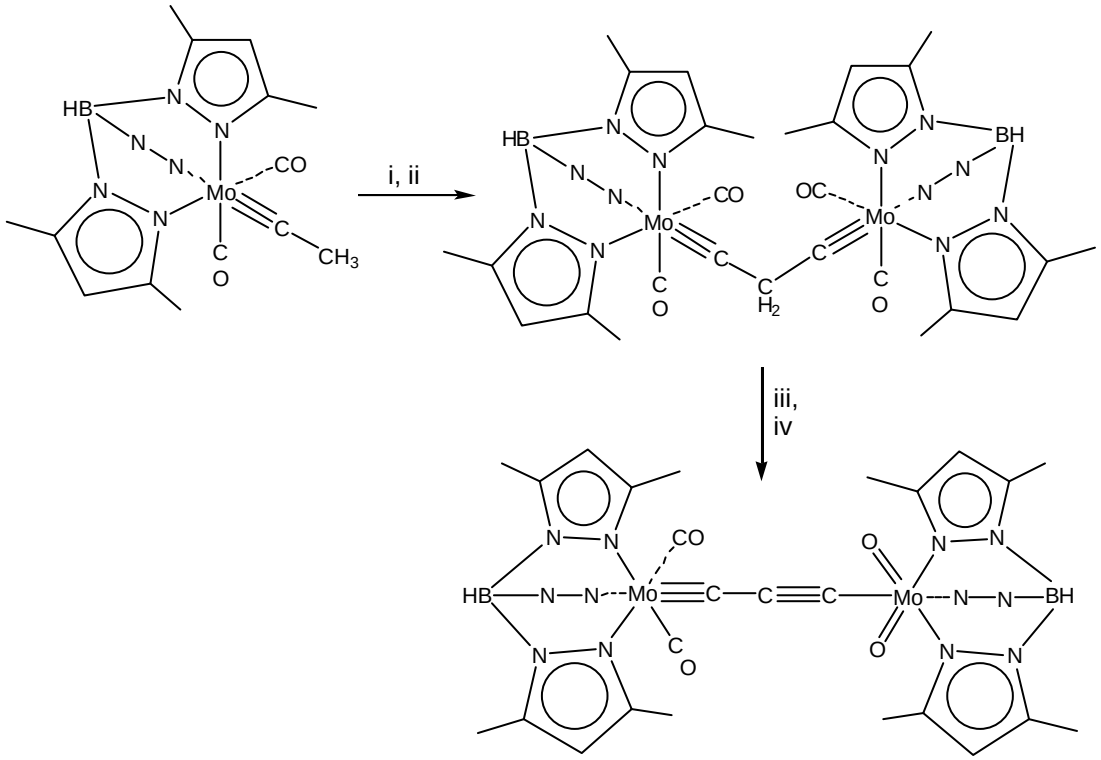

Reagents: i, KO^{t}Bu; ii, Tp*(CO)$_2$Mo≡CCl; iii, 2KO^{t}Bu; iv, O_2.
In this and other schemes, the third pyrazolyl group is indicated by N-N.

Scheme 3.1

3.1.1.2 Synthetic Strategy Two

The lithiated conjugate bases of transition metal ethynyl complexes can react with metal carbonyl complexes to form anionic adducts which can be methylated to give Fischer alkynyl carbene complexes, $L_nMC{\equiv}CC(OMe){=}M'L'_m$. The alkoxy groups can be removed from the carbene complexes with electrophilic agents to give either cationic or neutral carbyne complexes depending on the metal fragment and procedure used.

Employing this synthetic strategy and Re(C≡CH)(NO)(PPh_3)Cp* as the initial ethynyl complex, the complexes {Re(NO)(PPh_3)Cp*}{μ-C≡CC(OMe)=}{$M(CO)_x$} [M = W, x = 5; M = MnCp', (Cp' = Cp, Cp*) x = 2; M = Fe, x = 4] have been isolated.[106] Treatment of the iron and manganese complexes with BF_3 gives the desired carbyne complexes. The spectroscopic data, such as the downfield shift of

the chain carbons in the ^{13}C NMR spectrum and three intense bands at around 1890 cm^{-1} in the IR spectrum suggest the cumulenylidene structure predominates for the $Re^{+}=C=C=C=Mn$ bridge (Scheme 3.2).[106]

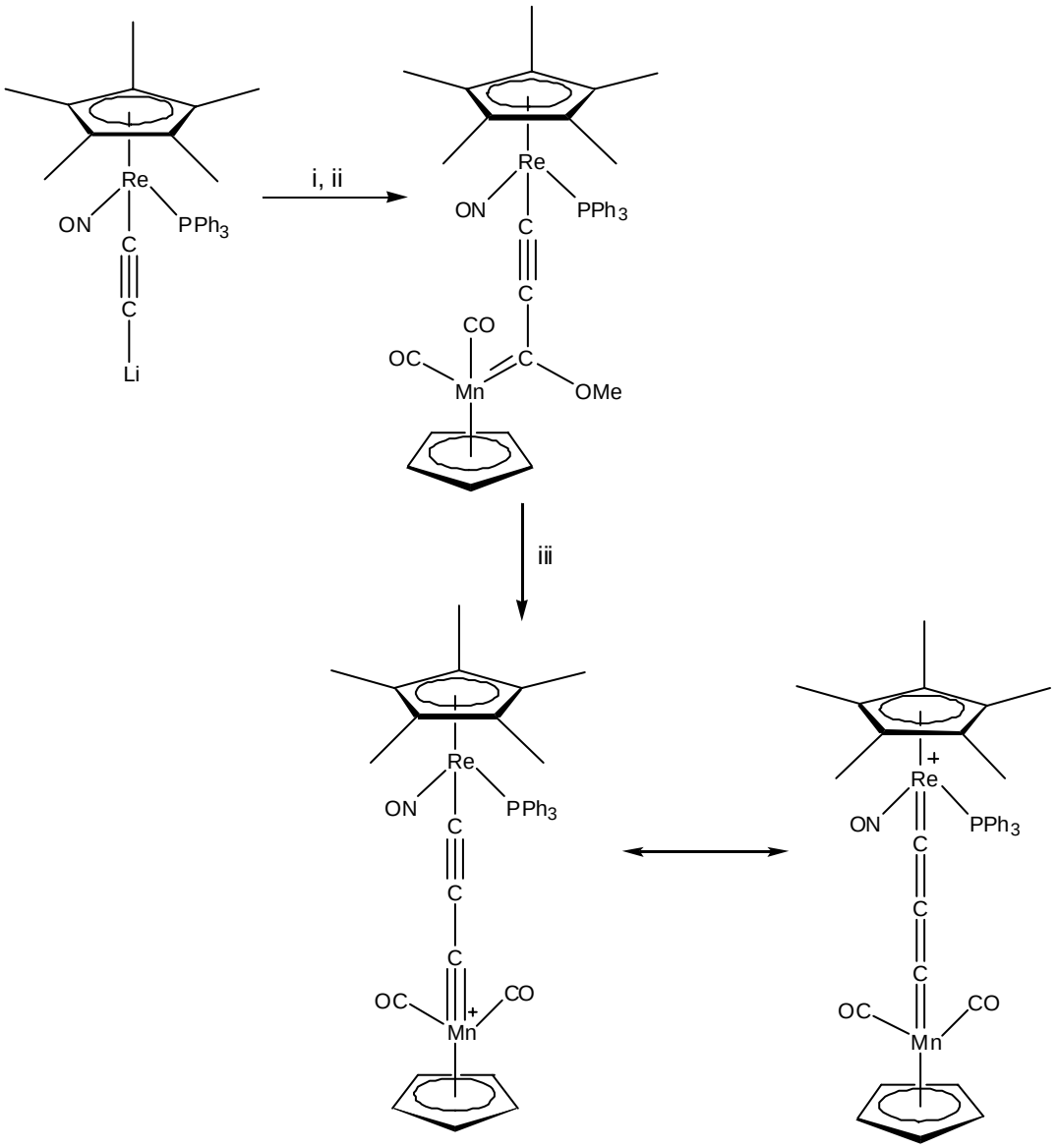

Reagents: i, $Mn(CO)_3Cp$; ii, $[Me_3O]^+[BF_4]^-$; iii, BF_3.

Scheme 3.2

3.1.1.3 Synthetic Strategy Three

The final synthetic strategy involves two alkynes capped by metal centres taking part in a metathesis reaction. This approach has been used in the synthesis of the mixed metal C_3 complex Cp*Re(NO)(PPh_3)(C≡CC≡)W(O^tBu)$_3$ which was formed in 79% yield upon combining the ditungsten tert-butoxy complex, (^{t}BuO)$_3$W≡W(^{t}BuO)$_3$ and rhenium complex Cp*Re(NO)(PPh_3)(C≡CC≡CMe) in toluene[107] (Scheme 3).

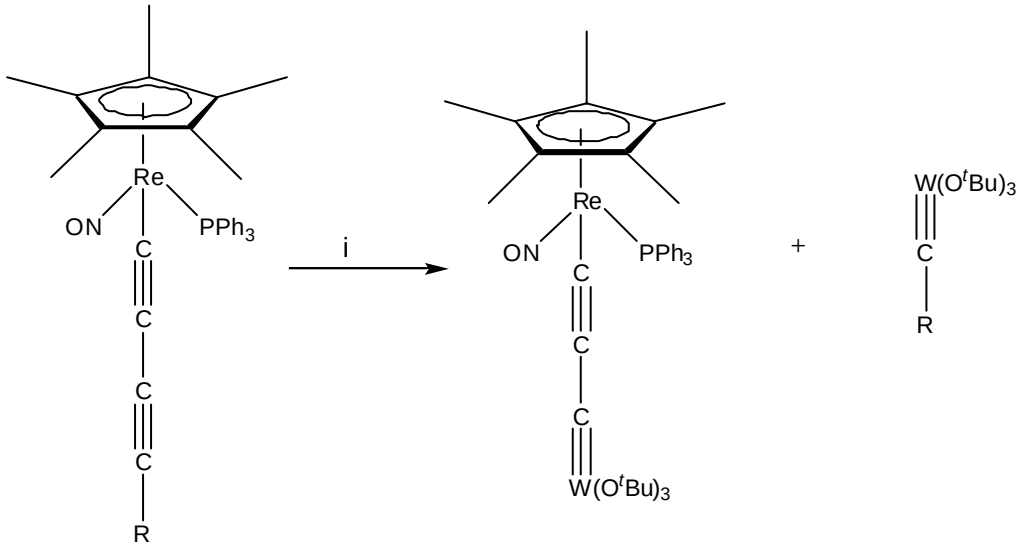

Reagents: i, (^{t}BuO)$_3$W≡W(O^tBu)$_3$; R = Me, H

Scheme 3.3

More recently halide metathesis reactions using nucleophilic anions [L_mM≡C−C≡C]$^-$ have been investigated, with the bimetallic complexes [M≡C−C≡C−RuH(L_n)(PPh_3)$_2$] (M = W(CO)$_2$Tp/Tp*, MoF(CO)$_2$(tmeda)/(bipy); L_n = Hpz', CO, PPh_3, 2,4,6-Me_3-CNC_6H_2) being obtained by treating a range of silylpropargylidynes with [Bu^n_4N]F in the presence of the hydrido complex [RuHCl(CO)L_n(PPh_3)$_2$].[108] Employing this synthetic strategy with [RhCl(CO)(PPh_3)$_2$] gives the expected rhodium analogue, [{(PPh_3)$_2$(CO)$_2$TpW}≡C−C≡C−{Rh(CO)(PPh_3)$_2$}].[109] However, reacting Vaska's complex [IrCl(CO)(PPh_3)$_2$] in the same way results in the formation of the

bis(tricarbido) complex $[IrH(C_3W(CO)_2Tp)_2(CO)(PPh_3)_2]$, most likely due to oxidative addition of reaction intermediates.[110]

3.1.2 Bimetallic Compounds Containing C_5 or Higher Odd-Membered Chains

Some of the methodology used to prepare C_3 complexes has been extended to the synthesis of longer carbon chain analogues. In particular lithiation of the butadiynyl complex $[Cp^*Re(NO)(PPh_3)(C{\equiv}CC{\equiv}CH)]$ followed by successive reactions with $Mn(CO)_3(\eta^5\text{-}C_5Cl_5)$ and $[Me_3O]^+[BF_4]^-$ gives the dark purple C_5OMe complex, $Cp^*Re(NO)(PPh_3)(C{\equiv}CC{\equiv}CC(OMe)=)Mn(CO)_2(\eta^5\text{-}C_5Cl_5)$. Removal of the methoxy group with an excess of BF_3 then gives the C_5 complex $[Cp^*Re(NO)(PPh_3)=C=C=C=C=Mn(CO)_2(\eta^5\text{-}C_5Cl_5)]^+[BF_4]^-$ in 52% yield.[111] Similar reactions were used to prepare analagous $Mn(CO)_2(\eta^5\text{-}C_5Br_5)$ and $Fe(CO)_4$ derivatives. Comparison of the spectroscopic properties with those of the analagous C_3 complex suggests a cumulenic structure, however these complexes are light sensitive and readily decompose.[111]

It has been suggested that the stability of alkyl cumulenes can be improved through the addition of phenyl groups to the two terminal carbons.[112] Thus there have been attempts to synthesise a C_7 cumulene with two ferrocenyl termini by cross-coupling the iodo-alkyne derivative of ferrocenyl(phenyl)methoxypropyne with the homopropargylic ether to give the dimethoxyheptadiyne. Addition of one equivalent of tetrafluoroboric acid results in a two-fold elimination of methanol, to give the air sensitive cumulenium salt, in 15% yield. This salt can be deprotonated by potassium tert-butoxide / n-butyllithium to give the neutral cumulene (Scheme 4).[113] However, this product was still not stable enough to be isolated and was identified only by mass spectrometry.

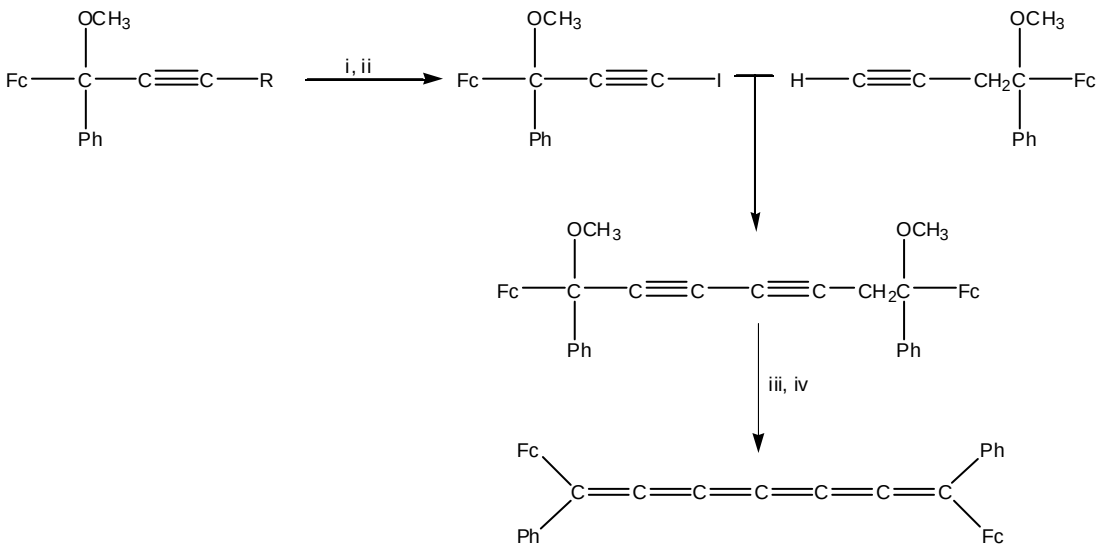

Reagents: i, BuLi; ii, I_2; iii, HBF_4; iv, BuLi/KO^tBu

Scheme 3.4

3.1.3 Carbon Chains Capped by Metal Clusters

The use of metal clusters as end-caps provides another method for the preparation of metal complexes with odd-numbered carbon chains. Complexes of this type usually involve terminal carbons interacting with three metal atoms (Figure 3.3).

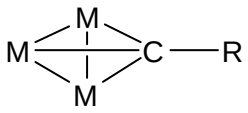

Figure 3.3: *Molecular structure of a trimetallic cluster.*

One such method of producing odd-numbered bridging carbon chains is the coupling of a poly-ynyl gold(I) complex, $\{L_yM\}(C{\equiv}C)_nAuPPh_3$, with a metal cluster of the type $\{L_xM_3\}(\mu_3\text{-}CBr)$ [M = Co, Os], in the presence of catalytic amounts of CuI and $Pd(PPh_3)_4$ (Equation 3.1).[89]

$$\{Cp^*(dppe)Ru\}(C{\equiv}C)_2AuPPh_3 + \{Co_3(dppm)(CO)_7\}(\mu_3\text{-}CBr) \rightarrow \{Cp^*(dppe)Ru\}(C{\equiv}C)_2C{\equiv}\{Co_3(dppm)(CO)_7\}$$

Equation 3.1

Even-numbered carbon chains can also be produced using similar reaction conditions. It has been shown that even-numbered bis(cluster) complexes, $\{L_xM_3\}{\equiv}C(C{\equiv}C)_{2m+n}C{\equiv}\{L_xM_3\}$, can be produced when a diiodo complex, $I(C{\equiv}C)_nI$, and two equivalents of a metal cluster poly-ynyl gold complex, $\{L_xM_3\}{\equiv}C(C{\equiv}C)_mAuPPh_3$, react in the presence of catalytic amounts of CuI and $Pd(PPh_3)_4$ (Equation 3.2).[89]

$$2\{(CO)_7(dppm)Co_3\}{\equiv}C(C{\equiv}C)_2AuPPh_3 + I(C{\equiv}C)_3I \rightarrow \{(CO)_7(dppm)Co_3\}{\equiv}C(C{\equiv}C)_7C{\equiv}\{Co_3(dppm)(CO)_7\}$$

Equation 3.2

New precursors to odd-numbered chains are required to enable bridging chains of varying length to be easily accessed. The use of the gold reaction and mono-metallic carbyne complexes should enable the isolation of a variety of metal-capped complexes with an odd-numbered bridging carbon chain.

3.2 Results and Discussion

Earlier reports have described the synthesis of alkynylcarbyne-molybdenum complexes by treatment of $Mo(CO)_6$ with $LiC{\equiv}CBu^t$, followed by addition of $(CF_3CO)_2O$ and *N,N,N',N'*-tetramethyldiaminoethane (tmeda) to give $Mo({\equiv}CC{\equiv}CBu^t)\{OC(O)CF_3\}(CO)_2(tmeda)$.[114] The $SiMe_3$ analogue **13** (Scheme 3.5) was made via this route and orange crystals obtained, on which a single-crystal structure determination was performed (Figure 3.4). The spectroscopic properties are consistent with the solid state structure being retained in solution, with ν(CC) at 2046 cm^{-1}, ν(CO) at 2013 and 1934 cm^{-1} and the ester ν(CO) at 1711 cm^{-1}. The NMR spectra contain resonances for the $SiMe_3$ group at δ_H 0.17 and δ_C 0.54, for the tmeda ligand at δ_H 3.02 (Me) and 2.80 (CH_2) and δ_C 50.85, 55.69 and 60.81, and the CF_3CO_2 group at δ_C 116.88 and 160.88 [quartets with *J*(CF) 289 and 36 Hz, respectively]. The alkynyl carbons are found at δ_C 73.33 and 112.74 and the carbons attached to Mo are at δ_C 224.76 (CO) and 261.16 (C≡Mo).

The molybdenum atom is octahedrally coordinated by the $CC{\equiv}CSiMe_3$ fragment, the CF_3CO_2 anion [Mo-O 2.192(4) Å], two CO groups [Mo-C(10, 10) 2.009(9), 1.992(7) Å] and the chelating tmeda ligand [Mo-N(01), N(02) 2.281(6), 2.275(7) Å], with angles subtended at Mo by *cis* pairs of ligands ranging between 88.9 and 93.2(3)°, with the exception of the tmeda ligand which, with its small bite angle, subtends an angle of only 79.4(2)°; other X-Mo-N(n) angles are larger as a result, ranging from 87.9 to 109.3(5)°. In the context of the present work, the geometry of the alkynylcarbyne is of interest. The distances in the Mo≡C-C≡C-Si fragment [1.82(1), 1.38(2), 1.21(2), 1.84(1) Å] confirm its formulation, with angles at C(1,2,3) of 174.2(12), 177.0(16) and 178.3(13)°. This atom string is disordered, with an equal population in a second site, located with C(1)-Mo-C(1') 18.0(8)° and having essentially identical geometrical parameters.

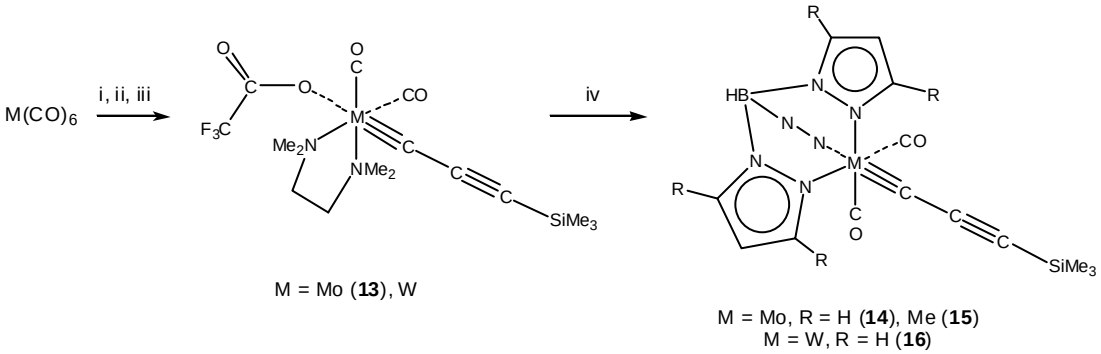

Reagents: i, $HC{\equiv}CSiMe_3$ / LiBu; ii, $(CF_3CO)_2O$; iii, tmeda; iv, KTp' (Tp' = Tp, Tp*).
In this and other schemes, the thrid pyrazolyl group is indicated by N-N.

Scheme 3.5

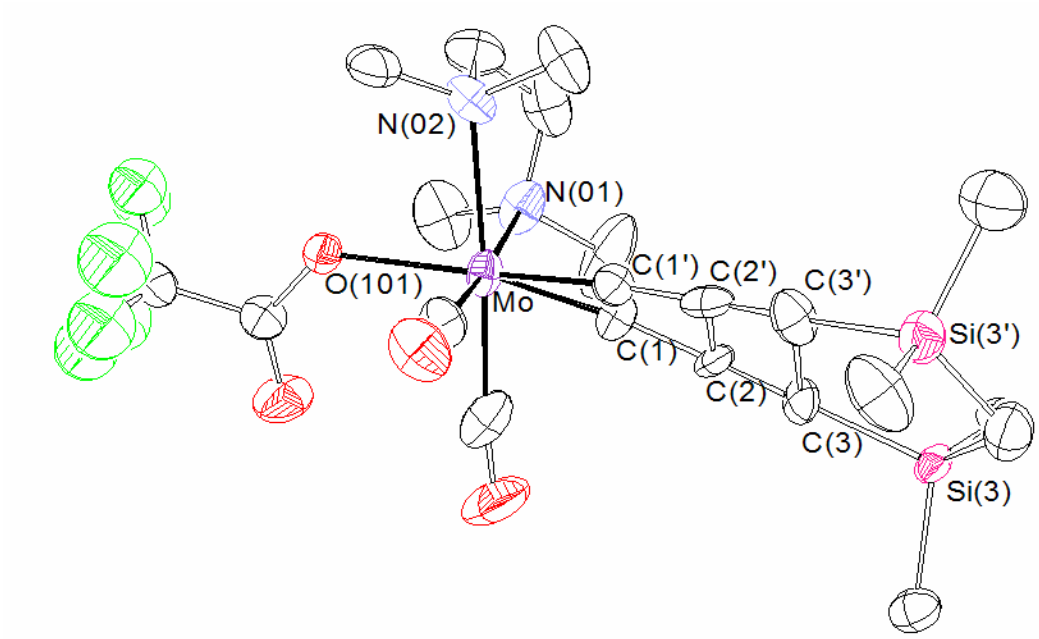

Figure 3.4: *ORTEP view of Mo(≡CC≡CSiMe$_3$){OC(O)CF$_3$}(CO)$_2$(tmeda)(**13**).*

Table 3.1: *Selected structural data for Mo(≡CC≡CSiMe$_3$){OC(O)CF$_3$}(CO)$_2$(tmeda)(**13**). Italicised values refer to molecule 2.*

Bond Distances (Å)		**Bond Angles (˚)**	
Mo-O(101)	2.192(4)	N(01)-Mo-N(02)	79.4(2)
Mo-C(10, 20)	2.009(9), 1.992(7)	O(101)-Mo-N(02)	81.8(2)
Mo-N(01, 02)	2.281(6), 2.275(7)	C(10)-Mo-O(101)	93.2(2)
Mo-C(1)	1.81(1), *1.81(1)*	C(20)-Mo-C(10)	88.9(4)
C(1)-C(2)	1.38(2), *1.36(1)*	C(1)-Mo-C(10)	75.8(6), *92.0(6)*
C(2)-C(3)	1.21(2), *1.22(2)*	Mo-C(1)-C(2)	174(1), *171(1)*
C(3)-Si	1.84(1), *1.84(1)*	C(1)-C(2)-C(3)	177(2), *180(2)*
		C(2)-C(3)-Si	178(1), *172(1)*

Reactions of **13** with KTp or KTp* (KTp = K[BH(pz)$_3$], KTp* = K[BH(dmpz)$_3$]) overnight give Mo(≡CC≡CSiMe$_3$)(CO)$_2$Tp' [Tp' = Tp (**14**), 34%; Tp* (**15**), 30%]. The IR spectrum of **14** contains a ν(BH) band at 2482 cm^{-1}, ν(CC) at 2046 cm^{-1} and terminal ν(CO) bands at 2004 and 1925 cm^{-1}. For **14** and **15**, the Tp' ligands give rise to characteristic ^{1}H and ^{13}C resonances which have a 2/1 relative intensity as a result of the MoA$_2$B ligand coordination. These occur between δ_c 104.9 and 107.8, between 134.8 and 145.7 and between 143.1 and 152.1, being assigned to C^4, C^3 and C^5 respectively. For **15,** the latter two resonances are found *ca* 8 ppm upfield from those in **14**. In a few cases, the two resonances overlap, as in **15**, where only one signal at δ_c 106.46 is observed. In the ^{13}C NMR spectrum of **15** resonances for the three methyl groups are found at δ12.97, 14.84 and 16.00. IR absorptions for the ν(CC) and ν(CO) vibrations are found in the usual regions, while the carbons of the Mo≡CC≡C systems are now found at δ_c 259.41, 113.52 and 76.48 (for **14**) and at δ_c 255.41, 113.49 and 75.28 (for **15**). The analogous tungsten complexes W(≡CC≡CSiMe$_3$)(CO)$_2$Tp' [Tp' = Tp(**16**), Tp*] have been reported on earlier occasions.[115]

The molecular structure of **14** was confirmed by single-crystal X-ray studies. (Figure 3.5) Important bond parameters are shown in Table 3.2. The Mo(CO)$_2$Tp fragment

is similar to that found in many other derivatives which have been studied earlier, of which Mo(≡Ctol)$(CO)_2$Tp* is perhaps the most closely related recent example.[116] The molybdenum atom is octahedrally coordinated, with the Tp ligand occupying three facial positions. The Mo-N(12, 22) bonds [2.234(6), 2.222(6) Å] *trans* to CO are shorter than Mo-N(32) [2.308(5) Å] which is *trans* to the carbyne ligand, as a result of better back-bonding into the latter. The other three sites are occupied by the two CO ligands [Mo-C(20, 30) 2.010(8), 2.007(8) Å] and the ≡CC≡C group. The Mo≡C(1) bond is considerably shorter, [1.833(7) Å], than the two Mo-CO bonds, as expected from its multiple-bond character, but longer than that in Mo(≡Ctol)$(CO)_2$Tp* [1.804(4) Å]. The carbon chain is essentially linear, angles at C(1,2,3) being 176.8(8), 178.9(7) and 179.3(6)˚, respectively.

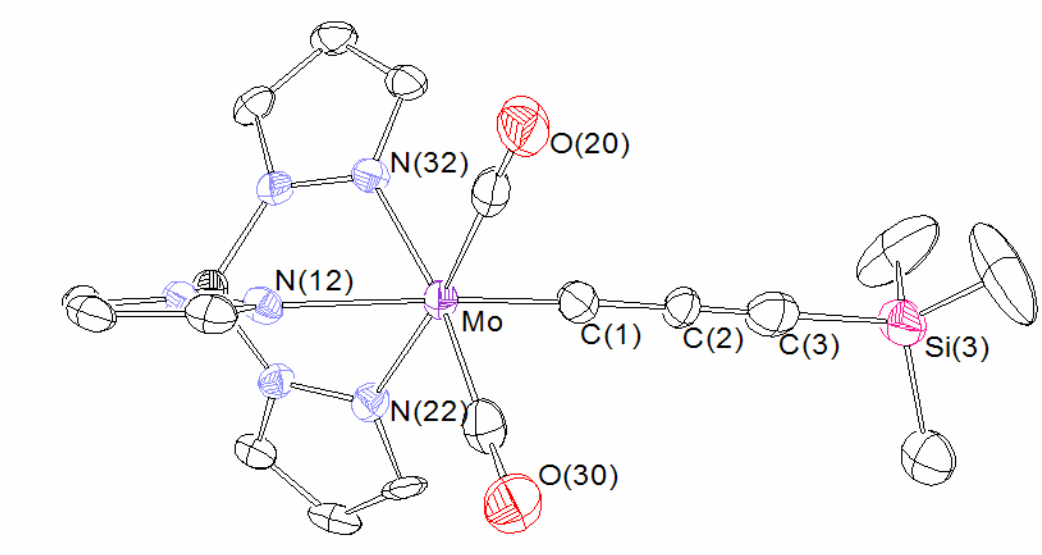

Figure 3.5: *ORTEP view of Mo(≡CC≡CSiMe$_3$)$(CO)_2$Tp* ***(14)****.*

Table 3.2: *Selected structural data for Mo(≡CC≡CSiMe$_3$)(CO)$_2$Tp (**14**) and Mo(≡Ctol)(CO)$_2$Tp*.*

Complex	**14**	**Mo(≡Ctol)(CO)$_2$Tp*[116]**
Bond Distances (Å)		
Mo-C(10,20)	2.010(8), 2.007(8)	1.987(4), 1.987(4)
Mo-N(12,22)	2.234(6), 2.222(6)	2.218(3), 2.212(3)
Mo-N(32)	2.308(5)	2.306(3)
Mo-C(1)	1.833(7)	1.804(4)
C(1)-C(2)	1.399(10)	1.449(5)
C(2)-C(3)	1.258(11)	
C(3)-Si	1.846(9)	
Bond Angles (˚)		
C(1)-Mo-N(12,22)	101.6(3), 98.4(3)	
C(1)-Mo-N(32)	176.9(3)	
C(1)-Mo-C(10,20)	86.5(4), 87.8(3)	
Mo-C(1)-C(2)	176.8(8)	163.1(3)
C(1)-C(2)-C(3)	178.9(7)	
C(2)-C(3)-Si	179.3(6)	

Red crystalline Mo{≡CC≡CAu(PPh$_3$)}(CO)$_2$Tp (**17**) was obtained in 88% yield by reaction of **14** with AuCl(PPh$_3$) in the presence of potassium carbonate (Scheme 3.6). The IR spectrum of this complex contains two strong ν(CO) bands at 1982 and 1904, ν(CC) at 2015 and ν(BH) at 2483 cm^{-1}. In the ^{1}H NMR spectrum, the pyrazole (pz) protons occur as two triplets which have a relative intensity 1:2 at δ 5.62 and 5.72 and four doublets with relative intensities of 1:1:2:2 at δ 7.21, 7.26, 7.30 and 7.91, being differentiated by the asymmetry at the molybdenum centre. Carbons of the pz groups resonate at δ 106.22 and 106.27 C^4, at 136.48 and 136.56 C^3, and at 144.69 and 144.82 C^5 in the ^{13}C NMR spectrum, with two of the C(*sp*) atoms found at δ 104.65 and 115.49. The Mo-CO and Mo≡C resonances are at δ 228.42 and 265.15, respectively. The ^{31}P NMR spectrum contains a singlet at δ 41.6 for the PPh$_3$ ligand. The electrospray (ES) mass spectrum contains various aggregate ions at *m/z* 1321 ([M + Au(PPh$_3$)]$^+$), 1125 ([M + HPPh$_3$]$^+$), 885 ([M + Na]$^+$) and 721 ([Au(PPh$_3$)$_2$]$^+$),

these being commonly observed in the mass spectra of $Au(PR_3)$ complexes.[117,118] The analogous tungsten complex **18** was prepared in a similar fashion in 69% yield and has similar spectroscopic properties, including ν(BH) at 2483, ν(CC) at 2020 and ν(CO) at 1970 and 1886 cm^{-1}. In the ^{13}C NMR spectrum, the W≡C and W−CO resonances are at δ 258.25 and 226.73, but the other carbons of the C_3 chain were not resolved. Complex **18** was also reported by Hill and his group[119] during the preparation of this thesis.

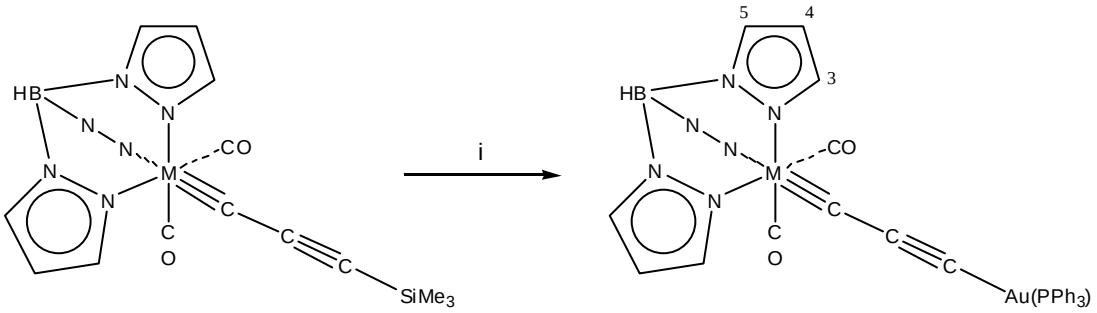

M = Mo (**14**), W (**16**)

M = Mo (**17**), W (**18**)

Reagents: i, $AuCl(PPh_3)$ / K_2CO_3, MeOH.

Scheme 3.6

It has previously been shown that the Pd(0) / Cu(I)-catalysed elimination of $AuX(PR_3)$ from reactions of compounds containing C(sp)-X [X = halide and $Au(PR_3)$] groups is an efficient method of forming C-C bonds which, in contrast to the well-known Sonogashira reaction, does not require the presence of a base (amine), which may attack the organometallic reactants and products.[89] The reactions between **17** or **18** and $Co_3(\mu_3\text{-CBr})(\mu\text{-dppm})(CO)_7$[120] proceed under mild conditions (thf, r.t., 2 h) to give $\{Tp(OC)_2M\}{\equiv}CC{\equiv}CC{\equiv}\{Co_3(\mu\text{-dppm})(CO)_7\}$ [M = Mo (**19**) (39%), W (**20**) (37%)] as brown solids (Scheme 3.7). These complexes were characterised by elemental microanalysis and spectroscopically. The IR spectra contain five terminal ν(CO) bands between 2060 and 1904 cm^{-1} and in the ^1H NMR spectra pz protons are found at δ 5.68, 5.77 (Mo) and 5.60, 5.70 (W). In the ^{13}C NMR spectra the pz carbons are found at δ 105.44/105.58, 135.47/135.65, 143.09/144.51 (Mo), 106.65/106.71, 135.44/135.76, 144.57/146.05 (W), C≡C

carbons at δ 87.79, 125.19 (Mo), Co-CO at δ 201.26, 209.90 (br) (Mo), M-CO at δ 230.49 (Mo), 229.97 (W) and M≡C at δ 252.92 (Mo), 246.80 (W). The ES-MS contain, $[M + Na]^+$ at *m/z* 1195 (Mo), $[M – H]^-$ at *m/z* 1257 (W).

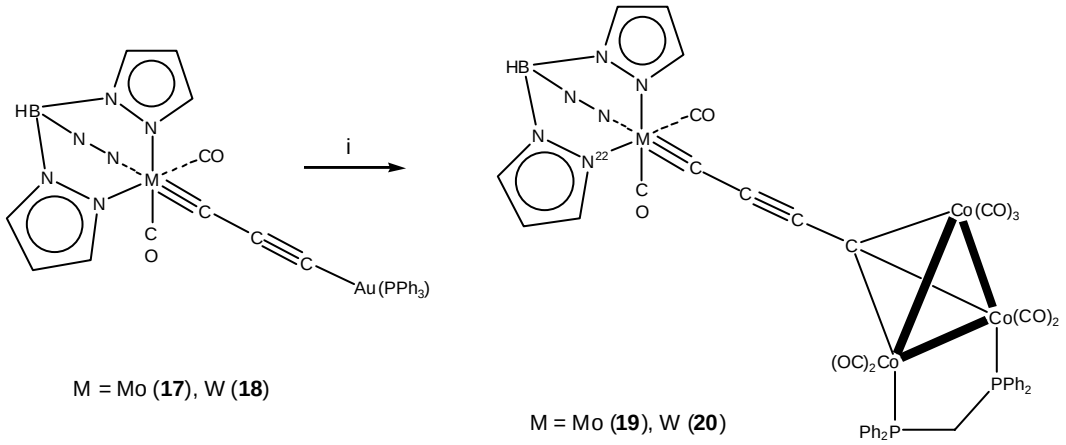

Reagents: $Co_3(\mu_3\text{-}CBr)(\mu\text{-}dppm)(CO)_7$, $Pd(PPh_3)_4$ / CuI.

Scheme 3.7:

The reverse reaction, i.e., between $Mo(\equiv CBr)(CO)_2Tp^*$ and $Co_3(\mu_3\text{-}CC{\equiv}CC{\equiv}CAuPPh_3)(\mu\text{-}dppm)(CO)_7$, afforded the corresponding $Tp^*Mo\text{-}C_6$ derivative **21** in 72% yield (Scheme 3.8). The IR spectrum contains ν(C≡C) bands at 2109 cm^{-1} and ν(CO) between 2060 and 1908cm^{-1}. The ^1H NMR spectrum has two pairs of pyrazolyl-Me resonances at δ 2.32, 2.38 and 2.34, 2.61 and the two pyrazolyl protons with relative intensity 1:2 at δ 5.71 and 5.88. In the ^{13}C NMR spectrum, the pyrazolyl-Me carbons are found at δ 12.68, 14.65 and 15.93 while the ring carbons are at δ 106.34/106.36, 144.45/145.07 and 151.28, the Co-CO at δ 201.29, 209.49, the Mo-CO at δ 229.48 and the Mo≡C at δ 261.02. We assign resonances at δ 52.55, 96.73, 100.92 and 107.95 to four of the six carbon chain nuclei; that attached to the Co_3 cluster is likely to be broadened by the ^{59}Co nuclear quadrupole.[121,122] The ES MS contains $[M + Na]^+$ at *m/z* 1302.

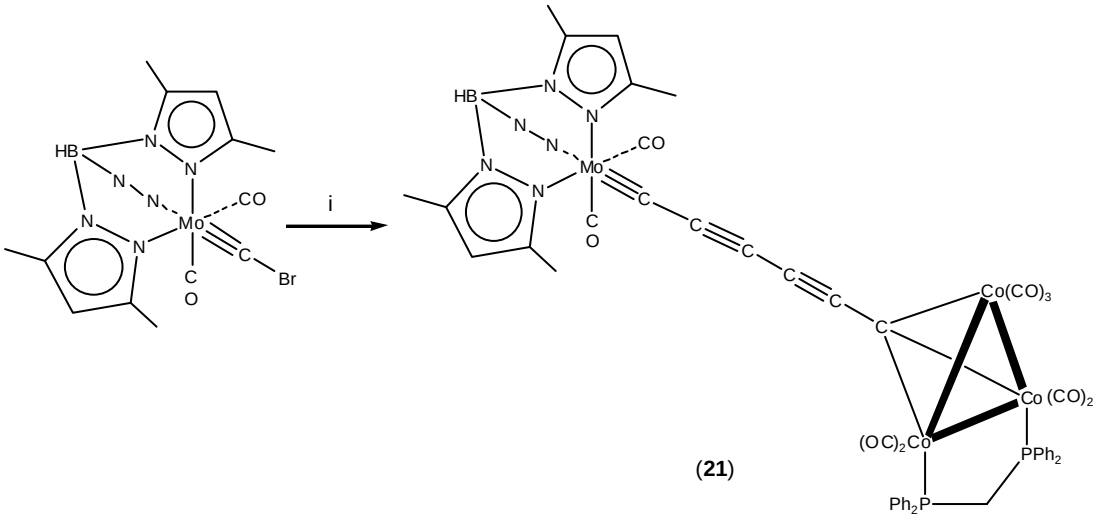

(**21**)

Reagents: $Co_3\{\mu_3\text{-}CC{\equiv}CC{\equiv}CAu(PPh_3)\}(\mu\text{-dppm})(CO)_7$, $Pd(PPh_3)_4$ / CuI.

Scheme 3.8

The molecular structures of **19**, **20** and **21** were confirmed by single crystal X-ray studies (Figures 3.6-8). Along the Mo-C(1)-C(2)-C(3)-X chain, C(1)-C(2) is between 1.35(1) and 1.355(6) Å, while C(2)-C(3) is between 1.24(1) and 1.25(1) Å, somewhat longer than expected for a normal C(sp)-C(sp) bond. In the longer chain in **21**, alternation with C(sp)-C(sp) single bonds of 1.332(6) and 1.371(6) Å and the second C≡C triple bond of 1.231(6) Å, for example, shows that there is a small amount of electron delocalisation occurring. The $Co_3(\mu\text{-dppm})(CO)_7$ clusters are similar to those found in many related examples that have been reported recently, with the dppm ligand occupying equatorial coordination sites bridging the Co(1)-Co(2) bond.[120,123-125] The other bond parameters are unexceptional, with Co-Co distances between 2.483 and 2.502(1) Å, Co-P bonds of 2.198-2.216(3) Å , and Co-C(4 or 6) being in the range 1.880 to 1.953(8) Å.

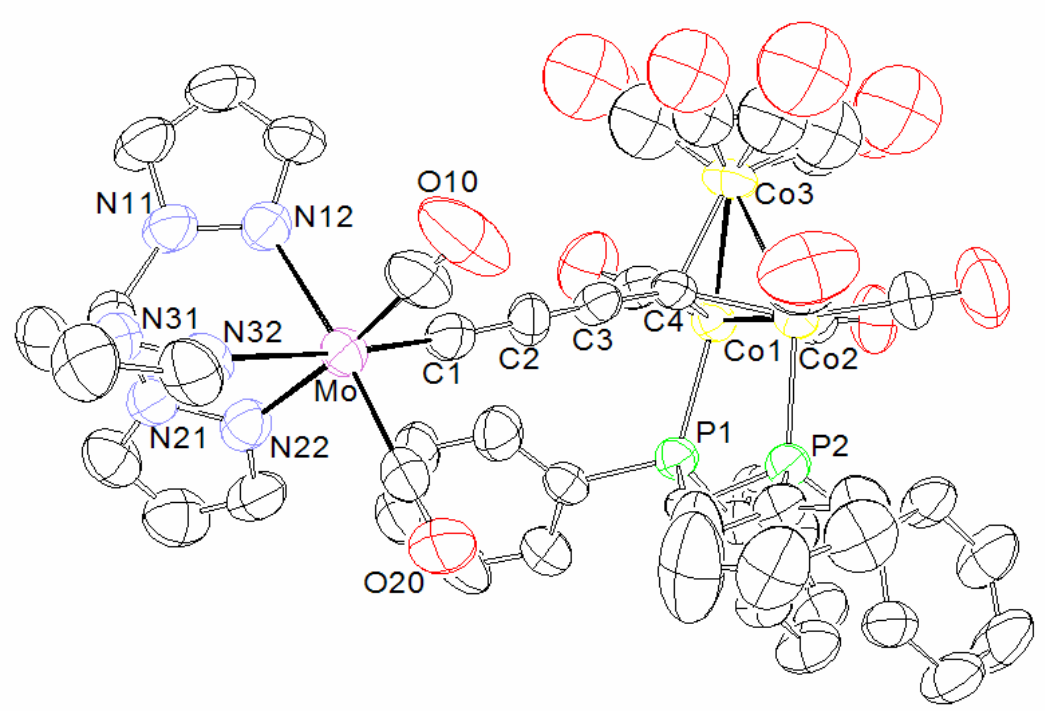

Figure 3.6: *ORTEP view of {Tp(OC)$_2$Mo}≡CC≡CC≡{Co$_3$(μ-dppm)(CO)$_7$}* ***(19)****.*

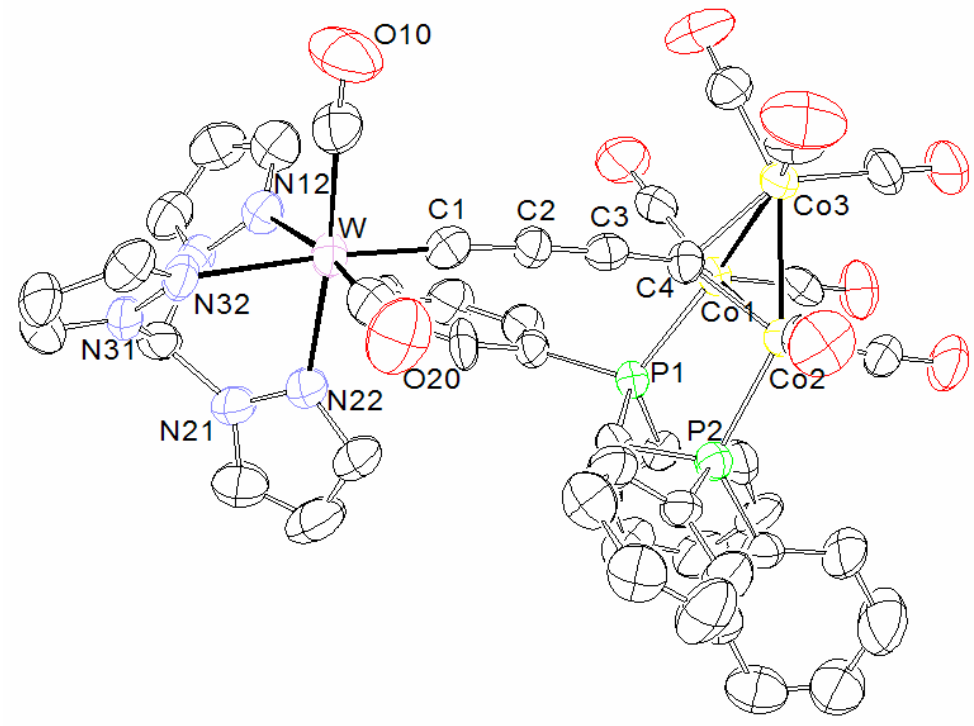

Figure 3.7: *ORTEP view of {Tp(OC)$_2$W}≡CC≡CC≡{Co$_3$(μ-dppm)(CO)$_7$}* ***(20)****.*

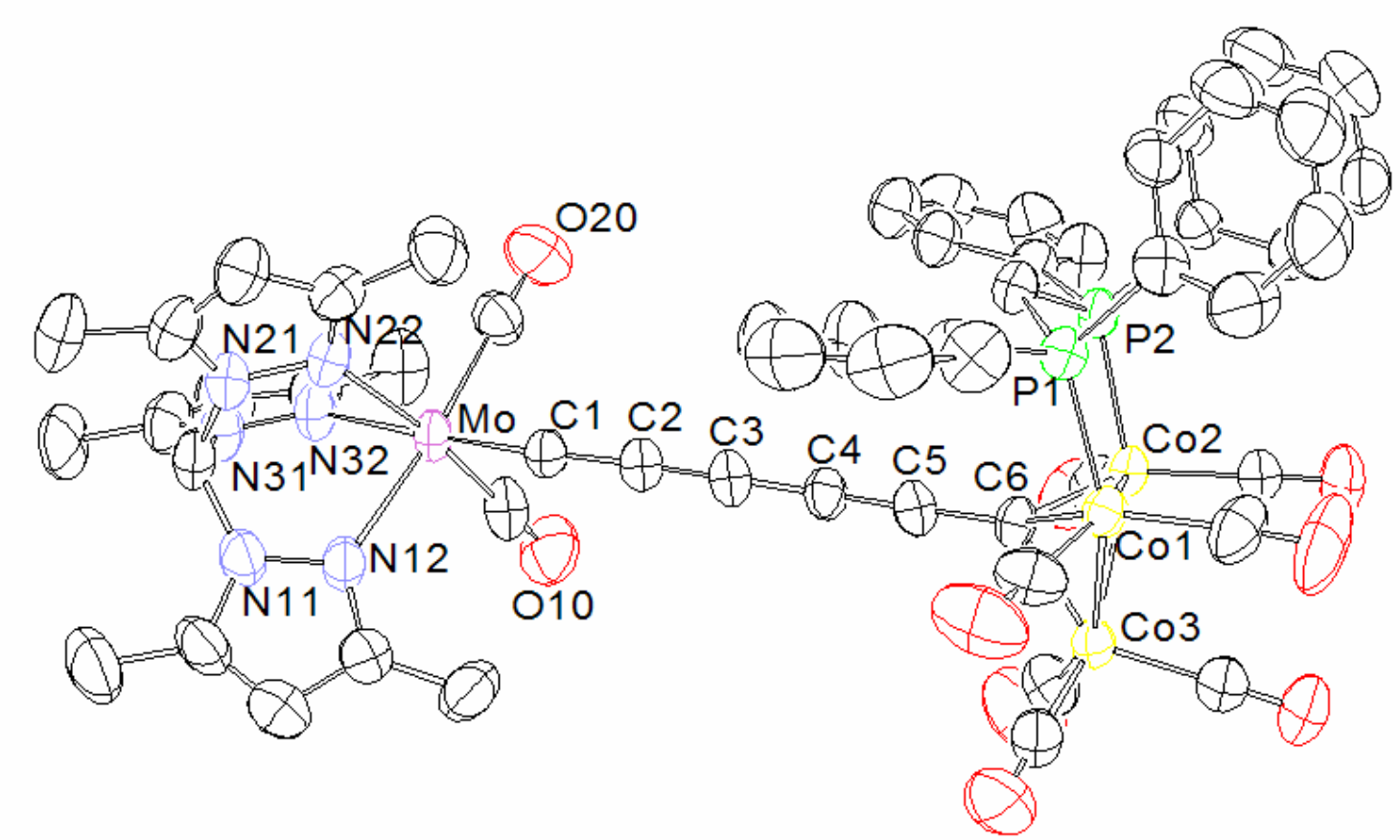

Figure 3.8: *ORTEP view of {Tp(OC)$_2$Mo}≡CC≡CC≡CC≡{Co$_3$(μ-dppm)(CO)$_7$}* ***(21)****.*

Table 3.2: *Selected structural data for {Tp(OC)$_2$M}≡CC≡CC≡{Co$_3$(μ-dppm)(CO)$_7$} M = Mo (**19**), W (**20**) and {Tp(OC)$_2$Mo}≡CC≡CC≡CC≡{Co$_3$(μ-dppm)(CO)$_7$} (**21**).*

Complex	**19**	**20**	**21**
Bond Distances (Å)			
Mo-C(10,20)	1.99(2), 1.993(9)	2.010(9), 1.96(1)	2.004(7), 1.983(7)
Mo-N(12,22)	2.213(6), 2.231(9)	2.198(7), 2.231(6)	2.223(5), 2.216(5)
Mo-N(32)	2.313(6)	2.296(6)	2.289(5)
Mo-C(1)	1.838(7)	1.857(7)	1.842(5)
C(1)-C(2)	1.35(1)	1.35(1)	1.355(6)
C(2)-C(3)	1.25(1)	1.24(1)	1.246(6)
C(3)-C(4)	1.40(1)	1.38(1)	1.332(6)
Co(1)-Co(2,3)	2.501, 2.485(2)	2.475(1), 2.491(1)	2.490, 2.483(1)
Co(2)-Co(3)	2.502(1)	2.477(1)	2.472(1)
Co(n)-P(n) (n = 1,2)	2.216, 2.215(3)	2.219(2), 2.211(2)	2.214, 2.198(2)
Co(1,2,3)-C(n) [C(n)]	1.880, 1.916, 1.953(8) [C(4)]	1.909(7), 1.905(7), 1.950(7) [C(4)]	1.904, 1.910, 1.950(5) [C(6)]
Bond Angles (˚)			
C(1)-Mo-N(12,22)	97.5(3), 103.2(4)	103.1(3), 96.2(3)	102.1, 105.9
C(1)-Mo-N(32)	174.7(4)	174.7(4)	169.6(2)
C(1)-Mo-C(10,20)	85.0(4), 86.3(3)	88.4(3), 86.7(4)	81.5, 83.5(2)
Mo-C(1)-C(2)	172.9(9)	176.9(6)	166.2(4)
C(1)-C(2)-C(3)	177.4(9)	175.0(7)	176.7(6)
C(2)-C(3)-C(4)	177.1(7)	175.8(7)	177.8(6)
C(5)-C(6)-Co(1,2,3)	138.4(8), 126.0(5), 128.6(6) [C(3,4)]		131.6, 134.4, 129.2(4)

For **8** C(4)-C(5) 1.231(6), C(5)-C(6) 1.371(6) Å; C(3)-C(4)-C(5) 179.9(6), C(4)-C(5)-C(6) 178.7(7)°.

An alternative method of preparing M-C(sp) bonds is via fluoride-catalysed metallo-desilylation, which has been shown to be particularly effective in reactions of trimethylsilyl-substituted alkynes with halides of electron-rich metal centres, such as $RuCl(PPh_3)_2Cp$.[81] The reaction of **14** with RuCl(dppe)Cp* in the presence of KF in methanol afforded red $\{Tp(OC)_2Mo\}\equiv CC\equiv C\{Ru(dppe)Cp^*\}$ (**22**) in 60% yield. (Scheme 3.9) The IR spectrum of this complex contains a ν(CC) band at 1975 and terminal ν(CO) bands at 1902 and 1863 cm^{-1}. In the ^1H NMR spectrum, the pz protons are found at δ 5.65 and 5.85, with the Cp* Me resonance at δ 1.50. Corresponding features are found in the ^{13}C NMR spectrum at δ 9.98 and 94.70 (Me and ring C of Cp*), 104.91/105.10, 136.13/136.46, 143.46/144.32 (pz) and 230.65 (Mo-CO); the Mo≡C resonance was not found. Finally, the ES-MS contains $[M + H]^+$ at *m/z* 1036. The tungsten analogue $\{Tp(OC)_2W\}\equiv CC\equiv C\{Ru(dppe)Cp^*\}$ (**23**) was obtained similarly from **16** in 36% yield and has comparable spectroscopic properties.

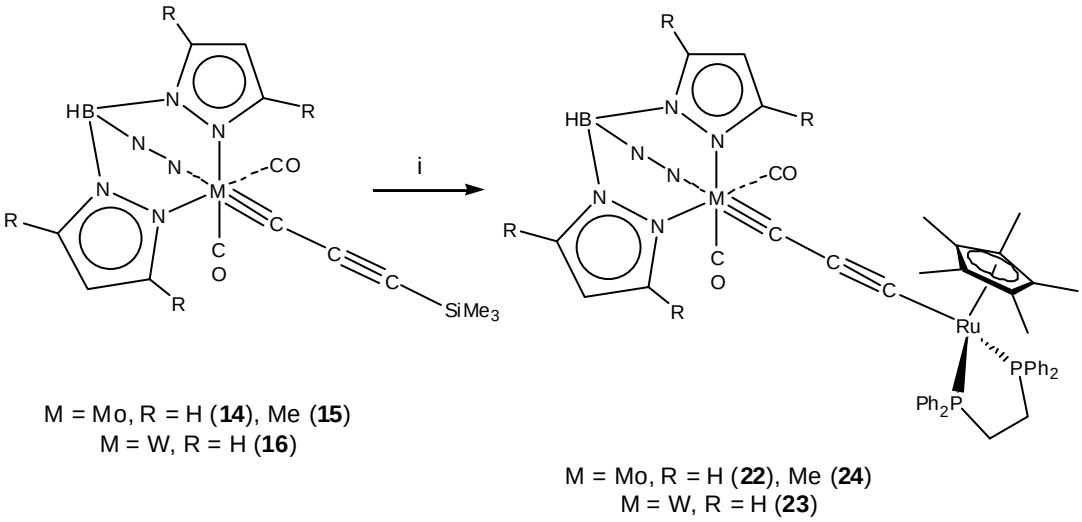

M = Mo, R = H (**14**), Me (**15**)
M = W, R = H (**16**)

M = Mo, R = H (**22**), Me (**24**)
M = W, R = H (**23**)

Reagents: i, RuCl(dppe)Cp*, KF, MeOH.

Scheme 3.9:

A reaction between **15** and RuCl(dppe)Cp* gave the Tp* analogue (**24**) as an orange solid in 36% yield. Spectral features are similar to those of **22**, with the dmpz Me groups resonating at δ_H 2.18, 2.24, 2.63 and 2.69 and the remaining pz H atoms at δ

5.46 and 5.65. In the ^{13}C NMR spectrum the Cp* Me and ring carbons are at δ 10.67 and 95.07, respectively, with the pz Me groups at δ 13.30, 15.59 and 16.62; the ring carbons are found at δ 106.28/106.47, 143.51/143.86, 151.51/151.66, while the Mo-bonded CO and carbyne carbons resonate at δ 230.95 and 254.47, respectively.

The structure of **24** was confirmed by X-ray studies of crystals obtained from dichloromethane/methanol (Figure 3.8). Two independent molecules were found in which the molybdenum atom displays the usual octahedral coordination with the Mo-C(1) bond, 1.868 Å, being longer than the Mo-CO bonds, 1.97, 1.98(1) Å. Along the carbon chain C(1)-C(2) is 1.34(1) Å while C(2)-C(3) is 1.24(2) Å. The Ru-C(3) distance is 1.95(1) Å, somewhat shorter than that found in $Ru(C{\equiv}CC{\equiv}CSiMe_3)(dppe)Cp^*$ [1.983(2) Å], for example.[126] The carbon chain is essentially linear, angles at C(1,2,3) being 173(1), 172(1) and 178(1)°, respectively. The Ru(dppe)Cp* fragment has the expected geometry, with Ru-P 2.269-2.297(3) Å and Ru-C(Cp*) 2.223-2/279(9) (av. 2.25_8 Å).

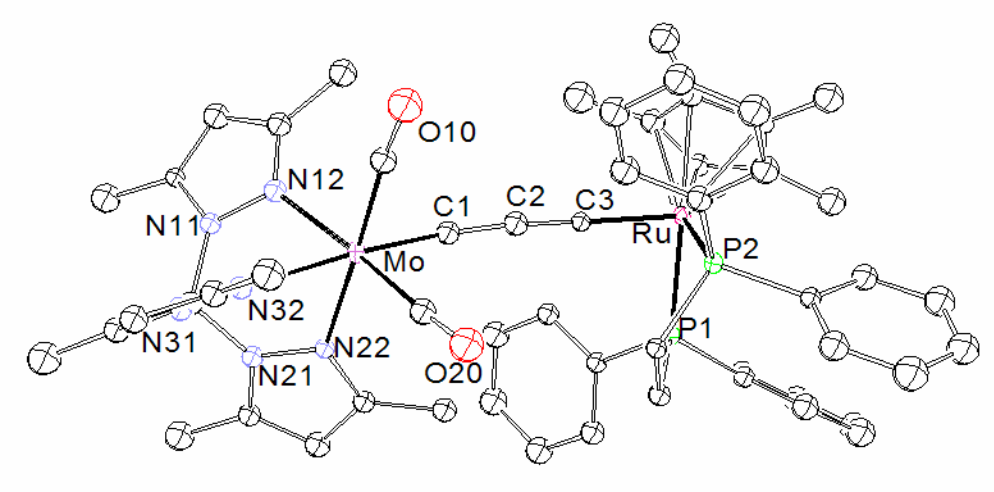

Figure 3.9: *ORTEP view of {Tp*(OC)$_2$Mo}≡CC≡C{Ru(dppe)Cp*}* ***(24)****.*

Table 3.4: *Selected structural data for {Tp*(OC)$_2$Mo}≡CC≡C{Ru(dppe)Cp*}* ***(24)****.*

Bond Distances (Å)		**Bond Angles (˚)**	
Mo-C(10,20)	1.97, 1.98(1)	C(1)-Mo-N(12,22)	102.5(4), 95.8(4)
	1.96, 1.97(1)		*100.0(4), 95.6(4)*
Mo-N(12,22)	2.23(1), 2.235(9)	C(1)-Mo-N(32)	175.6(5) *176.9(4)*
	2.23, 2.25(1)		
Mo-N(32)	2.328(7), *2.324(8)*	C(1)-Mo-C(10,20)	83.9(5), 83.1(4)
			85.7(4), 84.6(5)
Mo-C(1)	1.868(9), *1.849(9)*	Mo-C(1)-C(2)	172.8(10), *174.5(9)*
C(1)-C(2)	1.34(1), *1.36(1)*	C(1)-C(2)-C(3)	172.2(10), *174.7(12)*
C(2)-C(3)	1.24(2), *1.25(2)*	C(2)-C(3)-Ru	177.8(10), *176.7(10)*
C(3)-Ru	1.97(1), *1.95(1)*	P(1)-Ru-P(2)	81.7(1), *82.3(1)*
Ru-P(1,2)	2.272(3), 2.276(2)	P(1,2)-Ru-C(3)	86.3(3), 84.6(3)
	2.269(3), 2.297(3)		*86.6(3), 85.4(3)*
Ru-C(Cp*)	2.223-2.279(9)		
	2.23-2.28(1)		
Ru-C(Cp*) (av.)	2.26(2), *2.25(2)*		

Italicised values refer to molecule 2.

Lengthening of the carbon chain was achieved by Pd(0) / Cu(I)-catalysed reactions between Mo(≡CBr)$(CO)_2$Tp* and Ru{$(C\equiv C)_n$Au(PPh_3)}(dppe)Cp* (n = 2, 3) which afforded the red C_5 and C_7 complexes {Tp*$(OC)_2$Mo}≡C$(C\equiv C)_n${Ru(dppe)Cp*} (n = 2 **25**, 3 **26**) in 67 and 49% yield, respectively. Elemental analyses and their ES mass spectra confirmed the formulations of these complexes, supported by the usual spectroscopic data. Thus, the IR spectra contain two ν(CO) bands at 1899 and 1856 (for **25**) and 1916 and 1868 cm^{-1}(for **26**). In the ^{1}H NMR spectrum, the usual resonances for the ligands are found, while in the ^{13}C NMR spectrum, characteristic resonances at δ 10.42 and 94.87 (for **25**) or 10.55, 95.30 (for **26**) (Cp* Me and ring carbons), between δ 13 and 17 (pz Me groups) and at 106.62/106.67, 144.80/144.38, 151.64/152.08 (**25**) and 107.81, 144.00/145.65, 151.77/152.03 (**26**) (pz ring carbons) are accompanied by signals at δ 53.66, 92.65 (carbon chain), 230.29 (Mo-CO) and 260.85 (Mo≡C).

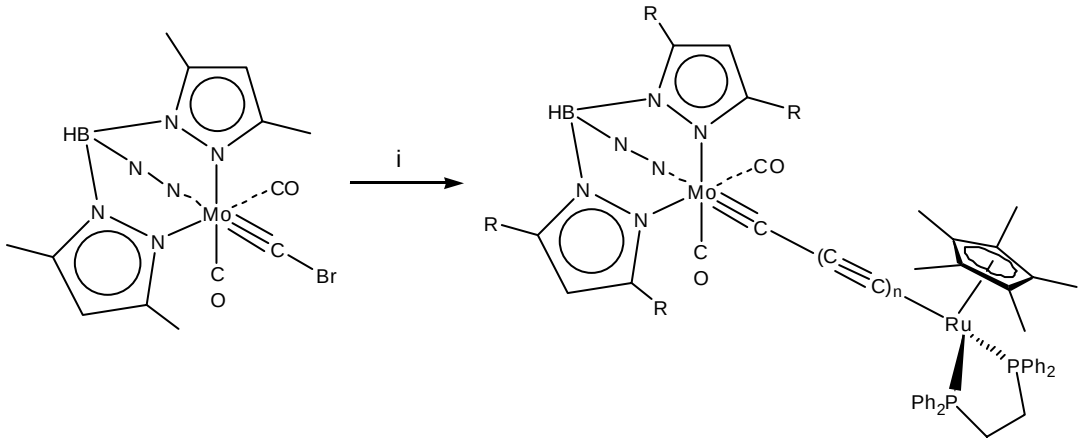

n = 2 (**25**), 3 (**26**)

Reagents: i, Ru{$(C\equiv C)_n$Au(PPh_3)}(dppe)Cp*, $Pd(PPh_3)_4$ / CuI.

Scheme 3.10

3.3 Electrochemistry

Electrochemical studies of the Tp-Mo/W complexes **14** and **16** show one oxidation event at E^1 = +0.89 and +0.82 V (vs SCE), respectively. Values for the corresponding bromocarbyne complex, Mo(≡CBr)$(CO)_2$Tp*, are similar to those of **14**, at +0.83 V. As none of these complexes contains any other redox-active centre it may be reasonably assumed that these events involve the metal centres.

Complexes **19** and **21**, which also contain the Co_3 cluster as a second redox-active centre, each show a reduction wave between -1.06 and -1.02 V, which by comparison with $Co_3(\mu_3\text{-}CC{\equiv}CSiMe_3)(dppm)(CO)_7$ (E^1 = -1.16, E^2 = +0.79 V) may confidently be assigned to processes centred on the Co_3 clusters. Complex **19** also shows a multi-electron oxidation event, as evidenced by the large ΔE_p and i_p values, at +0.66 V (Figure 3.10a) followed by an irreversible wave at +1.16 V. These oxidation events cannot be assigned definitively to either end-cap, however the chemical instability of the second oxidation wave was evident from the observation of a new stripping wave at -0.44 V (Figure 3.10b). With an added C≡C unit in **21** the first oxidation potential increases by 110 mV and is quasi-reversible. This is followed by a second quasi-reversible wave at +0.92 V and an irreversible wave at +1.14 V.

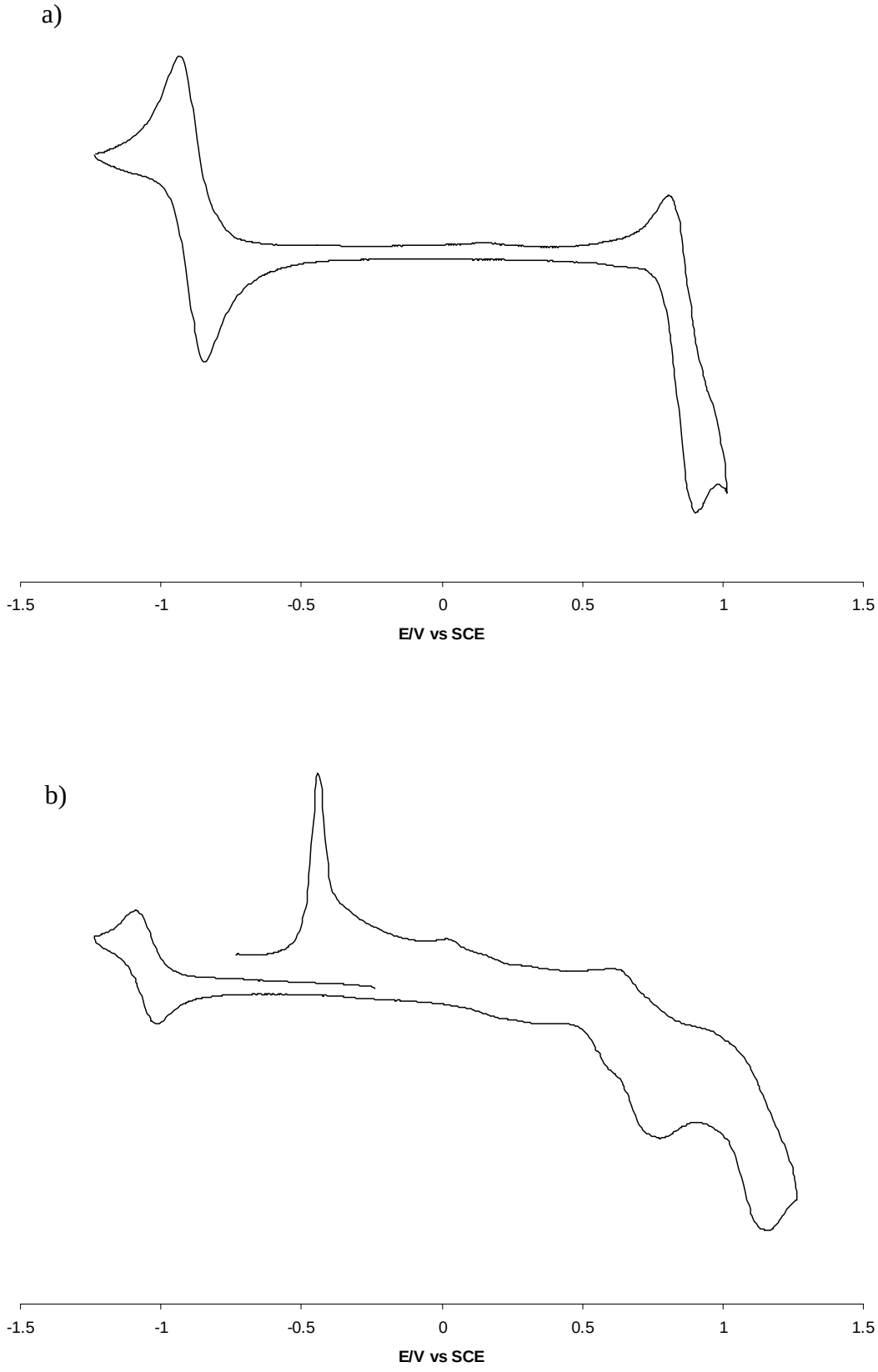

***Figure 3.10**: Cyclic voltammograms of **19** recorded in CH_2Cl_2, 0.1M $[Bu^n{}_4N][PF_6]$.*

Similar trends were observed for the Mo-C_n-Ru complexes **22**-**26.** Replacing the Tp in **22** by Tp* in **24** has little observable effect on the potentials, while the tungsten complex **23** is somewhat more difficult to oxidise than its molybdenum analogue (by 90 mV). Two oxidation events are found for **24**, the first at +0.20 V is fully chemically reversible, whilst the second at +0.73 V is irreversible. As the chain length increases from C_3 to C_5 to C_7 the first oxidation potentials increase by 110 and 60 mV and the second by 20 and 90 mV per added C≡C unit (Table 3.5). Comparison of these potentials with those of related mononuclear complexes such as Ru(C≡CC≡CSiMe_3)(dppe)Cp* (E^1 = +0.43 V)[70] and Mo(≡CC≡CSiMe_3)$(CO)_2$Tp (E^1 = +0.89 V) collected under analogous conditions, strongly supports the assumption that the first oxidation is ruthenium-centred and the second is more associated with the molybdenum centre. For the shorter chain complexes **24** and **25** E^1 may be reduced by the electron donating power of the molybdenum centre. However for the C_7 complex **26**, there is essentially no difference between the two oxidation events and those for the individual end groups when attached to a non-redox-active group (SiMe_3), suggesting that no electronic effect is communicated between the end groups.

***Table 3.5**: Electrochemical Data*

Complex	Electrochemical data[a]				^{13}C NMR[b]	IR[c]
	E^1 (V)	$i_{p,c}/i_{p,a}$	E^2 ($E_{p,a}$)[d] (V)	$i_{p,c}/i_{p,a}$	δMo(CO) (ppm)	ν(CO) (cm^{-1})
Mo(≡CBr)(CO)2Tp*	+0.83	0.99				2008, 1924
Mo(≡CC≡CSiMe$_3$)(CO)$_2$Tp (**14**)	+0.89	0.97			227.17	2004, 1925
W(≡CC≡CSiMe$_3$)(CO)$_2$Tp (**16**)	+0.82	0.66				1991, 1906
{Tp(OC)$_2$Mo}≡CC≡CC≡{Co$_3$(μ-dppm)(CO)$_7$}[e] (**19**)	-1.07	0.97	+0.66	0.92	230.49	2060, 2011, 1997, 1981, 1904
{Tp(OC)$_2$Mo}≡C(C≡C)$_2$C≡{Co$_3$(μ-dppm)(CO)$_7$}[f] (**21**)	-1.02	1.00	+0.71	0.43	229.48	2060, 2012, 1989, 1973, 1908
{Tp(OC)$_2$Mo}≡CC≡C{Ru(dppe)Cp*} (**22**)	+0.23	0.69	(+0.78)			1902, 1863
{Tp(OC)$_2$W}≡CC≡C{Ru(dppe)Cp*} (**23**)	+0.32	0.97	(+0.76)		228.46	1900, 1849
{Tp*(OC)$_2$Mo}≡CC≡C{Ru(dppe)Cp*} (**24**)	+0.20	0.81	(+0.73)		230.95	1899, 1856
{Tp*(OC)$_2$Mo}≡C(C≡C)$_2${Ru(dppe)Cp*}[g] (**25**)	+0.31	0.98	+0.75	0.98	230.29	2021, 1947, 1881
{Tp(OC)$_2$Mo}≡C(C≡C)$_3${Ru(dppe)Cp*} (**26**)	+0.47	0.78	+0.84	0.85	227.55	1990, 1916, 1868

[a] $E_{1/2}$ potentials in CH_2Cl_2, 0.1 M $[Bu^n_4N]BF_4$, at ambient temperature with Pt electrodes ($FcH/[FcH]^+$ = 0.46 V) and at a scan rate of 0.1 V s^{-1}. [b] Recorded in C_6D_6. [c] Recorded in thf. [d] For chemically irreversible oxidations, $E_{p,a}$ is reported in parentheses. [e] Also shows third, irreversible oxidation wave at +1.16 V. [f] Also shows a quasi-reversible process at +0.92 V and an irreversible oxidation at +1.14 V. [g] Also shows a third, irreversible process at +1.17 V.

In general as the chain length increases in the Mo-C_n-M complexes the oxidation potentials increase, reflecting the increasing electron transfer from the metal centres to the C_n chain. This feature has previously been observed in the series $\{Cp(OC)_3W\}(C{\equiv}C)_nFc$ where, for n = 2-4, the potential increases by about 50 mV per added C≡C unit.[127] This is probably a result of the increasing localisation of the HOMO on the C_n chain. The carbonyl stretching frequencies and chemical shifts of the carbonyl carbons for these complexes also reflect the effect of the increasing chain length. In the Mo-C_n-Ru* series the ν(CO) frequencies increase as the chain length is increased from three to five carbons and then decrease again as the chain length is increased to seven carbons. In the ^{13}C NMR spectrum the resonance for the carbonyl carbons moves upfield as the chain length increases and they become increasingly shielded.

3.4 Conclusions

The reactions described above have added significantly to the series of complexes containing the Tp'M(CO)$_2$ group (Tp' = Tp, Tp*; M = Mo, W) end-capping a carbon chain, examples containing three, four, five and seven carbons in the chain having been obtained. These compounds have been characterised by several spectroscopic methods, most distinctive being the ν(BH), ν(CO) and ν(CC) bands in the IR spectra and the characteristic resonances of the Tp' and Cp* groups (if present) in the ^{1}H and ^{13}C NMR spectra. Not all of the carbon atoms in the chains were found in the latter: the carbyne carbon attached to the Group 6 metal centre occurs at the expected downfield location (δ 253-265 for Mo≡C, 246.8 for W≡C in **20**), at higher frequencies than the M-CO resonances (δ 224-231). Single crystal X-ray structures of the C_3 complexes **13**, **14** and **24**; C_4 complexes **19** and **20** and C_6 complex **21** have been determined. The data confirmed the formulation of these complexes with alternating C(sp)-C(sp) single and triple bonds.

Synthetic approaches have employed either the AuX(PR$_3$)-elimination reaction between Au(C≡CR)(PPh$_3$) and halo-carbyne complexes[89] or the metalla-desilylation reaction which occurs between trimethylsilyl-substituted alkynes and chlororuthenium precursors such as RuCl(dppe)Cp'.[81] Interesting cluster-capped carbon chains are present in **19-21**, formed by linking of the well-known carbon-tricobalt complex with the Group 6 precursors by means of the AuX(PR$_3$) elimination reaction. These compounds, in which the Co$_3$ cluster has been stabilised against possible fragmentation by incorporation of a bridging dppm ligand,[89] are obtained as brown solids, which have the expected spectroscopic properties.

Electrochemical measurements show that as the chain length increases these complexes become harder to oxidise. Comparison with similar measurements carried out on the individual end-caps, suggests that no electronic effect is communicated between the metals once a chain length of C_7 is reached.

3.5 Experimental

Reagents. The complexes $Mo(\equiv CBr)(CO)_2Tp^*$,[128,129] $Co_3(\mu_3\text{-}CBr)(\mu\text{-}dppm)(CO)_7$[120] and RuCl(dppe)Cp*[130] were prepared as described previously.

$Mo(\equiv CC\equiv CSiMe_3)\{OC(O)CF_3\}(CO)_2(tmeda)$ (13)

A mixture of $HC\equiv CSiMe_3$ (0.7 ml, 5 mmol) in diethyl ether (30 ml) was cooled to -30˚C and nBuLi (2.5 M, 2 ml, 5 mmol) added and stirred at -30˚C for 30 min before $Mo(CO)_6$ (1.32 g, 5 mmol) in thf (5 ml) was added. The resulting mixture was stirred at 20˚C for 1 h, cooled to -78˚C and $(CF_3CO)_2O$ (0.7 ml, 5 mmol) added. At -50˚C tmeda (0.75 ml, 5 mmol) was added and the reaction mixture slowly warmed to 20˚C. Pentane (60 ml) was then added and the resulting orange precipitate collected and washed with pentane followed by pentane / dichloromethane (3/1) to give $Mo(\equiv CC\equiv CSiMe_3)\{OC(O)CF_3\}(CO)_2(tmeda)$ (**13**) (980 mg, 40%). Single crystals suitable for the X-ray study were grown from CH_2Cl_2 / hexane. Anal. Calcd ($C_{16}H_{25}F_3MoN_2O_4Si$): C, 39.19; H, 5.24; N, 5.71. Found: C, 39.07; H, 5.24; N, 5.73. IR (thf, cm^{-1}): ν(C≡C) 2046w, ν(CO) 2013s, 1934vs. ^1H NMR: δ 0.17 (s, 9H, $SiMe_3$) 3.02 (s, 6H, NMe), 2.80 (m, 4H, NCH_2), 2.60 (s, 6H, NCH_3). ^{13}C NMR: δ 0.54 (s, $SiMe_3$), 50.85, 55.69, 60.81 (3 x s, tmeda), 73.33 (s, C*C*$SiMe_3$), 112.74 (s, C≡C) 116.88 [q, ^1J(CF) 289 Hz, CF_3], 160.88 [q, ^1J(CF) 36 Hz, O_2CCF_3], 224.76 (s, CO), 261.16 (s, Mo≡C). ES MS (*m/z*): 378, $[M - O_2CCF_3]^+$.

$Mo(\equiv CC\equiv CSiMe_3)(CO)_2Tp$ (14)

A mixture of $Mo(\equiv CC\equiv CSiMe_3)(O_2CCF_3)(CO)_2(tmeda)$ (230 mg, 0.47 mmol) and K[Tp] (150 mg, 0.60 mmol) in dichloromethane (5 ml) was stirred at r.t. for 16 h. The solvent was then removed, and the deep purple residue extracted into dichloromethane and chromatographed on basic alumina column eluting with hexane/acetone (8/2). The purple band was collected to give $Mo(\equiv CC\equiv CSiMe_3)(CO)_2Tp$ (**14**) (75.6 mg, 34%) as micro crystals. Single crystals suitable for X-ray studies were grown from CH_2Cl_2/hexane. Anal. Calcd ($C_{17}H_{19}BMoN_6O_2Si$): C, 43.06; H, 4.04; N, 17.72. Found: C, 43.09; H, 4.06; N, 17.61. IR (thf, cm^{-1}): ν(BH) 2482w, ν(C≡C) 2046w, ν(CO) 2004s, 1925vs. ^1H

NMR (C_6D_6): δ 0.23 (s, 9H, $SiMe_3$), 6.14 [t, $^3J_{HH}$ = 2.4 Hz, 1H, pz-H^4), 6.25 [t, $^3J_{HH}$ = 2.4 Hz, 2H, pz-H^4), 7.54, 7.61 [2d, $^3J_{HH}$ = 2.1 Hz, 2 x 1H, pz-H], 7.68, 7.94 [2d, $^3J_{HH}$ = 2.4 Hz, 2 x 2H, pz-H]. ^{13}C NMR: δ 0.44 (s, $SiMe_3$), 76.48 (s, C≡C), 106.05/106.20, 136.26/136.34, 143.43/144.79 (6 x s, pz-ring C), 113.52 (s, C≡C), 227.17 (s, CO), 259.41 (s, C≡Mo). ES MS (*m/z*): 499, $[M + Na]^+$.

Mo(≡CC≡CSiMe$_3$)(CO)$_2$Tp* (15)

A mixture of Mo(≡CC≡CSiMe$_3$)(O_2CCF_3)(CO)$_2$(tmeda) (180 mg, 0.37 mmol) and K[HB($dmpz_3$)] (124 mg, 0.37 mmol) in dichloromethane (20 ml) was stirred at r.t. for 72 h. The solvent was then removed and the deep purple residue extracted into dichloromethane and chromatographed on basic alumina column, eluting with hexane / acetone (8 / 2). The purple band was collected to give Mo(≡CC≡CSiMe$_3$)(CO)$_2$Tp* (**15**) (60 mg, 30%). Anal. Calcd ($C_{23}H_{31}BMoN_6O_2Si$): C, 49.47; H, 5.60; N, 15.05. Found: C, 49.50; H, 5.62; N, 15.01. IR (thf, cm^{-1}): ν(BH) 2549w, ν(C≡C) 2045w, ν(CO) 1995s, 1915s. ^{1}H NMR (C_6D_6): δ 0.20 (s, 9H, $SiMe_3$), 2.32 (s, 3H, 5Me), 2.33 (s, 6H, 5Me), 2.37 (s, 3H, 3Me), 2.55 (s, 6H, 3Me). ^{13}C NMR: δ 0.04 (s, $SiMe_3$), 12.97, 14.84, 16.00 (3 x s, pz-Me), 75.28 (s, C≡C), 106.46, 144.49/145.16, 151.25/151.52 (5 x s, pz-ring C), 113.49 (s, C≡C), 227.42 (s, CO), 255.41 (s, C≡Mo). ES MS (*m/z*): 583, $[M + Na]^+$; 504, $[M – 2CO]^+$.

Mo{≡CC≡CAu(PPh$_3$)}(CO)$_2$Tp (17)

A mixture of Mo(≡CC≡CSiMe$_3$)(CO)$_2$Tp (400 mg, 0.81 mmol) and AuClPPh$_3$ (400 mg, 0.81 mmol) and K_2CO_3 (112 mg, 0.81 mmol) in a 4:1 mixture of thf / MeOH (150 ml) was stirred at r.t. for 2 h. The solvent volume was then reduced (*ca* 15 ml), and the resulting precipitate collected to afford Mo{≡CC≡CAu(PPh_3)}(CO)$_2$Tp (613 mg, 88%) as red microcrystals. Anal. Calcd ($C_{32}H_{25}AuBMoN_6O_2P$): C, 44.68; H, 2.93; N, 9.77. Found: C, 44.61; H, 2.81; N, 9.66. IR (thf, cm^{-1}): ν(BH) 2483w, ν(C≡C) 2015w, ν(CO) 1982s, 1904s. ^{1}H NMR (C_6D_6): δ 5.62 [t, ^3J(HH) = 2.1 Hz , 1H, pz-H^4], 5.72 [t, $^3J_{HH}$ = 2.1 Hz , 2H, pz-H^4], 6.83-7.14 (m, 15H, Ph), 7.21, 7.26 [2 x d, ^3J(HH) = 2.1 Hz, 2 x 1H, pz-H], 7.30, 7.91 [2 x d, ^3J(HH) = 2.1 Hz, 2 x 2H, pzH]. ^{13}C NMR (d_6-acetone): δ 104.65 (s, C≡C), 106.22/106.27, 136.48/136.56, 144.69/144.82 (6 x s, pz-ring C), 115.49 (s, C≡C), 129.06-134.97 (m, Ph), 228.42 (s,

CO), 265.15 (s, C≡Mo). ^{31}P NMR (C_6D_6): δ 41.64 (s, 1P, PPh_3). ES MS (*m/z*): 1321.6, $[M + AuPPh_3]^+$; 1125.5, $[M + HPPh_3]^+$; 885, $[M + Na]^+$; 721, $[Au(Ph_3P)_2]^+$.

W{≡CC≡CAu(PPh$_3$)}(CO)$_2$Tp (18)

A mixture of W(≡CC≡CSiMe$_3$)(CO)$_2$Tp (500 mg, 0.9 mmol) and AuCl(PPh_3) (445 mg, 0.9 mmol) and K_2CO_3 (125 mg, 0.9 mmol) in a 4:1 mixture of thf / MeOH (150 ml) was stirred at r.t. for 4 h. After this time the solvent volume was reduced (*ca* 15 ml), and the resulting precipitate collected to afford W{≡CC≡CAu(PPh_3)}(CO)$_2$Tp (**6**) (580 mg, 69%) as red microcrystals. Anal. Calcd ($C_{32}H_{25}AuBN_6O_2PW$): C, 40.54; H, 2.66; N, 8.86. Found: C, 40.57; H, 2.61; N, 8.76. IR (thf, cm^{-1}): ν(BH) 2483w, ν(C≡C) 2020w, ν(CO) 1970s, 1886s. ^{1}H NMR (C_6D_6): δ 5.55 [t, $^3J_{HH}$ = 2.4 Hz , 1H, pz-H^4], 5.65 [t, $^3J_{HH}$ = 2.4 Hz , 2H, pz-H^4], 6.87-6.92 (m, 15H, Ph), 7.11, 7.31 [2d, $^3J_{HH}$ = 2.4 Hz, 2 x 1H, pz-CH], 7.21, 7.97 [2d, $^3J_{HH}$ = 2.4 Hz, 2 x 2H, pz-CH]. ^{13}C NMR (d_6-acetone / C_6D_6): δ 67.60 (s, C≡C), 78.34 (t, ^3J = 34 Hz, C≡C), 106.12/106.17, 135.67/135.85, 144.05/145.23 (6 x s, pz-ring C), 127.58-135.85 (m, Ph), 226.73 (s, CO), 258.25 (s, C≡W). ^{31}P NMR (C_6D_6): δ 42.85 (s, 1P, PPh_3). ES MS (*m/z*): 1406, $[M + AuP - H]^+$; 1351, $[M + AuPPh_3 - 2CO]^+$; 1089, $[M + AuP - 2CO]^+$; 971, $[M + Na]^+$; 721, $[Au(PPh_3)_2]^+$; 500, $[Au(MeCN)]^+$; 459, $[Au(PPh_3)]^+$.

{Tp(OC)$_2$Mo}≡CC≡CC≡{Co$_3$(μ-dppm)(CO)$_7$} (19)

A mixture of Mo{≡CC≡CAu(PPh_3)}(CO)$_2$Tp (50 mg, 0.06 mmol), Co$_3$(μ$_3$-CBr)(μ-dppm)(CO)$_7$ (98 mg, 0.06 mmol), Pd(PPh_3)$_4$ (15 mg, 0.013 mmol) and CuI (5 mg, 0.026 mmol) was stirred in thf (15 ml) at r.t. for 2 h. The solvent was then removed and the resulting dark purple residue purified by preparative t.l.c. eluting with acetone / hexane (3:7) to obtain {Tp(OC)$_2$Mo}≡CC≡CC≡{Co$_3$(μ-dppm)(CO)$_7$} (**7**) as a yellow-brown band (R_f 0.23) (48 mg, 39%). Anal. Calcd ($C_{47}H_{32}BCo_3MoN_6O_9P_2$): C, 48.24; H, 2.76; N, 7.18. Found: C, 48.16; H, 2.81; N, 7.02. IR (thf, cm^{-1}): ν(BH) 2482w, ν(CO) 2060s, 2011s, 1997 (sh), 1981m, 1904m. ^{1}H NMR (C_6D_6): δ 3.10, 4.58 (2m, 2 x 1H, CH_2), 5.68 (s, br, 1H, pz-H^4), 5.77 (s, br, 2H, pz-H^4), 6.69-7.74 (m, 26H, Ph and pz-H^{3,5}). ^{13}C NMR: δ 40.35 (s, CH_2), 105.44/105.58, 135.47/135.65, 143.09/144.51 (6 x s, pz-ring C), 87.79, 125.19 (s, C≡C), 128.54-135.65 (m, Ph), 201.26, 209.90 (2s, br, Co-CO), 230.49 (s, Mo-CO), 252.92 (s, C≡Mo). ^{31}P NMR: δ

41.64 (s, 2P, dppm). ES MS (*m/z*): 1195, $[M + Na]^+$; 1171, $[M - H]^+$; 1142, $[M - CO]^+$.

$\{Tp(OC)_2W\}\equiv CC\equiv CC\equiv\{Co_3(\mu\text{-dppm})(CO)_7\}$ (20)

A mixture of $W(\equiv CC\equiv CAuPPh_3)(CO)_2Tp$ (57 mg, 0.06 mmol), $Co_3(\mu_3\text{-CBr})(\mu\text{-dppm})(CO)_7$ (98 mg, 0.06 mmol), $Pd(PPh_3)_4$ (20 mg, 0.017 mmol) and CuI (5 mg, 0.026 mmol) was stirred in thf (10 ml) at r.t. for 2 h. The solvent was then removed and the resulting residue purified by preparative t.l.c. eluting with acetone / hexane (3:7) to obtain $\{Tp(OC)_2W\}\equiv CC\equiv CC\equiv\{Co_3(\mu\text{-dppm})(CO)_7\}$ as a brown band (R_f 0.36) (28 mg, 37%). Anal. Calcd ($C_{47}H_{32}BCo_3N_6O_9P_2W$): C, 44.84; H, 2.56; N, 6.68. Found: C, 44.72; H, 2.58; N, 6.54. IR (thf, cm^{-1}): ν(CO) 2058s, 2010s, 1994 (sh), 1970m, 1885m. ^{1}H NMR (C_6D_6): δ 3.11, 4.70 (2m, 2 x 1H, CH_2), 5.60 [t, $^3J_{HH}$ = 2.1 Hz , 1H, pz-H^4), 5.70 [t, $^3J_{HH}$ = 2.1 Hz , 2H, pz-H^4], 6.66-8.04 (m, 26H, Ph and pz-$H^{3,5}$). ^{13}C NMR: δ 41.93 (s, CH_2), 106.65/106.71, 135.44/135.76, 144.57/146.05 (6 x s, pz-ring C), 128.08-141.41 (m, Ph), 198.89, 202.00 (2s, br, Co-CO), 229.97 (s, Mo-CO), 246.80 (s, C≡W). ^{31}P NMR: δ 32.15 (s, 2P, dppm). ES MS (*m/z*): 1257, $[M - H]^-$; 1229, $[M - H - CO]^-$.

$\{Tp^*(OC)_2Mo\}\equiv C(C\equiv C)_2C\equiv\{Co_3(\mu\text{-dppm})(CO)_7\}$ (21)

A mixture of $Mo(\equiv CBr)(CO)_2Tp^*$ (28 mg, 0.05 mmol), $Co_3\{\mu_3\text{-}C(C\equiv C)_2Au(PPh_3)\}(\mu\text{-dppm})(CO)_7$ (60 mg, 0.05 mmol), $Pd(PPh_3)_4$ (15 mg, 0.01 mmol) and CuI (5 mg, 0.03 mmol) was stirred in thf (10 ml) at r.t. for 1 h. The solvent was then removed and the resulting residue purified by preparative t.l.c. eluting with acetone / hexane (3:7) to obtain $\{Tp^*(OC)_2Mo\}\equiv C(C\equiv C)_2C\equiv\{Co_3(\mu\text{-dppm})(CO)_7\}$ as a brown band (R_f 0.34) (43 mg, 72%). An analytically pure sample was obtained through crystallisation from chloroform. Anal. Calcd ($C_{55}H_{44}BCo_3MoN_6O_9P_2.2CHCl_3$): C, 45.12; H, 3.06; N, 5.54. Found: C, 45.20; H, 3.00; N, 5.51. IR (thf, cm^{-1}): ν(C≡C) 2109w, ν(CO) 2060s, 2012s, 1989m, 1973m, 1908m. ^{1}H NMR ($CDCl_3$): δ 2.32 (s, 3H, Me), 2.34, (s, 3H, Me), 2.38 (s, 6H, Me), 2.61 (s, 6H, Me), 3.42, 4.26 (2m, 2 x 1H, CH_2), 5.71 (s, 1H, pz-H^4), 5.88 (s, 2H, pz-H^4), 7.23-7.54 (m, 26H, Ph and pz-$H^{3,5}$). ^{13}C NMR: δ 12.68, 14.65, 15.93 (3 x s, pz-Me), 44.45 [t, *J*(CP) 22Hz, CP_2], 52.55, 100.92, 96.73, 107.95 (4s, C≡C),

106.34/106.36, 144.45/145.07, 151.28 (5s, pz-ring C), 128.57-135.06 (m, Ph), 201.29, 209.49 (2s, br, Co-CO), 229.48 (s, Mo-CO), 261.02 (s, C≡Mo). ^{31}P NMR: δ 34.13 (s, 2P, dppm). ES MS (*m/z*): 1302, $[M + Na]^+$.

{Tp(OC)$_2$Mo}≡CC≡C{Ru(dppe)Cp*} (22)

To a mixture of RuCl(dppe)Cp* (40 mg, 0.06 mmol) and KF (3.5 mg, 0.06 mmol) in methanol at 0˚C was added Mo(≡CC≡CSiMe$_3$)(CO)$_2$Tp (22.5 mg, 0.06 mmol). The resulting mixture was allowed to warm to r.t. and stirred for 2 h. The precipitate which formed was then collected and washed with MeOH (10 ml) followed by hexane (20 ml) to obtain {Tp(OC)$_2$Mo}≡CC≡C{Ru(dppe)Cp*} as a red solid (37 mg, 60%). Anal. Calcd ($C_{50}H_{49}BMoN_6O_2P_2Ru$): C, 57.98; H, 4.77; N, 8.11. Found: C, 57.94; H, 4.69; N, 8.80. IR (thf, cm^{-1}): ν(BH) 2469w, ν(CC) 1975m, ν(CO) 1902s, 1863s. ^{1}H NMR (C_6D_6): δ 1.50 (s, 15H, Cp*), 1.79, 2.61 (2m, 2 x 2H, CH_2CH_2), 5.65 (s, br, 1H, pz-H^4), 5.85 [t, $^3J_{HH}$ = 2.4 Hz, 2H, pz-H^4], 6.93-7.85 (m, 26H, Ph and pz-H^{3,5}). ^{13}C NMR (C_6D_6): δ 9.98 (s, C_5*Me*$_5$), 29.78 (m, CH_2CH_2), 94.70 (s, *C*$_5$Me$_5$), 104.91/105.10, 136.13/136.46, 143.46/144.32 (6s, pz-ring C), 127.58-137.95 (m, Ph), 230.63 (s, CO). ^{31}P NMR (C_6D_6): δ 79.38 (s, 2P, dppe). ES MS (*m/z*): 1036, $[M + H]^+$; 1058, $[M + Na]^+$.

{Tp(OC)$_2$W}≡CC≡C{Ru(dppe)Cp*} (23)

Similarly, the reaction between W(≡CC≡CSiMe$_3$)(CO)$_2$Tp (34 mg, 0.06 mmol) and RuCl(dppe)Cp* (40 mg, 0.06 mmol) and KF (3.5 mg, 0.06 mmol) in methanol at 0˚C gave {Tp(OC)$_2$W≡CC≡C{Ru(dppe)Cp*} (**23**), obtained as an orange solid (24 mg, 31%). Anal. Calcd ($C_{50}H_{49}BN_6O_2P_2RuW$): C, 53.37; H, 4.39; N, 7.47. Found: C, 53.23; H, 4.28; N, 7.31. IR (thf, cm^{-1}): ν(BH) 2478w, ν(CC) 1976m, ν(CO) 1900s, 1849s. ^{1}H NMR (C_6D_6): δ 1.55 (s, 15H, Cp*), 1.85, 2.73 (2m, 2 x 2H, CH_2CH_2), 5.60 (s, br, 1H, pz-H^4), 5.82 (s, br, 2H, pz-H^4), 6.90-7.92 (m, 26H, Ph). ^{13}C NMR (C_6D_6): δ 10.41 (s, C_5*Me*$_5$), 30.79 (m, CH_2CH_2), 94.90 (s, *C*$_5$Me$_5$), 105.94/106.04, 134.84/135.15, 145.40/145.51 (6s, pz-ring C), 145.24 (s, pz-C$_5$), 129.95-141.03 (m, Ph), 228.46 (s, CO). ^{31}P NMR (C_6D_6): δ 78.87 (s, 2P, dppe). ES MS (*m/z*): 1147, $[M + Na]^+$; 1124, $[M]^+$; 635, $[Ru(dppe)Cp^*]^+$.

{Tp*(OC)$_2$Mo}≡CC≡C{Ru(dppe)Cp*} (24)

Similarly, from RuCl(dppe)Cp* (36 mg, 0.05 mmol) and KF (3 mg, 0.05 mmol) was obtained {Tp*(OC)$_2$Mo}≡CC≡C{Ru(dppe)Cp*} as an orange solid (20 mg, 36%). Anal. Calcd ($C_{56}H_{61}BMoN_6O_2P_2Ru$): C, 60.06; H, 5.49; N, 7.50. Found: C, 58.98; H, 5.33; N, 7.44. IR (thf, cm^{-1}): ν(BH) 2524w, ν(CC) 1971w, ν(CO) 1899s, 1856s. ^{1}H NMR (C_6D_6): δ 1.59 (s, 15H, Cp*), 1.98, 2.81 (2m, 2 x 2H, CH_2CH_2), 2.18 (s, 3H, 5Me), 2.24 (s, 6H, 5Me), 2.63 (s, 3H, 3Me), 2.69 (s, 6H, 3Me), 5.46 (s, 1H, H^4), 5.65 (s, 2H, H^4), 6.93-7.87 (m, 20H, Ph). ^{13}C NMR (C_6D_6): δ 10.67 (s, C_5*Me*$_5$), 13.30 (pz-C_5Me), 15.59 (pz-C_3Me), 16.62 (pz-C_3Me), 29.78 (m, CH_2CH_2), 56.41 (s, C≡C), 95.07 (s, *C*$_5$Me$_5$), 106.28/106.47, 143.51/143.86, 151.51/151.66 (6s, pz-ring C), 123.80-141.57 (m, Ph), 230.95 (s, CO), 254.47 (s, Mo≡C). ^{31}P NMR (C_6D_6): δ 78.44 (s, 2P, dppe). ES MS (*m/z*): 1143, [M + Na]$^+$; 1121, [M + H]$^+$; 667, [Ru(MeOH)(dppe)Cp*]; 635, [Ru(dppe)Cp*]$^+$.

{Tp*(OC)$_2$Mo}≡CC≡CC≡C{Ru(dppe)Cp*} (25)

A mixture of Mo(≡CBr)(CO)$_2$Tp* (25 mg, 0.05 mmol), Ru{C≡CC≡CAu(PPh$_3$)}(dppe)Cp* (53 mg, 0.05 mmol), Pd(PPh$_3$)$_4$ (10 mg, 0.01 mmol) and CuI (5 mg, 0.03 mmol) was stirred in thf (10 ml) at r.t. for 1 h. The solvent was then removed and the resulting residue purified by preparative t.l.c. eluting with acetone / hexane (3:7) to obtain {Tp*(OC)$_2$Mo}≡CC≡CC≡C-{Ru(dppe)Cp*} as a red band (R_f 0.38) (20 mg, 67%). A solid sample was obtained by adding the desolved product [CH_2Cl_2 (2 ml)] dropwise into hexane (20 ml). Anal. Calcd ($C_{58}H_{61}BMoN_6O_2P_2Ru.CH_2Cl_2$): C, 59.38; H, 5.32; N, 7.04. Found: C, 59.62; H, 5.32; N, 6.90. IR (thf, cm^{-1}): ν(BH) 2484w, ν(CO) 2021s, 1947s, 1881s. ^{1}H NMR (C_6D_6): δ 1.45 (s, 15H, Cp*), 1.68, 2.32 (2m, 2 x 2H, CH_2CH_2), 2.11(s, 3H, 5Me), 2.19 (s, 6H, 5Me), 2.43 (s, 3H, 3Me), 2.75 (s, 6H, 3Me), 5.30 (CH_2Cl_2), 5.37 (s, 1H, H^4), 5.56 (s, 2H, H^4), 6.79-7.73 (m, 20H, Ph). ^{13}C NMR (C_6D_6): δ 10.42 (s, C_5*Me*$_5$), 13.03, 15.40, 16.58 (3 x s, pz-CMe), 29.99 (m, CH_2CH_2), 53.66, 92.65 (s, C≡C), 94.87 (s, *C*$_5$Me$_5$), 106.62/106.67, 143.80/144.38, 151.64/152.80 (6 x s, pz-ring C), 128.08-148.65 (m, Ph), 230.29 (s, CO), 260.85 (s, Mo≡C). ^{31}P NMR (C_6D_6): δ 53.66 (CH_2Cl_2), 79.05 (s, 2P, dppe). ES MS (*m/z*): 1167, [M + Na]$^+$; 676, [Ru(MeCN)(dppe)Cp*]$^+$; 635, [Ru(dppe)Cp*]$^+$.

{Tp*(OC)$_2$Mo}≡C(C≡C)$_3${Ru(dppe)Cp*} (26)

A mixture of Mo(≡CBr)(CO)$_2$Tp* (23 mg, 0.04 mmol), Ru{(C≡C)$_3$Au(PPh$_3$)}(dppe)Cp* (50 mg, 0.04 mmol), Pd(PPh$_3$)$_4$ (10 mg, 0.01 mmol) and CuI (5 mg, 0.03 mmol) was stirred in thf (10 ml) at r.t. for 1 h. The solvent was then removed and the resulting residue purified by preparative t.l.c. eluting with acetone / hexane (3:7) to obtain {Tp*(OC)$_2$Mo}≡C(C≡C)$_3${Ru(dppe)Cp*} as a mauve band (R_f 0.33) (23 mg, 49%). A solid sample was obtained by adding the desolved product [CH_2Cl_2 (2 ml)] dropwise into hexane (20 ml). Anal. Calcd ($C_{60}H_{61}BMoN_6O_2P_2Ru.CH_2Cl_2$): C, 58.48; H, 5.07; N, 6.71. Found: C, 59.06; H, 5.01; N, 6.38. IR (thf, cm^{-1}): ν(C≡C) 2116w, 2069w, 2010w, ν(CO) 1990m, 1916m, 1868s. ^{1}H NMR (C_6D_6): δ 1.43 (s, 15H, Cp*), 1.72, 2.34 (2m, 2 x 2H, CH_2CH_2), 2.01 (s, 3H, Me), 2.10 (s, 6H, Me), 2.23 (s, 3H, Me), 2.53 (s, 6H, Me), 5.29 (s, 1H, H), 5.51 (s, 2H, H), 6.98-7.62 (m, 20H, Ph). ^{13}C NMR (C_6D_6): δ 10.55 (s, C_5*Me*$_5$), 13.06, 14.72, 16.44 (3 x s, pz-CMe), 28.54 (m, CH_2CH_2), 72.60, 78.20, 87.43 (s, C≡C), 95.30 (s, *C*$_5$Me$_5$), 107.17, 144.00/145.65, 151.77/152.03 (5 x s, pz-ring C), 127.95-170.80 (m, Ph), 227.55 (s, CO). ^{31}P NMR (C_6D_6): δ 78.88 (s, 2P, dppe). ES MS (*m/z*): 1191, [M + Na]$^+$.

Chapter 4

COMPLEXES WITH 1,4-BIS-DIETHYNYLAROMATIC LINKERS

4.1 Introduction

The extent of delocalisation through a complex containing two or more metal centres linked by bridging groups is influenced not only by the nature of the metal and supporting ligand structure but also by the bridging ligand itself. The electronic structure of a bridging ligand can be altered by introducing either an organic (**4a**) or organometallic (**4b**) linker into the chain.

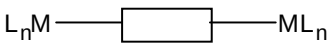

(**4a**)

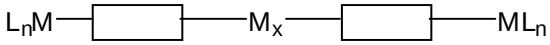

(**4b**)

A simple conjugated organic linker composed of sp^2 carbon atoms is the 1,4-phenylene unit. Incorporating an aromatic ring into the poly-yndiyl bridge of a bis-metallic complex has been found to provide radicals with improved stability[131] and may provide a route to further extending bridging carbon chains. However such compounds have been found generally to have low solubility, hindering the collection of data.[30]

While many examples 1,4-diethynylbenzene complexes, of the general formula 1,4-$\{ML_n(C{\equiv}C)\}_2C_6H_4$, have been synthesised, those in which the electronic properties have been examined are limited to platinum,[132] osmium,[133] ruthenium[99,134-136] and iron[134,137-140] systems. Electron delocalisation through the π-conjugated linker results in the loss of aromaticity (Figure 4.1) and should, in principle, have a high activation energy.[30] However the facile oxidation of these complexes and the progressive shift of the ν(CC) band to lower energies suggests that a cumulenic electronic structure is formed.[99,133] Furthermore, it should be noted that rotation about the alkynyl-aryl bond, which has been found to have a barrier of approximately 2.7 kJ,[141] will

diminish the electronic interaction. Despite these disadvantages, 1,4-diethynylbenzene is an attractive linker due to stability and synthetic versatility.

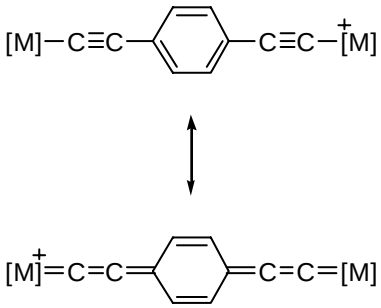

Figure 4.1: *Resonance structures of a mixed-valence bis-metallic 1,4-diethynylbenzene complex.*

4.1.1 Bis-Platinum and Bis-Osmium Complexes

The two terminal metal centres of the bis-platinum complex, $\{PtC_6H_3(CH_2NMe_2)_2\text{-}2,6\}_2(\mu\text{-}C{\equiv}CC_6H_4C{\equiv}C)$ display independent redox behaviour with only a single four electron oxidation event observed in its cyclic voltammogram.[99,132] Thus, the 1,4-diethynylbenzene linker is effectively blocking electronic communication between the two platinum centers. By contrast in the cyclic voltammogram of the bis-osmium complex, $\{Os(dppm)_2Cl\}_2(\mu\text{-}C{\equiv}CC_6H_4C{\equiv}C)$, two reversible one electron oxidation waves are observed.[133] These waves are separated by 0.30 V, suggesting that the metal centres can communicate through the 1,4-diethynylbenzene linker.

4.1.2 Bis-Ruthenium Complexes

The cyclic voltammograms of the bis-ruthenium complexes $\{Ru(PP)_2Cl\}_2\text{-}(\mu\text{-}C{\equiv}CC_6H_4C{\equiv}C)$ [PP = dppe (**27**) or dppm (**28**)] show two successive reversible one electron oxidation waves. These two waves are attributed to the formation of the Ru^{III}/Ru^{II} mono cation and the Ru^{III}/Ru^{III} dication respectively.[136] The two waves are separated by 0.40 V in **27**[134,136] and 0.30 V in **28**.[133] These large ΔE values suggest that in both of these complexes the ruthenium centres are able to communicate effectively through the 1,4-diethynylbenzene linker. The first oxidation potential in

the bis-metallic complex is much lower than that in the corresponding monometallic complex {Ru(PP)$_2$Cl}-(μ-C≡CC$_6$H$_4$C≡CH) due to the decrease in electron-donating ability of the proton compared to that of the ruthenium centre in bis-ruthenium complexes **27** and **28**. This decrease in E_1 supports communication between the two ruthenium centres through the 1,4-diethynyl linker.

Conversely the bis-bimetallic complex, {Ru$_2$(ap)$_4$}$_2$(μ-C≡CC$_6$H$_4$C≡C) (ap = 2-anilinopyridinate), displays three two-electron events in its cyclic voltammogram, corresponding to the three one-electron events observed for the mono-substituted spieces.[99,135] In this complex the 1,4-diethynylbenzene linker is blocking electronic communication between the two ruthenium centres, which thus display independent redox behaviour.

4.1.3 Bis-Iron Complexes

The bis-iron complexes {Fe(PP)$_2$Cl}$_2$-(μ-C≡CC$_6$H$_4$C≡C) [PP = dmpe (**29**) or depe (**30**)] show two successive reversible oxidation waves in their cyclic voltammograms. These waves are separated by 0.20 V in **29**[140] and 0.16 V in **30**.[133] While these ΔE values are smaller than those observed for the bis-ruthenium complexes they are significant and suggest communication between the iron centres through the 1,4-diethynylbenzene linker. The cyclic voltammogram of the complex {Fe(dppe)Cp*}$_2$-(μ-C≡CC$_6$H$_4$C≡C) also displays two reversible, one-electron, oxidation waves with ΔE = 0.26 V,[137] further demonstrating the ability of the 1,4-diethynylbenzene linker to delocalise an unpaired electron between two iron centres. It is therefore somewhat surprising that only a single, broad oxidation wave is found in the cyclic voltammogram of the bis-ferrocene complex, Fc$_2$(μ-C≡CC$_6$H$_4$C≡C), and that no significant difference was found in E_1 between this complex and its monometallic derivatives.[139] The broadness of these waves suggests the presence of multiple processes occurring at very similar potentials, hence it is clear that these bridges are not suited to enhancing electronic interactions between ferrocene termini.

These results suggest that the terminal metal centres can markedly influence the electrochemical response through the 1,4-diethynylbenzene linker in different ways.

Thus the suitability of this linker as a bridging ligand needs to be investigated for individual metal termini.

In this chapter the syntheses and properties of 1,4-diethynylbenzene complexes containing the electron-rich ruthenium end-groups are discussed. The use of the Ru(dppe)Cp* fragment allows direct comparisons to be made with the analogous extended chain complexes described in Chapter Two and the influence of the bridging group towards electronic interactions between two ruthenium centres to be investigated.

4.2 Results and Discussion

Earlier reports from our laboratory have described the synthesis of the 1,4-diethynylbenzene complex, $\{Ru(PPh_3)_2Cp\}_2(\mu\text{-}C{\equiv}CC_6H_4C{\equiv}C)$ (**31**) by treatment of the trimethylsilyl-substituted alkynes with $RuCl(PPh_3)_2Cp$ in the presence of potassium fluoride.[142]

As a part of this work the Ru(dppe)Cp (**32**) and Ru(dppe)Cp* (**33**) analogues were made via this route in 30% and 37% yields respectively (Scheme 4.1). Elemental analyses and the ES mass spectra confirmed the formulations of these complexes, supported by spectroscopic data; the IR spectra of **32** and **33** contain three ν(C≡C) bands between 2044 and 2146 cm^{-1}. In the ^1H NMR spectrum, the usual resonances for the ligands are found with the ethane portion of dppe at δ 1.96 and 2.54 (**32**), 1.88 and 2.69 (**33**) and Cp and Cp* at δ 4.26 and 1.68, respectively. In the ^{31}P NMR spectrum, characteristic resonances for dppe were found at δ 87.03 (for **32**) and 82.15 (for **33**). The ^{13}C NMR spectrum was not obtained for **32** as it was either too insoluble or decomposed in all common NMR solvents. A ^{13}C NMR spectrum was obtained for **33**, however resonances for the alkyne carbons were not found due too poor solubility. Characteristic resonances were found at δ 11.23 and 94.81 for the Cp* methyl and ring carbons, at δ 30.60 for the ethane portion of dppe and between, 127.17 and 143.14 for the aromatic carbons.

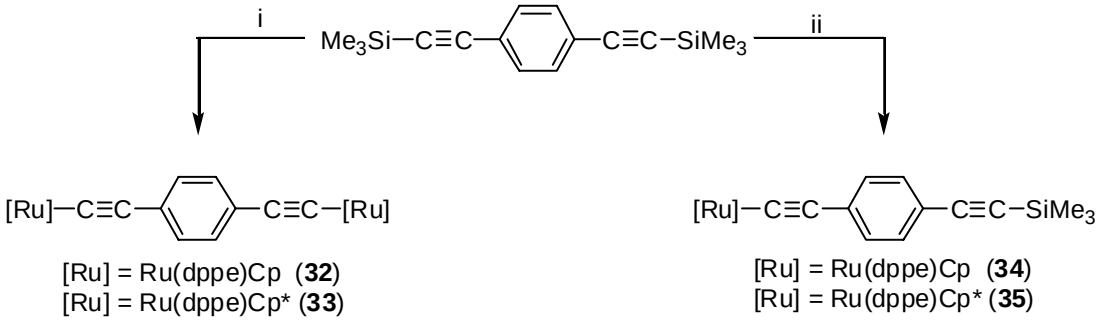

Reagents: i, RuCl(dppe)Cp' [Cp' = Cp (**32**), Cp* (**33**)], KF, MeOH/thf;
ii, RuCl(dppe)Cp' [Cp' = Cp (**34**), Cp* (**35**)], KF, MeOH

Scheme 4.1

Varying the stoichiometry in the method outlined above resulted in the formation of the monosubstituted congeners Ru(C≡CC_6H_4C≡C$SiMe_3$)(dppe)Cp', [Cp' = Cp (**34**) and Cp* (**35**)] (Scheme 4.1). These complexes were characterised by elemental analyses and spectroscopic techniques. The IR spectra contain three ν(C≡C) bands between 2042 and 2150 cm^{-1} and the ^{1}H NMR spectra exhibit $SiMe_3$ signals at δ 0.21 (**34**) and 0.56 (**35**) that integrate appropriately. ^{13}C NMR spectra for **34** and **35** exhibit resonances at δ 83.26 for the Cp ring carbons (for **34**) and at δ 10.68 and 93.26 for the Cp* Me and ring carbons (for **35**). The ES-MS contain ions consistent with $[M + Na]^+$ at *m/z* 785 (**34**) and at *m/z* 856 (**35**).

The structure of **34** was confirmed by an X-ray structure detemination after crystallisation from dichloromethane/methanol (Figure 4.1). The Ru(dppe)Cp fragment has the expected geometry with Ru-P 2.218, 2.242(1)Å and Ru-C(Cp) 2.230 – 2.243(4) Å and the carbon chain exhibits C-C contacts consistent with a C-C triple bond [C(1)-C(2) 1.210(5) Å] and a C-C single bond [C(2)-C(21) 1.430(5) Å]. The Ru-C(1) distance (2.007(4) Å), is somewhat longer than that found in Ru(C≡CC≡C$SiMe_3$)(dppe)Cp* [1.983(2) Å].[126] The carbon chain is essentially linear, with angles at C(1,2,3,4) of 178.6(3), 176.5(4), 177.0(5) and 173.8(4)˚ respectively

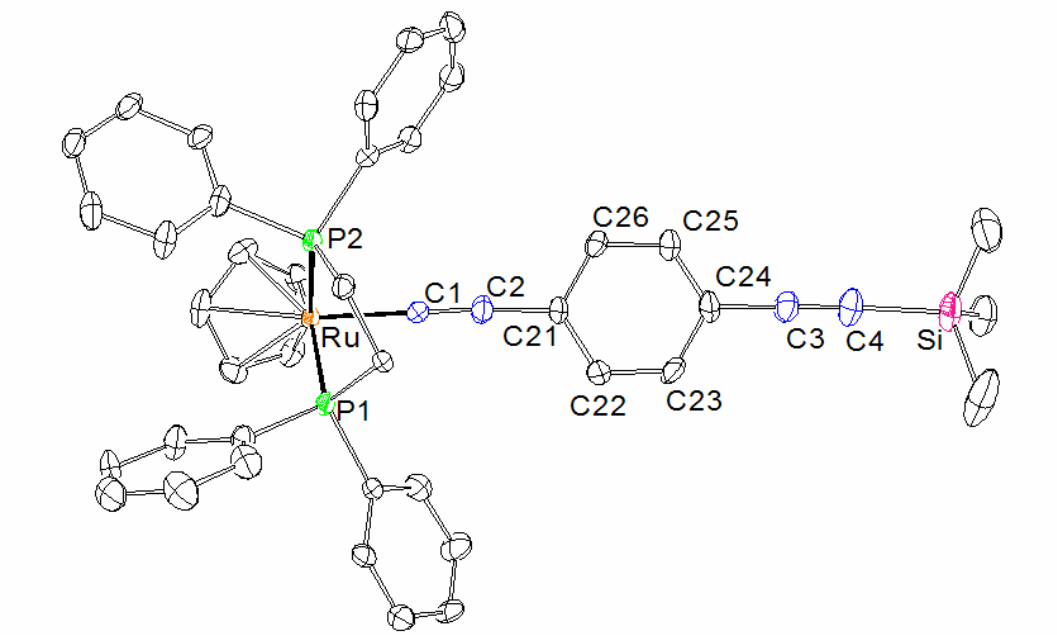

Figure 4.2 *ORTEP view of Ru(C≡CC_6H_4C≡C$SiMe_3$)(dppe)Cp (**34**).*

Table 4.1: *Selected structural data for Ru(C≡CC$_6$H$_4$C≡CSiMe$_3$)(dppe)Cp (**34**).*

Bond Distances (Å)		**Bond Angles (˚)**	
Ru-P(1,2)	2.218(9), 2.242(1)	Ru-C(1)-C(2)	178.6(3)
Ru-C(Cp)	2.230(4) – 2.243(4)	C(1)-C(2)-C(21)	176.5(4)
Ru-C(Cp) (av.)	2.235(4)	C(2)-C(21)-C(22)	122.9(4)
Ru-C(1)	2.007(4)	C(2)-C(21)-C(26)	119.6(3)
C(1)-C(2)	1.210(5)	C(22)-C(21)-C(26)	117.5(3)
C(2)-C(21)	1.430(5)	C(21)-C(22)-C(23)	121.0(4)
C(21)-C(22)	1.390(5)	C(22)-C(23)-C(24)	121.6(4)
C(22)-C(23)	1.38(6)	C(23)-C(24)-C(25)	117.6(4)
C(23)-C(24)	1.379(6)	C(23)-C(24)-C(3)	120.0(4)
C(24)-C(25)	1.378(6)	C(25)-C(24)-C(3)	122.3(4)
C(25)-C(26)	1.373(5)	C(24)-C(25)-C(26)	123.0(4)
C(26)-C(21)	1.432(6)	C(21)-C(26)-C(25)	119.2(3)
C(24)-C(3)	1.442(6)	C(24)-C(3)-C(4)	177.0(5)
C(3)-C(4)	1.193(6)	C(3)-C(4)-Si(4)	173.8(4)
C(4)-Si	1.840(5)		

4.2.1 Gold Reactions

Reactions of **34** and **35** with AuCl(PPh$_3$) in sodium methoxide solution gives Ru{C≡CC$_6$H$_4$C≡CAu(PPh$_3$)}(dppe)Cp' [Cp' = Cp (**36**) and Cp* (**37**)] in 63 and 82% yields. ES mass spectra confirm the formulations of these complexes which are also supported by spectroscopic data. Thus, ^{1}H NMR resonances for the dppe ligands are found at δ 1.96 and 2.48 (for **36**), 1.87 and 2.64 (for **37**) while the resonances for Cp and Cp* were found at δ 4.73 and 1.65, respectively. Due to the poor solubility of **36** a ^{13}C NMR spectrum was not obtained however, characteristic resonances were found for **37** at δ 10.72 and 93.11 for the Cp* methyl and ring carbons, at δ 26.14 for the ethane portion of dppe and at δ 68.15 for a chain carbon.

The bis-gold complex 1,4-{$Ph_3PAu(C\equiv C)\}_2C_6H_4$ has been reported previously[143] and was found to undergo Pd(0)/Cu(I)-catalysed elimination of $AuBr(PPh_3)$ when reacted with $Co_3(\mu_3\text{-}CBr)(\mu\text{-}dppm)(CO)_7$.[89] Accordingly, similar reactions involving the diiodo analogue 1,4-{$IC\equiv C\}_2C_6H_4$ (**38**) were of interest. This compound has been synthesised previously by treating 1,4-diethynylbenzene, obtained by deprotecting 1,4-trimethylsilylethynylbenzene with two equivalents of n-butyllithium and adding an equivalent of iodine at -78˚C.[144] However by using a similar method to that outlined in Chapter Two for the synthesis of Ru{C≡CC≡CAu(PPh_3)}(dppe)Cp* (**7**) it was found that the 1,4-trimethylsilylethynylbenzene could be converted directly to the diiodo compound by deprotection using sodium methoxide and adding iodine at 20˚C. This reduces the number of steps required to obtain **38**, significantly shortens the reaction time and increases the yield from 48 to 64%. All spectroscopic data agreed with those previously reported, with the IR spectrum showing a ν(C≡C) band at 2107 cm^{-1}, while the ^1H NMR spectrum exhibits a single resonance at δ 7.27.

Similar organic compounds to 1,4-diethynylbenzene have been reported. For example, 1,4-bis(phenylbutadiynyl)benzene (**39**) and 4-(phenylbutadiynyl)-phenylacetylene (**40**) have been prepared through the slow addition of 1-bromo-2-phenylacetylene to an aqueous solution containing copper chloride and 1,4-diethynylbenzene (Scheme 4.2).[145] The resulting crude product required several days of drying before it could be fractionally crystallised to obtain **39** and **40** in 35% yield each.

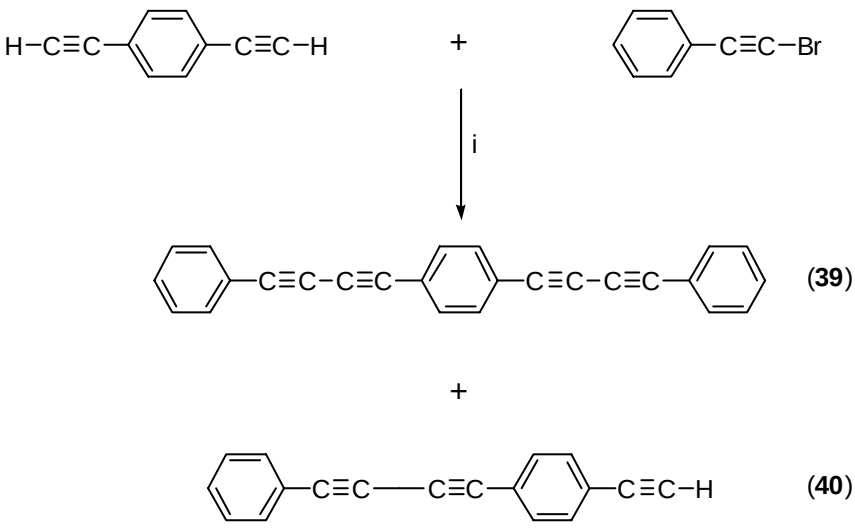

Reagents: i, CuCl / NEt_3 / H_2O, $NH_2OH.HCl$, DMF

Scheme 4.2

The $SiMe_3$ analogue of **39**, 1,4-bis(trimethylsilylbutadiynyl)benzene (**41**) has also been reported previously.[146] This compound was prepared by the oxidation of a diol with pyridinium chlorochromate (PCC) followed by dibromoolefination and treatment of the resulting tetrabromide with an excess of *n*-BuLi (Scheme 4.3). This three-step synthesis gave **41** in an overall yield of 50%.

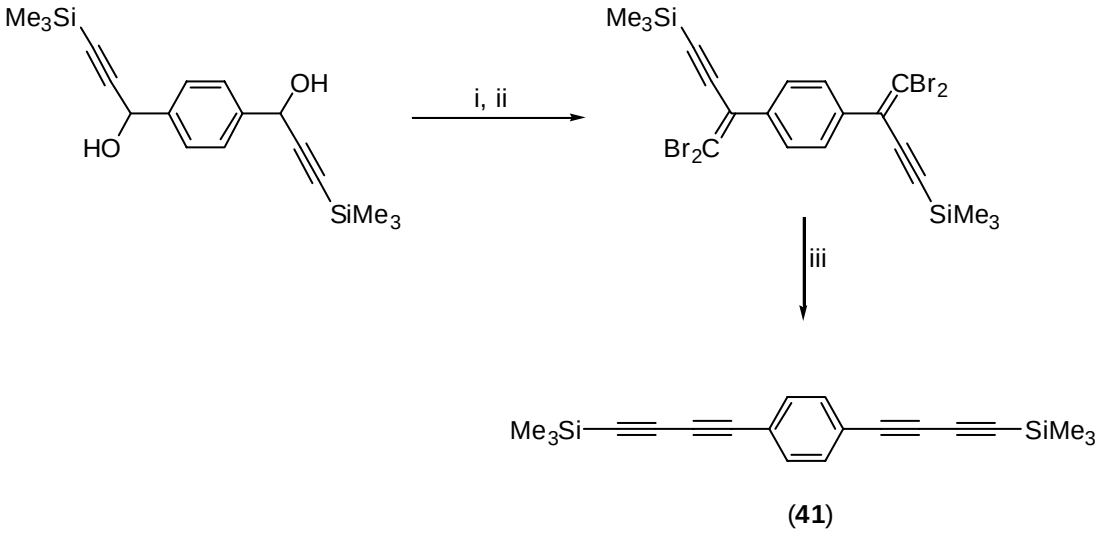

Reagents: i, PCC, Celite, molecular sieves, CH_2Cl_2; ii, PPh_3, CBr_4, CH_2Cl_2; iii, *n*-BuLi

Scheme 4.3

As a part of this work it was found that the gold-elimination reaction provides a more convenient route to these compounds. Reacting **38** with two equivalents of $Au(C{\equiv}CPh)PPh_3$ or $Au(C{\equiv}CSiMe_3)(PPh_3)$ in the presence of catalytic amounts of $Pd(PPh_3)_4$ and CuI afforded the corresponding 1,4-bis(butadiynyl)benzene complexes **39** and **41** in 26 and 87% yields respectively (Scheme 4.4). All spectroscopic values agreed with those previously reported.[145,146] The FAB-mass spectra of the products contain $[M]^+$ at *m/z* 326 (for **39**) and *m/z* 318 (for **41**).

Similarly, reacting **38** with only one equivalent of $Au(C{\equiv}CR)(PPh_3)$ (R = Ph, $SiMe_3$) under the standard gold coupling conditions gave compound **40** and the previously unreported 4-(trimethylsilylbutadiynyl)phenylacetylene (**42**) (Scheme 4.4). All spectroscopic values for **40** agreed with those previously reported.[145] Mass spectrometry confirmed the formulation of **42** with $[M]^+$ at *m/z* 222 in the FAB-mass spectrum. In the IR spectrum two $\nu(C{\equiv}C)$ bands were found at 2196 and 2104 cm^{-1}. In the ^1H NMR spectrum, three singlets were found: one at δ 7.47 for the four aromatic protons, another at δ 3.22 for the acetylenic proton and one singlet at δ 0.25 for the $SiMe_3$ protons. In the ^{13}C NMR spectrum all six of the chain carbons were found between δ 76.98 and 92.89. However consistent microanalyses were not obtained, this is probably due to the decomposition of **42** at higher temperatures.

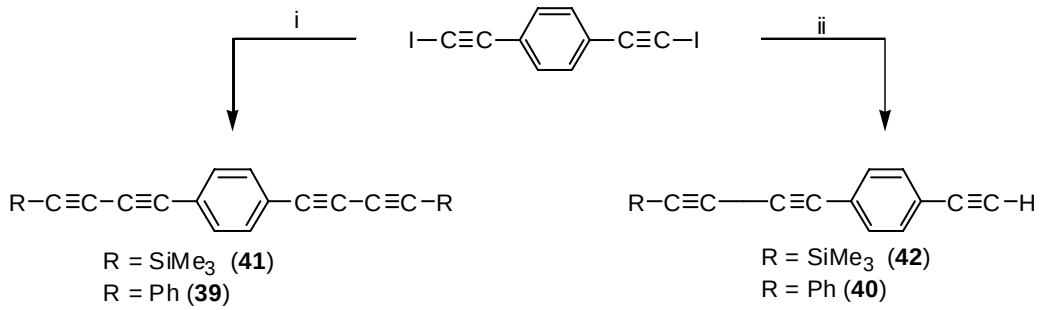

Reagents: i, $Au(C{\equiv}CR)PPh_3$ (2 eq) / $Pd(PPh_3)_4$ / CuI; ii, $Au(C{\equiv}CR)PPh_3$ (1 eq) / $Pd(PPh_3)_4$ / CuI

Scheme 4.4

4.2.2 Fluorinated linkers

Due to the electron withdrawing capabilities of fluorine, it was proposed that replacing the hydrogen atoms around the linking aromatic unit with fluorine atoms would improve the electron transport properties of the molecule. The electronegative fluorine substituents withdraw electron density from the bridging ligand and hence the metal centres thus increasing the kinetic stability of the molecule. This should increase the oxidation potential of the molecule. The larger fluorine atoms also provide steric protection for the chain.

It has been found previously that (pentafluorophenyl)ethynyl compounds undergo nucleophilic substitution of the *para* fluorine to give the corresponding *para*-substituted tetrafluorophenyl compound.[147-149] Hence, it was proposed that a convenient method for synthesising bis-metallo-1,4-diethynyltetrafluorobenzenes would be to react monometallic ethynylpentafluorobenzene with an alkyne nucleophile (Scheme 4.5).

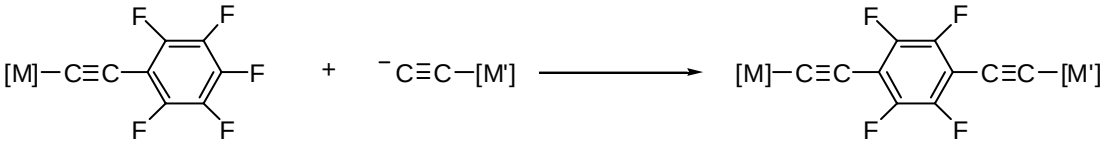

Scheme 4.5

Earlier reports have described the synthesis of $Ru(C{\equiv}CC_6F_5)(PPh_3)_2Cp$ by treatment of pentafluorophenylacetylene with $RuCl(PPh_3)_2Cp$ in the presence of sodium methoxide.[150] The analogues $Ru(C{\equiv}CC_6F_5)(dppe)Cp$ (**43**) and $Ru(C{\equiv}CC_6F_5)(dppe)Cp^*$ (**44**) were synthesised by reacting the trimethylsilyl-substituted alkyne, $Me_3SiC{\equiv}CC_6F_5$, with RuCl(dppe)Cp' (Cp' = Cp, Cp*)in the presence of potassium fluoride in 63% and 54% yield respectively. This route eliminated the need to deprotect the alkyne and avoided using sodium methoxide which could potentially attack the para-fluorine as the methoxy group is nucleophilic. Elemental analyses confirmed the formulations of these complexes, supported by spectroscopic data. Thus, in the ^{19}F NMR spectrum three resonances

are observed as AA'MM'X systems. The *ortho* and *meta* fluorines of **43** are observed as multiplets with a relative intensity of two at δ 9.13 and -14.10 respectively. The *para*-fluorine is observed as a triplet at δ -13.61, due to coupling with the *meta* fluorines, with a coupling constant of 21 Hz. Replacing the Cp group by Cp* in **44** has little effect on the *ortho*-fluorine which is found at δ 8.96, while the *para*-fluorine (δ -14.30) is now observed upfield of the *meta*-fluorine (δ -14.04). In the ^{31}P NMR spectrum, characteristic resonances at δ 86.98 (for **43**) and 81.72 (for **44**) were found. The ES mass spectra of these complexes contained $[M]^+$ at *m/z* 756 (**43**) and *m/z* 826 (**44**) followed by $[M - F]^+$ at *m/z* 738 (**43**) and *m/z* 808 (**44**).

The structures of **43** (Figure 4.2) and **44** (Figure 4.3) were confirmed by X-ray studies of crystals grown from dichloromethane/hexane. The Ru(dppe)Cp' fragments have the expected geometry, with Ru-P 2.238 - 2.2694(8) Å and Ru-C(Cp) 2.218 – 2.269(3) Å. Along the carbon chain of **43** C(1)-C(2) is 1.204(9) Å and C(2)-C(21) is 1.440(8) Å while in **44** C(1)-C(2) is 1.217(5) Å and C(2)-C(21) is 1.442(5) Å. The Ru-C(1) distance in **43** is 1.979(6) Å, and much closer to that reported for Ru(C≡CC≡CSiMe$_3$)(dppe)Cp* [1.983(2) Å][126] than in **44** in which the Ru-C(1) distance is 2.000(3) which is nearer to that found for **34** [2.007(4) Å]. The carbon chain of **43** is significantly more linear, angles at C(1,2) 178.6(6) and 177.4(7)° respectively, than that of **44**, angles at C(1,2) 168.9(3) and 170.3(3)° respectively.

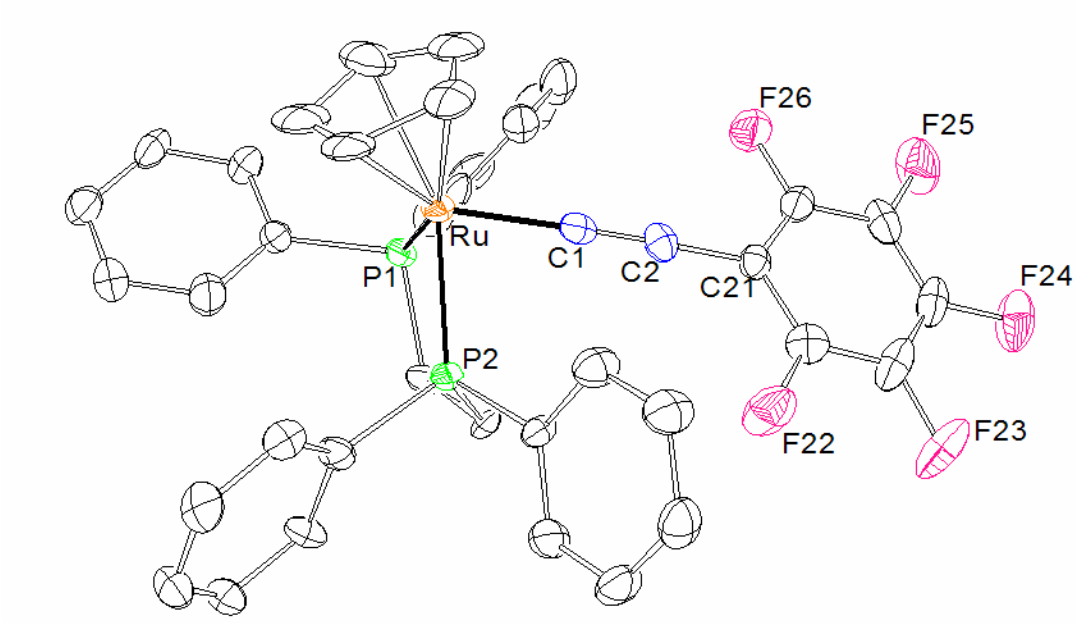

Figure 4.3 *ORTEP view of Ru(C≡CC$_6$F$_5$)(dppe)Cp (**43**).*

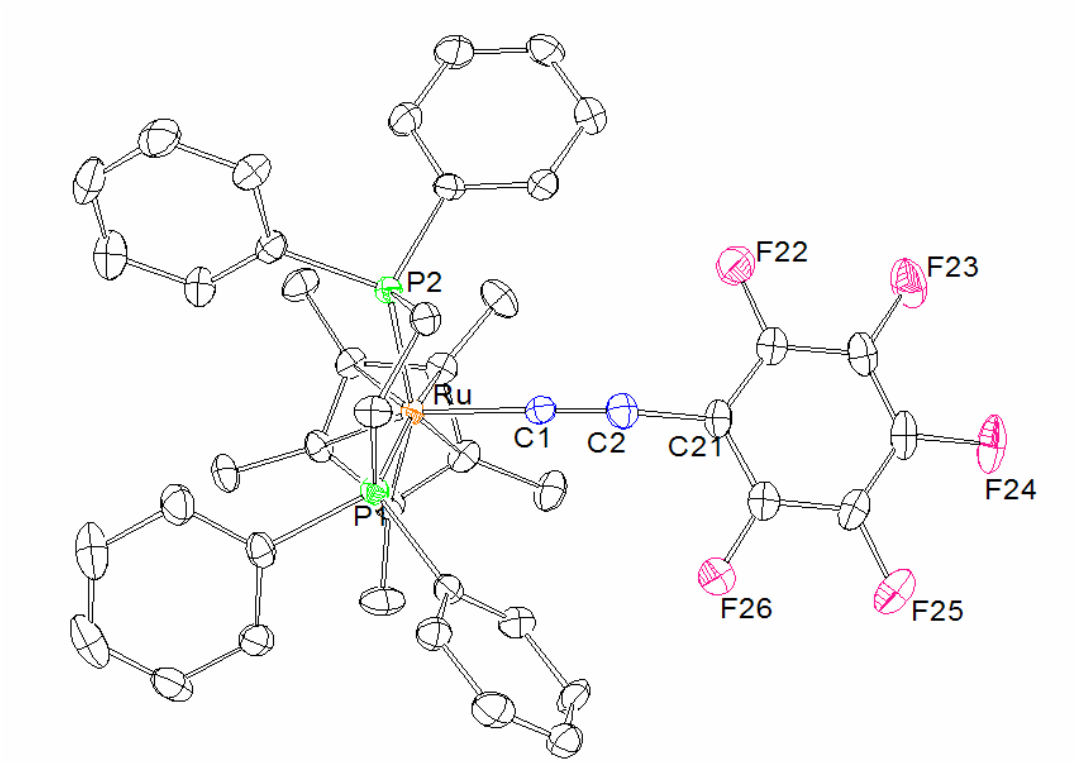

Figure 4.4 *ORTEP view of Ru(C≡CC$_6$F$_5$)(dppe)Cp* (**44**).*

Table 4.2: *Selected structural data for Ru(C≡CC$_6$F$_5$)(dppe)Cp (**43**) and Ru(C≡CC$_6$F$_5$)(dppe)Cp* (**44**).*

Complex	Ru(C≡CC$_6$F$_5$)(dppe)Cp (**43**)	Ru(C≡CC$_6$F$_5$)(dppe)Cp* (**44**)
Bond Distances (Å)		
Ru-P(1,2)	2.238(2), 2.261(2)	2.2694(8), 2.2592(8)
Ru-C(Cp*)	2.218(9) – 2.248(8)	2.225(3)-2.269(3)
Ru-C(Cp*) (av.)	2.231(8)	2.254(3)
Ru-C(1)	1.979(6)	2.000(3)
C(1)-C(2)	1.204(9)	1.217(5)
C(2)-C(21)	1.440(8)	1.442(5)
C(21)-C(22)	1.37(1)	1.398(5)
C(22)-C(23)	1.37(1)	1.384(6)
C(23)-C(24)	1.36(1)	1.373(6)
C(24)-C(25)	1.37(1)	1.353(5)
C(25)-C(26)	1.362(9)	1.371(6)
C(26)-C(21)	1.384(9)	1.395(5)
C(n)-F(n)	1.346(8) – 1.333(9)	1.338(5) – 1.353(5)
(n = 22-26)		
C(n)-F(n) (av.)	1.340(9)	1.344(5)
Bond Angles (˚)		
Ru-C(1)-C(2)	178.6(6)	168.9(3)
C(1)-C(2)-C(21)	177.4(7)	170.3(3)
C(2)-C(21)-C(22)	121.4(6)	122.5(3)
C(2)-C(21)-C(26)	115.7(6)	114.7(3)

Reacting the gold complex Au(C≡CC$_6$F$_5$)(PPh$_3$)[151] with a halogen-capped trimetallic complex, Co$_3$(μ_3-CBr)(μ-dppm)(CO)$_7$ or monometallic Mo(≡CBr)(CO)$_2$Tp* under standard gold coupling conditions gives the C$_3$-pentafluorophenyl complexes, Co$_3$(μ_3-CC≡CC$_6$F$_5$)(dppm)(CO)$_7$ (**45**) and Mo(≡CC≡CC$_6$F$_5$)(CO)$_2$Tp* (**46**) in 36 and 18% yield respectively. The ES mass spectra confirmed the formulations of these complexes, containing [M + Na]$^+$ at *m/z* 982 (**45**) and at *m/z* 677 (**46**). The IR spectrum of **45** contains one ν(C≡C) band at 2122 cm^{-1} and three ν(C≡O) bands

between 2062 and 1976 cm^{-1} while that of **46** contains two ν(C≡C) bands at 2110 and 2061 cm^{-1} and two ν(C≡O) bands at 2006 and 1926 cm^{-1}. In the ^{19}F NMR the *ortho* and *meta* fluorines have AA'MM' patterns and are found at δ 15.47 (**45**), 17.95 (**46**) and δ -10.30 (**45**), -9.16 (**46**). The *para*-fluorines are observed as triplets with a coupling constant of 20 Hz at δ -3.12 (**45**) and 1.09 (**46**). The broadening of each line within the triplet suggests that there is also coupling between the *para* and *ortho* fluorines which should give a triplet of triplets.

The structure of **45** was confirmed by an X-ray structure determination. The carbon chain is essentially linear [C(1)-C(2)-C(31) 175.8(2)˚] with C(1)-C(2) [1.403(2) Å] consistent with a carbon-carbon single bond and C(2)-C(3) [1.213(2) Å] with a carbon-carbon triple bond. The Co_3(μ-dppm)$(CO)_7$ cluster is similar to those found in related examples including **7**, **8** and **9**.

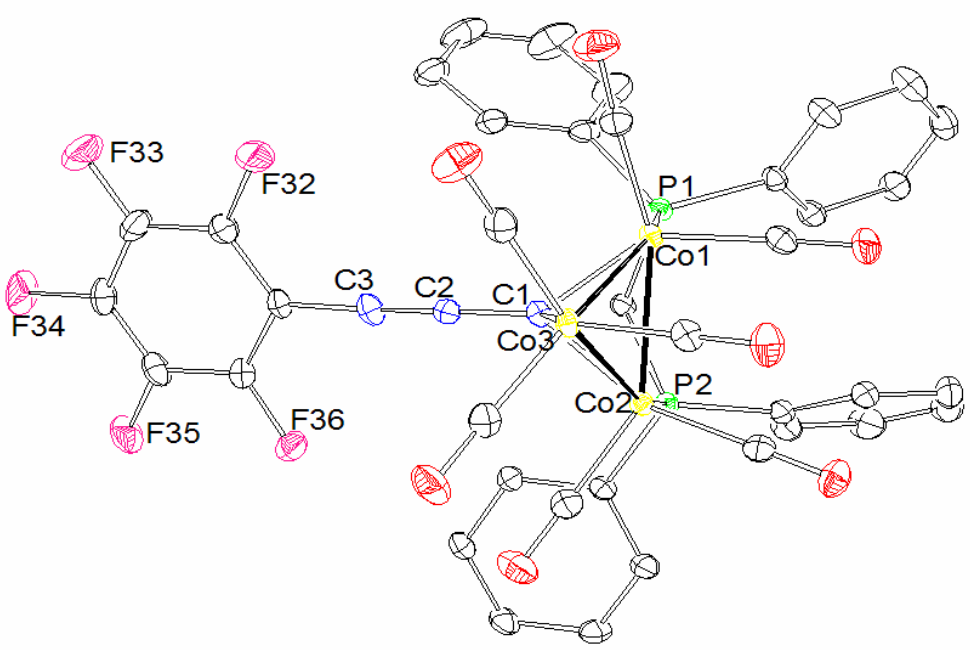

Figure 4.5 *ORTEP view of $Co_3(\mu_3\text{-}CC{\equiv}CC_6F_5)(dppm)(CO)_7$ (**45**).*

Table 4.3: *Selected structural data for $Co_3(\mu_3\text{-}CC{\equiv}CC_6F_5)(dppm)(CO)_7$ (**19**).*

Bond Distances (Å)		**Bond Angles (˚)**	
Co(1)-Co(2,3)	2.4781(5), 2.4810(4)	Co(1)-C(1)-C(2)	136.3(1)
Co(2)-Co(3)	2.4805(4)	Co(2)-C(1)-C(2)	131.4(1)
Co(n)-P(n) (n = 1,2)	2.2014(5), 2.2035(4)	Co(3)-C(1)-C(2)	81.05(6)
Co(1)-C(1)	1.8998(1)	C(1)-C(2)-C(3)	179.1(2)
Co(2)-C(1)	1.914(2)	C(1)-C(2)-C(31)	175.8(2)
Co(3)-C(1)	1.947(1)	C(3)-C(31)-C(32)	121.9(1)
C(1)-C(2)	1.403(2)	C(3)-C(31)-C(36)	121.8(1)
C(2)-C(3)	1.213(2)		
C(3)-C(32)	1.428(2)		

Similarly reacting $Au(C{\equiv}CC_6F_5)(PPh_3)$ and iodoethynylferrocene, $Fc(C{\equiv}CI)$ under standard gold coupling conditions gives the C_4-pentafluorophenyl compound $Fc(C{\equiv}C)_2C_6F_5$ (**47**) (Scheme 4.6). Elemental analysis confirmed the formulation of this complex, supported by the usual spectroscopic data. Thus in the IR spectrum a single $\nu(C{\equiv}C)$ band was observed at 2220 cm^{-1}. In the ^{13}C NMR spectrum resonances at δ 62.10, 69.53, 86.86 and 99.55 are assigned to the carbon chain nuclei. In the ^{19}F NMR three characteristic multiplets are found with two multiplets at δ 17.13 and -8.97 for the *ortho* and *meta* fluorines respectively and a triplet at δ 0.97 for the *para*-fluorine. Finally the ES-mass spectrum contains $[M]^+$ at *m/z* 400.

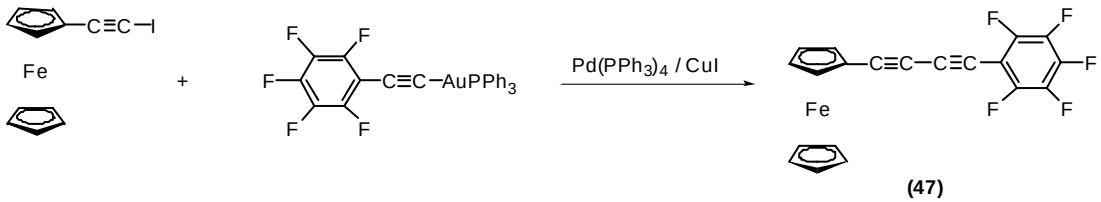

(47)

Scheme 4.6

4.2.2.1 Organometalic Linkers

The insertion of an organometallic fragment into a conjugated chain will also alter the communication between terminal metal centres. An organometallic linker which has been found to enhance electronic communication between two iron centres when incorporated into the bridging carbon chain is the di-platinum fragment $Pt_2(\mu\text{-dppm})_2$.[152,153]

Reacting two equivalents of the $C_6F_5C{\equiv}CSiMe_3$ with the dichloro precursor, $Pt_2Cl_2(\mu\text{-dppm})_2$, in the presence of sodium methoxide gives the organometallic linker, $Pt_2\{C{\equiv}CC_6F_5\}_2(dppm)_2$ (**48**) (Scheme 4.7). The IR spectrum of this complex contains a single ν(C≡C) band at 2079 cm^{-1}. In the ^1H NMR spectrum, characteristic resonances are found for the dppm at δ 4.62 for the methylene portion and between δ 6.96 and 7.90 for the phenyl protons. In the ^{31}P NMR spectrum a resonance is found at δ 2.13 along with satellite peaks with a coupling constant of 2816 Hz due to the coupling between the phosphorus and platinum atoms. In the ^{19}F NMR spectrum the usual three multiplets are found at δ -13.64, -11.16 and 11.52. Finally, the ES-MS contains $[M + H]^+$ at *m/z* 1541. No evidence was found to suggest that the *para*-fluorine of this complex was undergoing nucleophilic attack by the methoxide present. This is most likely due to the desired coupling occurring at a much faster rate and the product precipitating out before any nucleophilic attack can take place.

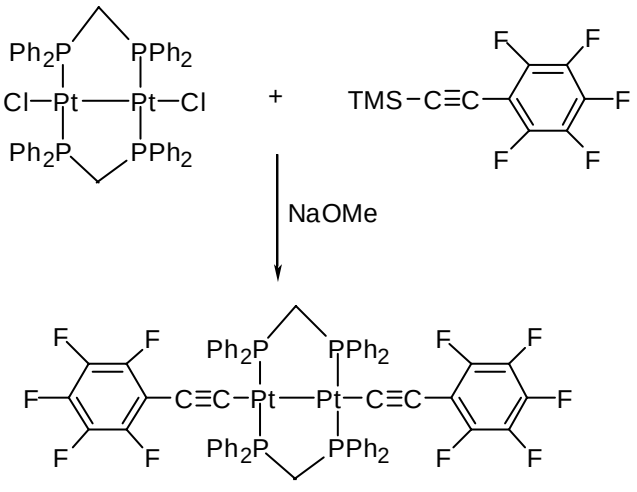

(**48**)

Scheme 4.7

4.2.2.2 1,4-diethynyltetrafluorobenzene

All attempts to synthesise bis-metallic-1,4-diethynyltetrafluorobenzene by reacting these monometallic ethynylpentafluorobenzenes with nucleophilic alkynes (Scheme 4.5) were unsuccessful. This is probably due to the instability of the nucleophilic alkynes which were prepared *in situ*. Hence the previously reported 1,4-bis[(trimethylsilyl)ethynyl]tetrafluorobenzene[154] was reacted with RuCl(PP)Cp' (where PP = $(PPh_3)_2$, dppe Cp' = Cp, Cp*) in the presence of potassium fluoride,[142] in a method analogous to that used to prepare **29** and **30**.

The bis-ruthenium complexes 1,4-$\{Cp(PPh_3)_2Ru(C\equiv C)\}_2C_6F_4$ (**49**) and 1,4-$\{Cp(dppe)Ru(C\equiv C)\}_2C_6F_4$ (**50**) were made via this route in 60% and 26% yield respectively. Elemental analyses and the ES mass spectra confirmed the formulations of these complexes with $[M]^+$ found at *m/z* 1578 (for **49**) and *m/z* 1326 (for **50**). The IR spectra contain two ν(C≡C) bands between 2072 and 2039 cm^{-1}. In the ^1H NMR spectrum, the usual resonance for the Cp ligand is found at δ 4.86 (**49**) and 4.71 (**50**). In the ^{31}P NMR spectrum, characteristic resonances at δ 51.72 (for **49**) and 86.65 (for **50**) were found. The ^{19}F NMR spectra contain only one resonance at δ 7.59 (for **49**) and δ 6.89 (for **50**), as expected due to the 1,4-disubstitution.

A third bis-ruthenium complex, 1,4-$\{Cp^*(dppe)Ru(C\equiv C)\}_2C_6F_4$ (**51**), was obtained in high yield (63%) using this synthetic method and characterised by elemental microanalyses and spectroscopic tehniques. The IR spectrum contains two ν(C≡C) bands at 2063 and 2032 cm^{-1} and the ^1H NMR spectrum exhibits a methyl proton Cp* resonance at δ 1.68. In the ^{13}C NMR spectra resonances were observed at δ 93.71 for the Cp* ring carbons and at δ 10.68 for the Cp* methyl carbons, while in the ^{19}F NMR a single resonance was observed at δ 6.83.

The structure of **51** was confirmed by an X-ray structure determination of crystals obtained after recrystallisation from dichloromethane (Figure 4.6). The Ru(dppe)Cp fragment has the expected geometry, with Ru-P(1,2) 2.2542 and 2.2607(7) Å and Ru-C(Cp) 2.223 – 2.264(3) Å. Along the carbon chain C(1)-C(2) is 1.221(3) Å

while C(2)-C(3) is 1.427(3) Å and the Ru-C(1) distance is 1.996(2) Å. The carbon chain is essentially linear, with angles of 172.6(2) at C(1),and 172.2(3) ˚at C(2).

Table 4.4 *Selected structural data for 1,4-{Ru(dppe)Cp*(C≡C)}$_2$C$_6$F$_4$ (**50**).*

Bond Distances (Å)		**Bond Angles (˚)**	
Ru-P(1,2)	2.2542(7), 2.2607(7)	Ru-C(1)-C(2)	172.6(2)
Ru-C(Cp*)	2.223(3) – 2.264(3)	C(1)-C(2)-C(3)	172.2(3)
Ru-C(Cp*) (av.)	2.250(3)	C(2)-C(3)-C(4)	123.4(2)
Ru-C(1)	1.996(2)	C(2)-C(3)-C(5)	122.1(2)
C(1)-C(2)	1.221(3)	C(4)-C(3)-C(5)	114.5(2)
C(2)-C(3)	1.427(3)	C(3)-C(4)-C(5)	123.1(2)
C(3)-C(4)	1.394(3)		
C(4)-C(5)	1.337(3)		
C(3)-C(5)	1.406(3)		
C(4)-F(4)	1.356(3)		
C(5)-F(5)	1.342(3)		

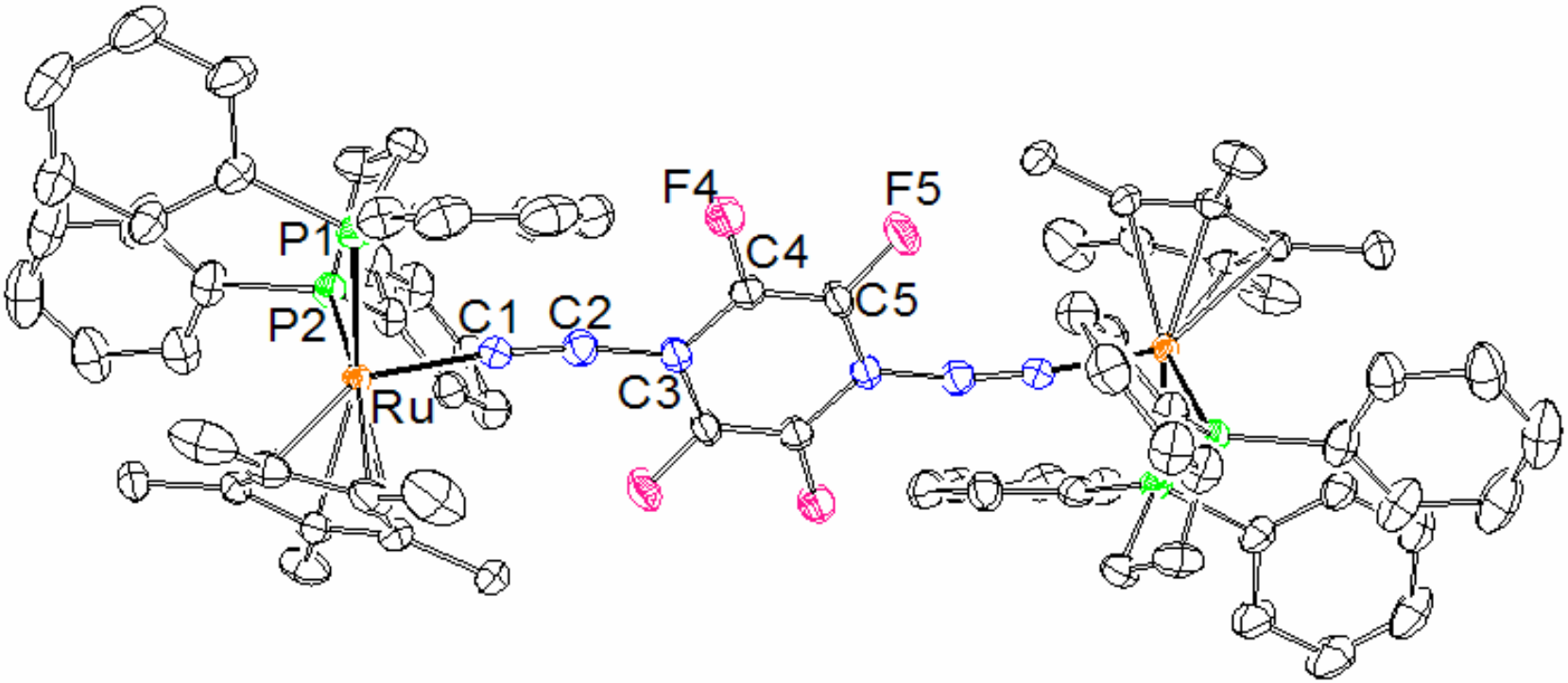

Figure 4.6: *ORTEP view of 1,4-{Cp*(dppe)Ru(C≡C)}$_2$C$_6$F$_4$ (**50**).*

4.3 Electrochemistry

Electrochemical studies of the 1,4-diethynylbenzene complexes **32** and **33** show two reversible oxidation waves with E_1 = +0.14 and -0.4 V respectively. Values for the corresponding monometallic complexes, Ru(C≡CPh)(dppe)Cp and Ru(C≡CPh)(dppe)Cp*, are much higher at +0.38 and +0.20 V respectively. This is a clear indication that there is some electronic communication between the two ruthenium centres in **32** and **33** through the 1,4-diethynylbenzene linker. Electronic communication is also evidenced by $\Delta E_{½}$ values of approximately 0.22 V in these complexes.

The cyclic voltammogram of the tetrafluoro analogues **50** and **51** also show two reversible oxidation waves with E_1 = +0.29 and +0.11 respectively. The monometallic complexes **43** and **44** have E_1 values which are higher still at +0.56 and +0.42 V respectively. In these complexes the fluorine atoms withdraw electron density from the bridge making the first oxidation much harder compared to that of **32** and **33** (Figure 4.5). Complexes **50** and **51** have larger $\Delta E_{½}$ values (*ca* 0.30 V) than those found for **32** and **33** (*ca* 0.22 V). Thus it appears that the C_6F_4 bridge enhances electronic communication relative to the C_6H_4 bridge.

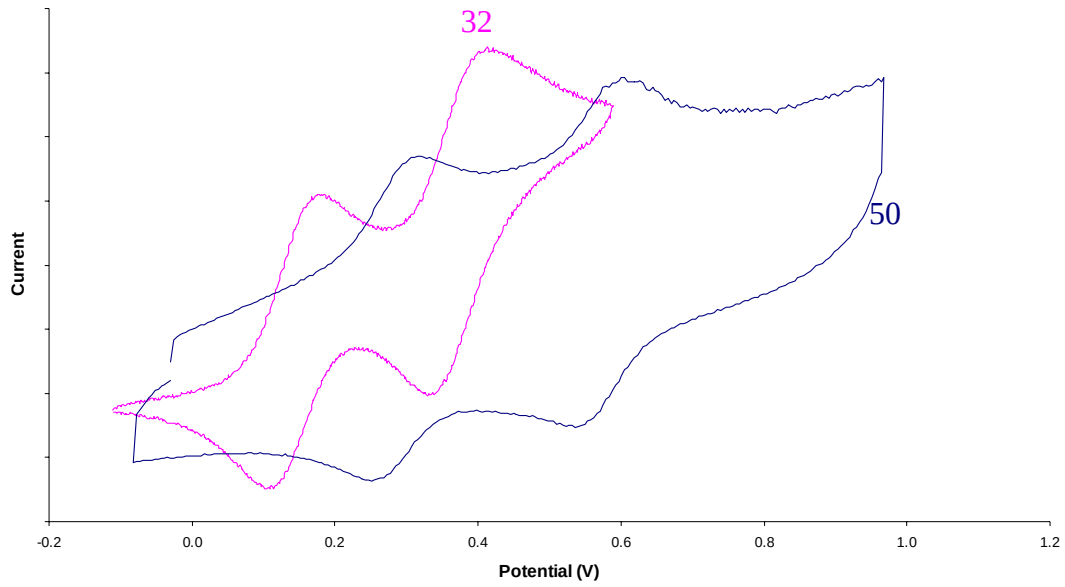

Figure 4.7: *Cyclic voltammograms of 1,4-{Ru(dppe)Cp(C≡C)}$_2$C$_6$H$_4$ (**32**) and 1,4-{RuCp(dppe)(C≡C)}$_2$C$_6$F$_4$ (**50**) recorded in CH$_2$Cl$_2$, 0.01M [Bu$^n_4$N][PF$_6$].*

Interestingly this increase in $\Delta E_{½}$ values was not seen for the triphenylphosphine complexes **31** (0.29 V) and **49** (0.30 V). This suggests that in these complexes the fluorine atoms have no overall effect on electronic communication. However the E_1 values follow the previous trend with decreasing values from the monometallic complex (+0.49 V) to **49** (+0.37 V) and finally to **31** (+0.16 V).

The K_c values of complexes **33** and **51** (Table 4.3) can be compared to those reported in Chapter Two for the bis-ruthenium series $\{Cp^*(dppe)Ru\}_2(C{\equiv}C)_n$ which contain pure polyynyl bridging ligands. The K_c value of **33** (2.40×10^3) is most comparable with that of the C_{12} complex (2.91×10^3) while that of **51** (2.56×10^5) is similar with that in the C_8 complex (9.5×10^5). Interestingly the two ruthenium atoms of **51** are separated by 12.12 Å, which is very close to that of the estimated value for the C_8 complex.

Table 4.3: *Electrochemical Data*

Complex	E_1	E_2	$\Delta E_{1/2}$	K_c (0/+1/+2) [a]
$Ru(C{\equiv}CC_6H_4C{\equiv}CSiMe_3)(PPh_3)_2Cp$	+0.49	+1.14[b]		
1,4-$\{Cp(PPh_3)_2Ru(C{\equiv}C)\}_2C_6H_4$ (**31**)	+0.16	+0.45	0.29	7.95×10^4
1,4-$\{Cp(dppe)Ru(C{\equiv}C)\}_2C_6H_4$ (**32**)	+0.14	+0.37	0.23	7.70×10^3
1,4-$\{Cp^*(dppe)Ru(C{\equiv}C)\}_2C_6H_4$ (**33**)	−0.04	+0.24	0.20	2.40×10^3
$Ru(C{\equiv}CPh)(dppe)Cp$	+0.38	+1.14[b]		
$Ru(C{\equiv}CPh)(dppe)Cp^*$	+0.20	+1.04[b]		
1,4-$\{Cp(PPh_3)_2Ru(C{\equiv}C)\}_2C_6F_4$ (**49**)	+0.37	+0.67	0.30	1.17×10^5
1,4-$\{Cp(dppe)Ru(C{\equiv}C)\}_2C_6F_4$ (**50**)	+0.29	+0.57	0.28	5.39×10^4
1,4-$\{Cp^*(dppe)Ru(C{\equiv}C)\}_2C_6F_4$ (**51**)	+0.11	+0.43	0.32	2.56×10^5
$Ru(C{\equiv}CC_6F_5)(dppe)Cp$ (**43**)	+0.56			
$Ru(C{\equiv}CC_6F_5)(dppe)Cp^*$ (**44**)	+0.42	+1.15[b]		

Electrochemical data (V), measured in CH_2Cl_2 with $[Bu^n{}_4N][PF_6]$ supporting electrolyte, values referenced to $[FeCp_2]/[FeCp_2]^+ = 0.46$ V. [a] *All values calculated from ΔE and Equation 1.6.* [b] *Peak potential of an irreversible process*

4.4 Conclusion

This work has demonstrated the efficient synthesis of bis-ruthenium 1,4-diethynyl benzene and 1,4-diethynyltetrafluorobenzene complexes by treating the $SiMe_3$-protected bridging ligand with two equivalents of the metal-halide precursor in a fluoride-catalysed desilylation reaction. The gold reaction provided a convenient synthetic route to organic 1,4-bis(butadiynyl)benzene and 4-(butadiynyl)phenylethyne compounds.

Electrochemical measurements show that the insertion of an aromatic ring into the poly-yndiyl bridge makes these complexes easier to oxidise. Electronic interactions appear to be stronger in the tetrafluoro complexes within the Ru(dppe)Cp' (Cp' = Cp, Cp*) series, thus making the 1,4-diethynyltetrafluorobenzene group a better linker for potential molecular wires. Interestingly both the K_c value and metal seperation of the tetrafluoro complex **51** are comparable to that of the C_8 complex, $\{Cp^*(dppe)Ru\}_2(C{\equiv}C)_4$. Hence it would seem that, at least in this system, the 1,4-diethynyltetrafluorobenzene linker is as effective as a polyynyl bridge of similar length.

4.5 Experimental

Reagents. The complexes 1,4-{Cp(PPh$_3$)$_2$Ru(C≡C)}$_2$C$_6$H$_4$,[155] RuCl(dppe)Cp,[156] RuCl(dppe)Cp*[130], RuCl(PPh$_3$)$_2$Cp[155] Mo(≡CBr)(CO)$_2$Tp*,[128,129] Pd(PPh$_3$)$_4$[100] Au(C≡CSiMe$_3$)(PPh$_3$)[157] Co$_3$(μ_3-CBr)(μ-dppm)(CO)$_{7,}$[120] I-C≡CFc,[158] Pt$_2$Cl$_2$(dppm)$_2$,[159] Au(C≡CC$_6$F$_5$)PPh$_3$,[160] 1,4-{Me$_3$SiC≡C}$_2$C$_6$F$_4$,[154] Ru(C≡CPh)(dppe)Cp[161] and Ru(C≡CPh)(dppe) Cp*[161] were prepared as described previously.

1,4-{Ru(dppe)Cp(C≡C)}$_2$C$_6$H$_4$ (32)

A mixture of 1,4-(Me$_3$SiC≡C)$_2$C$_6$H$_4$ (50 mg, 0.19 mmol), RuCl(dppe)Cp (222 mg, 0.37 mol) and KF (21 mg, 0.37 mmol) in MeOH (30 ml) was heated under reflux for 16 h and a yellow precipitate formed, which was collected and washed with MeOH followed by ether and hexane to give 1,4-{Cp(dppe)Ru(C≡C)}$_2$C$_6$H$_4$ (69 mg, 30%). Anal. Calcd (C$_{72}$H$_{62}$P$_4$Ru$_2$): C, 69.00; H, 4.99. Found: C, 68.98; H, 5.06. IR (Nujol, cm^{-1}): ν(C≡C) 2146 w, 2072 m, 2044 sh. ^{1}H NMR (C$_6$D$_6$): δ 1.96, 2.54 (2m, 2 x 2H, CH$_2$CH$_2$), 4.26 (s, 5H, Cp), 6.75 – 7.97 (m, 22H, Ph and C$_6$H$_4$). ^{31}P NMR: δ 87.03 (s, 2P, dppe). ES-mass spectrum (*m/z*): 1255, [M + H]$^+$; 1275, [M + Na]$^+$.

1,4-{Ru(dppe)Cp*(C≡C)}$_2$C$_6$H$_4$ (33)

A mixture of 1,4-(Me$_3$SiC≡C)$_2$C$_6$H$_4$ (50 mg, 0.18 mmol), RuCl(dppe)Cp* (232 mg, 0.29 mol) and KF (55 mg, 0.95 mmol) in thf (5 ml) and MeOH (20 ml) containing dbu (18.5 mg, 0.12 mmol) was heated under reflux for 16 h. The mixture was then chromatographed on a basic alumina column gradient eluting with hexane/acetone. Concentration of the red fraction gave 1,4-{Ru(dppe)Cp*(C≡C)}$_2$C$_6$H$_4$ (10 mg, 4%). Anal. Calcd (C$_{82}$H$_{82}$P$_4$Ru$_2$): C, 70.65; H, 5.93. Found: C, 70.61; H, 5.95. IR (Nujol, cm^{-1}): ν(C≡C) 2143 w, 2084 s, 2049 sh. ^{1}H NMR (C$_6$D$_6$): δ 1.68 (s, 15H, Cp*), 1.88, 2.69 (2m, 2 x 2H, CH$_2$CH$_2$), 6.89 – 7.96 (m, 22H, Ph and C$_6$H$_4$). ^{13}C NMR: (C$_6$D$_6$) δ 11.23 (s, C$_5$*Me*$_5$), 30.60 (m, CH$_2$CH$_2$), 94.81 (s, *C*$_5$Me$_5$), 127.17 – 143.14 (m, Ph). ^{31}P NMR: δ 82.15 (s, 2P, dppe). ES-mass spectrum (*m/z*): 1418, [M + Na]$^+$; 1394, [M]$^+$.

Ru(C≡CC$_6$H$_4$C≡CSiMe$_3$)(dppe)Cp (34)

A mixture of 1,4-(Me$_3$SiC≡C)$_2$C$_6$H$_4$ (100 mg, 0.36 mmol), RuCl(dppe)Cp (222 mg, 0.37 mol) and KF (21 mg, 0.37 mmol) in MeOH (20 ml) was heated under reflux for 2 h and an orange precipitate formed, which was collected and washed with MeOH followed by ether and hexane to give Ru(C≡CC$_6$H$_4$C≡CSiMe$_3$)(dppe)Cp (175 mg, 62%). Anal. Calcd (C$_{44}$H$_{42}$P$_2$RuSi): C, 69.36; H, 5.56. Found: C, 69.37; H, 5.47. IR (Nujol, cm^{-1}): ν(C≡C) 2145 m, 2067 s, 2042 sh. ^{1}H NMR (C$_6$D$_6$): δ 0.21 (s, 9H, SiMe$_3$), 1.96, 2.50 (2m, 2 x 2H, CH$_2$CH$_2$), 4.73 (s, 5H, Cp), 6.74 – 7.93 (m, 24H, Ph). ^{13}C NMR: (C$_6$D$_6$) δ 0.56 (s, SiMe$_3$), 28.66 [t, ^2J(CP) 44 Hz, CH$_2$CH$_2$], 83.26 (s, Cp), 128.07 – 145.02 (m, Ph). ^{31}P NMR: δ 86.84 (s, 2P, dppe). ES-mass spectrum (*m/z*): 785, [M + Na]$^+$; 762, [M]$^+$; 565, [Cp(dppe)Ru]$^+$.

Ru(C≡CC$_6$H$_4$C≡CSiMe$_3$)(dppe)Cp* (35)

A mixture of 1,4-(Me$_3$SiC≡C)$_2$C$_6$H$_4$ (100 mg, 0.36 mmol), RuCl(dppe)Cp* (232 mg, 0.29 mol) and KF (22 mg, 0.48 mmol) in MeOH (30 ml) with dbu (18 mg, 0.12 mmol) was heated under reflux for 16 h and a rust orange precipitate formed, which was collected and washed with MeOH followed by ether and hexane to give Ru(C≡CC$_6$H$_4$C≡CSiMe$_3$)(dppe)Cp* (60 mg, 20%). Anal. Calcd (C$_{49}$H$_{50}$P$_2$RuSi): C, 70.90; H, 6.07. Found: C, 70.97; H, 6.02. IR (Nujol, cm^{-1}): ν(C≡C) 2150 m, 2082 w, 2058 s 2045 sh. ^{1}H NMR (C$_6$D$_6$): δ 0.25 (s, 9H, SiMe$_3$), 1.63 (s, 15H, Cp*), 1.85, 2.56 (2m, 2 x 2H, CH$_2$CH$_2$), 7.01 – 7.94 (m, 24H, Ph and C$_6$H$_4$). ^{13}C NMR: (C$_6$D$_6$) δ 0.62 (s, SiMe$_3$), 10.68 (s, C$_5$*Me*$_5$), 30.02 [t, ^2J(CP) 46 Hz, CH$_2$CH$_2$], 93.26 (s, *C*$_5$Me$_5$), 127.88 – 139.89 (m, Ph). ^{31}P NMR: δ 81.88 (s, 2P, dppe). ES-mass spectrum (*m/z*): 856, [M + Na]$^+$; 833, [M + H]$^+$.

Ru{C≡CC$_6$H$_4$C≡CAu(PPh$_3$)}(dppe)Cp (36)

To a stirred suspension of AuCl(PPh$_3$) (64 mg, 0.13 mmol) in thf (5 ml) and NaOMe (MeOH 5 ml, Na 14 mg) was added Ru(C≡CC$_6$H$_4$C≡CSiMe$_3$)(dppe)Cp (100 mg, 0.13 mmol). This mixture was stirred at r.t. for 4 h before the resulting yellow precipitate was collected and washed with MeOH followed by hexane to give Ru{C≡CC$_6$H$_4$C≡CAu(PPh$_3$)}(dppe)Cp (94 mg, 63%). IR (Nujol, cm^{-1}): ν(C≡C) 2146 m, 2069 s. ^{1}H NMR (C$_6$D$_6$): δ 1.96, 2.48 (2m, 2 x 2H, CH$_2$CH$_2$), 4.73 (s, 5H,

Cp), 6.75 – 7.93 (m, 39H, Ph and C_6H_4). ^{31}P NMR: δ 33.91 (s, 1P, $AuPPh_3$), 86.83 (s, 2P, dppe). ES-mass spectrum (*m/z*): 1149, $[M + H]^+$; 721, $[(PPh_3)_2Au]^+$.

Ru{C≡CC_6H_4C≡CAu(PPh_3)}(dppe)Cp* (37)

To a stirred suspension of $AuCl(PPh_3)$ (60 mg, 0.12 mmol) in thf (5 ml) and NaOMe (MeOH 5 ml, Na 14 mg) was added Ru(C≡CC_6H_4C≡C$SiMe_3$)(dppe)Cp* (100 mg, 0.12 mmol). This mixture was stirred at r.t. for 4 h before the resulting yellow precipitate was collected and washed with MeOH followed by hexane to give Ru{C≡CC_6H_4C≡CAu(PPh_3)}(dppe)Cp* (120 mg, 82%). Anal. Calcd ($C_{64}H_{56}AuP_3Ru$): C, 63.21; H, 4.64. Found: C, 63.17; H, 4.71. IR (Nujol, cm^{-1}): ν(C≡C) 2083 sh, 2070 s, 2043 m. ^{1}H NMR (C_6D_6): δ 1.65 (s, 15H, Cp*), 1.87, 2.64 (2m, 2 x 2H, CH_2CH_2), 6.84 – 7.94 (m, 39H, Ph and C_6H_4). ^{13}C NMR: (C_6D_6) δ 10.72 (s, C_5*Me*$_5$), 26.14 (s, CH_2CH_2), 68.15 (s, C≡C), 93.11 (s, *C*$_5$Me$_5$), 123.52 – 137.38 (m, Ph). ^{31}P NMR: δ 43.44 (s, 1P, $AuPPh_3$), 81.99 (s, 2P, dppe). ES-mass spectrum (*m/z*): 1241, $[M + Na]^+$; 1218, $[M]^+$; 721, $[(PPh_3)_2Au]^+$.

1,4-(IC≡C)$_2$$C_6H_4$ (38)

To a solution of 1,4-(Me_3SiC≡C)$_2$$C_6H_4$ (500 mg, 1.8 mmol) in sodium methoxide [Na (40 mg) in MeOH (30 ml)] was added solid I_2 (~ 100 mg) until the iodine colour remained. The mixture was then washed with sodium thiosulphate (100 ml of 20% solution in H_2O) and extracted with dichloromethane (3 x 100 ml). The organic phase was then concentrated and chromatographed on a silica column eluting with hexane. The pale yellow fraction was collected and the solvent removed to obtain 1,4-(IC≡C)$_2$$C_6H_4$ (450 mg, 64%). ^{1}H NMR ($CDCl_3$): δ 7.27 (s, 4H, C_6H_4). ES-mass spectrum (*m/z*): 378, $[M]^+$.

1,4-Bis(phenylbutadiynyl)benzene (39)

A mixture of Au(C≡CPh)(PPh_3) (100 mg, 0.18 mmol), 1,4-bis(iodoethynyl)benzene (34 mg, 0.09 mmol), Pd(PPh_3)$_4$ (15 mg, 0.01 mmol) and CuI (5 mg, 0.02 mmol) in thf (30 ml) was heated under reflux for 6 h. The solvent was then removed and the black residue purified by preparative t.l.c. using hexane/dichloromethane (4:1) as an elutant. The UV active fraction was collected and the solvent removed to give 1,4-bis(phenylbutadiynyl)benzene (29 mg, 26%) as pale brown needles, mp 250−253˚C.

^{1}H NMR ($CDCl_3$) δ 7.30 – 7.59 (m, 14H, Ph). FAB-mass spectrum *(m/z)* 326, $[M]^+$; 202, $[M - C_4Ph]^+$. All values agreed with those previously reported.[145]

4-(Phenylbutadiynyl)phenylacetylene (40)

A mixture of Au(C≡CPh)(PPh_3) (100 mg, 0.18 mmol), 1,4-bis(iodoethynyl)benzene (68 mg, 0.18 mmol), Pd(PPh_3)$_4$ (15 mg, 0.01 mmol) and CuI (5 mg, 0.02 mmol) in thf (30 ml) was stirred at r.t. for 2 h. The solvent was then removed and the residue purified by preparative t.l.c. using hexane/dichloromethane (4:1) as an elutant. The UV active fraction was collected and the solvent removed give 4-(phenylbutadiynyl)phenylacetylene (23 mg, 55%) as a pale yellow powder, mp 142−145˚C. ^{1}H NMR ($CDCl_3$) δ 7.30 –7.57 (m, 9H, Ph), 3.15 (s, 1H, C≡CH). FAB-mass spectrum *(m/z)* 226, $[M]^+$; 202, $[M - C_2H]^+$. All values agreed with those previously reported.[145]

1,4-Bis(trimethylsilylbutadiynyl)benzene (41)

A mixture of Au(C≡CSiMe_3)(PPh_3) (600 mg, 1 mmol), 1,4-bis(iodoethynyl)benzene (204 mg, 0.54 mmol), Pd(PPh_3)$_4$ (25 mg, 0.02 mmol) and CuI (10 mg, 0.05 mmol) in thf (40 ml) was heated under reflux for 4 h. The solvent was then removed and the black residue purified by silica column using hexane/dichloromethane (4:1) as an elutant. The dark yellow fraction was collected and the solvent removed. The residue was then extracted into hot hexane and the solvent removed to give 1,4-bis(trimethylsilylbutadiynyl)benzene (149.8 mg, 87%) as a yellow powder. ^{1}H NMR ($CDCl_3$) δ 7.42 (s, 4H, C_6H_4), 0.25 (s, 18H, SiMe_3). FAB-mass spectrum *(m/z)* 318, $[M]^+$; 303, $[M - CH_3]^+$. All values agreed with those previously reported.[146]

4-(Trimethylsilylbutadiynyl)phenylacetylene (42)

A mixture of Au(C≡CSiMe_3)(PPh_3) (100 mg, 0.18 mmol), 1,4-bis(iodoethynyl)benzene (68 mg, 0.18 mmol), Pd(PPh_3)$_4$ (15 mg, 0.01 mmol) and CuI (5 mg, 0.02 mmol) in thf (30 ml) was stirred at r.t. for 2 h. The mixture was concentrated under vacuum and preparative t.l.c. of the residue using hexane/ dichloromethane (4:1) as an eluant afforded 4-(trimethylsilylbutadiynyl)-phenylacetylene (16 mg, 40%) as a pale yellow powder (R_f) (0.79), mp 74−76˚C. IR (Nujol, cm^{-1}): ν(C≡C) 2196 w, 2104 w. ^{1}H NMR ($CDCl_3$) δ 7.47 (s, 4H, Ph), 3.22 (s,

1H, C≡CH), 0.25 (s, 9H, $SiMe_3$). ^{13}C NMR (d_6 benzene): δ 0.20 (s, $SiMe_3$), 76.98, 80.53, 83.51, 89.16, 92.41, 92.89 (6s, C≡C), 122.34 – 133.21 (m, Ph). FAB-mass spectrum (*m/z*): 222, $[M]^+$; 207, $[M - CH_3]^+$.

Ru(C≡CC_6F_5)(dppe)Cp (43)

A mixture of $Me_3SiC{\equiv}CC_6F_5$ (300 mg, 1.13 mmol), RuCl(dppe)Cp (456 mg, 0.76 mmol) and KF (44 mg, 0.15 mmol) in MeOH (20 ml) was heated under reflux for 5 h. The resulting yellow precipitate was collected and washed with MeOH followed by hexane to give Ru(C≡CC_6F_4)(dppe)Cp (575 mg, 63%). Anal. Calcd ($C_{39}H_{29}F_5P_2Ru$): C, 61.99; H, 3.87. Found: C, 61.93; H, 3.83. IR (Nujol, cm^{-1}): ν(C≡C) 2097 m, 2070 w. ^1H NMR (C_6D_6): δ 2.16, 2.71 (2m, 2 x 2H, CH_2CH_2), 4.73 (s, 5H, Cp) 6.95 – 7.99 (m, 24H, Ph). ^{13}C NMR: (C_6D_6) δ 27.83 [t, ^2J(CP) 23 Hz, CH_2CH_2], 82.96 (s, Cp), 126.07 – 142.47 (m, Ph). ^{19}F NMR: δ -14.10 (m, 2F, m-F), -13.61 [t, $^3J_{FF}$ = 21 Hz, 1F, p-F], 9.13 (m, 2F, o-F). ^{31}P NMR: δ 86.98 (s, 2P, dppe). ES-mass spectrum (*m/z*): 779, $[M + Na]^+$; 756, $[M + H]^+$; 738, $[M – F]^+$; 593, $[Cp(dppe)Ru + CO]^+$; 565, $[Cp(dppe)Ru]^+$.

Ru(C≡CC_6F_5)(dppe)Cp* (44)

A mixture of $Me_3SiC{\equiv}CC_6F_5$ (200 mg, 0.76 mmol), RuCl(dppe)Cp* (508 mg, 0.76 mmol) and KF (44 mg, 0.76 mmol) and MeOH (20 ml) was heated under reflux for 5 h. The resulting pale green precipitate was collected and washed with MeOH followed by hexane to give Ru(C≡CC_6F_4)(dppe)Cp* (339 mg, 54%). Anal. Calcd ($C_{44}H_{39}F_5P_2Ru$): C, 64.00; H, 4.76. Found: C, 63.98; H, 4.80. IR (Nujol, cm^{-1}): ν(C≡C) 2078 m, 2033 s. ^1H NMR (C_6D_6): δ 1.66 (s, 15H, Cp*), 2.01, 2.81 (2m, 2 x 2H, CH_2CH_2), 7.02 – 7.87 (m, 20H, Ph). ^{13}C NMR: (C_6D_6) δ 10.59 (s, C_5Me_5), 29.91 [t, ^2J(CP) 23 Hz, CH_2CH_2], 92.74 (s, C≡C), 93.84 (s, C_5Me_5), 127.06 – 144.67 (m, Ph). ^{19}F NMR: δ -14.30 [t, $^3J_{FF}$ = 21 Hz, 1F, p-F], -14.04 (m, 2F, m-F), 8.96 (m, 2F, o-F). ^{31}P NMR: δ 81.72 (s, 2P, dppe). ES-mass spectrum (*m/z*): 848, $[M + Na]^+$; 827, $[M + H]^+$; 808, $[M – F]^+$; 662, $[Cp^*(dppe)Ru + CO]^+$; 635, $[Cp^*(dppe)Ru]^+$.

$Co_3(\mu_3\text{-}CC{\equiv}CC_6F_5)(\mu\text{-dppm})(CO)_7$ (45)

A mixture of $Au(C{\equiv}CC_6F_5)(PPh_3)$ (60 mg, 0.09 mmol), $Co_3(\mu_3\text{-}CBr)(\mu\text{-dppm})(CO)_7$ (30 mg, 0.09 mmol), $Pd(PPh_3)_4$ (15 mg, 0.01 mmol) and CuI (5 mg, 0.02 mmol) in thf (10 ml) was stirred at r.t. for 2 h. The solvent was then removed and the residue purified by preparative t.l.c. using acetone/hexane (3:7) as an eluant. The major fraction was collected as a brown/green band to give $Co_3(\mu_3\text{-}CC{\equiv}CC_6F_5)(\mu\text{-dppm})(CO)_7$ (10 mg, 36%). IR (Nujol, cm^{-1}): ν(C≡C) 2122 w, ν(CO) 2062 s, 2015 s, 1976 sh. ^1H NMR ($CDCl_3$): δ 3.49, 4.24 (2m, 2 x 1H, CH_2), 7.18 – 7.73 (m, 20H, Ph). ^{13}C NMR: δ 29.60 (s, CH_2), 72.17 (s, C≡C), 128.73 – 132.43 (m, Ph). ^{19}F NMR: δ -10.30 (m, 2F, m-F), -3.12 [t, $^3J_{FF}$ = 21 Hz, 1F, p-F], 15.47 (m, 2F, o-F). ^{31}P NMR: δ 34.71 (s, br, 2P, dppm). ES-mass spectrum (*m/z*): 982, $[M + Na]^+$; 960, $[M]^+$.

$Mo(\equiv CC{\equiv}CC_6F_5)(CO)_2Tp^*$ (46)

A mixture of $Au(C{\equiv}CC_6F_5)(PPh_3)$ (60 mg, 0.09 mmol), $Mo(\equiv CBr)(CO)_2Tp^*$ (50 mg, 0.09 mmol), $Pd(PPh_3)_4$ (15 mg, 0.01 mmol) and CuI (5 mg, 0.02 mmol) in thf (10 ml) was stirred at r.t. for 2 h. The solvent was then removed and the residue purified by preparative t.l.c. using acetone/hexane (3:7) as an eluant. The major fraction was collected as a green band to give $Mo(\equiv CC{\equiv}CC_6F_5)(CO)_2Tp^*$ (11 mg, 18%). IR (Nujol, cm^{-1}): ν(C≡C) 2110 w, 2061 w, ν(CO) 2006 s, 1926 s. ^1H NMR ($CDCl_3$): δ 2.33(s, 6H, pz-Me), 2.38 (s, 6H, pz-Me), 2.56 (s, 6H, pz-Me), 5.73 (s, 1H, H^4), 5.89 (s, 2H, H^4). ^{13}C NMR ($CDCl_3$): δ 12.84, 14.76, 15.90 (3 x s, pz-CMe), 94.06, 108.87 (2s, C≡C), 106.69/107.52, 144.86/145.58, 151.55/151.60 (6 x s, pz-ring C), 227.43 (s, CO), 248.80 (s, Mo≡C). ^{19}F NMR: δ -9.16 (m, 2F, m-F), -1.09 [t, $^3J_{FF}$ = 21 Hz, 1F, p-F], 17.95 (m, 2F, o-F). ES-mass spectrum (*m/z*): 677, $[M + Na]^+$; 487, $[M\text{-}C_6F_5]^+$.

$Fc(C{\equiv}C)_2C_6F_5$ (47)

A mixture of $Au(C{\equiv}CC_6F_5)(PPh_3)$ (60 mg, 0.09 mmol), IC≡CFc (30 mg, 0.09 mmol), $Pd(PPh_3)_4$ (15 mg, 0.01 mmol) and CuI (5 mg, 0.02 mmol) in thf (10 ml) was stirred at r.t. for 2 h. The solvent was then removed and the residue purified by preparative t.l.c. using acetone/hexane (3:7) as an eluant. The major fraction was collected as a

bright orange band to give $Fc(C{\equiv}C)_2C_6F_5$ (19 mg, 50%). Anal. Calcd ($C_{20}H_9F_5Fe$): C, 60.04; H, 2.27. Found: C, 59.96; H, 2.15. IR (Nujol, cm^{-1}): ν(C≡C) 2220 m. ^1H NMR (C_6D_6): δ 4.29, 4.58 (2m, 9H, $C_5\underline{H}_5$). ^{13}C NMR: (C_6D_6) δ 62.10, 69.53, 86.86, 99.55 (4s, C≡C), 70.39, 70.79, 72.91 (3s, $\underline{C}_5H_5$), 132.29 – 137.46 (m, Ph). ^{19}F NMR: δ -8.97 (m, 2F, m-F), -0.97 [t, $^3J_{FF}$ = 21 Hz, 1F, p-F], 17.13 (m, 2F, o-F). ES-mass spectrum (*m/z*): 400, $[M]^+$.

$Pt_2(C{\equiv}CC_6F_5)_2(\mu\text{-dppm})_2$ (48)

To a stirring suspension of $Pt_2Cl_2(\mu\text{-dppm})_2$ (100 mg, 0.08 mmol) in NaOMe (MeOH 10 ml, Na 50 mg) was added an excess of $C_6F_5C{\equiv}CSiMe_3$ (50 mg). This mixture was stirred at r.t. for 6 h before the resulting precipitate was collected and washed with MeOH followed by hexane to give $Pt_2(C{\equiv}CC_6F_5)_2(\mu\text{-dppm})_2$ (33 mg, 26%). Anal. Calcd ($C_{66}H_{44}F_{10}P_4Pt_2$): C, 51.44; H, 2.88. Found: C, 51.39; H, 2.80. IR (Nujol, cm^{-1}): ν(C≡C) 2079 m. ^1H NMR (C_6D_6): δ 4.62 (m, 4H, 2 x CH_2), 6.96 – 7.90 (m, 40H, Ph). ^{19}F NMR: δ -13.64 (m, 2F, m-F), -11.16 [t, $^3J_{FF}$ = 21 Hz, 1F, p-F], 11.52 (m, 2F, o-F). ^{31}P NMR: δ 2.13 (s, 4P, dppm, $^1J_{PtP}$ = 2816 Hz). ES-mass spectrum (*m/z*): 1541 $[M + H]^+$.

1,4-$\{Cp(PPh_3)_2Ru(C{\equiv}C)\}_2C_6F_4$ (49)

A mixture of 1,4-$(Me_3SiC{\equiv}C)_2C_6F_4$ (24 mg, 0.07 mmol), $RuCl(PPh_3)_2Cp$ (100 mg, 0.14 mol) and KF (8 mg, 0.15 mmol) in thf (5 ml) and MeOH (20 ml) was heated under reflux for 5 h. The resulting yellow precipitate was collected and washed with MeOH followed by hexane to give 1,4-$\{Ru(PPh_3)_2Cp(C{\equiv}C)\}_2C_6F_4$ (66 mg, 60%). Anal. Calcd ($C_{92}H_{70}P_4Ru_2F_4$): C, 70.04; H, 4.47. Found: C, 70.09; H, 4.47. IR (Nujol, cm^{-1}): ν(C≡C) 2073 m, 2039 m. ^1H NMR (C_6D_6): δ 4.86 (s, 5H, Cp), 6.94 – 7.75 (m, 30H, Ph). ^{13}C NMR: ($CDCl_3$) δ 93.48 (s, Cp), 127.57 – 137.33 (m, Ph). ^{19}F NMR (C_6D_6): δ 7.59 (s, 2F). ^{31}P NMR (C_6D_6): δ 51.72 (s, 2P, PPh_3). ES-mass spectrum (*m/z*): 1578, $[M]^+$; 731, $[Cp(PPh_3)_2Ru + MeCN]^+$; 691, $[Cp(PPh_3)_2Ru]^+$.

1,4-$\{Cp(dppe)Ru(C{\equiv}C)\}_2C_6F_4$ (50)

A mixture of 1,4-$(Me_3SiC{\equiv}C)_2C_6F_4$ (28 mg, 0.08 mmol), RuCl(dppe)Cp (100 mg, 0.17 mmol) and KF (9 mg, 0.16 mmol) in thf (5 ml) and MeOH (20 ml) was heated under reflux for 5 h. The resulting yellow precipitate was collected and washed with

MeOH followed by hexane to give 1,4-{Cp(dppe)Ru(C≡C)}$_2$C$_6$F$_4$ (28 mg, 26%). Anal. Calcd ($C_{72}H_{58}P_4Ru_2F_4.CHCl_3$): C, 60.69; H, 4.12. Found: C, 60.92; H, 4.11. IR (Nujol, cm^{-1}): ν(C≡C) 2072 m, 2037 m. ^{1}H NMR (C_6D_6): δ 2.07, 2.70 (2m, 2 x 2H, CH_2CH_2), 4.71 (s, 5H, Cp), 6.91 – 7.99 (m, 20H, Ph). ^{13}C NMR: ($CDCl_3$) δ 32.19 (m, CH_2CH_2), 88.38 (s, Cp), 126.03 – 133.80 (m, Ph). ^{19}F NMR (C_6D_6): δ 6.89 (s, 2F). ^{31}P NMR: δ 86.65 (s, 2P, dppe). ES-mass spectrum (*m/z*): 1326, $[M]^+$; 605, $[Cp(dppe)Ru + MeCN]^+$; 565, $[Cp(dppe)Ru]^+$.

1,4-{Cp*(dppe)Ru(C≡C)}$_2$C$_6$F$_4$ (51)

A mixture of 1,4-($Me_3SiC≡C)_2C_6F_4$ (26 mg, 0.07 mmol), RuCl(dppe)Cp* (100 mg, 0.15 mmol) and KF (8 mg, 0.15 mmol) in thf (5 ml) and MeOH (20 ml) was heated under reflux for 5 h. The resulting yellow precipitate was collected and washed with MeOH followed by hexane to give 1,4-{Cp*(dppe)Ru(C≡C)}$_2$C$_6$F$_4$ (65 mg, 63%). Anal. Calcd ($C_{82}H_{78}P_4Ru_2F_4$): C, 67.20; H, 5.36. Found: C, 67.21; H, 5.40. IR (Nujol, cm^{-1}): ν(C≡C) 2063 m, 2032 m. ^{1}H NMR (d_6 benzene): δ 1.68 (s, 15H, $C_5\mathit{Me}_5$), 1.99, 2.88 (2m, 2 x 2H, CH_2CH_2), 7.03 – 7.95 (m, 20H, Ph). ^{13}C NMR: ($CDCl_3$) δ 10.68 (s, $C_5\mathit{Me}_5$), 30.05 (m, CH_2CH_2), 93.71 (s, C_5Me_5), 95.89 (s, br, Ru−C), 127.90 – 147.80 (m, Ph). ^{19}F NMR (d_6 benzene): δ 6.83 (s, 2F). ^{31}P NMR: δ 80.86 (s, 2P, dppe). ES-mass spectrum (*m/z*): 1467, $[M + H]^+$; 675, $[Cp*(dppe)Ru + MeCN]^+$; 635, $[Cp*(dppe)Ru]^+$.

Chapter5

SOME CLUSTER CHEMISTRY

5.1 Introduction

Early motivation towards cluster chemistry came from the proposal that their reactivity could resemble that found on the surfaces of metals.[162,163] The binding of alkynes to clusters was found to be different to that seen with mononuclear metal centres. The new structural forms may offer clues for surface chemistry, where direct structural data is still hard to obtain.[162] Metal clusters have also enabled the stabilisation of certain molecules, exhibited novel catalytic functions and are regarded as a bridge between mononuclear complexes and colloids.[164]

Carbon chain complexes with cluster capping groups usually involve the terminal carbon atom of the chain being attached to all three metal atoms by between one and three σ-type bonds, the μ_3-η^1 mode (**5a**). Such capping groups include $M_3(\mu\text{-}H)_3(CO)_9$ (M = Ru, Os), $Co_3(CO)_9$ and $M_3Cp'_3$ (M = Co, Rh, Ir; Cp' = Cp, Cp*). However there are far fewer examples of complexes in which a C_n chain is attached by two of the carbon atoms in a μ_3-η^2 mode (**5b**).

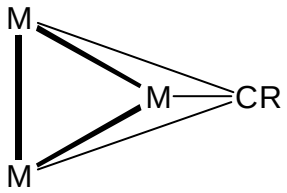

5a

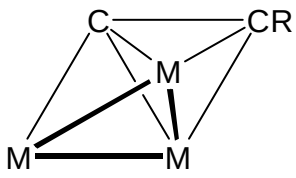

5b

Di- and tri- metal carbonyl complexes are known to react readily with alkynes to give polynuclear complexes.[165,166] Thus poly-ynediyl M-$(C\equiv C)_n$-M and polyynyl complexes M-$(C\equiv C)_n$-H are precursors for cluster compounds containing a one dimensional carbon chain, with adduct formation typically occuring at the least hindered alkyne linkage.[10] This can stabilise otherwise unstable poly-ynyl compounds. The commonly accepted route to these complexes is via initial

formation of a η^2-alkyne complex, which subsequently interacts with the other metal atoms of the cluster, becoming attached to all three metal atoms. A cluster-bound monosubstituted alkyne may then undergo hydrogen migration from the alkyne to the cluster to give a hydrido-alkynyl complex.[167] For example the reaction of $HC{\equiv}CSiMe_3$ with the ruthenium carbonyl cluster $Ru_3(\mu\text{-dppm})(CO)_{10}$ in refluxing thf gave the hydrido-alkynyl complex $Ru_3(\mu\text{-H})(\mu_3\text{-}C_2SiMe_3)(\mu\text{-dppm})(CO)_7$ (Scheme 5.1).[168] The hydride resonance was observed as a doublet in the ^{1}H NMR spectrum at δ -19.99 due to coupling with one phosphorus of the dppm ligand.

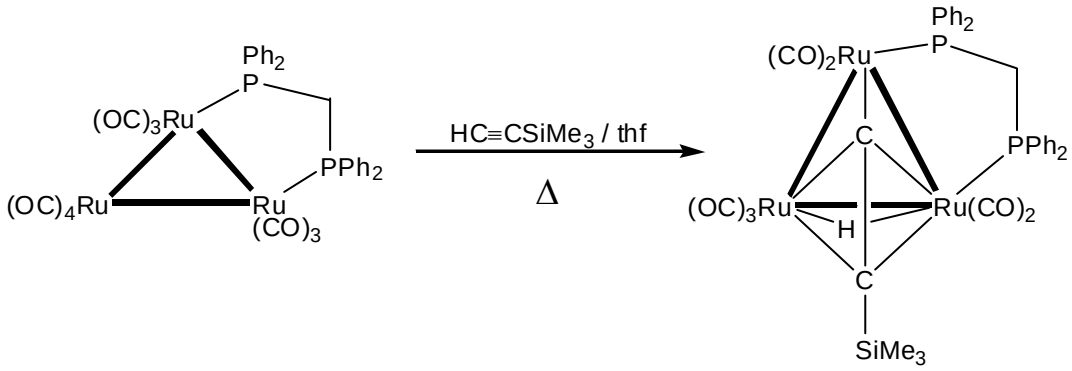

Scheme 5.1

It has been found that the cluster $Ru_3(CO)_{10}(NCMe)_2$, with labile NCMe ligands, reacts with alkynes at room temperature enabling the isolation of the alkyne-Ru_3 species.[169] The reaction of $Ru_3(CO)_{10}(NCMe)_2$ and $FcC{\equiv}CH$ at room temperature gave $Ru_3(\mu_3\text{-}HC_2Fc)(\mu\text{-CO})(CO)_9$ in 52% yield after one hour (Scheme 5.2). The IR spectrum of this complex contains a band at 1876 cm^{-1} characteristic of a bridging CO group, while a singlet was found at δ 8.09 in the ^{1}H NMR spectrum for the ≡CH proton. No Ru-H metallohydride resonance was observed.

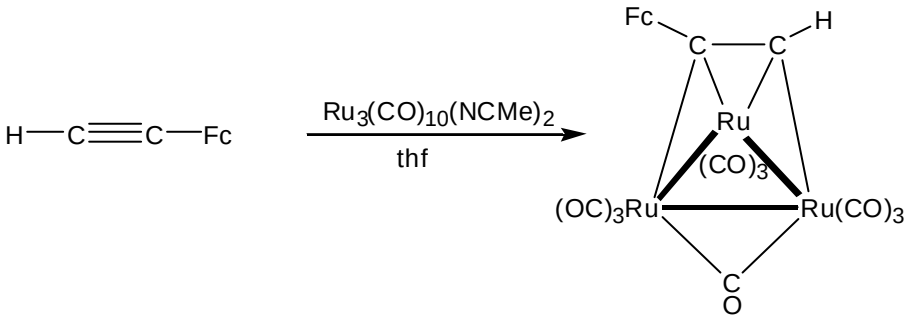

Scheme 5.2

Similarly the reaction of $Ru_3(CO)_{10}(NCMe)_2$ with the C_4 complex $W(C{\equiv}CC{\equiv}CH)(CO)_3Cp$ gave the μ_3-alkyne complex, $Ru_3\{\mu_3\text{-}\eta^2\text{-}HC_2C{\equiv}C[W(CO)_3Cp]\}(\mu\text{-}CO)(CO)_9$ in 40% yield.[170] The bridging CO ligand was identified without difficulty in the IR spectrum as a weak band at 1879 cm^{-1}, while in the ^1H NMR spectrum the ≡CH proton was observed at δ 7.86. This complex was readily converted into the corresponding hydrido-alkynyl cluster, $Ru_3(\mu\text{-}H)\{\mu_3\text{-}C_2C{\equiv}C[W(CO)_3Cp]\}(CO)_9$ by briefly heated at reflux in benzene (Scheme 5.3). The ^1H NMR spectrum of this complex contained the metallohydride resonance at δ -20.33.[170]

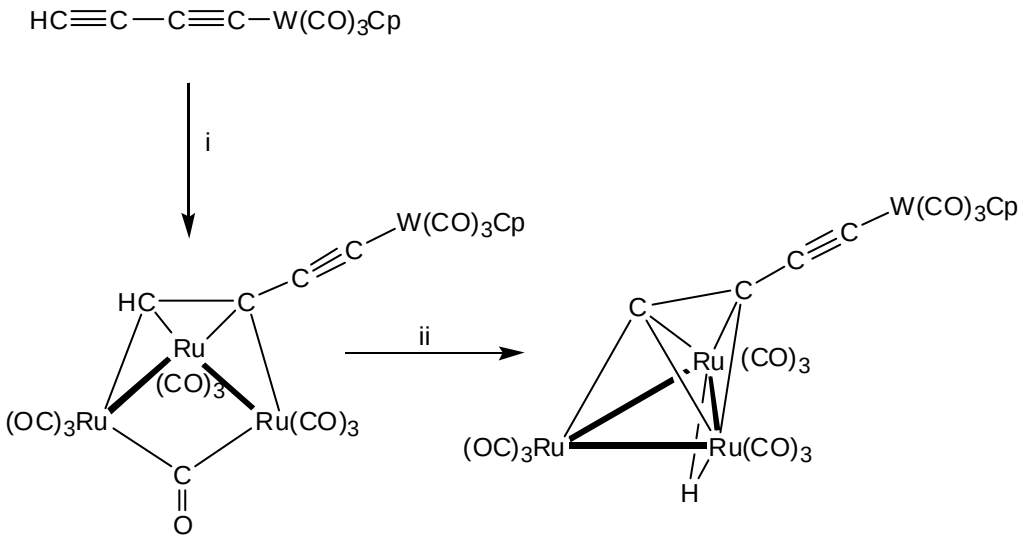

Reagents: i, $Ru_3(CO)_{10}(NCMe)_2$; ii C_6H_6/reflux

Scheme 5.3

Similar reactions with $Os(CO)_{10}(NCMe)_2$ and rhenium complexes of varying chain length, $Re\{(C{\equiv}C)_nC{\equiv}CH\}(NO)(PPh_3)Cp^*$ (n = 1-4) have also been investigated.[171,172] Reactions of the ethynyl, butadiynyl and hexatriynyl complexes gave the corresponding tri-osmium hydride complexes, $\{Cp^*Re(NO)(PPh)_3(C{\equiv}C)_{n-1}(CC)\}\{Os_3(\mu\text{-}H)(CO)_{10}\}$. The stabilities of these complexes, as with the mono-metallic complexes, were found to decrease with increased chain length. Thus the reaction of the analogous octatetraynyl rhenium complex gave a multitude of products.[171]

The isolobal nature of the proton and the $\{Au(PR_3)\}^+$ species has been used to rationalise new gold-containing clusters which differ structurally only by the replacement of a proton by the $\{Au(PPh_3)\}^+$ group.[173,174] Thus the reaction of $Ru_3(\mu\text{-dppm})(CO)_{10}$ with $Au(C_2Ph)\{P(tol)_3\}$ in thf at reflux generated the cluster $AuRu_3(\mu_3\text{-}C_2Ph)(\mu\text{-dppm})(CO)_7\{P(tol)_3\}$ in 92% yield (Scheme 5.4).[168] The X-ray structure of this complex was compared to that of $Ru_3(\mu\text{-H})(\mu_3\text{-}C_2Ph)(\mu\text{-dppm})(CO)_7\{P(tol)_3\}$ and both complexes have virtually identical parameters, emphasising the isolobal nature of H and $Au(PR_3)$. The only minor modification was an expansion of the Ru_3 cluster and a closer approach for the acetylide to the Ru_3 core.[168]

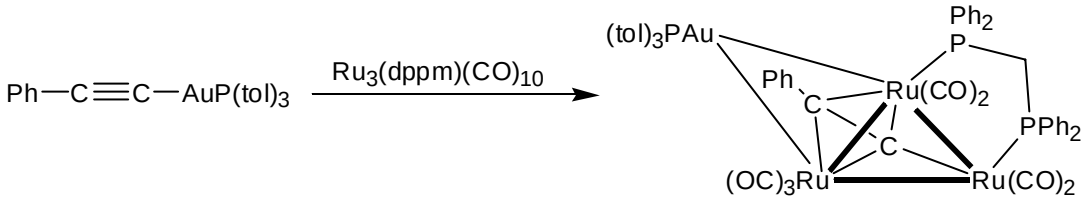

Scheme 5.4

Complexes containing more than one cluster nucleus can be synthesised by reacting poly-yne species with greater than one equivalent of the metal carbonyl. The reaction of $Ru_3(CO)_{12}$ and $\{Au[P(tol)_3]\}_2(\mu\text{-}C{\equiv}CC{\equiv}C)$ in refluxing thf gives a mixture of $\{AuRu_3(CO)_9[P(tol)_3]\}_2(\mu_3,\eta^2\text{:}\mu_3,\eta^2\text{-}C_2C_2)$ and the mono-cluster complex $AuRu_3\{\mu_3,\eta^2\text{-}C_2C{\equiv}CAu[P(tol)_3]\}(CO)_9\{P(tol)_3\}$ in 10 and 31% yield respectively (Scheme 5.5). The ^{31}P NMR spectra contained signals at δ 59.9 for the symmetrical di-cluster complex and at δ 40.0 and 59.5 for $C{\equiv}CAu\{P(tol)_3\}$ and $Ru_3Au\{P(tol)_3\}$ respectively in the mono-cluster complex.[175,176]

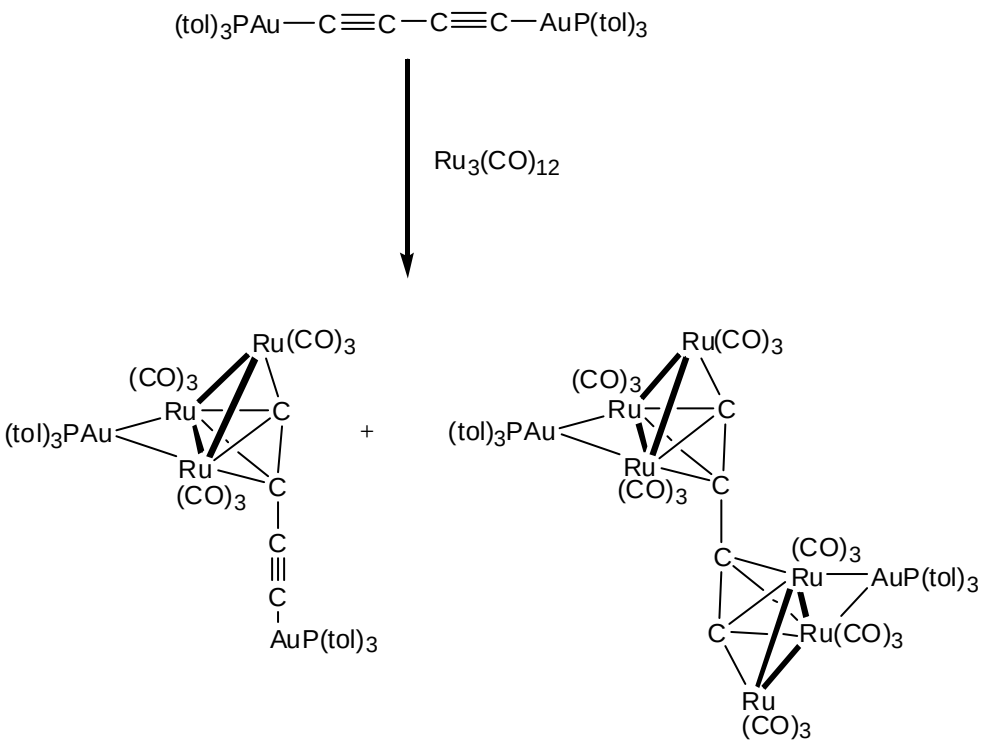

Scheme 5.5

Using polyynediyl complexes, M-$(C\equiv C)_n$-M, as precursors, where both termini of the chain are protected by metal groups, results in cluster formation along the chain, at the least hindered alkyne linkage. Reacting the C_8 bis-tungsten complex $\{W(CO)_3Cp\}_2(C\equiv C)_4$ with cobalt carbonyl at room temperature gives a mixture of the mono- and di-adducts, with $Co_2(CO)_6$ groups attached to just the C(3)-C(4) or C(3)-C(4) and C(3')-C(4') triple bonds respectively (Scheme 5.6).[177] The ^{1}H NMR spectrum of the mono-adduct contains two singlet resonances for the Cp protons at δ 5.64 and 5.67. The Cp groups of the di-adduct are equivalent and hence only one singlet, at δ 5.59, is observed in the ^{1}H NMR spectrum.

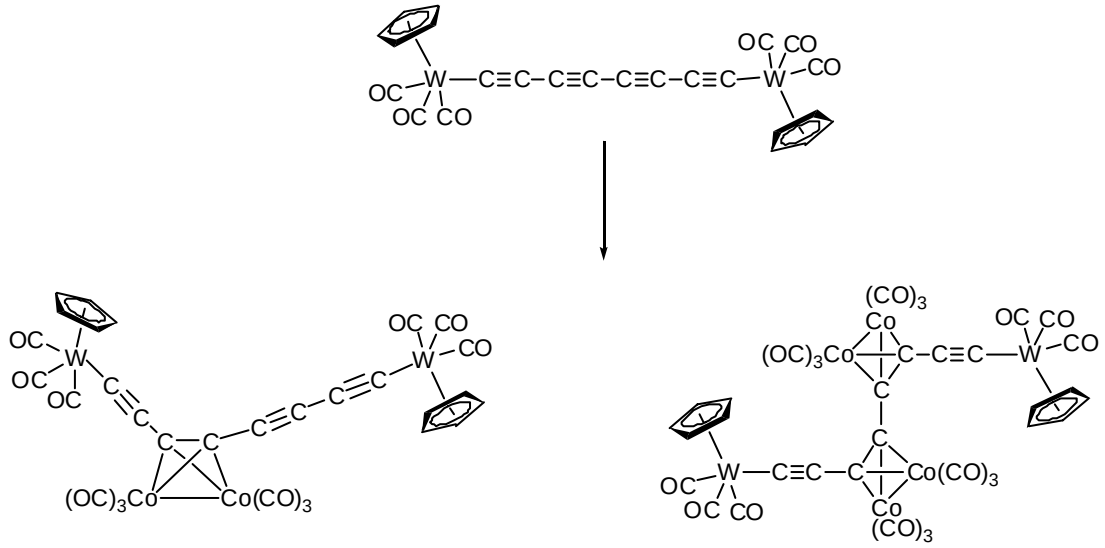

Scheme 5.6

Reacting shorter chains with metal carbonyls has been found to result in the formation of mixed-metal clusters containing a bridging carbon chain fragment. For example the trinuclear acetylide derivative $CpMoRu_2(CO)_8(C{\equiv}CPh)$ has been isolated in 42% yield by reaction of $Ru_3(CO)_{12}$ and $CpMo(CO)_3C{\equiv}CPh$ in toluene under reflux (Scheme 5.7).[178,179] This probably results from the incoming metal atom approaching close to the original metal centre, facile loss of a ligand (usually CO) resulting in condensation with M-M bond formation.

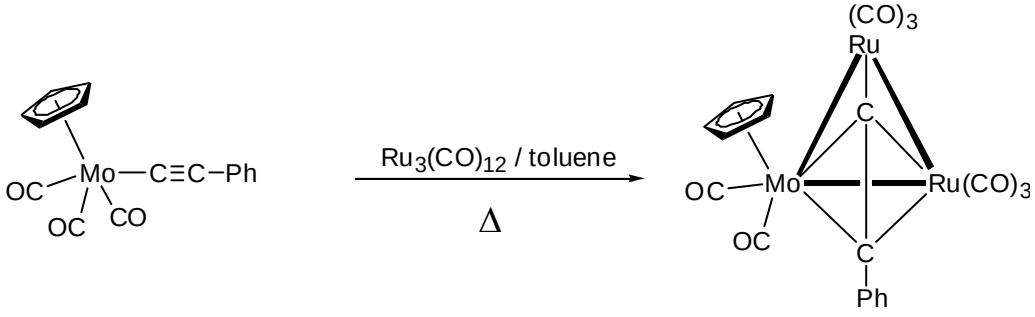

Scheme 5.7

5.2 Results and Discussion

The acetonitrile complex $Ru_3(CO)_{10}(NCMe)_2$ is readily prepared by amine oxide oxidation of the carbonyl groups in acetonitrile / dichloromethane solution, followed by coordination of the two MeCN ligands. As the nitrile ligands are only weakly coordinated, this complex was not isolated, but used *in situ*. The activated cluster reacted readily at room temperature with a variety of alkynyl-gold(I) phoshine complexes to give gold-containing Ru_3 clusters which were purified by preparative t.l.c.

A reaction between $Ru_3(CO)_{10}(NCMe)_2$ and the ruthenium complexes $Ru\{(C\equiv C)_nAu(PPh_3)\}(dppe)Cp^*$ (n = 2, 3) gave the new cluster complexes $AuRu_3(\mu_3\text{-}C_2C\equiv C[Ru(dppe)Cp^*]\}(CO)_9(PPh_3)$ (**52**) and $AuRu_3\{\mu_3\text{-}C_2(C\equiv C)_2[Ru\text{-}(dppe)Cp^*](CO)_9(PPh_3)$ (**53**) (vida infra) in 19 and 14% yields respectively (Scheme 5.8). The IR spectra of **52** and **53** contain ν(C≡C) bands at 2066 cm^{-1} (**52**) 2126 and 2076 cm^{-1} (**53**) and with terminal carbonyl bands between 2069 and 1952 cm^{-1}. In the ^{13}C NMR spectra, recorded in d_6-benzene at ambient temperature, characteristic resonances were found at δ 10.28 and 98.93 (**52**) and δ 10.47 and 94.21 (**53**) for the Cp* methyl and ring carbons, with the carbonyl resonances observed as a singlet at 198.98 (for **52**) and 227.63 (for **53**). Presumably the carbonyl resonances are observed as singlets due to fluxionality. The ^{31}P NMR spectra of **52** and **53** exhibit resonances at δ 61.35 and 80.65 (**52**) and δ 62.18 and 80.57 (**53**) that can be assigned to the $AuPPh_3$ and dppe respectively.

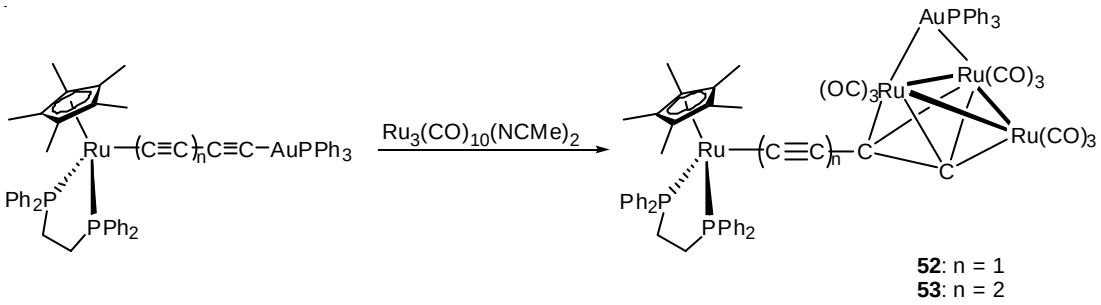

Scheme 5.8

The ES-mass spectrum of **52** gives a positive ion $[M]^+$ without prior derivatisation, in addition to the $[Ru(dppe)Cp^* + CO]^+$ fragment, as shown in Figure 5.1. Ionisation to give $[M]^+$ may occur by oxidation of **52** in the ES ionisation source which can act as an electrochemical cell.[180] Subjecting **52** to collision-induced dissociation (CID) by increasing the cone voltage enables CO-loss fragment ions to be observed (Figure 5.2). At a cone voltage of 55 V the formation of the fragment ion $[M - CO]^+$ is observed. Increasing the cone voltage results in further loss of CO ligands with $[M - 5CO]^+$ and $[M - 6CO]^+$ ions observed at 70 V and $[M - 7CO]^+$ at 80 V. Finally at a cone voltage of 110 V all nine CO ligands are stripped away by CID.

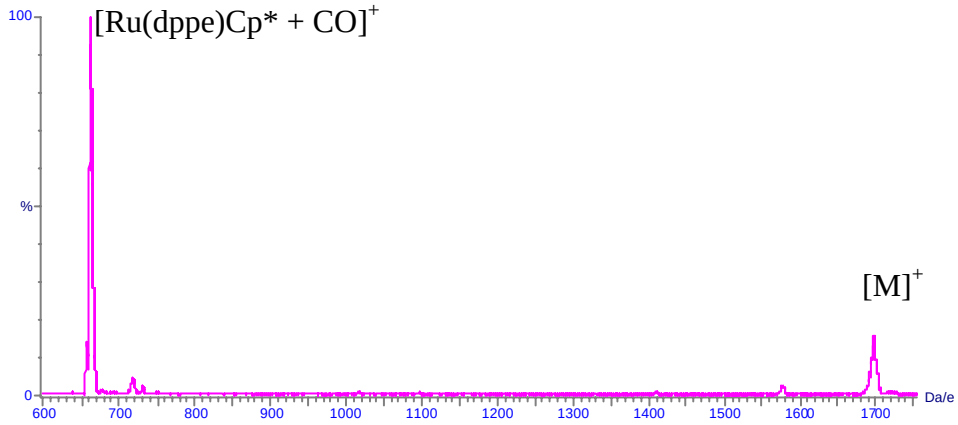

Figure 5.1: *Positive-ion ES-mass spectrum of $AuRu_3(\mu_3\text{-}C_2C{\equiv}C[Ru\text{-}(dppe)Cp^*](CO)_9(PPh_3)$ (**52**) in a methanol solution at a cone voltage of 15 V.*

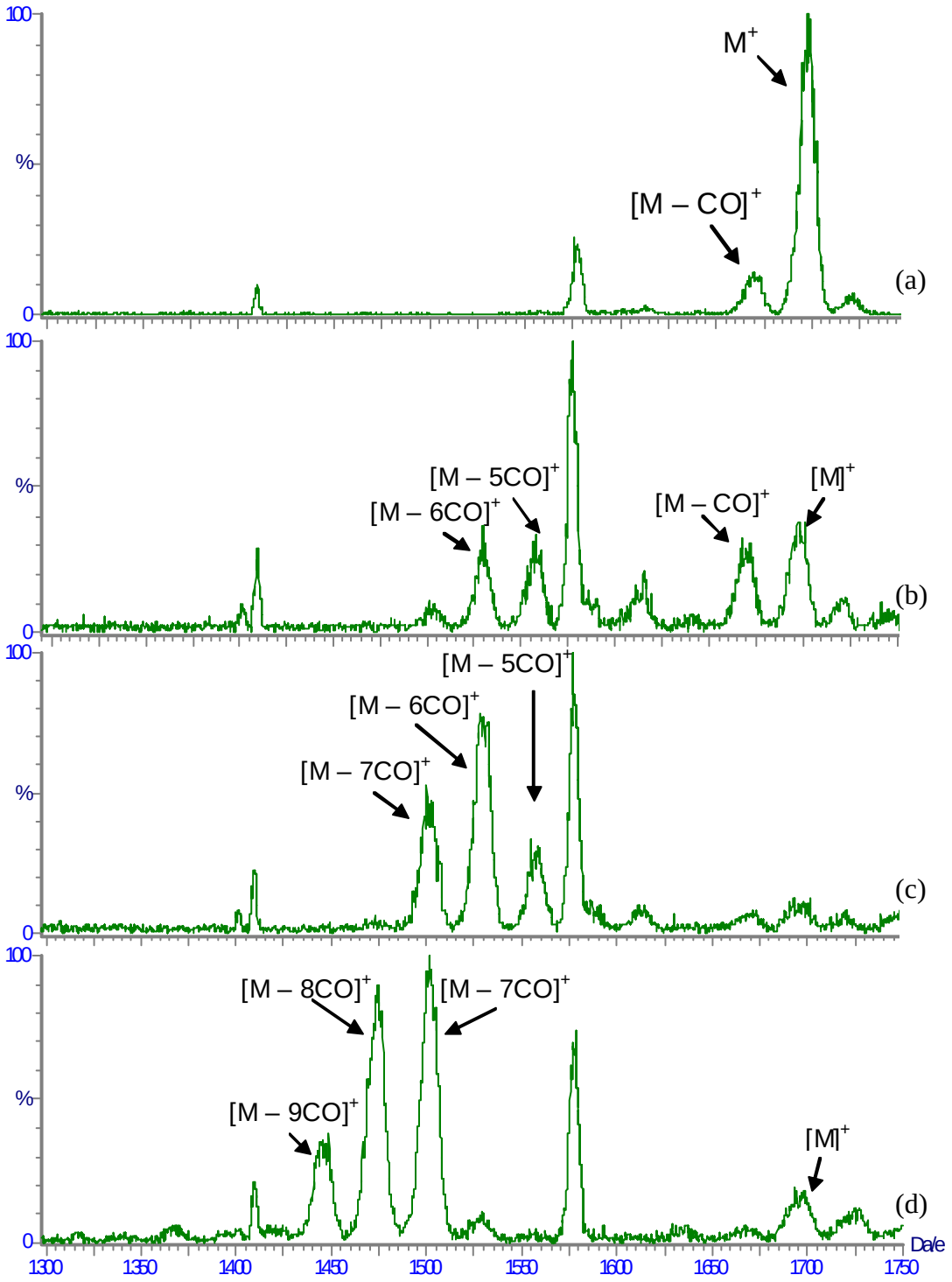

Figure 5.2: *(a) Positive-ion ES-mass spectrum of $AuRu_3(\mu_3\text{-}C_2C{\equiv}C[Ru\text{-}(dppe)Cp^*](CO)_9(PPh_3)$ (**52**) in methanol solution at a cone voltage of 55 V, showing the formation of $[M]^+$ and the fragment ion $[M – CO]^+$. At higher cone voltages (70 V, b; 80 V, c; 110 V, d), further loss of CO ligands occurs.*

The acetonitrile complex $Ru_3(CO)_{10}(NCMe)_2$ also reacted with the shorter C_3 chains in $M\{\equiv CC\equiv CAu(PPh_3)\}(CO)_2Tp$ to give $AuRu_3\{\mu_3\text{-}C_2C\equiv[M(CO)_2Tp]\}(CO)_9(PPh_3)$, [M = Mo (**54**), W (**55**)] in 28 and 21% yields respectively (Scheme 5.9). The IR spectrum of **54** contains eight terminal ν(C≡O) bands between 2074 and 1917 cm^{-1} while the IR spectrum of **55** exhibits only six ν(C≡O) bands between 2072 and 1902 cm^{-1}. In the ^1H NMR spectra pz protons are found at δ 5.62, 5.77 (Mo) and δ 5.54, 5.71 (W). In the ^{13}C NMR spectra the pz carbons are found at δ 105.98/106.23, 134.38/135.61, 143.80/144.83 (Mo), 106.51/106.79, 135.49/135.60, 144.77/146.70 (W), C≡O carbons at δ 227.54, 227.08 (Mo), 227.54, 225.12 (W) and M≡C at δ 267.23 (Mo), 257.79 (W). In the ^{31}P NMR spectra resonances for $AuPPh_3$ were found at δ 62.45 (Mo), 62.37 (W), significantly downfield compared to those observed in the starting materials $M\{\equiv CC\equiv CAu(PPh_3)\}(CO)_2Tp$ at δ 41.64 (M = Mo) and δ 42.85 (M = W). The ES-mass spectra contain $[M + Na]^+$ at *m/z* 1439 (Mo) and at *m/z* 1527 (W).

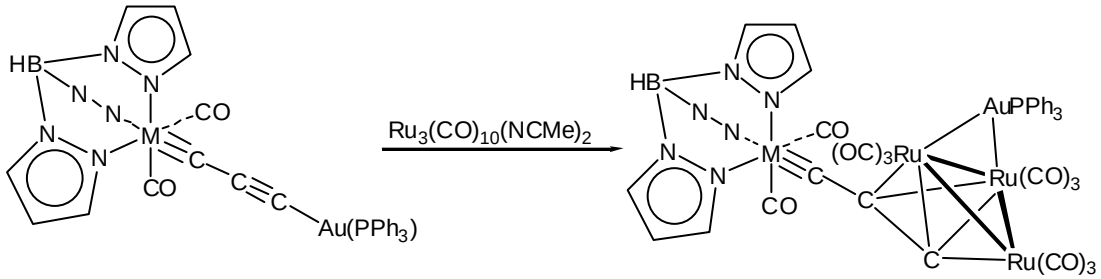

Scheme 5.9

The structure of **54** was confirmed by an X-ray study of crystals obtained from dichloromethane/methanol (Figure 5.1). The structure contains an approximately equilateral Ru_3 core, the Ru(2)-Ru(3) edge of which is bridged by an $Au(PPh_3)$ group. The C_2 fragment of the alkynyl group is attached to the Ru_3 core by one σ-type bond and two π-type bonds. The σ-bond Ru(1)-C(3) is the shortest at 1.915(8) Å and involves the only ruthenium atom which is not attached to the $Au(PPh_3)$ group. The π bonds Ru(2)-C(2,3) and Ru(3)-C(2,3) are significantly longer with separations between 2.173(8) and 2.243(6) Å. The carbon chain within this molecule

is notably bent due to the partial rehybridisation of the π-bonded carbon atoms, with Mo-C(1)-C(2) and C(1)-C(2)-C(3) angles of 171.0(6) and 155.7(7)˚, respectively. The Au-Ru(2,3) distances of 2.7562(7) and 2.745(1) Å, with an Au-P contact of 2.296(2) Å are similar to those values found previously for complexes of this type.[181] As with the addition of H, the addition of $Au(PPh_3)$ involves the electrons in the Ru(2)-Ru(3) bond. This bond therefore gets longer with **54** having a Ru(2)-Ru(3) bond distance of 2.8421(8) Å, while the non-bridged Ru(2,3)-Ru(1) separations are shorter at 2.8164(8) and 2.802(1) Å.

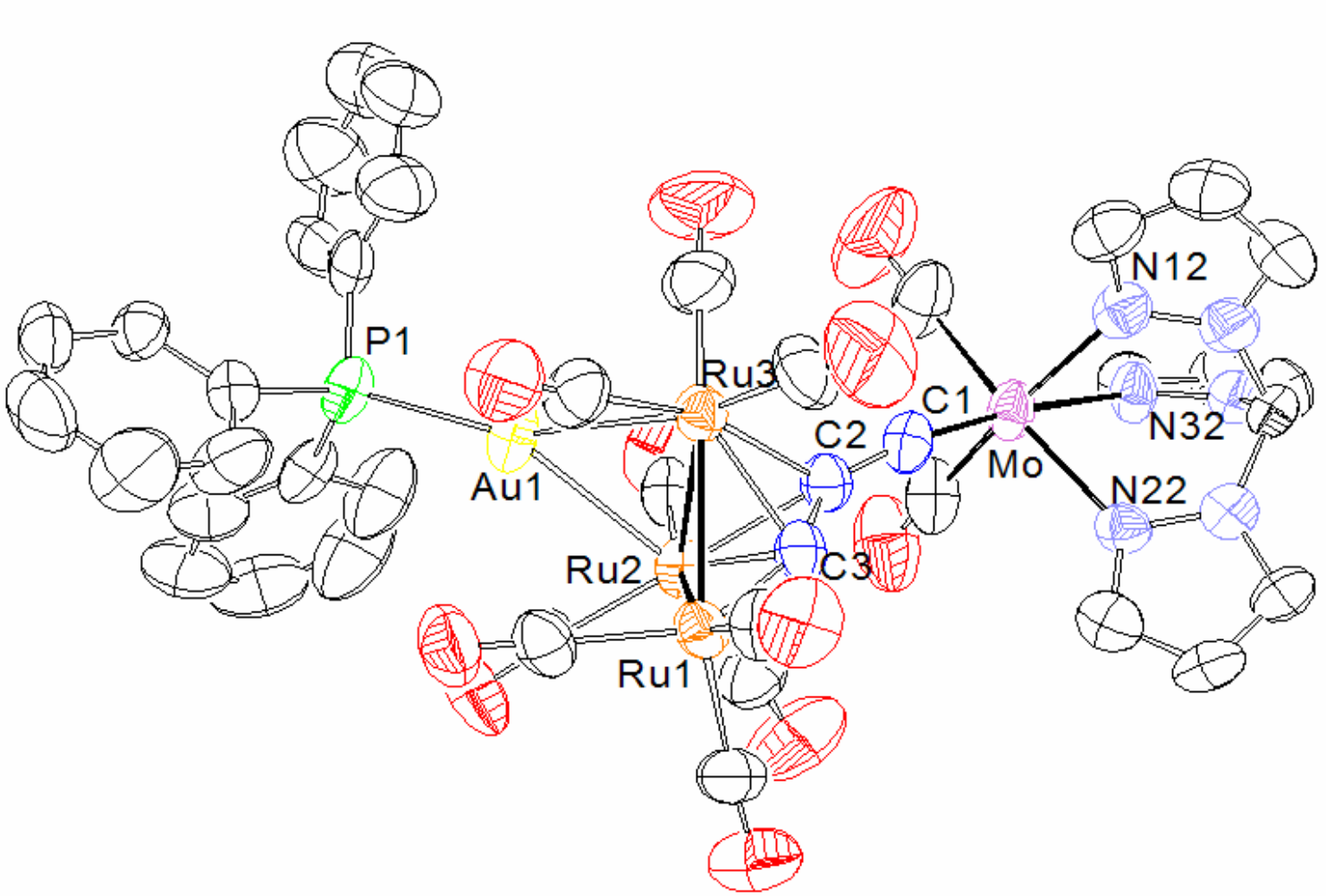

Figure 5.3 *ORTEP view of $AuRu_3\{\mu_3\text{-}C_2C{\equiv}[Mo(CO)_2Tp]\}(CO)_9(PPh_3)$* ***(54)***.

Table 5.1: *Selected structural data for $AuRu_3(\mu_3\text{-}C_2C{\equiv}[Mo(CO)_2Tp]\}\text{-}(CO)_9(PPh_3)$ (**54**).*

Bond Distances (Å)		**Bond Angles (˚)**	
Ru(1)-Ru(2)	2.8164(8)	Ru(2)-Au-P	143.04(5)
Ru(1)-Ru(3)	2.802(1)	Ru(3)-Au-P	154.51(5)
Ru(2)-Ru(3)	2.8421(8)	Ru(2)-Ru(1)-Ru(3)	60.77(2)
Ru(2)-Au	2.7562(7)	Ru(2)-Ru(1)-C(3)	50.4(2)
Ru(3)-Au	2.745(1)	Ru(3)-Ru(1)-C(3)	50.9(2)
Ru(1)-C(3)	1.915(8)	Ru(1)-Ru(2)-Ru(3)	59.37(2)
Ru(2)-C(2)	2.237(9)	Ru(1)-Ru(2)-C(2)	76.7(2)
Ru(2)-C(3)	2.173(8)	Ru(1)-Ru(2)-C(3)	42.7(2)
Ru(3)-C(2)	2.243(6)	Ru(3)-Ru(2)-C(2)	50.7(2)
Ru(3)-C(3)	2.179(7)	Ru(3)-Ru(2)-C(3)	49.3(2)
Au-P	2.296(2)	C(2)-Ru(2)-C(3)	34.9(3)
C(1)-C(2)	1.39(1)	Ru(1)-Ru(3)-C(2)	76.9(2)
C(2)-C(3)	1.32(1)	Ru(1)-Ru(3)-C(3)	43.0(2)
C(1)-Mo	1.818(9)	Ru(2)-Ru(3)-C(2)	50.5(2)
		Mo-C(1)-C(2)	171.0(6)
		C(1)-C(2)-C(3)	145.3(9)
		Ru(1)-C(3)-C(2)	155.7(7)

The carbon-carbon triple bond of the ethynyl complex $Au(C{\equiv}CC_6F_5)(PPh_3)$ also reacts with $Ru_3(CO)_{10}(NCMe)_2$ to afford the cluster complex $Ru_3(\mu\text{-}AuPPh_3)(\mu_3\text{-}C_2C_6F_5)$ (**56**) in 35% yield (Scheme 5.10). The ES mass spectrum confirmed the formulation of this complex, containing $[M]^+$ at *m/z* 1207. In the ^{13}C NMR spectrum the carbonyl carbons are found at δ 216.53 while in the ^{31}P NMR spectrum a single resonance for $Au(PPh_3)$ was found at δ 63.27. As expected in the ^{19}F NMR spectrum three resonances with the intensity ratio 2 : 1 : 2 are found at δ -9.82, -2.54 and 18.74.

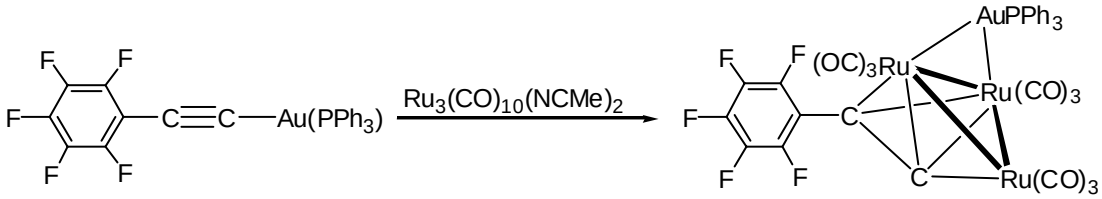

56

Scheme 5.10

The structure of **56** was confirmed by an X-ray study of crystals obtained from dichloromethane/methanol (Figure 5.4). Two molecular units were found in the asymmetric unit, bond parameters for both are comparable and herein only the first unit is discussed. As found in **54** the Ru_3 core forms approximately isoceles triangle with Ru-Ru distances of 2.822(1) - 2.804(1) Å. The pentafluorophenylacetylide ligand is π bonded to Ru(1) [Ru(1)-C(1,2) 2.18(1), 2.24(1) Å] and Ru(2) [Ru(2)-C(1,2) 2.19(1), 2.21(1)] and σ-bonded to Ru(3) through C(1) [1.930(9) Å]. Similarly to **54** the carbon chain within this molecule is notably bent with C(1)-C(2)-C(3) having an angle of 140.0(1)˚, as the sp carbon atoms are partialy rehybridised to sp^3. The cluster bound $AuPPh_3$ bridges the Ru(1)-Ru(2) edge [Ru(1)-Au 2.7417(9), Ru(2)-Au 2.779(1) Å]. As found for **54** the Ru-Ru edge bridged by the gold group is longest. A similar lengthening of metal-metal bonds is induced by the hydride in a number of triruthenium clusters including $Ru_3(\mu\text{-}H)(\mu_3\text{-}C_2{}^tBu)(\mu\text{-}dppm)(CO)_7$.[168]

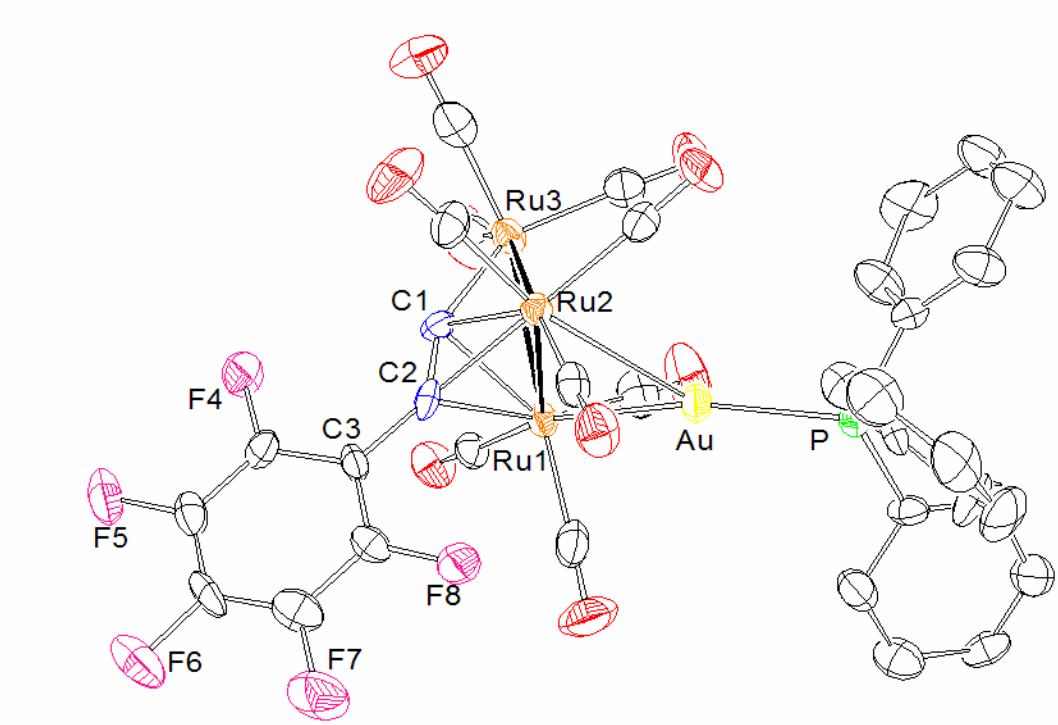

Figure 5.4 *ORTEP view of $AuRu_3(\mu_3\text{-}C_2C_6F_5)(CO)_9(PPh_3)$ (**56**).*

Table 5.2: *Selected structural data for $AuRu_3(\mu_3\text{-}C_2C_6F_5)(CO)_9(PPh_3)$ (**56**).*

Bond Distances (Å)		**Bond Angles (˚)**	
Ru(1)-Ru(2)	2.822(1), *2.810(1)*	Ru(1)-Au-P	154.16(7), *149.29(6)*
Ru(1)-Ru(3)	2.804(1), *2.804(1)*	Ru(2)-Au-P	143.47(4), *149.80(6)*
Ru(2)-Ru(3)	2.811(1), *2.806(1)*	Ru(2)-Ru(1)-Ru(3)	59.96(3), *59.98(3)*
Ru(1)-Au	2.7417(9), *2.7699(9)*	Ru(2)-Ru(1)-C(1)	49.9(3), *50.5(2)*
Ru(2)-Au	2.779(1), *2.7747(9)*	Ru(2)-Ru(1)-C(2)	50.1(3), *50.3(2)*
Ru(1)-C(1)	2.18(1), *2.19(1)*	Ru(1)-Ru(2)-Ru(3)	59.71(3), *59.91(3)*
Ru(1)-C(2)	2.24(1), *2.232(9)*	Ru(1)-Ru(2)-C(1)	49.7(3), *50.1(3)*
Ru(2)-C(1)	2.19(1), *2.21(1)*	Ru(1)-Ru(2)-C(2)	51.2(3), *51.1(2)*
Ru(2)-C(2)	2.21(1), *2.204(9)*	Ru(3)-Ru(1)-C(1)	43.3(2), *43.8(3)*
Ru(3)-C(1)	1.930(9), *1.95(1)*	Ru(3)-Ru(1)-C(2)	77.1(2), *77.1(3)*
Au-P	2.295(3), *2.291(3)*	C(1)-Ru(1)-C(2)	35.0(3), *34.74*
C(1)-C(2)	1.33(1), *1.32(1)*	Ru(3)-Ru(2)-C(1)	43.2(2), *43.7(3)*
C(2)-C(3)	1.45(1), *1.45(1)*	Ru(3)-Ru(2)-C(2)	77.5(2), *77.5(2)*
		Ru(1)-Ru(3)-Ru(2)	60.33(3), *60.12(3)*

The reaction of the 1,4-diethynylbenzene complex, $Ru\{C{\equiv}CC_6H_4C{\equiv}CAu(PPh_3)\}(dppe)Cp^*$ and $Ru_3(CO)_{10}(NCMe)_2$ gave the cluster complex $AuRu_3\{\mu_3\text{-}C_2C_6H_4C{\equiv}C[Ru(dppe)Cp^*]\}(CO)_9(PPh_3)$ (**57**), which is presumably structurally related to **54** and **56**. The formulation of this complex was confirmed by microanalysis and ES mass spectrometry and supported by the usual spectroscopic data. Thus, in the IR spectrum a ν(C≡C) band at 2068 cm^{-1} and five terminal ν(C≡O) bands between 2037 and 1961 cm^{-1} are observed. In the ^1H NMR spectrum a singlet is obsered at δ 1.64 for the methyl protons of Cp* and two multiplets at δ 1.95 and 2.60 for the ethane portion of the dppe ligand. In the ^{13}C NMR spectrum characteristic resonances were found for the Cp* methyl and ring carbons at δ 10.89 and 93.30 respectively with a carbonyl resonance at δ 216.42. In the ^{31}P NMR spectrum resonances were found at δ 62.6 and 81.94 for the cluster bound $AuPPh_3$ and dppe ligand respectively.

The bis-cluster complex $1,4\text{-}\{AuRu_3(CO)_9(PPh_3)C_2\}_2C_6H_4$ (**58**) was obtained by reacting the bis-gold complex $1,4\text{-}\{(Ph_3P)Au(C{\equiv}C)\}_2C_6H_4$ with two equivalents of $Ru_3(CO)_{10}(NCMe)_2$ (Scheme 5.11). Microanalysis and ES mass spectrometry confirmed the formulation of this complex, supported by the usual spectroscopic data. Thus, in the IR spectrum five terminal ν(C≡O) bands were observed between 2070 and 1991 cm^{-1}. In the ^{13}C NMR spectrum a singlet was found at δ 224.80 for the carbonyl carbons, while in the ^{31}P NMR spectrum a characteristic resonance at δ 61.9 for $Au(PPh_3)$ was observed.

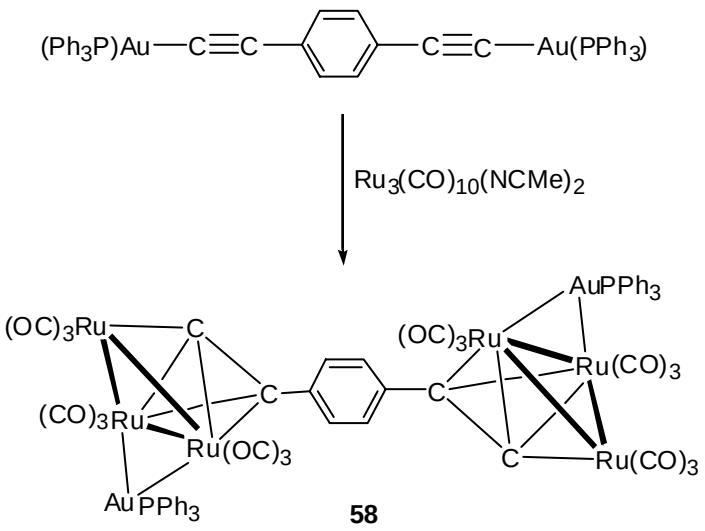

58

Scheme 5.11

The reactivity of the gold fragment within **54** was investigated using the gold coupling reaction described in Scheme 5.12. It was hoped that the gold coupling reaction between these cluster complexes and compounds containing C(sp)-X [X = halide] would enable the isolation of complexes containing an inorganic linker along the carbon chain with the elimination of $AuX(PPh_3)$ (Scheme 5.12).

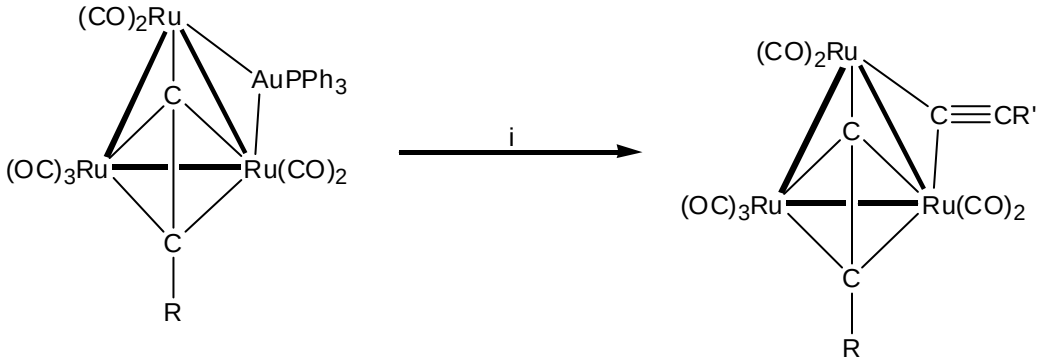

Reagents: R'C≡CX, $Pd(PPh_3)_4$ / CuI

Scheme 5.12

The progress of the reaction of **54** and $Co_3(\mu_3\text{-CBr})(\mu\text{-dppm})(CO)_7$ in thf in the presence of $Pd(PPh_3)_4$ and CuI was monitored by t.l.c.. It was found that the reaction did not proceed at room temperature so the reaction mixture was slowly heated to reflux. However after one day the reaction mixture was purified by preparative t.l.c.

to give back **54** in 100% yield. It was thought that the bulk of the cobalt cluster may have hindered this reaction hence the reaction of **54** and IC≡CSiMe$_3$ was also investigated. However, complex **54** was again isolated in 100% yield after purification of the reaction mixture suggesting that the gold fragment within the cluster complexes is unreactive under standard gold coupling conditions.

Reacting the SiMe$_3$ protected complex Mo(≡CC≡CSiMe$_3$)(CO)$_2$Tp with the activated ruthenium cluster Ru$_3$(CO)$_{10}$(NCMe)$_2$ at room temperature gave the di-ruthenium complex MoRu$_2$(μ$_3$-C$_2$Me)(CO)$_8$Tp (**59**) (Scheme 5.13). The SiMe$_3$ group was most likely lost after hydrogenation by hydrolysis during purification by t.l.c. due to the presence of water. Elemental analysis and the ES mass spectrum confirmed the formulation of this complex, supported by spectroscopic data. Thus the IR spectrum contains six ν(C≡O) bands between 2085 and 1786 cm^{-1}. In the ^{1}H NMR spectrum resonances are found at δ 1.99 for the methyl protons and at δ 6.25 and 6.29 for the pz protons. In the ^{13}C NMR spectrum characteristic resonances are found at δ 15.83 for the methyl carbon, δ 105.88/106.10, 135.91/135.98 and 143.87/144.44 for the pz carbons and at δ 213.60 for the carbonyl carbons. Resonances at δ 30.01 and 114.63 are assigned to the remaining carbons of the chain. The obsevation of a single carbonyl resonance indicates the presence of a fluxional, presumably similar to that previously reported for the tungsten complex CpWRu$_2$(CCPh)(CO)$_8$ where it was found that, at 300 K coalescence of the two tungsten carbonyl resonances as well as the six ruthenium carbonyl resonances occurred.[179]

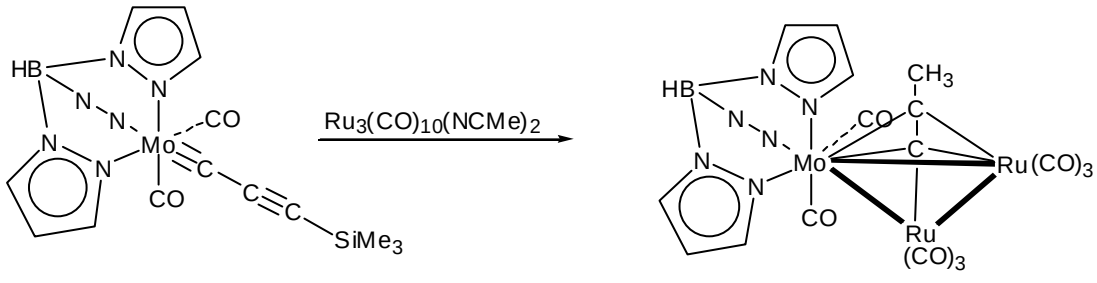

59

Scheme 5.13

The reaction of {Tp(CO)$_2$Mo}≡CC≡CSiMe$_3$ with Fe$_2$(CO)$_9$ at room temperature in diethyl ether overnight gave the iron analogue Fe$_2$Mo(μ$_3$-C$_2$Me)(CO)$_8$Tp (**60**)

(Scheme 5.14) as a maroon powder after purification by t.l.c.. The IR spectrum contains six ν(C≡O) bands between 2072 and 1879 cm^{-1}. In the ^{1}H NMR spectrum resonances are found at δ 2.17 for the methyl protons and at δ 6.25 and 6.32 for the pz protons. In the ^{13}C NMR spectrum characteristic resonances are found at δ 16.88 for the methyl carbon, δ 106.27/106.05, 136.17 and 144.52 for the pz carbons and at δ 203.26 and 217.16 for the carbonyl carbons. The ES mass spectrum contains $[M + Na]^{+}$ at *m/z* 708.

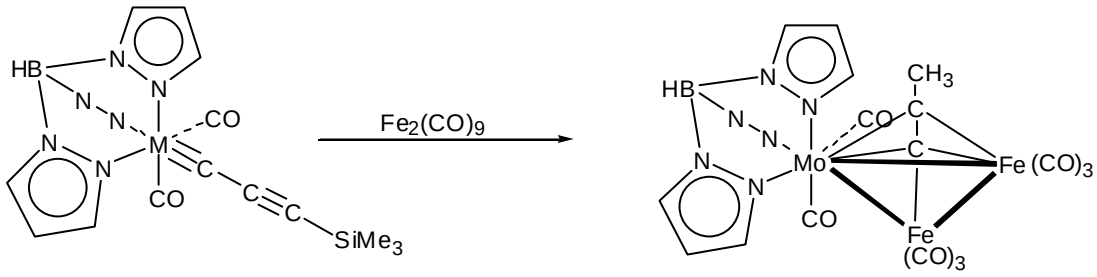

60

Scheme 5.14

The structure of **60** was confirmed by an X-ray study of crystals obtained from dichloromethane/methanol (Figure 5.5). This molecule has a triangular $MoFe_2$ core with bond distances of Mo-Fe(2) = 2.9244(7) Å, Mo-Fe(3) = 2.7679(8) Å and Fe(2)-Fe(3) = 2.638(9) Å. The molybdenum atom is also associated with a Tp and two CO ligands, while each of the iron atoms is linked to three terminal CO ligands. The carbon chain is coordinated to the cluster face with the α-carbon bound to all three metal atoms with bond distances of 1.804(4) - 2.249(4) Å and the β-carbon linked to molybdenum and Fe(3) with bond distances of 2.305(4) and 2.801(5) Å respectively. The C(1)-C(2) bond distance of 1.294(6) Å is significantly shorter than that found in $Mo(\equiv CC\equiv CSiMe_3)(CO)_2Tp$ (**14**) [1.40(1) Å]. The carbon chain is markedly bent with Mo-C(1)-C(2) and C(1)-C(2)-C(3) having angles of 75.9(3) and 146.6(4)˚ respectively. This bend at C(1) is much greater than found in the analogous complexes $Ru_2W(C_2Ph)(CO)_8Cp$ [162.5(6)˚][179] and $Fe_2W(C_2C_6H_4Me\text{-}4)(CO)_8Cp$ 163˚.[182]

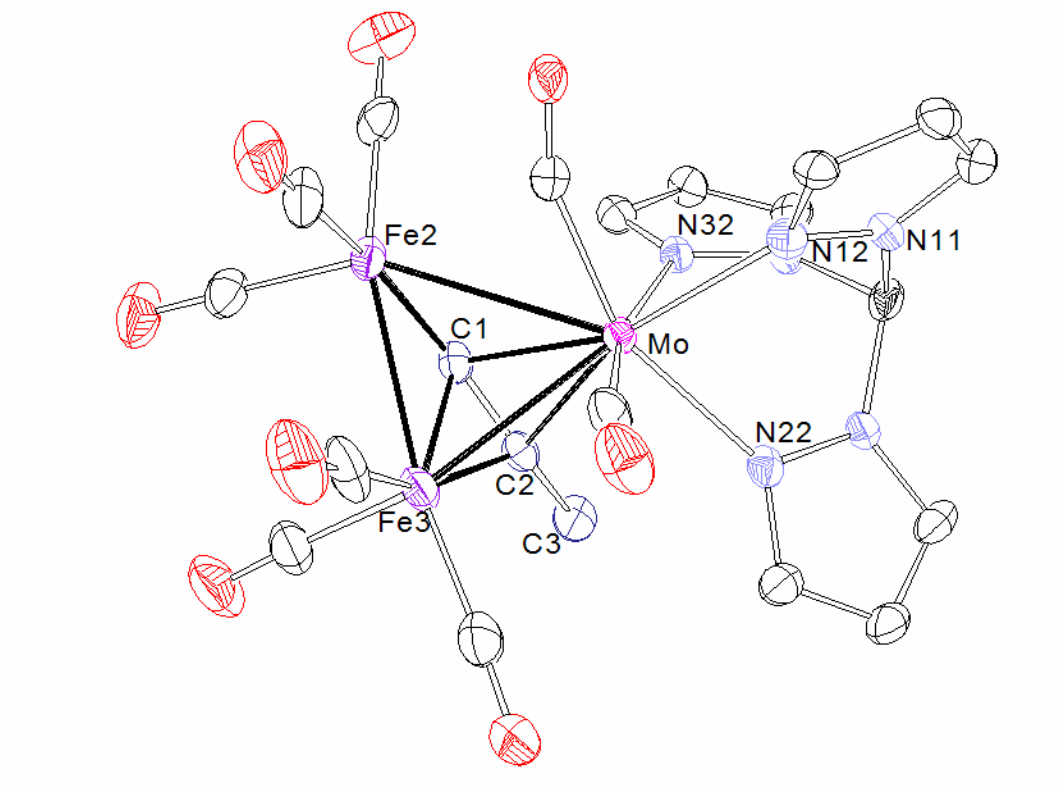

Figure 5.5: *ORTEP view of $Fe_2Mo(\mu_3\text{-}C_2Me)(CO)_8Tp$ (**60**).*

Table 5.3: *Selected structural data for $Fe_2Mo(\mu_3\text{-}C_2Me)(CO)_8Tp$ (**60**).*

Bond Distances (Å)		**Bond Angles (˚)**	
Fe(2)-Fe(3)	2.638(9)	Fe(2)-Mo-Fe(3)	55.27(2)
Mo-Fe(2)	2.9244(7)	Fe(2)-Mo-C(1)	38.1(1)
Mo-Fe(3)	2.7679(8)	Fe(3)-Mo-C(1)	46.7(1)
Fe(2)-C(1)	1.804(4)	C(1)-Mo-C(2)	33.0(2)
Fe(3)-C(1)	2.043(5)	Mo-Fe(2)-Fe(3)	59.36(2)
Mo-C(1)	2.249(4)	Fe(3)-Fe(2)-C(1)	50.5(2)
Fe(3)-C(2)	2.081(5)	Mo-Fe(3)-Fe(2)	65.37(2)
Mo-C(2)	2.305(4)	Mo-Fe(3)-C(1)	53.2(1)
C(1)-C(2)	1.294(6)	Mo-Fe(3)-C(2)	54.6(1)
C(2)-C(3)	1.492(7)	Fe(2)-Fe(3)-C(1)	42.9(1)
Mo-N(12)	2.221(4)	C(1)-Fe(3)-C(2)	36.6(2)
Mo-N(22)	2.231(3)	Mo-C(1)-C(2)	75.9(3)
Mo-N(32)	2.237(4)	C(1)-C(2)-C(3)	146.6(4)

Reactions between **14** and the cobalt carbonyls $Co_2(CO)_8$ and $Co_2(\mu\text{-dppm})(CO)_6$ afforded the corresponding di-cobalt derivatives, analogous to those found previously for the tertiary butyl derivatives,[114] $Mo\{\equiv CC\equiv CSiMe_3[Co_2(CO)_6]\}(CO)_2Tp$ (**61**) and $Mo\{\equiv CC\equiv CSiMe_3[Co_2(\mu\text{-dppm})(CO)_4\}(CO)_2Tp$ (**62**) (Scheme 5.15) in 26 and 49% yield respectively. The IR spectrum of **61** contains four terminal ν(C≡O) bands between 2021 and 1857cm^{-1}, while that of **62** contains five terminal ν(C≡O) bands between 2026 and 1895cm^{-1}. In the ^{1}H NMR, pz protons are found at δ 5.62, 5.87 (**61**) and 5.90, 6.09 (**62**). In the ^{13}C NMR spectra, $SiMe_3$ carbons are found at δ 0.96 (**61**), 1.17 (**62**) and the carbonyl carbons at δ 199.72, 227.17 (**61**), 202.20, 228.20 (**62**). The ES mass spectra contain $[M + Na]^+$ at *m/z* 785 (**61**) and 1113 (**62**).

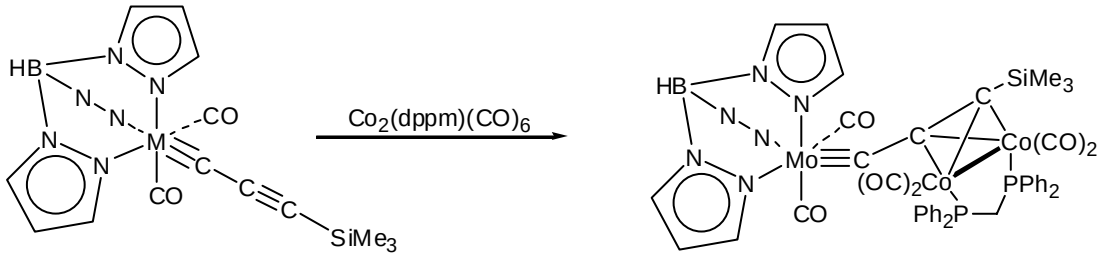

62

Scheme 5.15

The structure of **62** was confirmed by an X-ray structure determination after crystallisation from dichloromethane/methanol (Figure 5.6). The di-cobalt fragment is attached to the C≡C rather than the Mo≡C, perhaps owing to the steric constraints imposed by the dppm ligand as found for the addition of cobalt carbonyl to W≡C in $W\equiv CC\equiv CCMe_3(CO)_2Cp$.[114] Thus the molybdenum atom remains octahedrally coordinated, with the Tp ligand occupying three facial positions with Mo-N bonds distances of 2.222(3) – 2.299(3) Å. Two of the remaining three sites are occupied by two CO ligands while the third is occupied by the carbon chain. The Mo≡C(1) bond, [1.841(3)], is statistically identical to that found in $Mo(\equiv CC\equiv CSiMe_3)(CO)_2Tp$ [1.833(7)]. Angles at C(1), C(2) and C(3) are 167.3(3), 142.1(3) and 145.6(2) respectively giving the carbon chain a prominent bend. Back bonding from the Co_2 fragment results in a lengthening of the C(2)-C(3) bond distance to 1.379(6) Å compared to 1.26(1) Å in **14**.

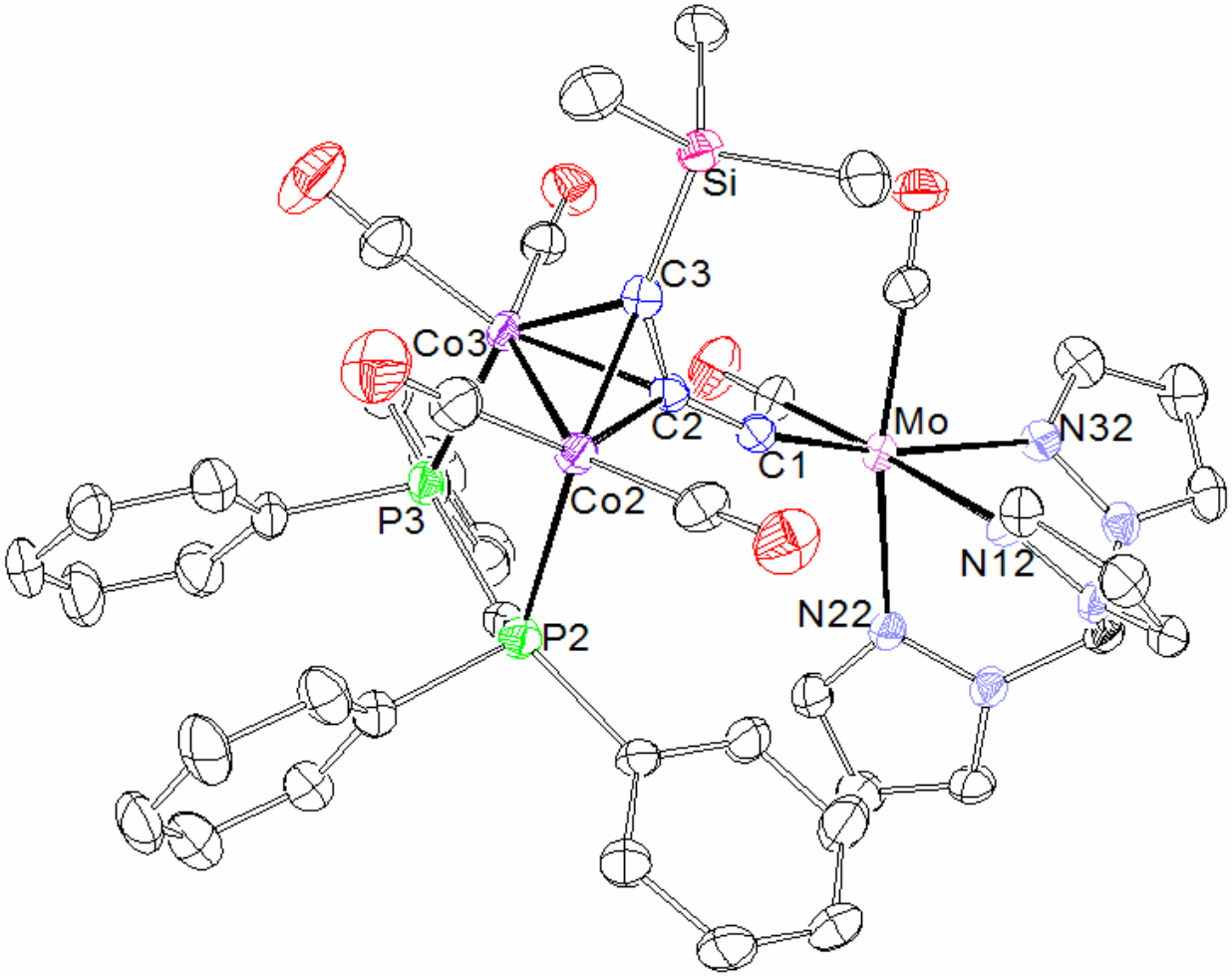

Figure 5.6: *ORTEP view of Mo{≡CC≡CSiMe$_3$[Co$_2$(μ-dppm)(CO)$_4$](CO)$_2$Tp* ***(62)****.*

Table 5.4: *Selected structural data for Mo{≡CC≡CSiMe$_3$[Co$_2$(μ-dppm)(CO)$_4$}(CO)$_2$Tp (**62**).*

Bond Distances (Å)		**Bond Angles (˚)**	
Mo-C(1)	1.841(3)	Mo-C(1)-C(2)	167.3(3)
Mo-N(12)	2.222(3)	C(2)-Co(2)-C(3)	40.8(2)
Mo-N(22)	2.239(3)	Co(2)-Co(3)-C(2)	51.02(9)
Mo-N(32)	2.299(3)	Co(2)-Co(3)-C(3)	50.51(9)
Co(2)-Co(3)	2.5046(8)	C(2)-Co(3)-C(3)	40.8(2)
Co(2)-C(2)	1.989(3)	Co(2)-C(2)-Co(3)	78.2(1)
Co(2)-C(3)	1.971(3)	Co(2)-C(2)-C(3)	68.9(2)
Co(2)-P(2)	2.232(1)	Co(3)-C(2)-C(1)	131.2(3)
Co(3)-C(2)	1.983(3)	Co(3)-C(2)-C(3)	69.3(2)
Co(3)-C(3)	1.976(4)	C(1)-C(2)-C(3)	142.1(3)
Co(3)-P(3)	2.224(1)	Co(2)-C(3)-Co(3)	78.79
C(1)-C(2)	1.392(5)	Co(2)-C(3)-C(2)	70.3(2)
C(2)-C(3)	1.379(6)	C(2)-C(3)-Si	145.6(2)
C(3)-Si(3)	1.846(4)		

A similar di-nickel complex, Mo{≡CC≡CSiMe$_3$[Ni$_2$Cp$_2$](CO)$_2$Tp (**63**) was isolated from the reaction of **14** with nickelocene at reflux in toluene. The IR spectrum of **63** contains ν(BH) as a weak band at 2483 cm^{-1} and two ν(C≡O) bands at 1885 and 1815 cm^{-1}. In the ^{1}H NMR spectrum SiMe$_3$ protons are found at δ 0.09 while pz protons are found at δ 5.16 and 5.82. In the ^{13}C NMR spectrum Cp ring carbons are found at δ 94.64, the pz ring carbons at δ 105.54/106.94, 134.85/135.84, 145.01/145.17 and the carbonyl carbons at δ 227.54. The ES mass spectrum contains $[M]^+$ at *m/z* 721 and $[M - CO]^+$ at *m/z* 693.

It was found that the alkyne linkages within the bis-metallic complex {Tp(OC)$_2$Mo}≡CC≡C{Ru(dppe)Cp*} (**24**) did not react with the activated ruthenium carbonyl complex, Ru$_3$(CO)$_{10}$(NCMe)$_2$. It was thought that this may be due to the size of the Ru$_3$ cluster, which hinders the approach to the carbon chain and thus the reaction. However attempts to react **24** with dinuclear cobalt and iron

carbonyls were also unsuccessful due to the decomposition of the $Fe_2(CO)_9$ or $Co_2(CO)_8$ prior to reaction with **24**. The results suggest **24** is too bulky to permit adduct formation at the C_3 chain. Considering the space-filling models in Figure 5.7, which illustrate the encapsulation of the C_3 chain within the bis-metallic complex {Tp*$(OC)_2$Mo}≡CC≡C{Ru(dppe)Cp*}, this may not be surprising. Comparison with the exposed C_3 chain found in Mo(≡CC≡C$SiMe_3$)$(CO)_2$Tp, with which reaction does occur further evidences the disparity in bulk.

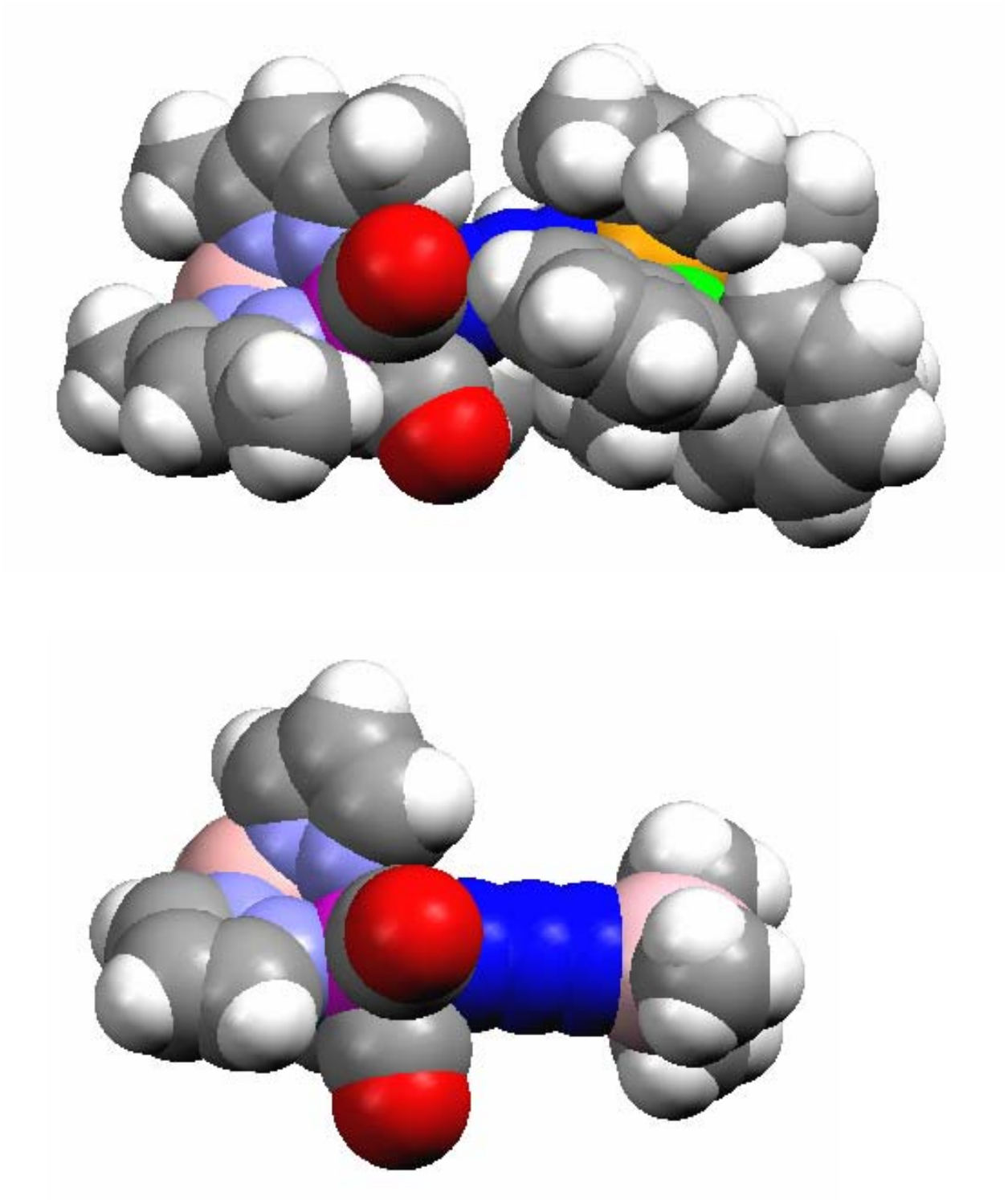

Figure 5.7: *Space-filling models of {Tp*(OC)$_2$Mo}≡CC≡C{Ru(dppe)Cp*}* ***(24)*** *and Mo(≡CC≡CSiMe$_3$)(CO)$_2$Tp* ***(14)****. Generated using Mercury (Version 1.2.1); grey = carbon; red = oxygen; purple = molybdenum; orange = ruthenium; green = phosphorus; blue = carbon atoms of the C_3 chain).*

5.3 Conclusions

A number of new gold containing cluster complexes have been prepared from the reaction of gold alkynyl complexes, M-$(C\equiv C)_n$-$Au(PPh_3)$, (n = 3, 4, 6) with the activated ruthenium carbonyl, $Ru_3(CO)_{10}(NCMe)_2$. Similar cluster complexes, $AuRu_3(\mu_3\text{-}C_2C_6F_5)(CO)_9(PPh_3)$ and 1,4-$\{Ru_3(\mu\text{-}AuPPh_3)(CO)_9(\mu_3\text{-}C_2)$ were obtained from the reaction of $Ru_3(CO)_{10}(NCMe)_2$ with the C_2 compounds $Au(C\equiv CC_6F_5)(PPh_3)$ and 1,4-$\{(Ph_3P)Au(C\equiv C)\}_2C_6H_4$ respectively. The cluster-bound gold within these complexes appears to be unreactive towards coupling with halo-alkynes with catalytic $Pd(PPh_3)_4$ and CuI.

The mixed metal cluster complexes, $MoRu_2(\mu_3\text{-}C_2Me)(CO)_8Tp$ and $MoFe_2(\mu_3\text{-}C_2Me)(CO)_8Tp$, were obtained from the reaction of the carbyne complex, $\{Tp(CO)_2Mo\}\equiv CC\equiv CSiMe_3$, with ruthenium and iron carbonyls respectively. Reactions of the same carbyne complex with the cobalt carbonyls $Co_2(L)(CO)_6$ (L = $(CO)_2$, dppm) and nickelocene afforded the corresponding di-cobalt and di-nickel derivatives. However the attempts to synthesis similar complexes from the C_3 complex $\{Tp(OC)_2Mo\}\equiv CC\equiv C\{Ru(dppe)Cp^*\}$ were unsuccessful most likely due to steric constraints.

5.4 Experimental

Reagents. The complexes $Ru\{(C{\equiv}C)_3Au(PPh_3)\}(dppe)Cp^*$,[98] 1,4-$\{Au(PPh_3)(C{\equiv}C)\}_2C_6H_4$,[143] and $Au(C{\equiv}CC_6F_5)(PPh_3)$[160] were prepared as described previously. Anhydrous Me_3NO was prepared by sublimation of the commercial dihydrate.

Reactions of $Ru_3(CO)_{10}(NCMe)_2$

General procedure. The gold complex (0.078 mmol) was added to a solution of $Ru_3(CO)_{10}(NCMe)_2$ [prepared from $Ru_3(CO)_{12}$ (50 mg, 0.078 mmol) and Me_3NO (12 mg, 0.16 mmol) in CH_2Cl_2 (25 ml) and MeCN (5 ml)] at -10˚C. On warming slowly to r.t. the colour darkened and the resulting mixture stirred for a further 2 h. Preparative t.l.c. (acetone/hexane 3:7) enabled separation of the major product.

$AuRu_3\{\mu_3\text{-}C_2C{\equiv}C[Ru(dppe)Cp^*]\}(CO)_9(PPh_3)$ (52)

(R_f 0.35) (25 mg, 19%). Anal. Calcd ($C_{67}H_{54}AuO_9P_3Ru_4$): C, 47.41; H, 3.21. Found: C, 47.21; H, 3.46. IR (cyclohexane, cm^{-1}): ν(C≡C) 2066 w, ν(C≡O) 2029 s, 1985 m, 1965 w, 1952 w. ^{1}H NMR (C_6D_6): δ 1.50 (s, 15H, Cp*), 1.88, 2.60 (2m, 2 x 2H, CH_2CH_2), 6.94 – 7.80 (m, 35H, Ph). ^{13}C NMR: (C_6D_6) δ 10.28 (s, $C_5\mathit{Me}_5$), 29.80(m, CH_2CH_2), 93.93 (s, C_5Me_5), 99.97 (s, C≡C), 127.52–148.96 (m, Ph), 198.98 (s, br, C≡O). ^{31}P NMR (C_6D_6): δ 61.4 (s, 1P, $AuPPh_3$), 80.7 (s, 2P, dppe). ES-mass spectrum (*m/z*): 1721, $[M + Na]^+$, 1699, $[M + H]^+$.

$AuRu_3\{\mu_3\text{-}C_2(C{\equiv}C)_2[Ru(dppe)Cp^*]\}(CO)_9(PPh_3)$ (53)

(R_f 0.34) (30 mg, 14%). Anal. Calcd ($C_{69}H_{54}AuO_9P_3Ru_4$): C, 48.15; H, 3.16. Found: C, 48.07; H, 3.14. IR (cyclohexane, cm^{-1}): ν(C≡C) 2126 w, 2076 w, ν(C≡O) 2064 m, 2047 s, 2036 s, 2000 m, 1963 w. ^{1}H NMR (C_6D_6): δ 1.51 (s, 15H, Cp*), 1.72, 2.41 (2m, 2 x 2H, CH_2CH_2), 6.98 – 7.81 (m, 35H, Ph). ^{13}C NMR: (C_6D_6) δ 10.47 (s, $C_5\mathit{Me}_5$), 30.56 (m, CH_2CH_2), 94.21 (s, C_5Me_5), 128.07 – 134.62 (m, Ph), 227.63 (s, C≡O). ^{31}P NMR (C_6D_6): δ 62.2 (s, 1P, $AuPPh_3$), 80.6 (s, 2P, dppe). ES-mass spectrum (*m/z*): 1745, $[M + Na]^+$.

$AuRu_3\{\mu_3\text{-}C_2C{\equiv}[Mo(CO)_2Tp]\}(CO)_9(PPh_3)$ (54)

(R_f 0.29) (31 mg, 28%). Anal. Calcd ($C_{41}H_{25}AuBMoN_6O_{11}PRu_3$): C, 34.79; H, 1.78; N, 5.94. Found: C, 34.74; H, 1.90; N, 6.02. IR (cyclohexane, cm^{-1}): ν(C≡O) 2074 m, 2043 s, 2003 s, 1996 sh, 1981 m, 1966 w, 1946 w, 1917 m. ^1H NMR (C_6D_6): δ 5.62 (t, $^3J_{HH}$ = 2.4 Hz , 1H, pz-C_4H), 5.77 (t, $^3J_{HH}$ = 2.4 Hz , 2H, pz-C_4H), 6.99 – 7.58 (m, 19H, Ph), 7.97 [d, $^3J_{HH}$ = 1.8 Hz, 2H, pz-C_3H]. ^{13}C NMR (C_6D_6): δ 105.98/106.23, 134.38/135.61, 143.80/144.83 (6 x s, pz-C) 128.71–163.69 (m, Ph), 227.54, 227.08 (s, C≡O), 267.23 (s, C≡Mo). ^{31}P NMR (C_6D_6): δ 62.5 (s, 1P, PPh_3). ES-mass spectrum (*m/z*): 1439, $[M + Na]^+$, 1416, $[M]^+$, 957, $[M - AuPPh_3]$.

$AuRu_3\{\mu_3\text{-}C_2C{\equiv}[W(CO)_2Tp]\}(CO)_9(PPh_3)$ (55)

(R_f 0.27) (24 mg, 21%). Anal. Calcd ($C_{41}H_{25}N_6AuBO_{11}PRu_3W$): C, 32.75; H, 1.68; N, 5.59. Found: C, 32.74; H, 1.73; N, 5.61. IR (cyclohexane, cm^{-1}): ν(C≡O) 2072 w, 2042 s, 2001 s, 1979 w, 1964 w, 1902 m. ^1H NMR (C_6D_6): δ 5.54 (t, $^3J_{HH}$ = 2.4 Hz , 1H, pz-C_4H), 5.71 (t, $^3J_{HH}$ = 2.4 Hz , 2H, pz-C_4H), 6.99–7.61 (m, 19H, Ph), 8.04 (d, $^3J_{HH}$ = 2.4 Hz, 2H, pz-C_3H]. ^{13}C NMR (C_6D_6): δ 106.51/106.79, 135.49/135.60, 144.77/146.70 (6 x s, pz-C), 129.23-135.49 (m, Ph), 227.54, 225.12 (s, C≡O), 257.79 (s, C≡W). ^{31}P NMR (C_6D_6): δ 62.4 (s, 1P, PPh_3). ES-mass spectrum (*m/z*): 1527, $[M + Na]^+$.

$AuRu_3(\mu_3\text{-}C_2C_6F_5)(CO)_9(PPh_3)$ (56)

(R_f 0.53) (20 mg, 35%). Anal. Calcd ($C_{35}H_{15}AuF_5O_9Ru_3$): C, 34.87; H, 1.25. Found: C, 34.90; H, 1.28. IR (CH_2Cl_2, cm^{-1}): ν(C≡O) 2076 w, 2043 s, 2000 m, 1514 w, 1495 w. ^1H NMR (C_6D_6): δ 6.97–7.56 (m, 15H, Ph). ^{13}C NMR (C_6D_6): δ 126.45−134.57 (m, Ph), 216.53 (s, C≡O). ^{19}F NMR (C_6D_6): δ -9.82 (m, 2F, o-F), -2.54 [t, $^3J_{FF}$ = 22 Hz, 2F, p-F], 18.74 (m, 2F, m-F). ^{31}P NMR (C_6D_6): δ 63.3 (s, 1P, PPh_3). ES-mass spectrum (*m/z*): 1207, $[M]^+$.

$AuRu_3(\mu_3\text{-}C_2C_6H_4C{\equiv}C[Ru(dppe)Cp^*]\}(CO)_9(PPh_3)$ (57)

(R_f 0.37) (25 mg, 15%). Anal. Calcd ($C_{73}H_{58}AuO_9P_3Ru_4$): C, 49.44; H, 3.30. Found: C, 49.50; H, 3.39. IR (cyclohexane, cm^{-1}): ν(C≡O) 2068 m, 2037 s, 1993 m, 1986 sh, 1975 w, 1961 w. ^1H NMR (C_6D_6): δ 1.64 (s, 15H, Cp*), 1.95, 2.60 (2m, 2 x 2H,

CH_2CH_2), 6.58 – 7.87 (m, 39H, Ph and C_6H_4). ^{13}C NMR: (C_6D_6) δ 10.89 (s, $C_5\mathit{Me}_5$), 30.64 (m, CH_2CH_2), 93.30 (s, C_5Me_5), 124.00–135.57 (m, Ph), 216.42 (s, C≡O). ^{31}P NMR: δ 62.6 (s, 1P, $AuPPh_3$), 81.9 (s, 2P, dppe). ES-mass spectrum (*m/z*): 1775, $[M + H]^+$.

1,4-{$AuRu_3(CO)_9(PPh_3)(\mu_3\text{-}C_2)\}_2C_6H_4$ (58)

(R_f 0.37) (26 mg, 15%). Anal. Calcd ($C_{64}H_{34}Au_2O_{18}P_2Ru_6$): C, 36.22; H, 1.61. Found: C, 36.30; H, 1.70. IR (cyclohexane, cm^{-1}): ν(C≡O) 2070 m, 2040 s, 2013 m, 1997 s, 1991 sh. ^1H NMR (C_6D_6): δ7.53 (s, 4H C_6H_4), 6.90 – 7.56 (m, 30H, Ph). ^{13}C NMR: (C_6D_6) δ 126.15 – 149.65 (m, Ph), 224.80 (s, C≡O). ^{31}P NMR: δ 61.9 (s, 1P, $AuPPh_3$). ES-mass spectrum (*m/z*): 2177, $[M + Na]^+$; 1695, $[M - AuPPh_3]^+$.

$MoRu_2(\mu_3\text{-}C_2Me)(CO)_8Tp$ (59)

To a solution of $Ru_3(CO)_{10}(NCMe)_2$ [prepared *in situ* from $Ru_3(CO)_{12}$ (50 mg, 0.078 mmol) and Me_3NO (12 mg, 0.16 mmol) in a mixture of CH_2Cl_2 (25 ml) and MeCN (5 ml)] at -10˚C was added $Mo(\equiv CC\equiv CSiMe_3)(CO)_2Tp$ (30 mg, 0.078 mmol). The resulting mixture was stirred at r.t. for 5 h before the solvent was removed and the residue purified by preparative t.l.c. (acetone/hexane 3:7) The major product was collected as a bright orange band (12 mg, 20%) Anal. Calcd ($C_{20}H_{13}BMoN_6O_8Ru_2$): C, 31.03; H, 1.69; N, 10.85. Found: C, 31.79; H, 1.92; N, 10.46. IR (CH_2Cl_2, cm^{-1}): ν(C≡O) 2085 s, 2051 s, 2020 s, 2006 sh, 1851 m, 1786 m. ^1H NMR ($CDCl_3$): δ 1.99 (s, 3H, CH_3), 6.25 [t, $^3J_{HH}$ = 2.3 Hz, 2H, pz-H^4], 6.29 [t, $^3J_{HH}$ = 2.3 Hz, 1H, pz-H^4], 7.68 (m, 4H, pz-$H^{3,5}$), 7.91 [d, $^3J_{HH}$ = 2.3 Hz, 1H, pz-$H^{3,5}$]. ^{13}C NMR ($CDCl_3$): δ 15.83 (s, CH_3), 30.01, 114.63 (2s, CC), 105.88/106.10, 135.91/135.98, 143.87/144.44 (6s, pz-C), 213.60 (s, C≡O). ES-mass spectrum (*m/z*): 796, $[M + Na]^+$.

$Fe_2Mo(\mu_3\text{-}C_2Me)(CO)_8Tp$ (60)

A mixture of $\{Tp(CO)_2Mo\}\equiv CC\equiv CSiMe_3$ (100 mg, 0.26 mmol) and $Fe_2(CO)_9$ (200 mg, 0.56 mmol) was stirred in diethyl ether (30 ml) at r.t. overnight. The resulting mixture was then filtered and the solvent removed. The resulting residue was purified by preparative t.l.c. eluting with acetone / hexane (3:7) to obtain $Fe_2Mo(\mu_3\text{-}C_2Me)(CO)_8Tp$ as a maroon band (R_f 0.43) (40 mg, 22%). Anal. Calcd

($C_{20}H_{13}BFe_2MoN_6O_8$): C, 35.13; H, 1.92; N, 12.29. Found: C, 36.05; H, 1.97; N, 12.25. IR (CH_2Cl_2, cm^{-1}): ν(CO) 2072 s, 2028 s, 2008 m, 1993 sh, 1972 m, 1879 m. ^{1}H NMR ($CDCl_3$): δ 2.17 (s, 3H, CH_3), 6.25 (s, br, 2H, pz-C_4H), 6.32 [t, $^3J_{HH}$ = 3.3 Hz, 1H, pz-CH), 7.71 (s,br, 3H, pz-CH), 7.93 [d, $^3J_{HH}$ = 2.7 Hz, 1H, pz-CH]. ^{13}C NMR: δ 16.88 (s, CH_3), 106.05/106.27, 136.17, 143.91/144.52 (5 x s, pz-ring C), 203.26, 217.16 (2s, CO). ES MS (*m/z*): 708, $[M + Na]^+$.

Mo{≡CC≡CSiMe$_3$[Co$_2$(CO)$_6$]}(CO)$_2$Tp (61)

A mixture of Mo(≡CC≡CSiMe$_3$)Tp(CO)$_2$ (100 mg, 0.26 mmol) and $Co_2(CO)_8$ (267 mg, 0.78 mmol) was stirred in diethyl ether (10 ml) at r.t. for 2 h. The resulting mixture was then filtered and the solvent removed. The resulting residue was purified by preparative t.l.c. eluting with acetone/hexane (3:7) to obtain Mo{≡CC≡CSiMe$_3$[Co$_2$(CO)$_6$]}(CO)$_2$Tp as a green band (R_f 0.60) (51 mg, 26%). IR (CH_2Cl_2, cm^{-1}): ν(BH) 2478 w, ν(CO) 2021 m, 1974 m, 1896 s, 1857 s. ^{1}H NMR (C_6D_6): δ 0.31 (s, 9H, $SiMe_3$), 5.62 [t, $^3J_{HH}$ = 2.1 Hz, 1H, pz-C_4H], 5.87 [t, $^3J_{HH}$ = 2.1 Hz, 2H, pz-CH), 7.19 [d, $^3J_{HH}$ = 2.4 Hz, 1H, pz-CH], 7.29, 7.95 [2d, $^3J_{HH}$ = 2.1 Hz, 2 x 2H, pz-CH]. ^{13}C NMR (C_6D_6): δ 0.96 (s, $SiMe_3$), 106.11, 135.85/135.76, 144.40/143.94 (5 x s, pz-ring C), 199.72 (s, Co-CO), 227.17 (s, Mo-CO), 262.84 (s, C≡Mo). ES MS (*m/z*): 785, $[M + Na]^+$.

Mo{≡CC≡CSiMe$_3$[Co$_2$(μ-dppm)(CO)$_4$]}(CO)$_2$Tp (62)

A mixture of {Tp(CO)$_2$Mo}≡CC≡CSiMe$_3$ (50 mg, 0.13 mmol) and $Co_2(CO)_6$(μ-dppm) (89 mg, 0.13 mmol) was stirred in diethyl ether (10 ml) at r.t. for 8 h. The solvent was then removed and the resulting residue was purified by preparative t.l.c. eluting with acetone/hexane (3:7) to obtain Mo{≡CC≡CSiMe$_3$[Co$_2$(μ-dppm)(CO)$_4$]}-(CO)$_2$Tp as a black band (R_f 0.36) (68.8 mg, 49%). Anal. Calcd ($C_{46}H_{41}BCo_2MoN_6O_6P_2Si$): C, 50.76; H, 3.80; N, 7.72. Found: C, 50.90; H, 3.94; N, 7.61. IR (CH_2Cl_2, cm^{-1}): ν(CO) 2026 s, 2000 s, 1978 s, 1967 sh 1895 m. ^{1}H NMR ($CDCl_3$): δ 0.48 (s, 9H, $SiMe_3$), 3.51, 3.83 (2m, 2 x 1H, CH_2), 5.90 (s, br, 2H, pz-CH), 6.09 (s, br, 1H, pz-CH), 6.89-7.61 (m, 26H, Ph and H^{3,5}pz). ^{13}C NMR ($CDCl_3$): δ 1.17 (s, $SiMe_3$), 26.38 (m, CH_2) 105.29/105.51, 134.59/135.16, 143.12/144.05 (6 x s, pz-ring C), 128.15-137.70 (m, Ph), 202.20 (s, Co-CO), 228.20

(s, Mo-CO). ^{31}P NMR: δ 35.40 (s, br, 2P, dppm). ES MS (*m/z*): 1113, $[M + Na]^+$; 1090 $[M]^+$; 1062, $[M – CO]^+$.

Mo{≡CC≡CSiMe$_3$[Ni$_2$Cp$_2$]}(Co)$_2$Tp (63)

A mixture of Mo(≡CC≡CSiMe$_3$)(CO)$_2$Tp (50 mg, 0.13 mmol) and NiCp$_2$ (50 mg, 0.26 mmol) was stirred in toluene (30 ml) under reflux for 24 h. The solvent was then removed and the resulting residue was purified by preparative t.l.c. eluting with acetone / hexane (3:7) to obtain Mo{≡CC≡CSiMe$_3$[Ni$_2$Cp$_2$]}(Co)$_2$Tp as a brown band (R_f 0.50) (27.4 mg, 29%). Anal. Calcd ($C_{27}H_{29}BMoN_6Ni_2O_2Si$): C, 44.93; H, 4.05; N, 11.64. Found: C, 45.05; H, 4.15; N, 11.41. IR (CH_2Cl_2, cm^{-1}): ν(BH) 2483 w, ν(CO) 1885 s, 1815 m. ^{1}H NMR (C_6D_6): δ 0.09 (s, 9H, SiMe$_3$), 5.16 (s, 10H, Cp), 5.82(m, 3H, pz-CH), 7.13 [d, $^3J_{HH}$ = 1.5 Hz, 2H, pz-CH], 7.31, (m, 3H, pz-CH), 8.31 [d, $^3J_{HH}$ = 1.8 Hz, 1H, pz-CH]. ^{13}C NMR (C_6D_6): δ 0.77 (s, SiMe$_3$), 94.64 (s, Cp), 105.54/106.94, 134.85/135.84, 145.01/145.17 (6 x s, pz-ring C), 227.54 (s, CO), 239.07 (s, C≡Mo). ES MS (*m/z*): 744, $[M + Na]^+$; 721, $[M]^+$; 693, $[M - CO]^+$.

References

(1) Diederch, F.; Rubin, Y. *Angew. Chem. Int. Ed. Engl.* **1992**, *31*, 1101.

(2) Weltner Jr., W.; Van Zee, R. J. *Chem. Rev.* **1989**, *89*, 1713.

(3) Bruce, M. I. *Coord. Chem. Rev.* **1997**, *166*, 91.

(4) Rohlfing, E. A.; Cox, D. M.; Kaldor, A. *J. Chem. Phys.* **1984**, *81*, 3322.

(5) Kroto, H. W.; Heath, J. R.; O'Brien, S. C.; Curl, R. F.; Smalley, R. E. *Nature* **1985**, *318*, 162.

(6) Krätschmer, W.; Lamb, L. D.; Fostiropoulos, K.; Huffman, D. R. *Nature* **1990**, *347*, 354.

(7) Smith, P. P. K.; Buseck, P. R. *Science* **1982**, *216*, 984.

(8) Diederch, F. *Nature* **1994**, *369*, 199.

(9) Eisler, S.; Slepkov, A. D.; Elliott, E.; Luu, T.; McDonald, R.; Hegmann, F. A.; Tykwinski, R. R. *J. Am. Chem. Soc.* **2005**, *127*, 2666.

(10) Bruce, M. I.; Low, P. J. *Adv. Organomet. Chem.* **2004**, *50*, 179.

(11) Hudson, S. A.; Maitlis, P. M. *Chem. Rev.* **1993**, *93*, 861.

(12) Nguyen, P.; Gómez-Elipe, P.; Manners, I. *Chem. Rev.* **1999**, *99*, 1515.

(13) Matsumi, N.; Chujo, Y.; Lavastre, O.; Dixneuf, P. H. *Organometallics* **2001**, *20*, 2423.

(14) Onittsuka, K.; Harada, Y.; Takei, S.; Takahashi, S. *Chem. Commun.* **1998**, 643.

(15) Lewis, J. L.; Raithby, P. R.; Wong, W.-Y. *J. Organomet. Chem.* **1998**, *556*, 219.

(16) Fillaut, J.-L.; Price, M.; Johnson, A. L.; Perruchon, J. *Chem. Commun.* **2001**, 739.

(17) Whittall, I. R.; McDonagh, A. M.; Humphrey, M. G.; Samoc, M. *Adv. Organomet. Chem.* **1999**, *42*, 291.

(18) Hurst, S. K.; Humphrey, M. G.; Isoshima, T.; Wostyn, K.; Asselberghs, I.; Clays, K.; Persoons, A.; Samoc, M.; Luther-Davies, B. *Organometallics* **2002**, *21*, 2024.

(19) Weyland, T.; Ledoux, I.; Brasselet, S.; Zyss, J.; Lapinte, C. *Organometallics* **2000**, *19*, 5235.

(20) Yam, V. W.-W.; Tang, R. P.-L.; Wong, K. M.-C.; Kung-Kai, C. *Organometallics* **2001**, *20*, 4476.

(21) Yam, V. W.-W.; Wong, K. M.-C.; Zhu, N. J. *J. Am. Chem. Soc.* **2002**, *124*, 6506.

(22) Bruce, M. I.; Hall, B. C.; Low, P. J.; Smith, M. E.; Skelton, B. W.; White, A. H. *Inorg. Chim. Acta* **2000**, *300-302*, 633.

(23) Lundstorm, M. *Science* **2003**, *299*, 210.

(24) Moore, G. E. *Electronics* **1965**, *38*, 114.

(25) Low, P. J. *Dalton Trans.* **2005**, 2821.

(26) Kleiner, K. *New Scientist* **2000**, *166*, 30.

(27) James, D. K.; Tour, J. M. *AldrichimicaACTA* **2006**, *39*, 47.

(28) Robertson, N.; McGowan, C. A. *Chem. Soc. Rev.* **2003**, *32*, 96.

(29) Ward, M. D. *Chem. Ind.* **1996**, 568.

(30) Paul, F.; Lapinte, C. *Coord. Chem. Rev.* **1998**, *178-180*, 431.

(31) Tour, J. M.; Rawlett, A. M.; Kozaki, M.; Yao, Y.; Jagessar, R. C.; Dirk, S. M.; Price, D. W.; Reed, M. A.; Zhou, C. W.; Chen, J.; Wang, W.; Campbel, I. *Chem. Eur. J.* **2001**, *7*, 5118.

(32) Fraysse, S.; Coudret, C.; Launay, J. P. *Eur. J. Inorg. Chem.* **2000**, 1581.

(33) Donhauser, Z. J.; Mantooth, B. A.; Kelly, K. F.; Bumm, L. A.; Monnell, J. D.; Stapleton, J. J.; Price Jr, D. W.; Rawlett, A. M.; Allara, D. L.; Tour, J. M.; Weiss, P. S. *Science* **2001**, *292*, 2303.

(34) Ward, M. D. *Chem. Ind.* **1997**, 640.

(35) Chen, J.; Reed, M. A.; Rawlett, A. M.; Tour, J. M. *Science* **1999**, *286*, 1550.

(36) Roth, K. M.; Dontha, N.; Dabke, R. B.; Gryko, D. T.; Clausen, C.; Lindsey, J. S.; Bocian, D. F.; Kuhr, W. G. *J. Vac. Sci. Technol. B* **2000**, *18*, 2359.

(37) Metzger, R. M. *Chem. Rev.* **2003**, *103*, 3803.

(38) Metzger, R. M.; Chen, B.; Höpfner, U.; Lakshmikantham, M. V.; Vuillaume, D.; Kawai, T.; Wu, X.; Tachibana, H.; Hughes, T. V.; Sakurai, H.; Baldwin, J. W.; Hosch, C.; Cava, M. P.; Brehmer, L.; Ashwell, G. J. *J. Am. Chem. Soc.* **1997**, *119*, 10455.

(39) Anderson, H. L. *J. Chem. Soc., Chem. Commun.* **1999**, 2323.

(40) Fink, H.-W.; Schonenberger, C. *Nature* **1999**, *398*, 407.

(41) Reed, M. A.; Zhou, C.; Muller, C. J.; Burgin, T. P.; Tour, J. M. *Science* **1997**, *278*, 252.

(42) Cygan, M. T.; Dunbar, T. D.; Arnold, J. J.; Bumm, L. A.; Shedlock, N. F.; Burgin, T. P.; Jones II, L.; Allara, D. L.; Tour, J. M.; Weiss, P. S. *J. Am. Chem. Soc.* **1998**, *120*, 2721.

(43) Fan, F.-R. F.; Yang, J.; Cai, L.; Price Jr, D. W.; Dirk, S. M.; Kosynkin, D. V.; Yao, Y.; Rawlett, A. M.; Tour, J. M.; Bard, A. J. *J. Am. Chem. Soc.* **2002**, *124*, 5550.

(44) Tour, J. M. *Chem. Rev.* **1996**, *96*, 537.

(45) Iijima, S. *Nature* **1991**, *354*, 56.

(46) http://www.ruf.rice.edu/smalleyg/image_gallery.htm.

(47) Guldi, D. M.; Aminur Rahman, G. M.; Sgobba, V.; Ehli, C. *Chem. Soc. Rev.* **2006**, *35*, 471.

(48) Yang, X. "Carbon Nanotubes: Synthesis, Applications and some new aspects," State University of New York, 2006.

(49) Tans, S. J.; Devoret, M. H.; Dai, H.; Thess, A.; Smalley, R. E.; Geerligs, L. J.; Dekker, C. *Nature* **1997**, *386*, 474.

(50) Collins, P. G.; Arnold, M. S.; Avouris, P. *Science* **2001**, *292*, 706.

(51) Nelsen, S. F.; Ismagilov, R. F.; Powell, D. R. *J. Am. Chem. Soc.* **1997**, *119*, 10213.

(52) Creutz, C.; Taube, H. *J. Am. Chem. Soc.* **1969**, *91*, 3988.

(53) Creutz, C.; Taube, H. *J. Am. Chem. Soc.* **1973**, *95*, 1086.

(54) Robin, M. B.; Day, P. *Adv. Inorg. Chem. Radiochem.* **1967**, *10*, 247.

(55) Demadis, K. D.; Hartshorn, C. M.; Meyer , T. J. *Chem. Rev.* **2001**, *101*, 2655.

(56) Datta, S.; Tian, W. *Phys. Rev. Let.* **1997**, *79*, 2530.

(57) Bumm, L. A.; Arnold, J. J.; Cygan, M. T.; Dunbar, T. D.; Burgin, T. P.; Jones II, L.; Allara, D. L.; Tour, J. M.; Weiss, P. S. *Science* **1996**, *271*, 1705.

(58) Reichert, J.; Ochs, R.; Beckmann, D.; Weber, H. B.; Mayor, M.; Lohneysen, H. V. *Phys. Rev. Let.* **2002**, *88*, 176804.

(59) Barriére, F.; Camire, N.; Geiger, W. E.; Müller-Westerhoff, U. T.; Sanders, R. *J. Am. Chem. Soc.* **2002**, *124*, 7262.

(60) Mc Cleverty, J. A.; Ward, M. D. *Acc. Chem. Res.* **1998**, *31*, 842.

(61) Flanagan, J. B.; Margel, S.; Bard, A. J.; Anson, F. C. *J. Am. Chem. Soc.* **1978**, *100*, 4248.

(62) Neyhart, G. A.; Hupp, J. T.; Curtis, J. C.; Timpson, C. J.; Meyer, T. J. *J. Am. Chem. Soc.* **1996**, *118*, 3724.

(63) LeSuer, R. J.; Geiger, W. E. *Angew. Chem., Int. Ed.* **2000**, *39*, 248.

(64) Sutton, J. E.; Sutton, P. M.; Taube, H. *Inorg. Chem.* **1979**, *18*, 1017.

(65) Richardson, D. E.; Taube, H. *J. Am. Chem. Soc.* **1983**, *105*, 40.

(66) Bruce, M. I.; Low, P. J.; Costuas, K.; Halet, J.; Best, S. P.; Heath, G. A. *J. Am. Chem. Soc.* **2000**, *122*, 1949.

(67) Dembinski, R.; Bartik, T.; Bartik, B.; Jaeger, M.; Gladysz, J. A. *J. Am. Chem. Soc.* **2000**, *122*, 810.

(68) Müller, T. E.; Choi, S. W. K.; Mingos, D. M. P.; Murphy, D.; Williams, D. J.; Yam, V. W. W. *J. Organomet. Chem.* **1994**, *484*, 209.

(69) Akita, M.; Terada, M.; Oyama, S.; Moro-oka, Y. *Organometallics* **1990**, *9*, 816.

(70) Ellis, B. Ph.D. thesis, University of Adelaide, 2003.

(71) Davies, J. A.; El-Ghanam, M.; Pinkerton, A. A.; Smith, D. A. *J. Organomet. Chem.* **1991**, *409*, 367.

(72) Koutsantonis, G. A.; Selegue, J. P. *J. Am. Chem. Soc.* **1991**, *113*, 2316.

(73) Appel, M.; Heidrich, J.; Beck, W. *Chem. Ber.* **1987**, *120*, 1087.

(74) Brady, M.; Weng, W.; Zhou, Y.; Seyler, J. W.; Amoroso, A. J.; Arif, A. M.; Böhme, M.; Frenking, G.; Gladysz, J. A. *J. Am. Chem. Soc.* **1997**, *119*, 775.

(75) Meyer, W. E.; Amoroso, A. J.; Horn, C. R.; Jaeger, M.; Gladysz, J. A. *Organometallics* **2001**, *20*, 1115.

(76) Le Narvor, N.; Toupet, L.; Lapinte, C. *J. Am. Chem. Soc.* **1995**, *117*, 7129.

(77) Brandsma, L. *Preparative Acetylenic Chemistry*; 2nd ed.; Elsevier: Amsterdam, 1988.

(78) Rappert, T.; Nürnberg; Werner, H. *Organometallics* **1993**, *12*, 1359.

(79) Werner, H.; Lass, R. W.; Gevert, O.; Wolf, J. *Organometallics* **1997**, *16*, 4077.

(80) Wong, A.; Kang, P. C. W.; Tagge, C. D.; Leon, D. R. *Organometallics* **1990**, *9*, 1992.

(81) Bruce, M. I.; Hall, B. C.; Kelly, B. D.; Low, P. J.; Skelton, B. W.; White, A. H. *J. Chem. Soc., Dalton. Trans.* **1999**, 3719.

(82) Roberts, R. L.; Puschmann, H.; Howard, J. A. K.; Yamamoto, J. H.; Carty, A. J.; Low, P. J. *Dalton Trans.* **2003**, 1099.

(83) Guillemot, M.; Toupet, L.; Lapinte, C. *Organometallics* **1998**, *17*, 1928.

(84) Bruce, M. I.; Kelly, B. D.; Skelton, B. W.; White, A. H. *J. Organomet. Chem.* **2000**, *604*, 150.

(85) Akita, M.; Chung, M.-C.; Sakurai, A.; Sugimoto, S.; Terada, M.; Tanaka, M.; Moro-oka, Y. *Organometallics* **1997**, *16*, 4882.

(86) Horn, C. R.; Martín-Alvarez, J. M.; Gladysz, J. A. *Organometallics* **2002**, *21*, 5386.

(87) Bruce, M. I.; Ke, M.; Low, P. J.; Skelton, B. W.; White, A. H. *Organometallics* **1998**, *17*, 3539.

(88) Mohr, W.; Stahl, J.; Hampel, F.; Gladysz, J. A. *Chem. Eur. J.* **2003**, *9*, 3324.

(89) Antonova, A. B.; Bruce, M. I.; Ellis, B. G.; Gaudio, M.; Humphrey, P. A.; Jevric, M.; Melino, G.; Nicholson, B. K.; Perkins, G. J.; Skelton, B. W.; Stapleton, B.; White, A. H.; Zaitseva, N. N. *Chem. Commun.* **2004**, 960.

(90) Bartik, T.; Bartik, B.; Brady, M.; Dembinski, R.; Gladysz, J. A. *Angew. Chem., Int. Ed. Engl.* **1996**, *35*, 414.

(91) Sakurai, A.; Akita, M.; Y, M.-o. *Organometallics* **1999**, *18*, 3241.

(92) Peters, T. B.; Bohling, J. C.; Arif, A. M.; Gladysz, J. A. *Organometallics* **1999**, *18*, 3261.

(93) Mohr, W.; Stahl, J.; Hampel, F.; Gladysz, J. A. *Inorg. Chem.* **2001**, *40*, 3263.

(94) Zheng, Q.; Gladysz, J. A. *J. Am. Chem. Soc.* **2005**, *127*, 10508.

(95) Rigaut, S.; Perruchon, J.; Le Pichon, L.; Touchard, D.; Dixneuf, P. H. *J. Organomet. Chem.* **2003**, *670*, 37.

(96) Szafert, S.; Gladysz, J. A. *Chem. Rev.* **2003**, *103*, 4175.

(97) Tanimoto, M.; Kuchitsu, K.; Morino, Y. *Bull. Chem. Soc. Jpn.* **1971**, *44*, 386.

(98) Parker, C. R. Honours, University of Adelaide, 2005.

(99) Low, P. J.; Roberts, R. L.; Cordiner, R. L.; Hartl, F. *J. Solid State Electrochem* **2005**, *9*, 717.

(100) Coulson, D. R. *Inorg. Synth.* **1990**, *28*, 107.

(101) Cataldo, F. *Fullerene Sci. Technol.* **2001**, *9*, 525.

(102) Johnson, T. J.; Alvey, L. J.; Brady, M.; Mayne, C. L.; Arif, A. M.; Gladysz, J. A. *Chem. Eur. J.* **1995**, *1*, 294.

(103) Holmes, A. B.; Sporikou *Org. Synth.* **1987**, *65*, 61.

(104) Takahashi, S.; Kuroyama, Y.; Sonogashira, K.; Hagihara, N. *Synthesis* **1980**, *8*, 627.

(105) Woodworth, B. E.; Templeton, J. L. *J. Am. Chem. Soc.* **1996**, *118*, 7418.

(106) Weng, W.; Ramsden, J. A.; Arif, A. M.; Gladysz, J. A. *J. Am. Chem. Soc.* **1993**, *115*, 3824.

(107) Dembinski, R.; Szafert, S.; Haquette, P.; Lis, T.; Gladysz, J. A. *Organometallics* **1999**, *18*, 5438.

(108) Dewhurst, R. D.; Hill, A. F.; Smith, M. K. *Angew. Chem., Int. Ed.* **2004**, *43*, 476.

(109) Dewhurst, R. D.; Hill, A. F.; Willis, A. C. *Organometallics* **2004**, *23*, 5903.

(110) Dewhurst, R. D.; Hill, A. F.; Willis, A. C. *Organometallics* **2004**, *23*, 1646.

(111) Bartik, B.; Weng, W.; Ramsden, J. A.; Szafert, S.; Falloon, S. B.; Arif, A. M.; Gladysz, J. A. *J. Am. Chem. Soc.* **1998**, *120*, 11071.

(112) Fischer, H. In *The Chemistry of Alkenes*; Patai, S., Ed.; Interscience/Wiley: London, 1964.

(113) Skibar, W.; Kopacka, H.; Wurst, K.; Salzmann, C.; Ongania, K.; Fabrizi de Biani, F.; Zanello, P.; Bildstein, B. *Organometallics* **2004**, *23*, 1024.

(114) Hart, I. J.; Hill, A. F.; Stone, F. G. A. *J. Chem. Soc., Dalton. Trans.* **1989**, 2261.

(115) Schwenzer, B.; Schleu, J.; Burzlaff, N.; Karl, C.; Fischer, H. *J. Organomet. Chem.* **2002**, *641*, 134.

(116) Wadepohl, H.; Arnold, U.; Pritzkow, H.; Calhorda, M. J.; Veiros, L. F. *J. Organomet. Chem* **1999**, *587*, 233.

(117) Blumenthal, T.; Bruce, M. I.; bin Shawkataly, O.; Green, B. N.; Lewis, I. *J. Organomet. Chem.* **1984**, *269*, C10.

(118) Bruce, M. I.; Liddell, M. J. *J. Organomet. Chem.* **1992**, *427*, 263.

(119) Dewhurst, R. D.; Hill, A. F.; Smith, M. K. *Organometallics* **2005**, *24*, 5576.

(120) Bruce, M. I.; Kramaczuk, K. A.; Perkins, G. J.; Skelton, B. W.; White, A. H.; Zaitseva, N. M. *J. Cluster Sci.* **2004**, *15*, 119.

(121) Aime, S.; Milone, L.; Valle, M. *Inorg. Chim. Acta* **1976**, *18*, 9.

(122) Yuan, P.; Richmond, M. G.; Schwarz, M. *Inorg. Chem.* **1991**, *30*, 679.

(123) Bruce, M. I.; Skelton, B. W.; Zaitseva, N. N. *J. Organomet. Chem.* **2003**, *683*, 398.

(124) Bruce, M. I.; Smith, M. E.; Zaitseva, N. N.; Skelton, B. W.; White, A. H. *J. Organomet. Chem.* **2003**, *670*, 170.

(125) Bruce, M. I.; Humphrey, P. A.; Melino, G.; Skelton, B. W.; White, A. H.; Zaitseva, N. N. *Inorg. Chim. Acta* **2005**, *358*, 1453.

(126) Bruce, M. I.; Ellis, B. G.; Gaudio, M.; Lapinte, C.; Melino, G.; Paul, F.; Skelton, B. W.; Smith, M. E.; Toupet, L.; White, A. H. *Dalton Trans.* **2004**, 1601.

(127) Bruce, M. I.; Smith, M. E.; Skelton, B. W.; White, A. H. *J. Organomet. Chem* **2001**, *637-639*, 484.

(128) Desmond, T.; Lalor, F. J.; Ferguson, G.; Parvez, M. *J. Chem. Soc., Chem. Commun.* **1983**, 457.

(129) Lalor, F. J.; Desmond, T. J.; Cotter, G. M.; Shanahan, C. A.; Ferguson, G.; Parvez, M.; Ruhl, B. *J. Chem. Soc., Dalton. Trans.* **1995**, 1709.

(130) Bruce, M. I.; Ellis, B. G.; Low, P. J.; Skelton, B. W.; White, A. H. *Organometallics* **2003**, *22*, 3184.

(131) Montigny, F.; Argouarch, G.; Costuas, K.; Halet, J.; Roisnel, T.; Toupet, L.; Lapinte, C. *Organometallics* **2005**, *24*, 4558.

(132) Back, S.; Lutz, M.; Spek, A. L.; Lang, H.; van Koten, G. *J. Organomet. Chem.* **2001**, *620*, 227.

(133) Colbert, M. C. B.; Lewis, J.; Long, N. J.; Raithby, P. R.; Younus, M.; White, A. J. P.; Williams, D. J.; Payne, N. N.; Yellowlees, L.; Beljonne, D.; Chawdhury, N.; Friend, R. H. *Organometallics* **1998**, *17*, 3034.

(134) Klein, A.; Lavastre, O.; Fiedler, J. *Organometallics* **2006**, *25*, 635.

(135) Hurst, S. K.; Ren, T. *J. Organomet. Chem.* **2002**, *660*, 1.

(136) Lavastre, O.; Plass, J.; Bachmann, P.; Guesmi, S.; Moinet, C.; Dixneuf, P. H. *Organometallics* **1997**, *16*, 184.

(137) Ghazala, S. I.; Paul, F.; Toupet, L.; Roisnel, T.; Hapiot, P.; Lapinte, C. *J. Am. Chem. Soc.* **2006**, *128*, 2463.

(138) Le Narvor, N.; Lapinte, C. *Organometallics* **1995**, *14*, 634.

(139) Jutzi, P.; Kleinebekel, B. *J. Organomet. Chem.* **1997**, *545-546*, 573.

(140) Field, L. D.; George, A. V.; Laschi, F.; Malouf, E. Y.; Zanello, P. *J. Organomet. Chem.* **1992**, *435*, 347.

(141) Greaves, S. J.; Flynn, E. L.; Futcher, E. L.; Wrede, E.; Lydon, D. P.; Low, P. J.; Rutter, S. R.; Beeby, A. *J. Phys. Chem. A* **2006**, *110*, 2114.

(142) Bruce, M. I.; Hall, B. C.; Low, P. J.; Skelton, B. W.; White, A. H. *J. Organomet. Chem.* **1999**, *592*, 74.

(143) Hurst, S. K.; Cifuentes, M. P.; McDonagh, A. M.; Humphrey, M. G.; Samoc, M.; Luther-Davies, B.; Asselberghs, I.; Persoons, A. *J. Organomet. Chem.* **2002**, *642*, 259.

(144) Yamamoto, H. M.; Yamaura, J. I.; Kato, R. *J. Am. Chem. Soc.* **1998**, *120*, 5905.

(145) White, D. M.; Quinn, C. B. *Journal of Polymer Science* **1977**, *15*, 2595.

(146) Shi Shun, A. L. K.; Chernick, E. T.; Eisler, S.; Tykwinski, R. R. *J. Org. Chem.* **2003**, *68*, 1339.

(147) Zhang, Y.; Wen, J.; Du, W. *J. Fluorine Chem.* **1990**, *49*, 293.

(148) Brooke, G. M.; Mawson, S. D. *J. Fluorine Chem.* **1990**, *50*, 111.

(149) Wiles, M. R.; Massey, A. G. *Tetrahedron Letters* **1967**, *51*, 5137.

(150) Bruce, M. I.; Wallis, R. C. *Aust. J. Chem.* **1979**, *32*, 1471.

(151) Bruce, M. I.; Horn, E.; Matisons, J. G.; Snow, M. R. *Aust. J. Chem.* **1984**, *37*, 1163.

(152) Yip, J. H. K.; Wu, J.; Wong, K.; Ho, K. P.; Pun, C. S.; Vittal, J. J. *J. Chin. Chem. Soc.* **2004**, *51*, 1245.

(153) Yip, J. H. K.; Wu, J.; Wong, K.-Y.; Ho, K. P.; Pun, C. S.; Vittal, J. J. *Organometallics* **2002**, *21*, 5292.

(154) Neenan, T. X.; Whitesides, G. M. *J. Org. Chem.* **1988**, *53*, 2489.

(155) Hall, B. C. Ph.D. thesis, University of Adelaide, 2000.

(156) Alonso, A. G.; Reventós, L. B. *J. Organomet. Chem.* **1988**, *338*, 249.

(157) Vicente, J.; Chicote, M.-T.; Abrisqueta, M.-D.; Jones, P. G. *Organometallics* **1997**, *16*, 5628.

(158) Bruce, M. I.; Smith, M. E.; White, A. H. *Aust. J. Chem.* **1999**, *52*, 431.

(159) Pringle, P. G.; Shaw, B. L. *J. Chem. Soc., Dalton. Trans.* **1983**, 889.

(160) Bruce, M. I.; Ernst, H.; Matisons, J. G.; Snow, M. R. *Aust. J. Chem.* **1984**, *37*, 1163.

(161) Bitcon, C.; Whiteley, M. W. *J. Organomet. Chem.* **1987**, *336*, 385.

(162) Crabtree, R. H. *The Organometallic Chemistry of the Transition Metals*; John Wiley & Sons, Inc, 2001.

(163) Band, E.; Mutterties, E. L. *Chem. Rev.* **1978**, *78*, 639.

(164) Dyson, P. J.; Mc Indoe, J. S. *Transition Metal Carbonyl Cluster Chemistry*; Gorden and Breach Science Publishers, 2000.

(165) Akita, M.; Sakurai, A.; Chung, M.-C.; Moro-oka, Y. *J. Organomet. Chem.* **2003**, *670*, 2.

(166) Shapley, J. R.; Richter, S. I.; Tachikawa, M.; Keister, J. B. *J. Organomet. Chem.* **1975**, *94*, C43.

(167) Bruce, M. I.; Skelton, B. W.; White, A. H.; Zaitseva, N. M. *J. Chem. Soc., Dalton Trans.* **1999**, 1445.

(168) Bruce, M. I.; Humphrey, P. A.; Horn, E.; Tiekink, E. R. T.; Skelton, B. W.; White, A. H. *J. Organomet. Chem.* **1992**, *429*, 207.

(169) Foulds, G. A.; Johnson, B. F. G.; Lewis, J. *J. Organomet. Chem.* **1985**, *296*, 147.

(170) Bruce, M. I.; Low, P. J.; Zaitseva, N. M.; Kahlal, S.; Halet, J. F.; Skelton, B. W.; White, A. H. *J. Chem. Soc., Dalton. Trans.* **2000**, 2939.

(171) Falloon, S. B.; Arif, A. M.; Gladysz, J. A. *Chem. Commun.* **1997**, 629.

(172) Falloon, S. B.; Szafert, S.; Arif, A. M.; Gladysz, J. A. *Chem. Eur. J.* **1998**, *4*, 1033.

(173) Ferguson, G.; Gallagher, J. F.; Kelleher, A.-M.; Spalding, T. R.; Deeney, F. T. *J. Organomet. Chem.* **2005**, *690*, 2888.

(174) Hoffman, R. *Angew. Chem., Int. Ed. Engl.* **1982**, *21*, 711.

(175) Bruce, M. I.; Zaitseva, N. M.; Skelton, B. W.; White, A. H. *J. Organomet. Chem* **2005**, *690*, 3268.

(176) Khairul, W. M.; Porres, L.; Albesa-Jove, D.; Senn, M. S.; Jones, M.; Lydon, D. P.; Howard, J. A. K.; Beeby, A.; Marder, T. B.; Low, P. J. *J. Cluster Sci.* **2006**, *17*, 65.

(177) Bruce, M. I.; Kelly, B. D.; Skelton, B. W.; White, A. H. *J. Chem. Soc., Dalton Trans.* **1999**, 847.

(178) Hwang, D.-K.; Chi, Y.; Peng, S.-M.; Lee, G.-H. *J. Organomet. Chem.* **1990**, *389*, C7.

(179) Chi, Y.; Liu, B.-J.; Lee, G.-H.; Peng, S.-M. *Polyhedron* **1989**, *8*, 2003.

(180) Henderson, W.; Mc Indoe, J. S. *Mass Spectrometry of Inorganic and Organometallic Compounds*; Wiley, 2005.

(181) Bruce, M. I.; Zaitseva, N. M.; Skelton, B. W.; White, A. H. *J. Organomet. Chem.* **2005**, *690*, 3268.

(182) Green, M.; Marsden, K.; Salter, I. D.; Stone, F. G. A. *Chem. Commun.* **1983**, 446.

Publications

"Alkynyl and poly-ynyl derivatives of carbon-tricobalt clusters." Antonova, A B.; Bruce, M. I.; Gaudio, M.; Humphrey, P. A.; Nicholson, B. K.; Scoleri, N.; Skelton, B. W.; White, A. H.; Zaitseva, N. N. *J. Organomet. Chem.*, **2006**, *691*, 4694.

"Some complexes containing carbon chains end-capped by $M(CO)_2Tp'$ [M = Mo, W; Tp' = $HB(pz)_3$, $HB(dmpz)_3$] groups." Bruce, M. I.; Cole, M. L.; Gaudio, M.; Skelton, B. W.; White, A. H. *J. Organomet. Chem.*, **2006**, *691*, 4601.

"A novel methodology for the synthesis of complexes containing long carbon chains linking metals centres: molecular structures of $\{Ru[dppe]Cp^*\}_2(\mu\text{-}C_{14})$ and $\{Co_3(\mu\text{-}dppm)(CO)_7\}_2(\mu_3\text{: }\mu_3\text{-}C_{16})$." Antonova, A. B.; Bruce, M. I.; Ellis, B. G.; Gaudio, M.; Humphrey, P. A.; Jevric, M.; Melino, G.; Nicholson, B. K.; Perkins, G. J.; Skelton, B. W.; Stapleton, B.; White, A. H.; Zaitseva, N. N. *Chem. Commun.*, **2004**, 960.

"Preparation, structures and some reactions of novel diynyl complexes of iron and ruthenium." Bruce, M. I.; Ellis, B. G.; Gaudio, M.; Lapinte, C.; Melino, G.; Paul, F.; Skelton, B. W.; Smith, M. E.; Toupet, L.; White, A. H., *Dalton Trans.*, **2004**, 1601.

"The series of carbon-chain complexes $\{Ru(dppe)Cp^*\}_2\{\mu\text{-}(C{\equiv}C)\}_n$: synthesis, structures and properties." *In preparation.*

"Synthesis and redox studies of ruthenium complexes containing polyfluoroaromatic-alkynyl linkers." *In preparation.*

"Formation of cluster-bonded carbon chains." *In preparation.*

Antonova, A.B., Bruce, M.I., Humphrey, P.A., Gaudio, M., Nicholson, B.K., Scoleri, N., Skelton, B.W., White, A.H. and Zaitseva, N.N. (2006) Alkynyl and poly-ynyl derivatives of carbon-tricobalt clusters.
Journal of Organometallic Chemistry, v.691, (22), pp. 4694-4707, November 2006

Bruce. M.I., Cole, M.L., Gaudio, M., Skelton, B.W. and White, A.H. *(2006)* Some complexes containing carbon chains end-capped by $M(CO)_2Tp'$ [M = Mo, W; $Tp' = HB(pz)_3$, $HB(dmpz)_3$] groups.
*Journal of Organometallic Chemistry, v.*691, *(22), pp. 4601-4614, November 2006*

Antonova, A.B., Bruce, M.I., Ellis, B.G., Gaudio, M., Humphrey, P.A., Jevric, M., Melino, G., Nicholson, B.K., Perkins, G.J., Skelton, B.W., Stapleton, B., White, A.H. and Zaitseva, N.N. (2004) A novel methodology for the synthesis of complexes containing long carbon chains linking metal centres: molecular structures of $\{Ru(dppe)Cp^*\}_2(\mu\text{-}C_{14})$ and $\{Co_3(\mu\text{-}dppm)(CO)_7\}_2(\mu_3\text{:}\mu_3\text{-}C_{16})$.
Chemical Communications, no. 8, pp. 960-961, 2004

Bruce, M.I., Ellis, B.G., Gaudio, M., Lapinte, C., Melino, G., Paul, F., Skelton, B.W., Smith, M.E., Toupet, L., and White, A.H. (2004) Preparation, structures and some reactions of novel diynyl complexes of iron and ruthenium.
Dalton Transactions, no. 10, pp. 1601-1609, 2004